Tropical Cyclone Tornadoes-Climatology, Convective modes, Environment and Case Study

Xiaoding YU
China Meteorological Administration

Tropical Cyclone Tornadoes in United States

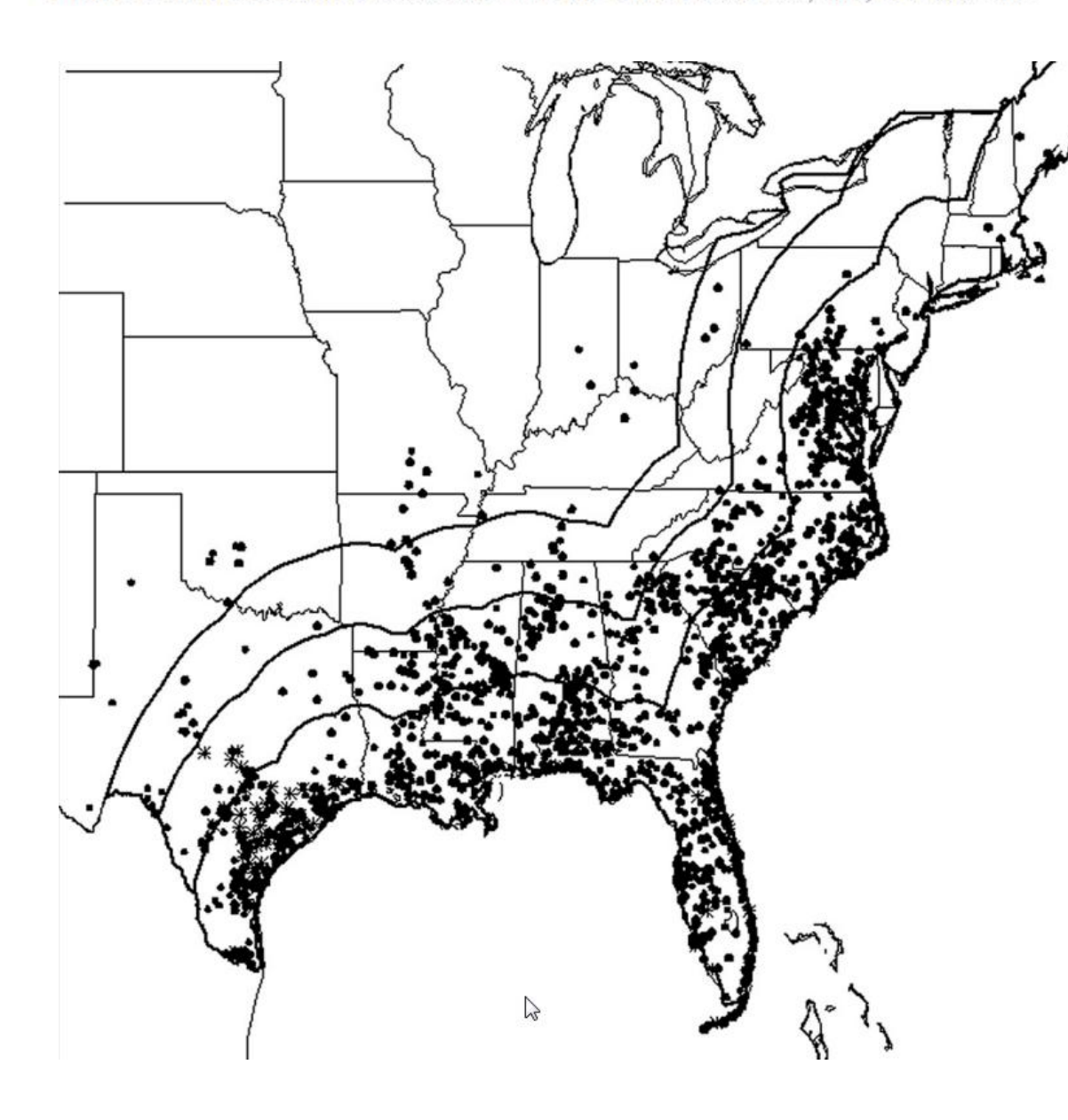
- Climatology
- Convective modes
- Environment Parameters

TC tornadoes Climatology-based on the work of Schultz and Cecil, 2009.

- Based on the data from 1950-2007, total TC tornadoes number is about 1800, making up about 3.4% of the total number of tornado records in U.S. since 1950.;
- Spatial distribution;
- Azimuthal distribution;

Spatial Distribution

. The U.S. tornado locations associated with Atlantic basin tropical cyclones, 1950–2007. Range lines moving inland from the coast are associated with the distances of 200, 400, and 600 km.



TC tornadoes occurrence is most likely within 200–400 km of the coast, with the coastal zone (within 50 km of the coast) incurring the largest percentage of hits.

It is emphasized the importance of the water-to-land transition with increased frictional effects, resulting in decreased wind speed near the surface. This increases the shear in the vertical direction, a key component in the development of rotation on the convective scale.

In addition, areas of increased convergence parallel to the coast can occur while the TC approaches, aiding in the rapid growth or intensification of supercellular storm structures.

Tornado records segmented by distance from the coast. The range values from the coast in the first column start along the coastline and move inland. The middle column lists the number of TC tornado records, and the third column gives the percentage of the total number of TC tornado records.

Range (km)	Count	% of TC tornadoes
0–50	789	44.7%
50-100	301	17.0%
100-150	149	8.4%
150-200	154	8.7%
200-250	90	5.1%
250-300	88	5.0%
300-350	82	4.6%
350-400	41	2.3%
400-450	23	1.3%
450+	50	2.9%

94% of the TC-spawned tornado records occur within 400 km of the coast, 44% (800) of which occur within 50 km of the coast.

Zooming in even further, 2 times as many tornadoes are located within the 0–25-km segment as opposed to the 25–50-km range.

The resultant distribution places 30% of the total TC tornado sample in the immediate coastal zone(0-25km).

Tornado record counts segmented by damage rating. The top half of the table uses the data from 1950–2007. The bottom part of the table shows the data spanning only 1995–2007. The "400 km, May–Nov" label refers to the limitation applied to the U.S. tornado dataset, corresponding to the 400-km-range ring and the months from May to November. The category UNK, or unknown, was used when a damage rating could not be obtained from the available data. This occurred mostly in the earlier part of the record and has not been used in recent years.

Years	Classification		F-scale rating						
		Tot	F0	F1	F2	F3	F4	F5	UNK
1950–2007	All U.S. tornadoes	Counts %Tot	21 487 42%	16 609 32.4%	8239 16.1%	2312 4.5%	621 1.2%	77 <1%	1864 3.6%
	All U.S. tornadoes: 400 km, May-Nov	Counts	3936	3657	1487	298	42	3	337
	25 15 2	%Tot	40.3%	37.5%	15.2%	3.1%	<1%	<1%	3.5%
	TC tornadoes	Counts	866	568	205	38	2	0	88
		%Tot	49%	32.1%	11.6%	2.2%	<1%	0%	5.0%
1995-2007	All U.S. tornadoes	Counts	10 530	4197	1252	383	82	6	0
		%Tot	64.0%	25.5%	7.6%	2.3%	<1%	<1%	0%
	All U.S. tornadoes: 400 km, May–Nov	Counts	1945	1044	227	49	12	1	0
	100 100 100 100 100 100 100 100 100 100	%Tot	59.3%	31.8%	6.9%	1.5%	<1%	<1%	0%
	TC tornadoes	Counts	620	306	70	3	0	0	0
		%Tot	62.1%	30.6%	7.0%	<1%	0%	0%	0%

TC tornadoes are typically weaker than those that occur in the Great Plains region. For the 58-yr dataset in Table, TC tornadoes have a larger number of F0 reports (49%) as compared with all U.S. tornadoes (42%);

The F1-rated numbers share a similar percentage of each dataset, whereas only 3% of TC tornadoes are rated F3 or stronger as compared with 6% of the full U.S. tornado database.

States with 10 or more TC tornado records. The middle column lists the number of TC tornadoes on record for that state. The right column gives the percentage of TC tornadoes in the total count for that state.

State	Count	% from TC
AL	160	11%
AR	20	2%
FL	393	14%
GA	115	10%
LA	115	8%
MD	26	10%
MS	132	9%
NC	153	16%
PA	20	3%
SC	169	22%
TX	296	4%
VA	119	23%

All of the Gulf coast and Atlantic coast states from Virginia southward have experienced over 100 TC tornadoes each.

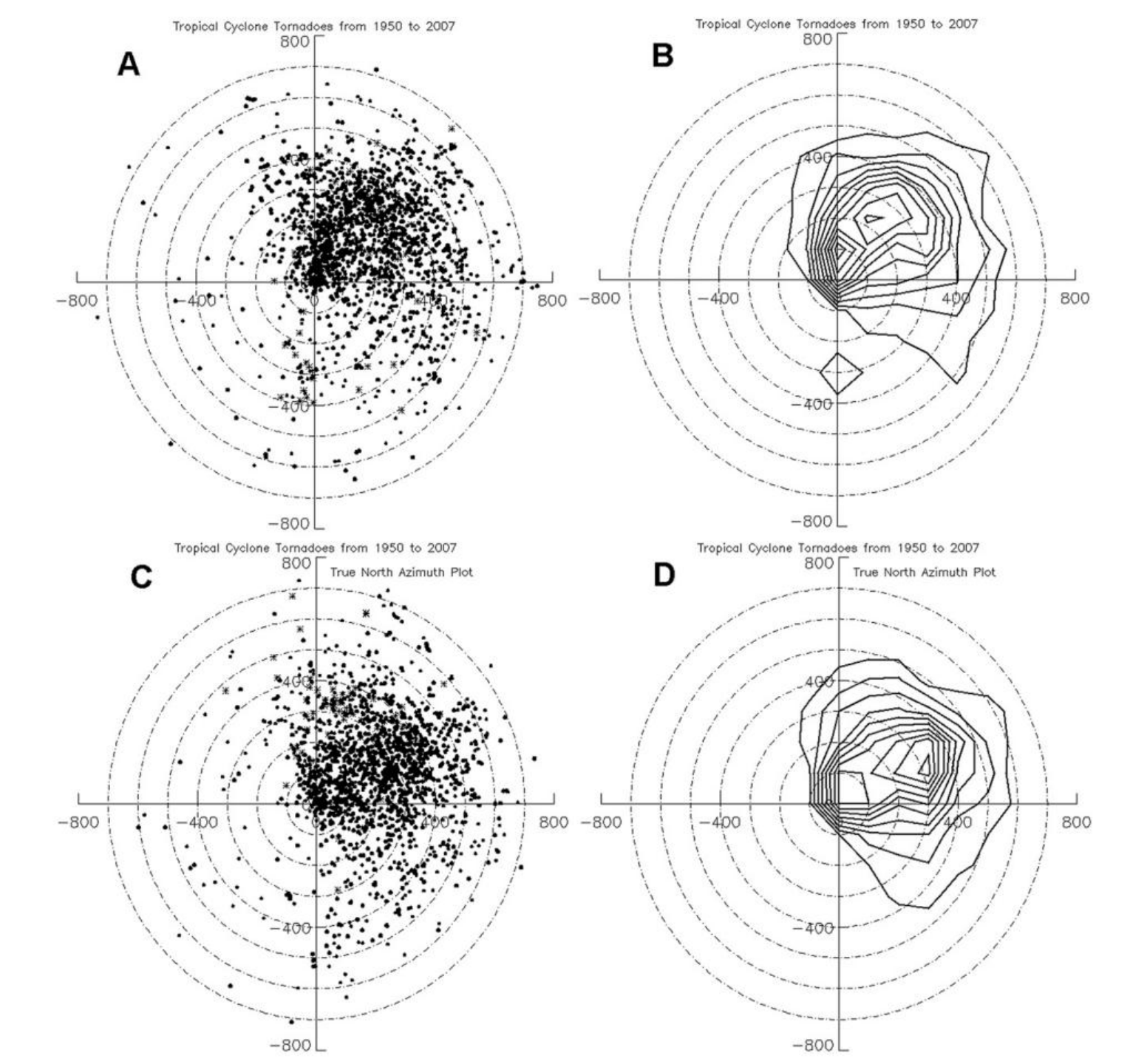
Although Florida leads the country with the most TC-spawned tornadoes by number, this classification of tornado only makes up 14% of the total tornado count for the state in the 58 yr reviewed.

In contrast, Virginia's TC tornado count makes up 23% of the state's total record, the highest in the United States, followed by South Carolina with 22%.

For the coastal states from Louisiana to Maryland, TC tornadoes account for 10%–25% of each state's total tornadoes reported.

Azimuthal Distribution

- It has become somewhat common knowledge from prior studies that TC tornadoes are typically clustered in the right-front quadrant with respect to TC motion or the northeast quadrant in a fixed reference frame (Smith1965; Hill et al. 1966; Novlan and Gray 1974; Gentry1983; McCaul 1991);
- The figure in next slide suggests that it is more appropriate to speak of a preferred sector or region instead of a preferred quadrant. Over 90% of tornadoes take place between 340° and 120°, relative to TC motion (over 80% in north-relative coordinates).
- There is a rightward shift with increasing distance from the center(Fig. c). Inside a 200-km radius, the mean tornado location is ~32° to the right of the storm motion vector(~52° to the right of true north). Between 200 and 400 km, the mean is ~50° to the right of storm motion(~60° to the right of true north), and beyond 400 km it is ~65° to the right of storm motion (~68° to the right of true north).
- Both reference frames have preferred sectors but also have outliers from individual cases. As an example, Hurricane Audrey (1957) produced 14 outlier tornadoes in the south–southeast region (north relative) and Hurricane Beulah (1967) produced over 30 tornadoes in the rear to left-rear region (storm relative).



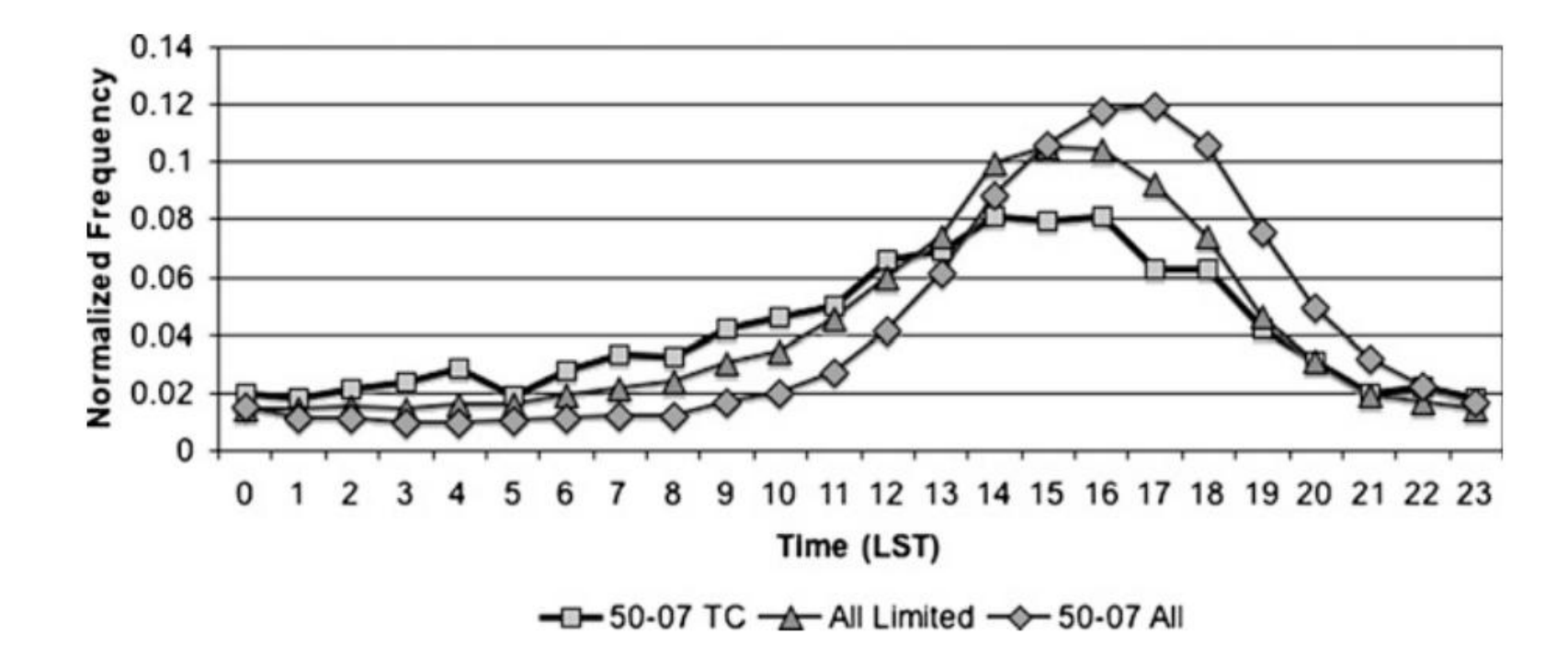
Tropical cyclone tornado locations in both storm-relative and Cartesian coordinates. Range rings are in 100-km increments. (a) Locations relative to TC motion vector. (b) 2D histogram of locations relative to TC motion vector, with 100 km \times 100 km bin spacing centered on the origin. Contour interval is 10 tornadoes per grid box. (c) Locations relative to true north. (d) As in (b), but relative to true north.

Spatial Distribution Summary

- TC tornadoes occurrence is most likely within 200–400 km of the coast, with the coastal zone (within 50 km of the coast) incurring the largest percentage of hits.
- All of the Gulf coast and Atlantic coast states from Virginia southward have experienced over 100 TC tornadoes each for the 58-yr dataset in Table. For the coastal states from Louisiana to Maryland, TC tornadoes account for 10%–25% of each state's total tornadoes reported.
- TC tornadoes are typically weaker than those that occur in the Great Plains region,
 TC tornadoes have a larger number of F0 reports (49%) as compared with all U.S.
 tornadoes (42%); Only 3% of TC tornadoes are rated F3 or stronger as compared
 with 6% of the full U.S. tornado database.

Time of Day

Histogram of the local solar time of TC tornadoes (thick black line with squares), all U.S. tornadoes limited by a 400-km distance from the coast and from May to November (black line with triangles), and all U.S. tornadoes (black line with diamonds).



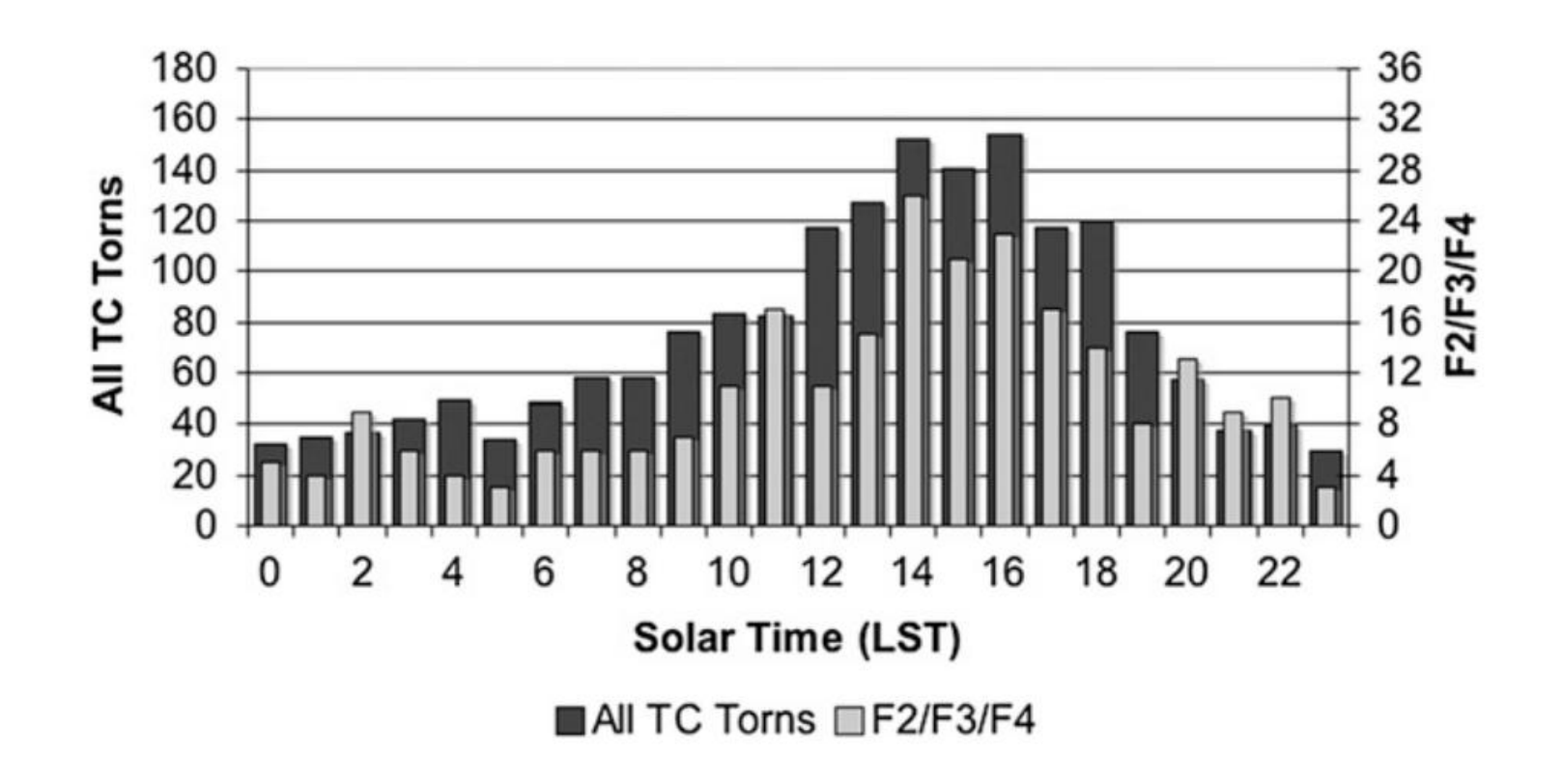
The peak for all U.S. tornadoes is in late afternoon from 1600 to 1800 LST, as compared with mid- to late afternoon (1400–1700 LST) for TC tornadoes.

For the amplitude of change over the day, the full U.S. tornado record showed the sharpest increase of a factor of ~12 from morning to afternoon as compared with about a fourfold increase in the TC tornado record.

Again limiting the U.S. dataset to within 400 km of the coast and to May–November results in an amplitude of a factor of ~7.

This suggests that TC tornadoes are a bit less dependent on daytime heating (buoyant forcing) than tornadoes are in general. This is reasonable, because extensive cloud cover and rain cooled air limit daytime heating over much of the region affected by a TC.

Histogram of TC tornadoes as a function of time of day (local solar time). Dark bars are for all TC tornadoes; light bars are significant (≥F2) tornadoes only. The scale between axes is 5.



The phase and amplitude of the histograms for ≥F2 TC tornadoes are very similar to those for all TC tornadoes, adding confidence to the result.

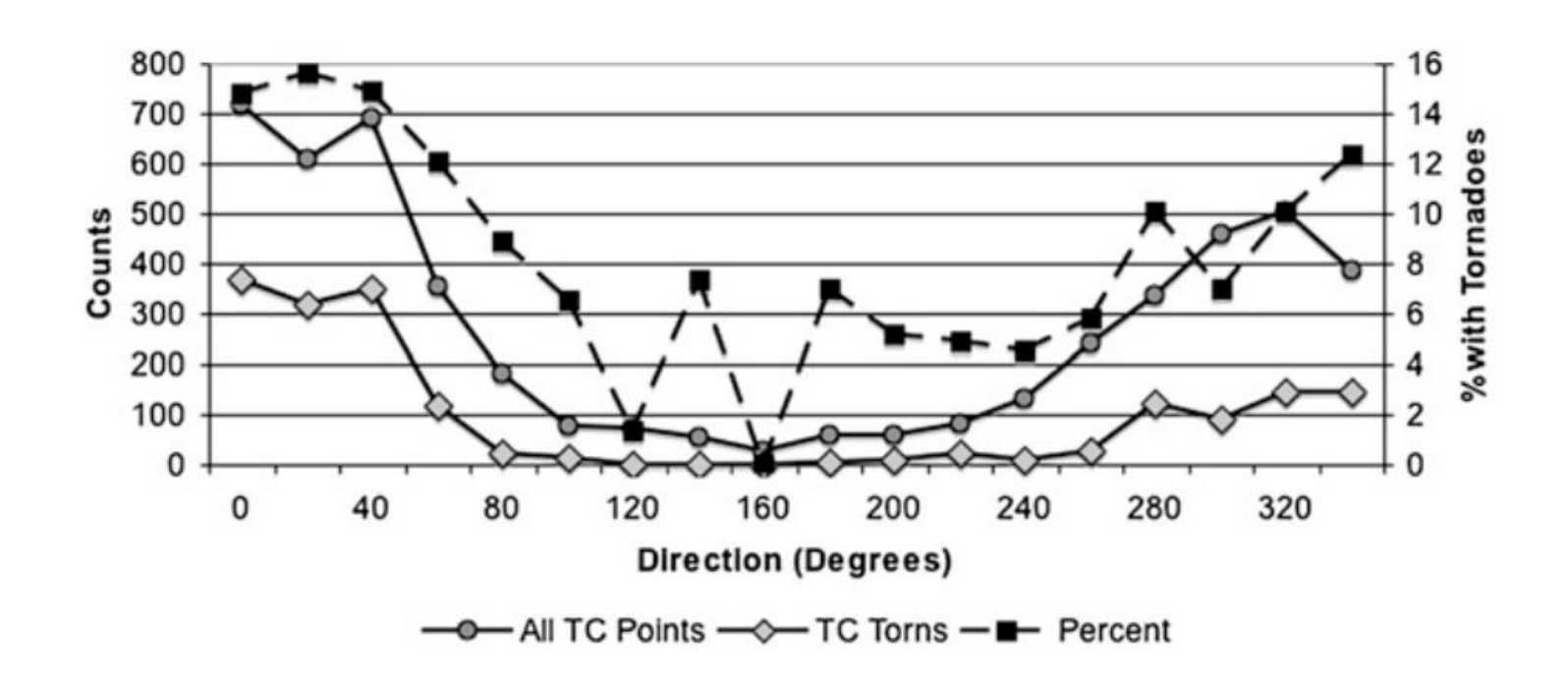
Time of Day Summary

- Pearson and Sadowski (1965), Smith (1965), and McCaul (1991) all presented work
 depicting the tornado counts as a function of time of day. In McCaul's (1991) 626-tornado
 sample, the peak occurrence was between 1500 and 1800 LST.
- With a threefold larger sample size, it is now practical to examine this on a finer time scale. The peak for all U.S. tornadoes is in late afternoon from 1600 to 1800 LST, as compared with mid- to late afternoon (1400–1700 LST) for TC tornadoes.
- For the amplitude of change over the day, the full U.S. tornado record showed the sharpest increase of a factor of ~12 from morning to afternoon as compared with about a fourfold increase in the TC tornado record. Again limiting the U.S. dataset to within 400 km of the coast and to May–November results in an amplitude of a factor of ~7. This suggests that TC tornadoes are a bit less dependent on daytime heating (buoyant forcing) than tornadoes are in general. This is reasonable, because extensive cloud cover and rain cooled air limit daytime heating over much of the region affected by a TC.
- The phase and amplitude of the histograms for ≥F2 TC tornadoes are very similar to those for all TC tornadoes, adding confidence to the result.
- A possible diurnal relationship to the time of landfall of the parent TC was investigated and was found to offer no distinct signal.

Tropical Cyclone Speed and Direction-Summary

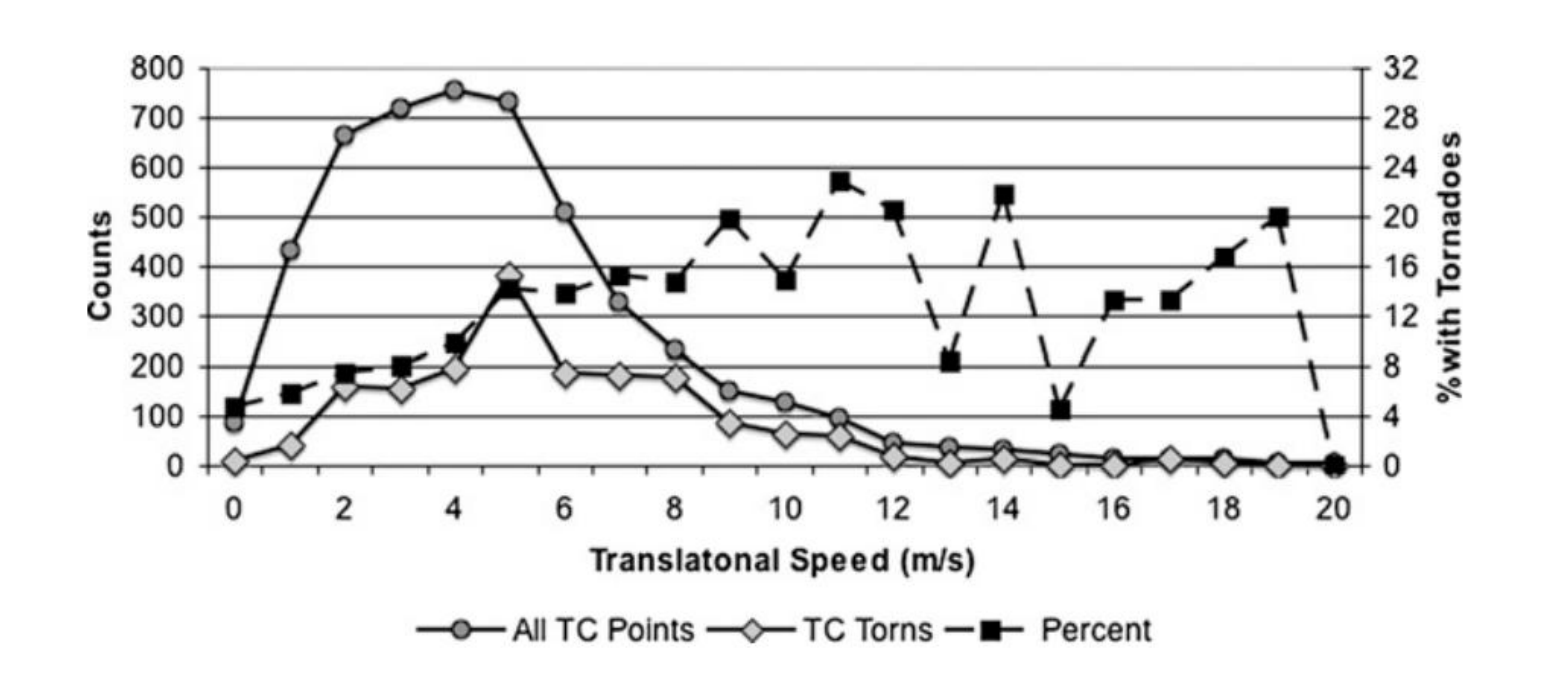
- Vertical wind shear profiles are more favorable for tornadoes in the right-front (northeast) region while being further enhanced when the tropical cyclone interacts with the mid-latitude westerlies (e.g., McCaul 1991; Verbout et al. 2006). This adds to the westerly shear and the upper-level forcing. Weiss (1987) found the forward translational speed of a TC was associated with tornado production. Verbout et al. (2007) showed that the occurrence of a large number of TC tornadoes (sometimes termed an outbreak, depending on how it is defined) is more likely with TCs that are recurving ahead of a mid-latitude trough approaching from the northwest.
- this relationship between TC recurvature and tornado occurrence is manifested in most of the tornadoes occurring while TCs are moving toward the north or northeast. These headings are more common for TCs in general in the U.S. region, but even more so when considering TCs that are spawning tornadoes.

Histograms as a function of TC direction of motion: TC tornadoes (solid line with small circles; left axis); 6-hourly time periods with that TC motion, regardless of tornado occurrence (solid line with large circles; left axis); and percentage of all 6-hourly time periods that have associated tornadoes (dashed lines with squares; right axis). Only time periods during which a TC is in the U.S. region (north of 23.5° lat and west of 70° lon) are included. The scale between axes is 50:1.



With the TC database in 6-hourly intervals, ~15% of the time periods with translational TC headings between 340° and 80° have tornadoes (dashed line with squares in Figure). For most other headings, ~5%–10% of the time periods have tornadoes.

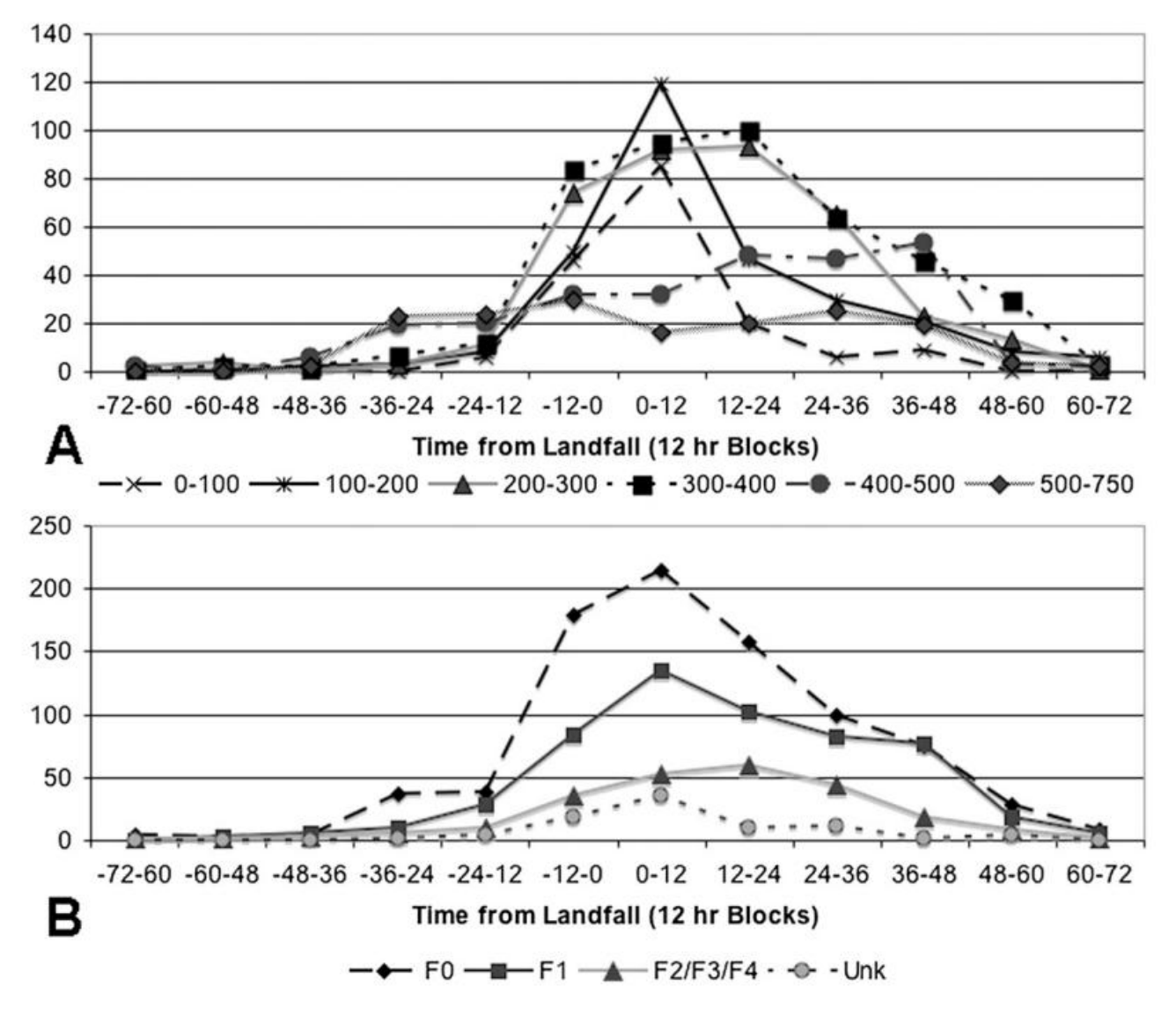
Histograms as a function of TC speed: TC tornadoes (solid line with small circles; left axis); 6-hourly time periods with that TC motion, regardless of tornado occurrence (solid line with large circles; left axis); and percentage of all 6-hourly time periods that have associated tornadoes (dashed lines with squares; right axis). Only time periods during which a TC is in the U.S. region (north of 23.5° lat and west of 70° lon) are included. The scale between axes is 25:1.



In a similar way, ~15%–25% of the time periods with TC forward speed of at least 5 m s⁻¹ have associated tornadoes. There is a spike in the number of tornado occurrences at TC forward speeds of 5 m s⁻¹, because the faster forward speeds are less common for TCs in general.

Time from Landfall

(a) The 1950–2007 TC tornado counts as a function of time from landfall (12-h bins) and distance from the TC center (km). (b) The TC tornado counts as a function of time from landfall (12-h bins) and damage rating.



In the composite, there is a rapid increase in tornado counts in the last 12 h while a TC approaches its landfall.

A majority of tornadoes occurs between 12 h before and 24 h after landfall. About 84% of the tornado record occurs from about 12 h before to 48 h after landfall, with the threat continuing out to 72 h.

More-damaging tornadoes (≥F2) have a broad distribution with a relative peak at 350 km from the center of the TC and tend to occur after landfall rather than before.

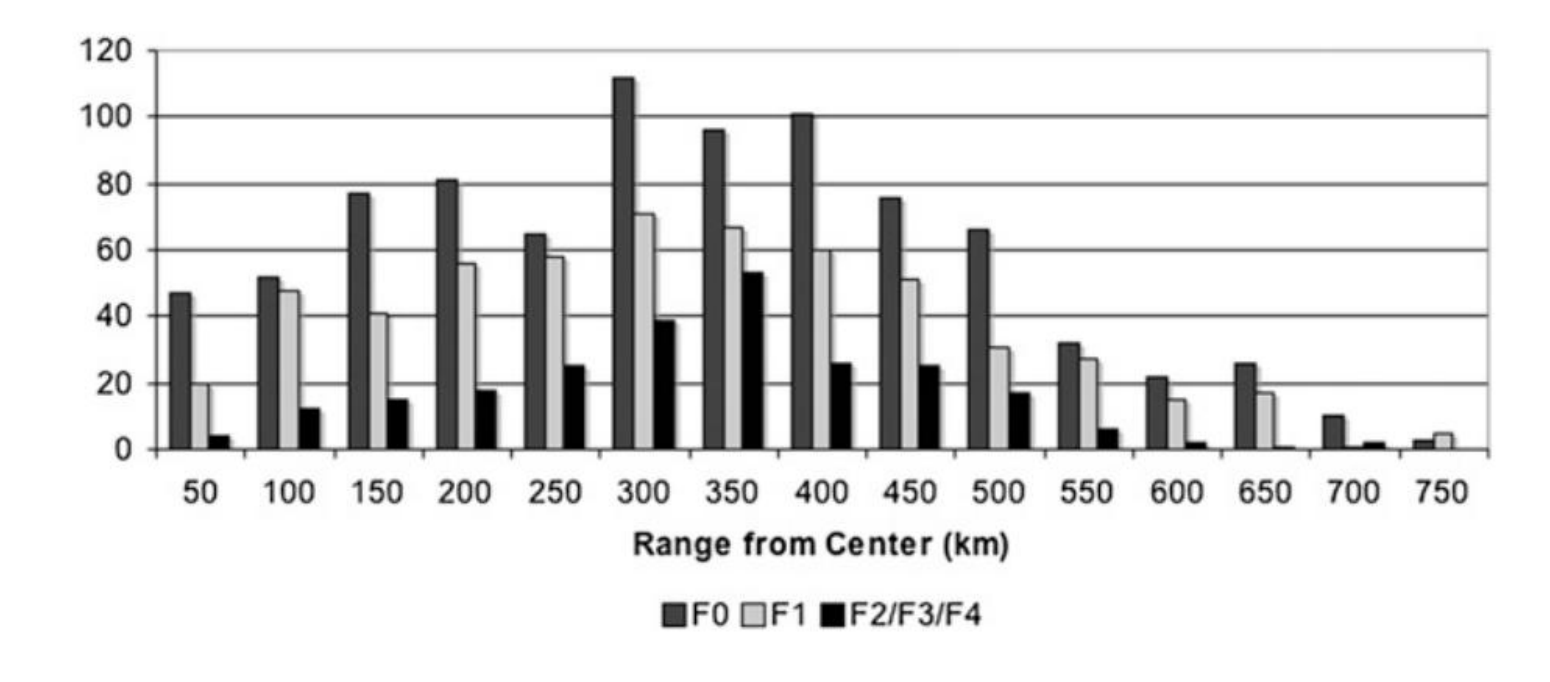
There are distinct spikes at landfall in the counts of tornadoes in the 0–100- and 100–200-km bins, whereas the other range bins have a broader distribution, with relative peaks in later time bins.

Time from Landfall - summary

- From a statistical standpoint, the majority of TC tornadoes begin occurring 1–2 days ahead of landfall (as the TC approaches or parallels the coast, with rainbands penetrating inland), although a few TC tornadoes have occurred as early as 4 days before landfall (e.g., Hurricane Georges in 1998). They continue to occur through 2–3 days after landfall (McCaul 1991), with some slow-moving, persistent TCs producing tornadoes into days 4 and 5.
- In the composite, there is a rapid increase in tornado counts in the last 12 h while a TC approaches its landfall (Figs.a,b). A majority of tornadoes occurs between 12 h before and 24 h after landfall. About 84% of the tornado record occurs from about 12 h before to 48 h after landfall, with the threat continuing out to 72 h.
- More-damaging tornadoes (≥F2) have a broad distribution with a relative peak at 350 km from the center of the TC and tend to occur after landfall rather than before .

Bimodal Segmentation

The 1950–2007 TC tornado F scale as a function of range from the TC center (km).

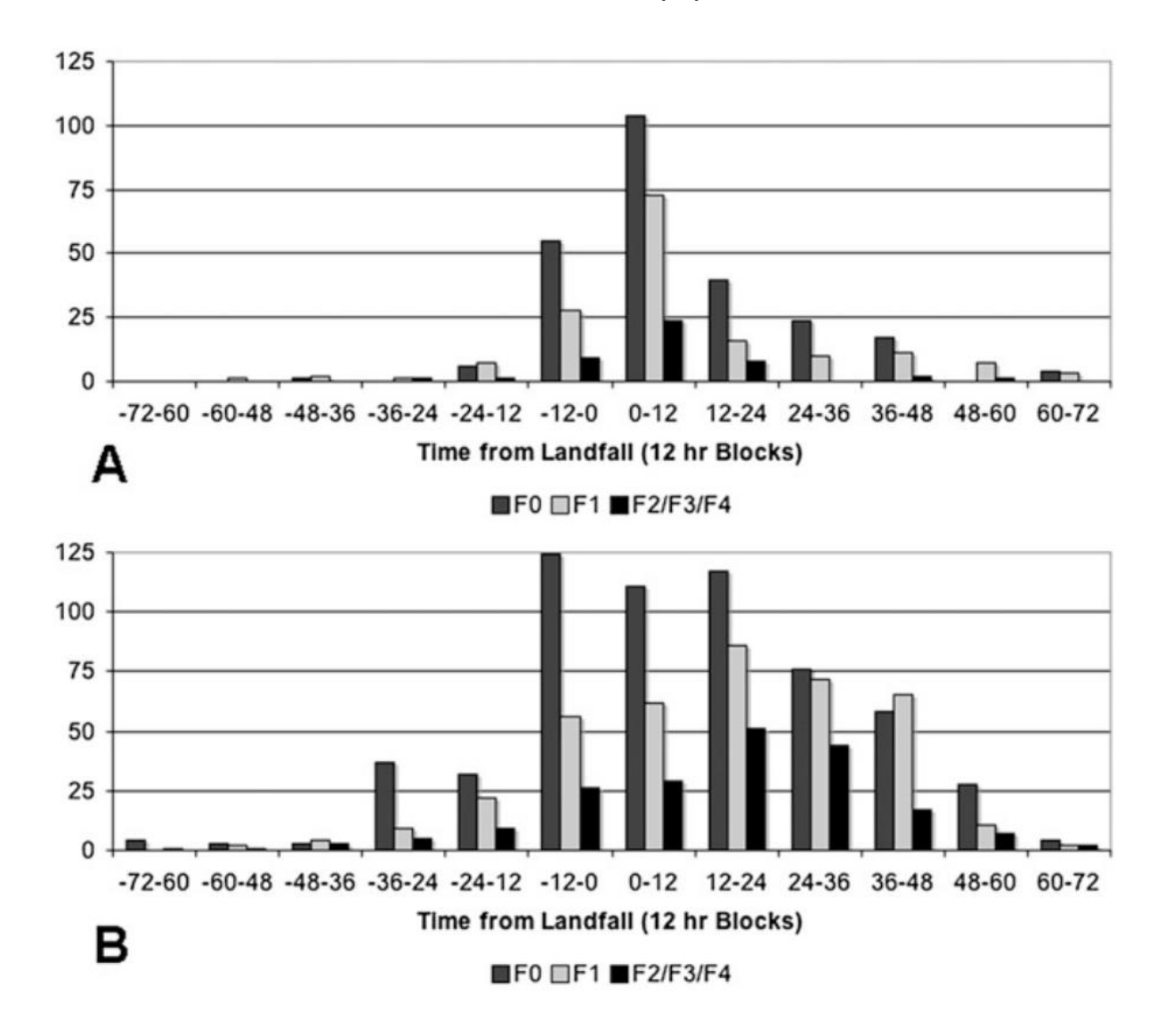


In McCaul (1991), the data showed a distinct peak from 200 to 400 km with a "shoulder" located approximately inside the 160-km range.

In the current data, the maximum falls between 250 and 500 km with a shoulder inside 250 km for the F0 distribution and located inside the 200-km range for the higher damage ratings.

For this study, the area described as "core region" is defined to be within 200 km of the center while the "outer rainband" classification describes tornadoes that occur outside the 200-km limit. For individual cases, smaller or larger distances might be preferable for this distinction.

(a) Core region (0–200 km from TC center) tornado F scale as a function of time from landfall (h). (b) Outer region (beyond 200 km from TC center) tornado F scale as a function of time from landfall (h).

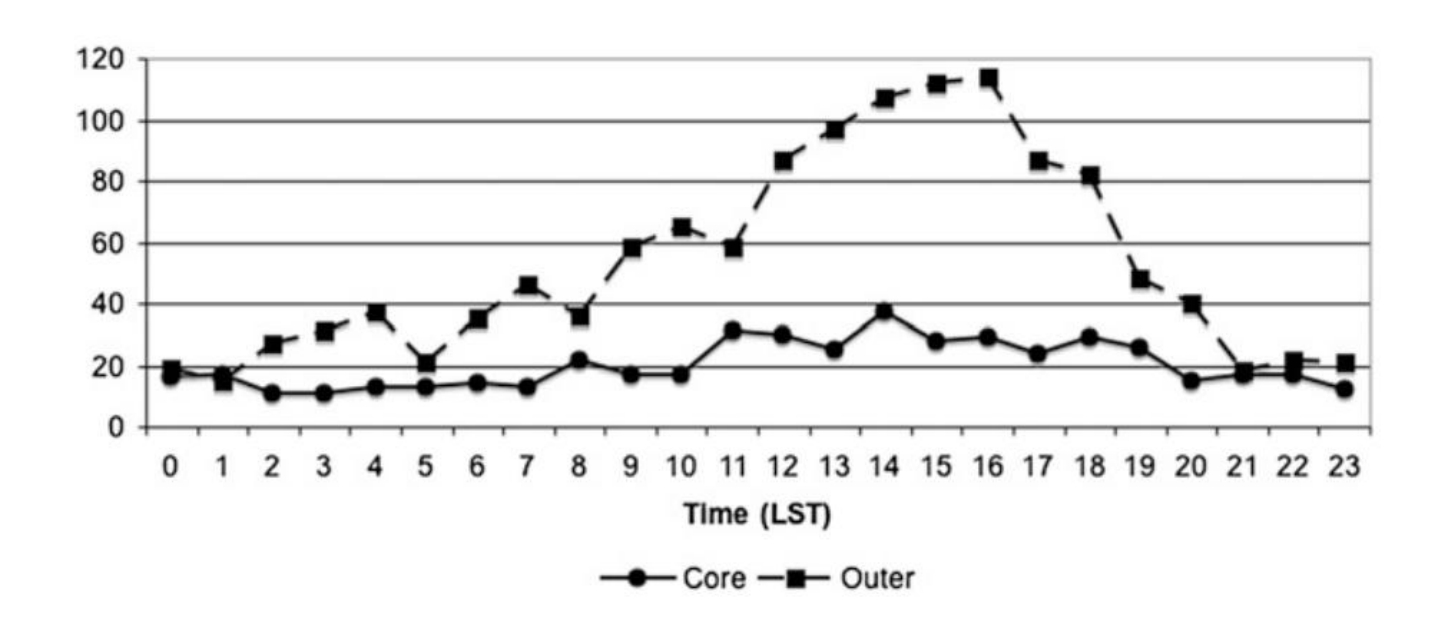


Tornadoes within 200 km of the center occur mostly near the time of landfall and tend to be relatively weak, mostly F0 and F1 (over 80% of subtotal), supporting the findings in McCaul (1991). It is important to note here that this type of TC tornado only makes up one-quarter of the entire dataset so that the numbers are arguably small overall.

At larger radii (beyond 200 km) from the TC center (Fig. b), there is less dependence on the time since landfall, with the distribution of each of the intensities being fairly well spread between the 12-h blocks.

The F1 counts in the outer region reach their maximum in the 12–24-h block and slowly decrease through 48 h, whereas ≥F2 tornadoes have a broader peak 12–36 h after landfall.

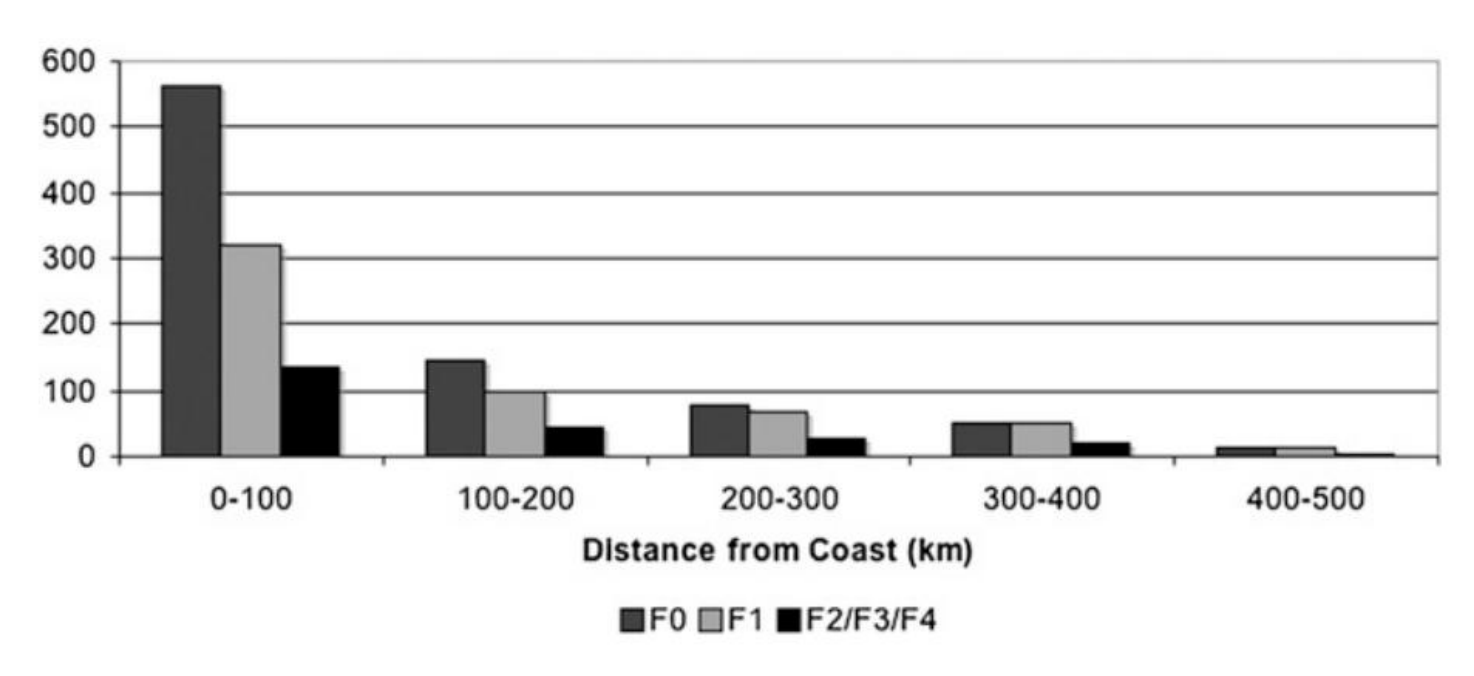
Diurnal distribution of core (0–200 km; solid line) and outer region (beyond 200 km; dashed line) TC tornadoes.



When considering the core- and outer-region tornadoes separately, it is seen that the diurnal signal is almost entirely a result of afternoon tornadoes in the outer regions. Coreregion tornado numbers remain fairly consistent throughout the day, with about a twofold increase from overnight to afternoon. In the outerrainband mode, the presence of a diurnal effect is similar to the climatological distribution shown in previous slides with over a fivefold increase from overnight to afternoon.

The TCs that produced a tornado were checked for a preference in the TC time of landfall. There was no obvious influence, ruling out the possibility of a preferred TC landfall time contributing to a preferred tornado diurnal distribution.

Tornado F scale as a function of distance from the coast (km).



The finding that stronger tornadoes tend to be in the outer regions and continue to occur more than a day after landfall leads to the question of whether they are found farther inland than most TC tornadoes. The difference in the damage rating as a function of distance from the coast is small.

There is a slight preference for F0-rated tornadoes near the coast in comparison with farther inland. It is obvious that the core-region tornadoes near the time of landfall are near the coast, and it would be tempting to conclude that most tornadoes within 100 km of the coast fit that description. In fact, only about one-third of the tornadoes located near the coast (the 0–100-km-range bin) are designated as core-region tornadoes. Nearly half of the coastal zone tornadoes occur more than 12 h from landfall (not shown). These tornado events within 100 km of the coast are therefore a combination of the inner-region tornadoes and more distant tornadoes related to outer rainbands coming ashore.

Bimodal Segmentation-summary

- Weiss (1987), Gentry (1983), and McCaul (1991) discussed a bimodal signal that occurs with respect to range from the center of the TC outward. In McCaul (1991), the data showed a distinct peak from 200 to 400 km with a "shoulder" located approximately inside the 160-km range. In the current data, the maximum falls between 250 and 500 km with a shoulder inside 250 km for the F0 distribution and located inside the 200-km range for the higher damage ratings.
- The area described as "core region" is defined to be within 200 km of the center while the "outer rainband" classification describes tornadoes that occur outside the 200-km limit.
- McCaul (1991) noted that these core tornadoes are more prominent on the day of landfall, with the
 threat in the outer regions sometimes persisting for a few days. This is also seen in the in 1950–2007
 dataset, with 62% of core-region tornadoes occurring in the 12 h bracketing landfall. There is a broad
 peak of tornado occurrence in the outer region from 12 h prior through 24 h after landfall, with a
 gradual decline thereafter.
- Tornadoes within 200 km of the center occur mostly near the time of landfall and tend to be relatively weak, mostly F0 and F1 (over 80% of subtotal), supporting the findings in McCaul (1991).
- A specific look at the distribution of tornadoes outside of 200 km shows that the major threat for more-damaging tornadoes extends through 2 days after landfall, with some occurring even later.

Summary 01 (Schultz and Cecil, 2009)

- An updated climatology based on almost 1800 tropical cyclone tornadoes for the period of 1950–2007 (making up about 3.4% of the total number of tornado records in U.S. since 1950) is consistent with many earlier findings. The vastly larger sample size allows for a reexamination of some of those findings and reveals additional aspects of a distinction between tornadoes near the TC core and those in the outer regions.
- The greatest frequency of TC tornadoes is along the coastline, with numbers decreasing rapidly over the first 150 km inland. Seventy-nine percent are within 200 km of the coast, and TC tornadoes account for ~10%–25% of all tornado records for each of the coastal states from Louisiana to Maryland.
- Other than a preference for F0 tornadoes near the coast, there is no strong relationship between TC tornado rating and distance inland.
- Significant (≥F2) tornadoes are less common with TCs (≤14% of TC tornadoes) than with non-TC tornado events (~20% of U.S. tornadoes). Since 1995, only ~7% of TC tornadoes and ~10% of U.S. tornadoes have received ≥F2 ratings.

Summary 02 (Schultz and Cecil, 2009)

- The right-front (northeast) region of the TC produces the largest number of tornadoes (as in previous studies), with 80% occurring between 350° and 120° relative to the TC motion vector (81% in the same sector relative to Cartesian north). The peak in mid- to late afternoon (1400–1700 LST) for TC tornadoes is slightly earlier than that reported by McCaul (1991) (1500–1800 LST) and slightly earlier than the peak in the overall U.S. tornado distribution (1600–1800 LST).
- The amplitude of the diurnal signal for TC tornadoes is smaller (a factor of 4 increase from overnight to afternoon) than for other tornadoes. Tornadoes are most common when TCs are moving northward or northeastward at 5 m/s or faster.
- Tornadoes near the center of the TC and/or near the time of TC landfall are disproportionately less damaging (more F0s) than those occurring farther away or later.
- Inner-region tornadoes (defined here as those within 200 km of the center) compose 26%
 of the population. Only 10% of these are significant tornadoes(≥F2), as compared with 15%
 of those in the outer regions.

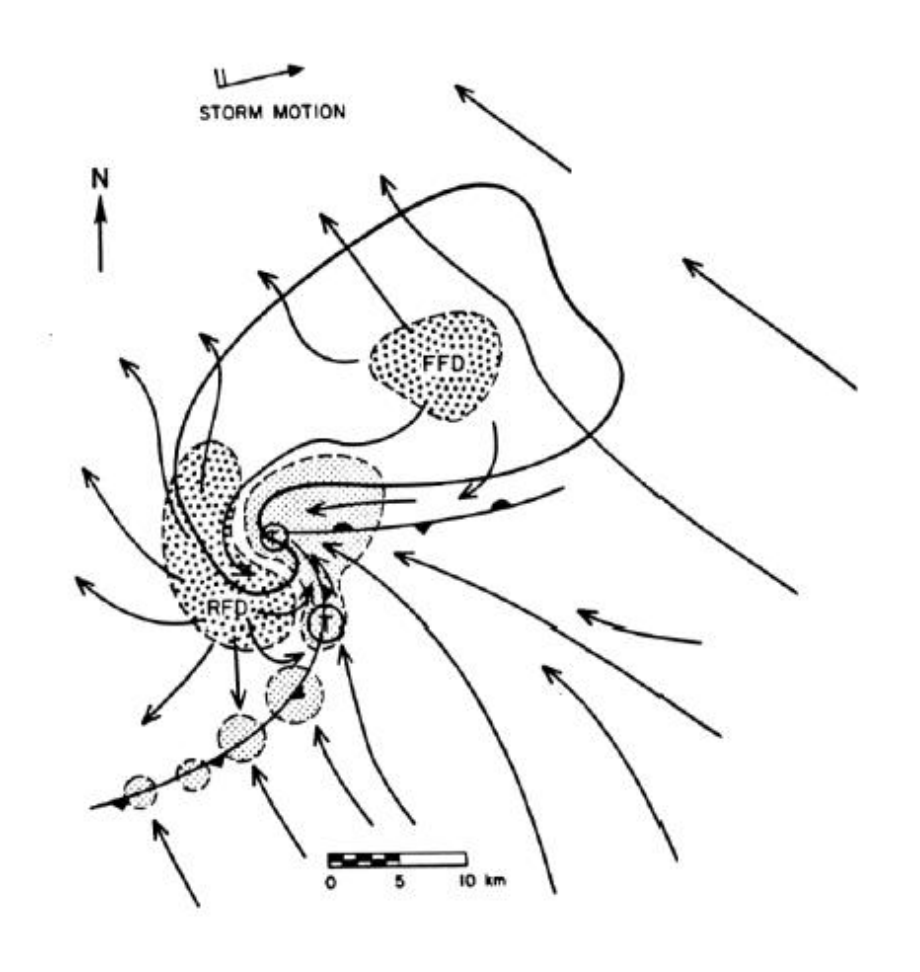
Summary 03 (Schultz and Cecil, 2009)

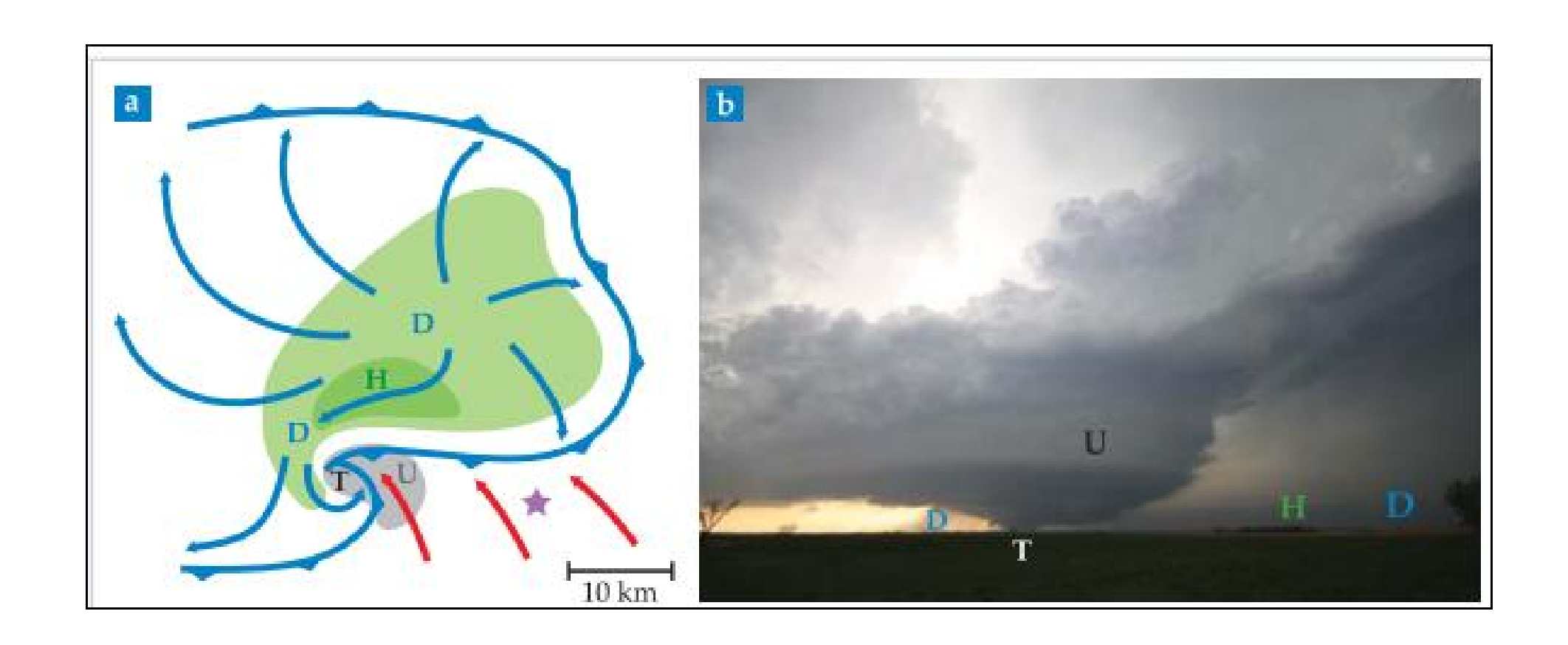
- The core-region tornadoes occur mostly near the time of landfall, with 75% from 12 h before to 24 h after landfall. Slightly over half of the outer-region tornadoes occur during the same time period; the outer region also poses a tornadic threat in the days preceding and following landfall.
- A vast majority (94%) of tornadoes occur within 48 h of landfall (12h before to 36h after).
- Tornadoes near the TC center mostly occur within a day of landfall and, for the most part, are relatively weak. Farther from the TC center (mostly 200–500 km away), tornadoes are a threat, especially during the afternoon as the TC nears the coast and for another afternoon or two during and after landfall.

Convective modes and Environmental Conditions for TC tornadoes in United States

- Based on the work of Edwards et al., 2012.
- A gridded, hourly, three-dimensional environmental mesoanalysis database at the Storm Prediction Center(SPC), based on objectively analyzed surface observations blended with the Rapid Update Cycle (RUC) model-analysis fields is applied to a 2003–11 subset of the SPC tropical cyclone (TC) tornado records.
- Distributions of environmental convective parameters, derived from SPC hourly
 mesoanalysis fields that have been related to supercells and tornadoes in the midlatitudes,
 are evaluated for their pertinence to TC tornado occurrence.
- Radar reflectivity and velocity data also are examined for the same subset of TC tornadoes, in order to determine parent convective modes (e.g., discrete, linear, clustered, supercellular vs nonsupercellular), and the association of those modes with several mesoanalysis parameters.
- For clarity, "storm" hereafter will refer to those convective elements, on horizontal scales of 10°–10¹ km, specifically responsible for tornadoes. This term is used instead of "cell" since (as shown herein) some tornadic storm modes are not unambiguously or discretely cellular. The acronym "TC" will be used to refer to the tropical cyclone as a whole.

Supercell storms conceptual model (Lemon and Doswell, 1979)

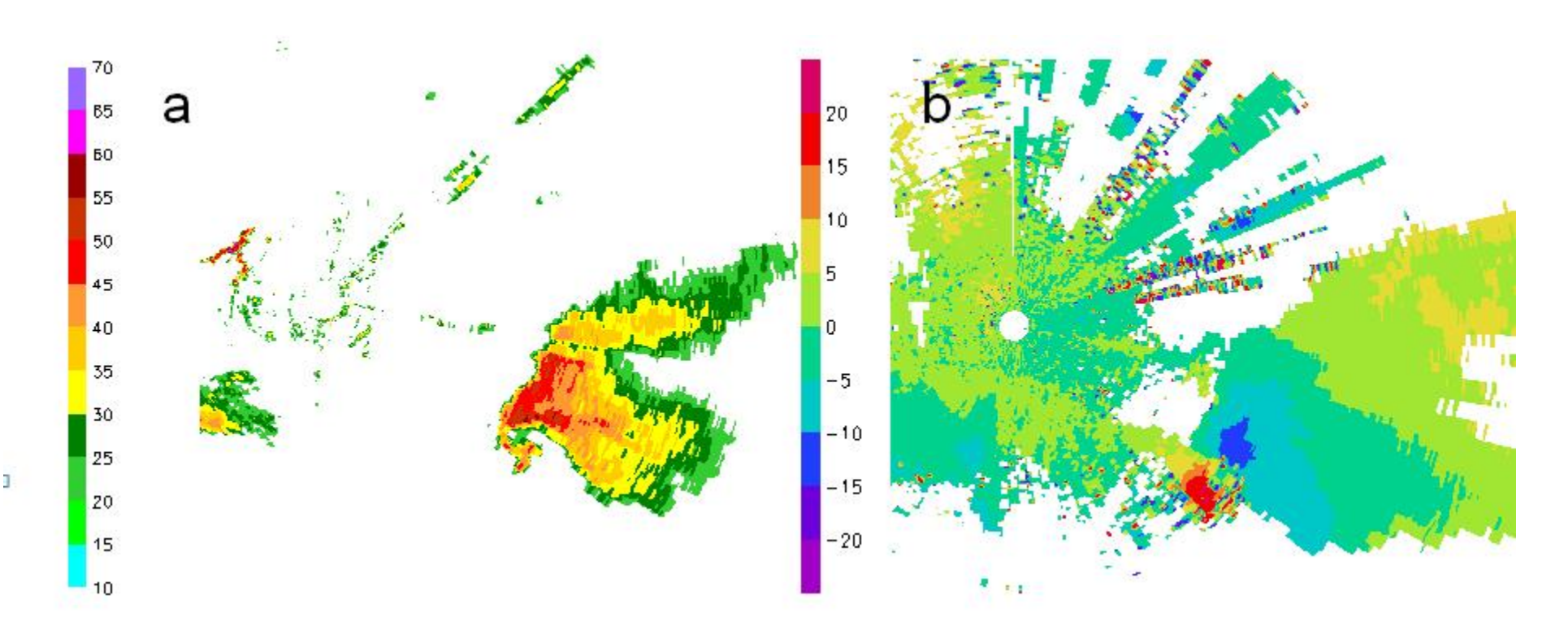






Supercell - convective storm with deep and persistent mesocyclone

May 31, 2005, supercell storms in Beijing



MESOCYCLONE CORE WARNING CRITERIA

(Operator Defined)

- Shear
 - Distance between max inbound and max outbound ≤ 5 nm
 - Rotational velocity (Vut + |Vin|) / 2

SEVERE THUNDERSTORM WARNING if minimal mesocyclone is recognized (use diagram).

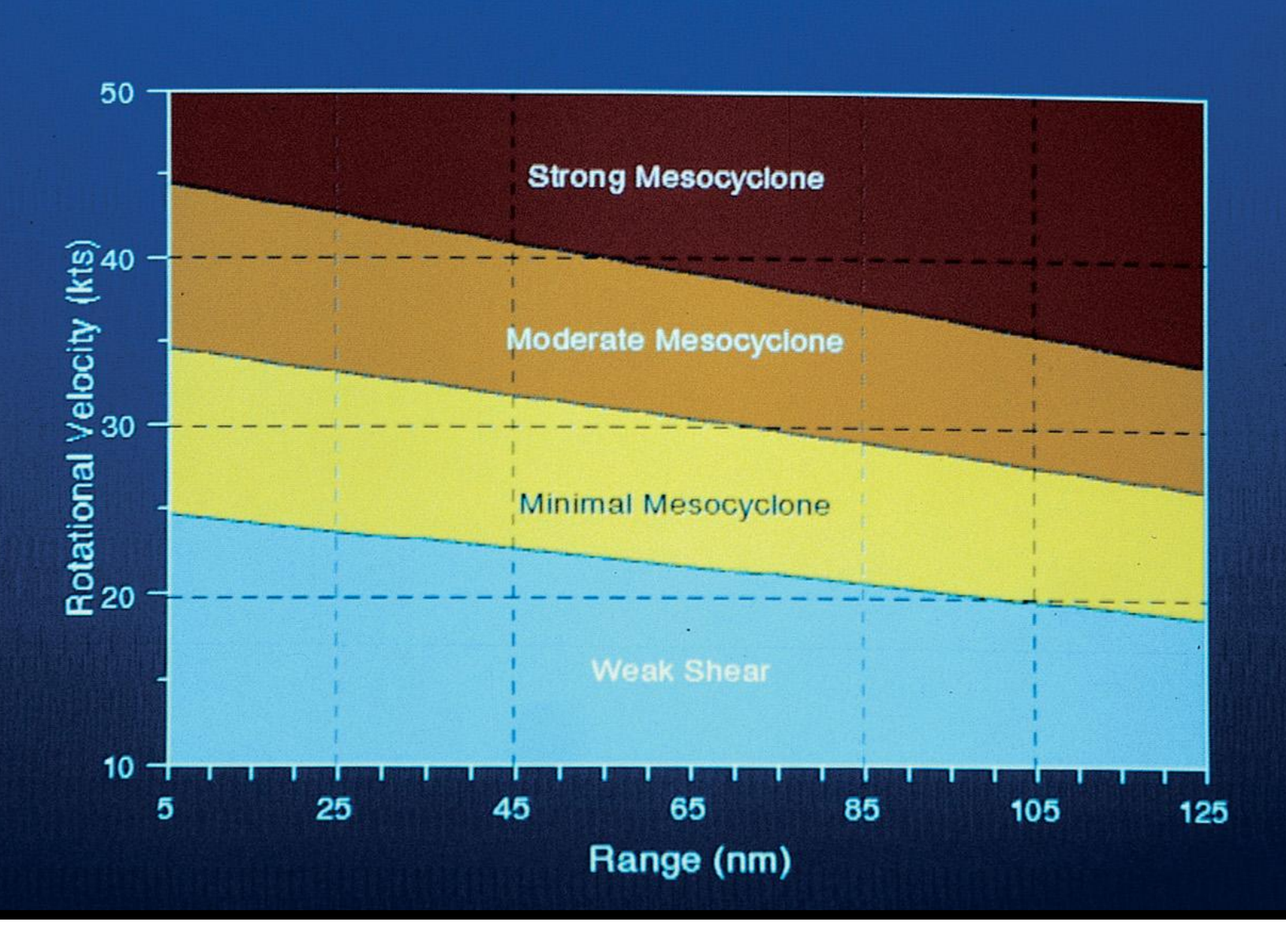
TORNADO WARNING if strong mesocyclone is recognized (use diagram).

MESOCYCLONE CORE WARNING CRITERIA (cont) (Operator Defined)

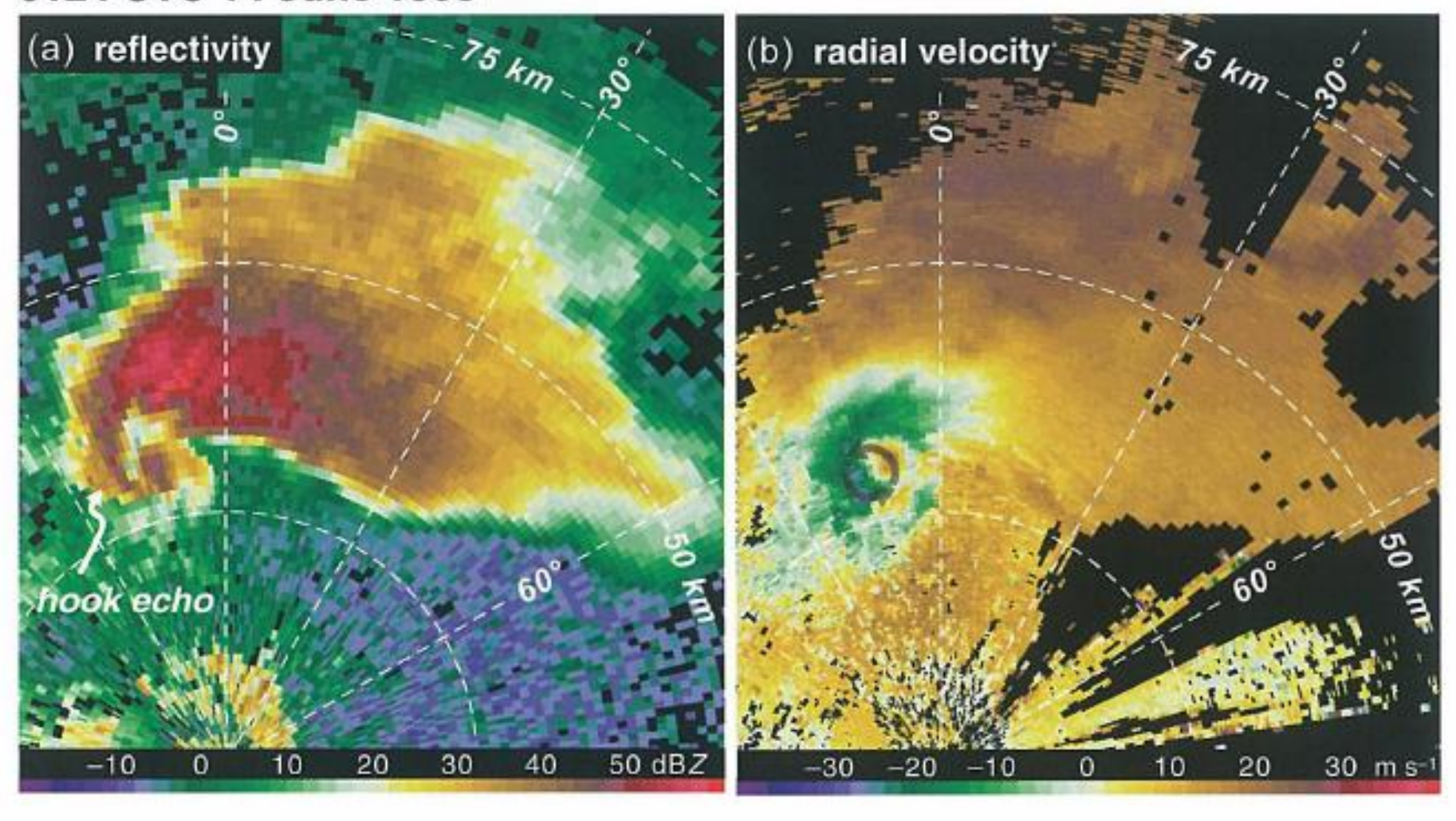
- Vertical Extent
 - Shear extends at least 10,000 ft in the vertical
- Persistence
 - Rotational signature persists for at least two volume scans

CAUTION: These are guidelines based on Oklahoma statistics. Other factors must also be taken into consideration when making warning decisions.

Mesocyclone Recognition Criteria



0124 UTC 14 June 1998





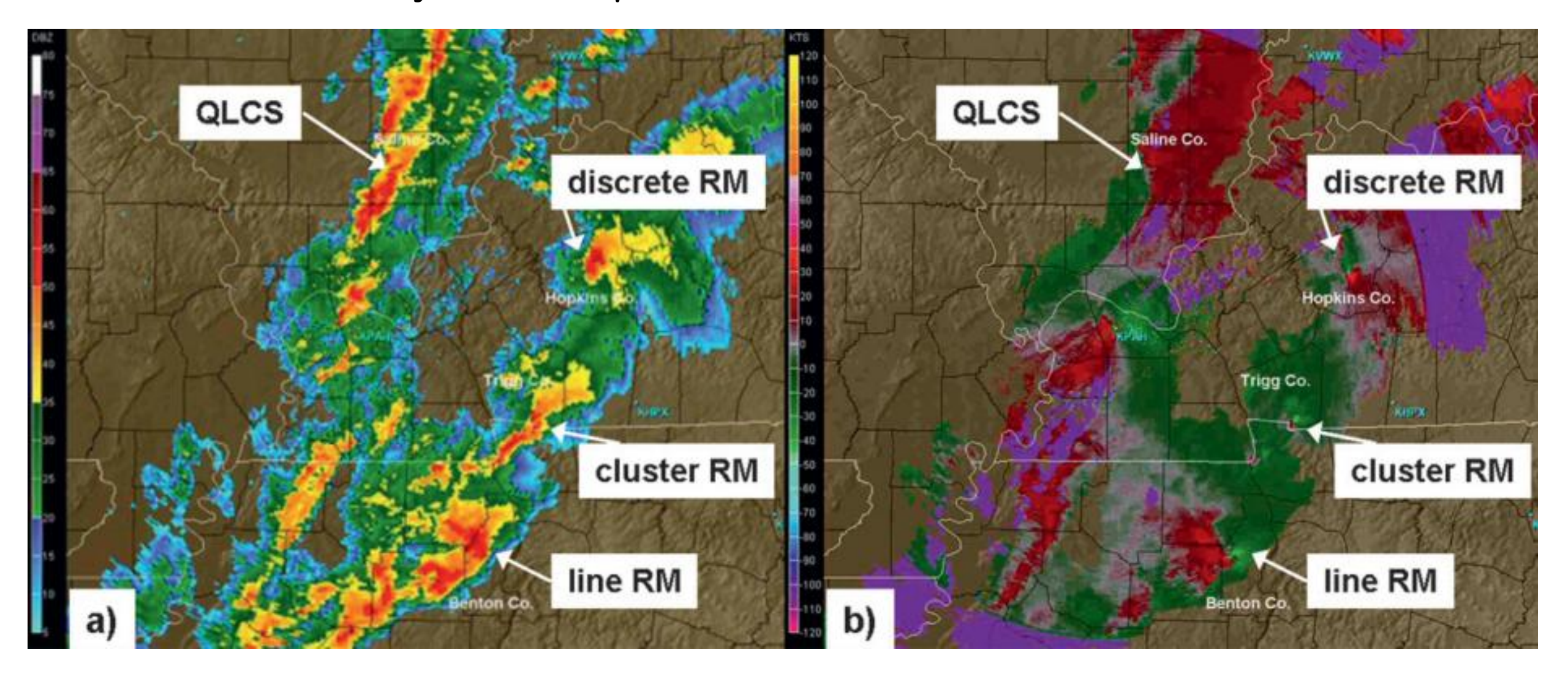
Convective Modes Classification 01

- discrete right-moving supercell (RM) —storms accompanied by deep, persistent
 mesocyclones, generally characterized by ≥20 kt (10 m/s) rotational velocity at
 most ranges, and distinct from surrounding echoes at ≥ 35 dBZ; 249 events (34%);
- quasi-linear convective system (QLCS)—contains contiguous reflectivities >35
 dBZ for a length ≥ 100 km at ≥ 3/1 aspect ratio; nonsupercellular; includes storms
 embedded in lines; 21 events (3%);
- cluster—as with QLCS, but with an aspect ratio <3 /1; nonsupercellular; included disorganized and/or amorphous reflectivity patterns; 25 events (3%);
- supercell in line—meets velocity and continuity guidelines for supercells but is embedded in a QLCS; 70 events (10%);
- supercell in cluster—meets velocity and continuity guidelines for supercells but is embedded in a cluster; 257 events (35%);

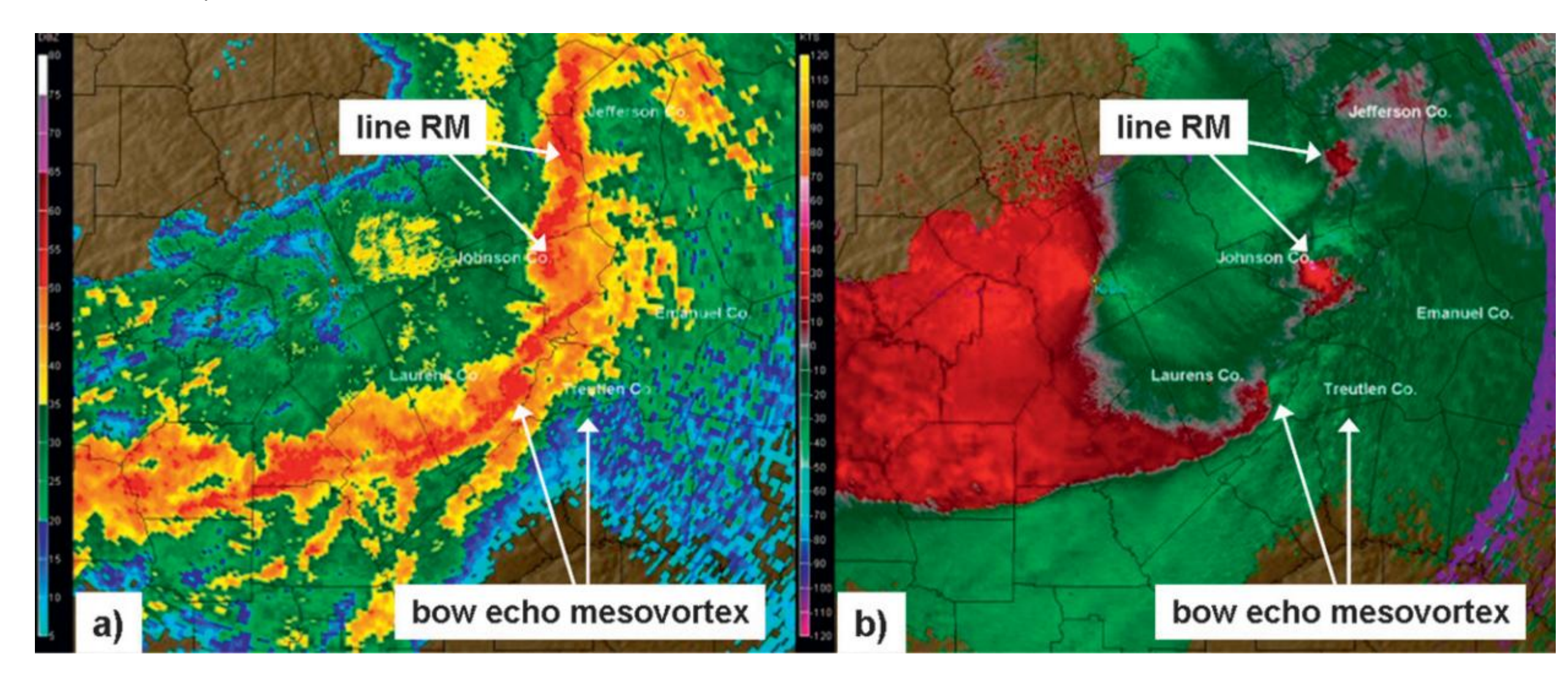
Convective Modes Classification 02

- discrete nonsupercell—lacks horizontal rotation, or rotational characteristics are too weak and transient to classify even as "marginal" (below); 13 events (2%);
- marginal discrete supercell—shows at least brief, weak rotational characteristics but not fulfilling supercellular guidelines; 19 events (3%);
- marginal supercell in cluster; 37 events (5%);
- marginal supercell in line; 7 events (1%);
- cell in cluster, nonsupercellular; 26 events (4%);
- The three unambiguously supercellular categories (discrete, in line, in cluster)
 were analyzed separately and as a subgroup for this study.
- Nonsupercell TC (NSTC) tornadoes likewise were examined in terms of their classified modes (e.g., clustered, linear, marginal supercell), distance from TC center, and as a second subgroup.
- Continuous spiral bands or segments of bands are treated as QLCSs if they meet the aforementioned mode criteria.

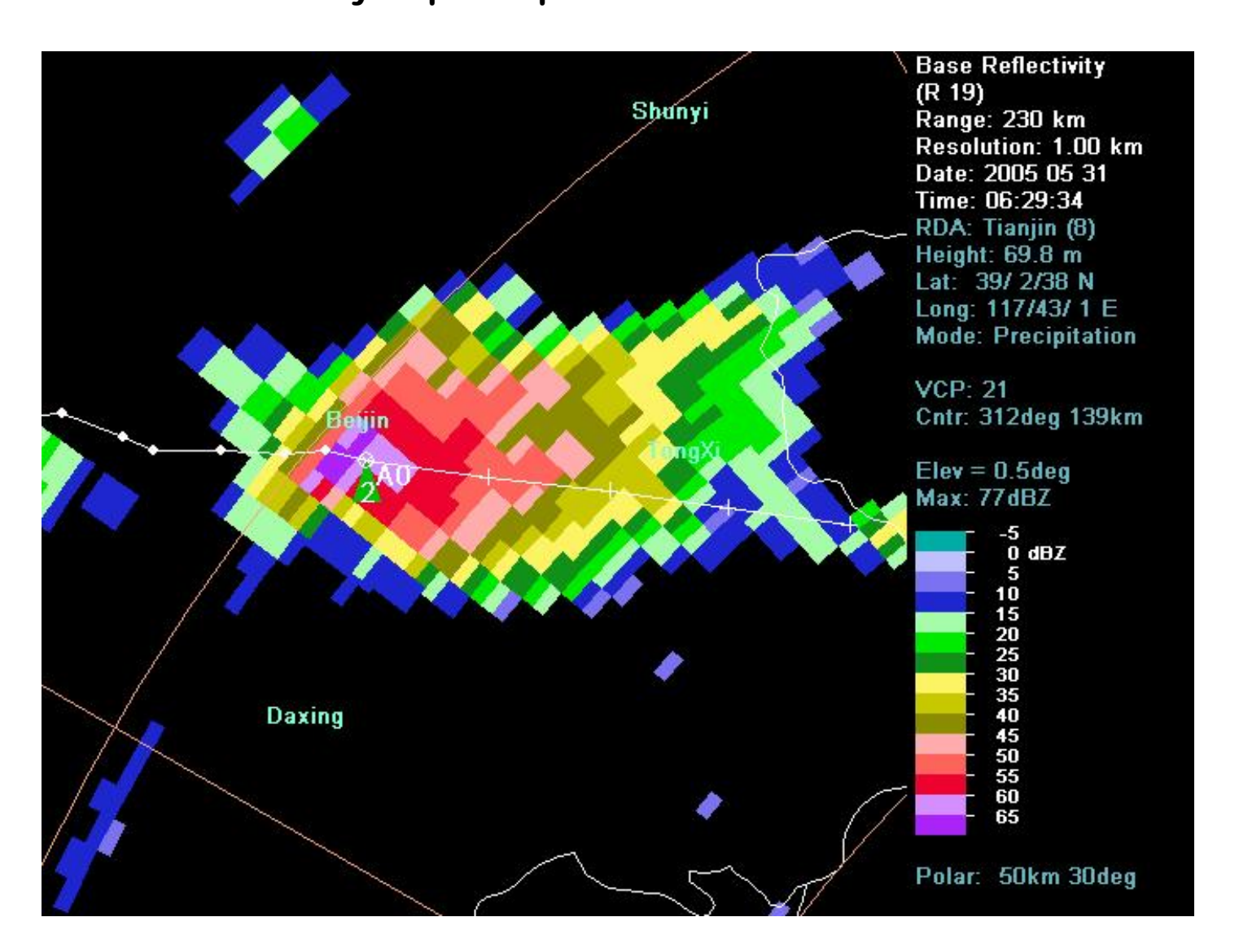
Discrete cell, cell in cluster and cell in line: 2005 11 15 21:32 UTC Paducah, KY (KPAH) WSR-88D 0.5° beam tilt reflectivity and SRM maps.



Cell in line. 2008 05 11 10:57 UTC Robins AFB, GA (KJGX) WSR-88D 0.5° beam tilt reflectivity and SRM maps.

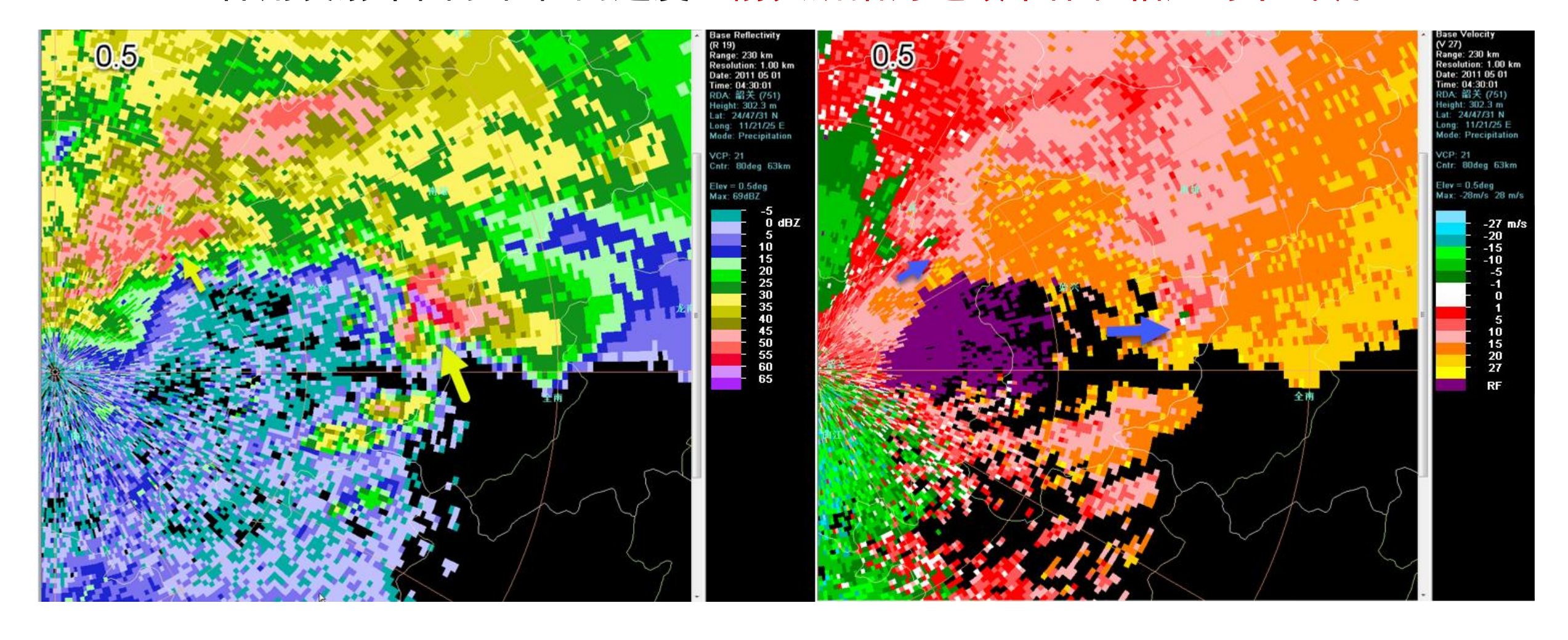


Discrete cell: 2005 05 31 14:29 BJT Tanggu (Tianjin) SA radar 0.5° elevation reflectivity superimposed with STI and HI.

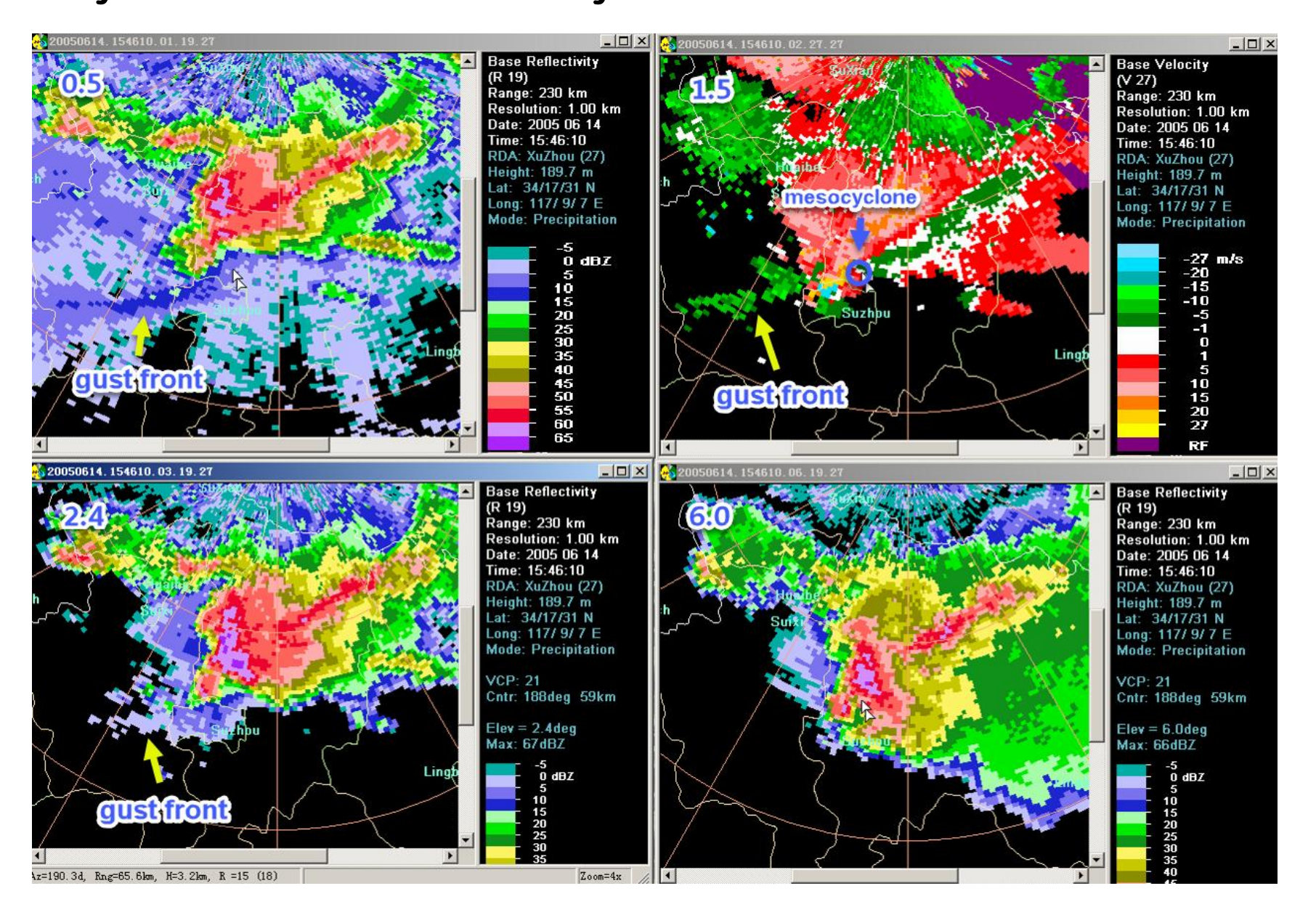


Discrete cell and Cell in Cluster: 2011 05 01 04:30 BJT 韶关SA雷达

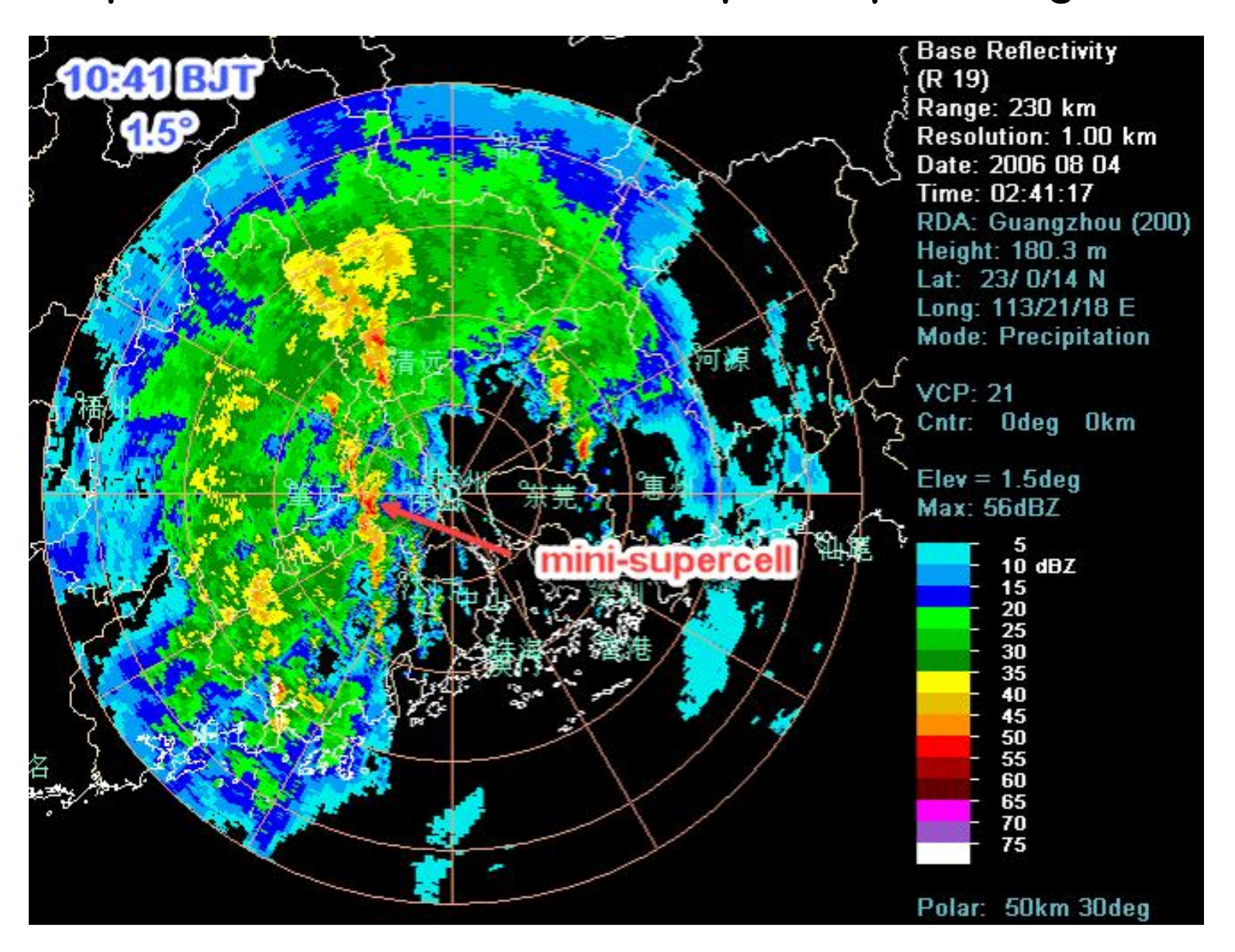
0.5° 仰角反射率因子和径向速度(箭头所指为超级单体和相应的中气旋)



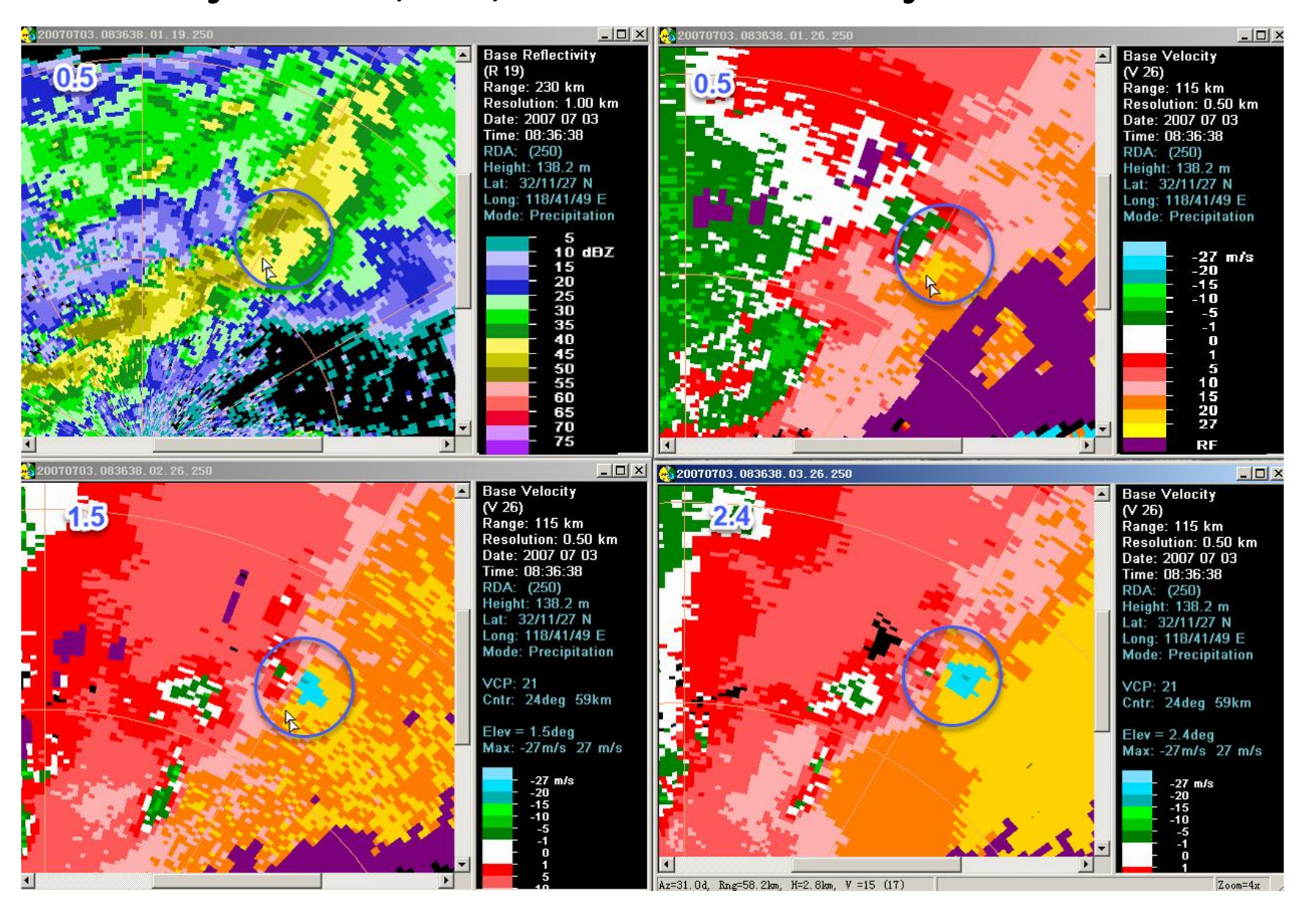
Cell in cluster: 2005 06 14 23:46 BJT Xuzhou SA radar 0.5°, 2.4°, 6.0° elevation reflectivity and 1.5° elevation velocity.



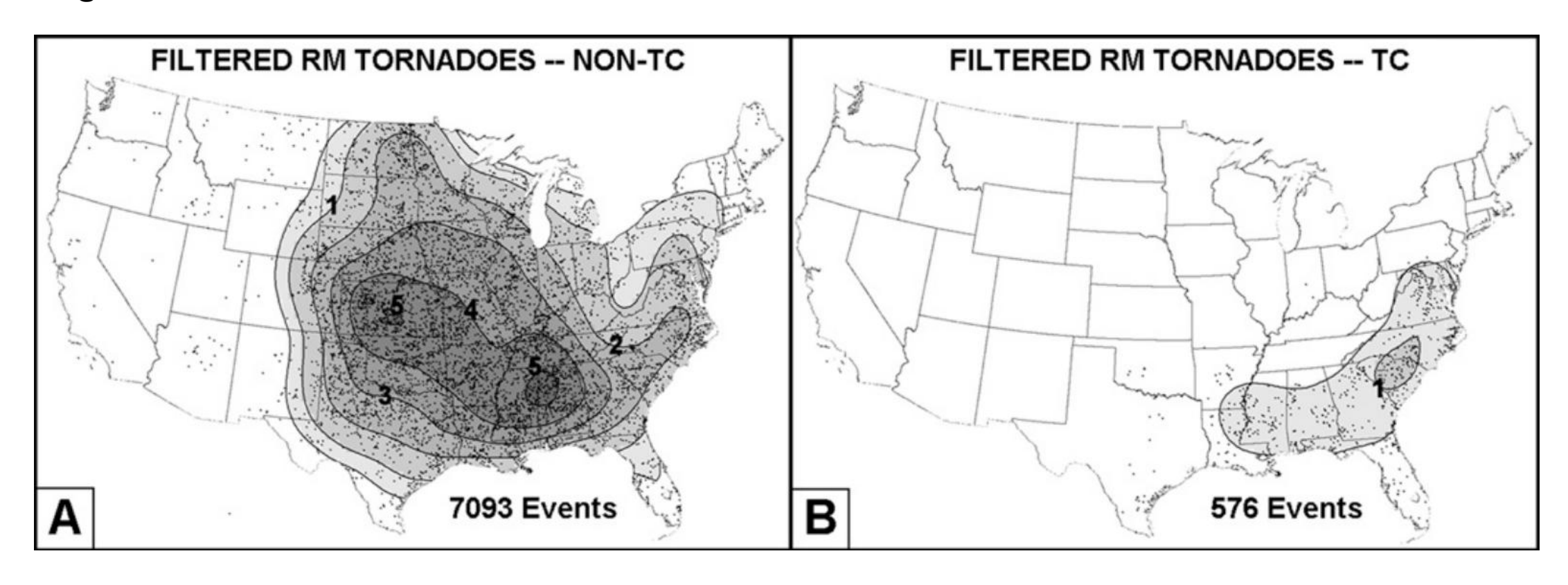
Cell in line: 2006 08 04 10:41 BJT Guangzhou SA radar 1.5° elevation reflectivity, the red arrow points to the embodied mini-supercell producing the tornado.



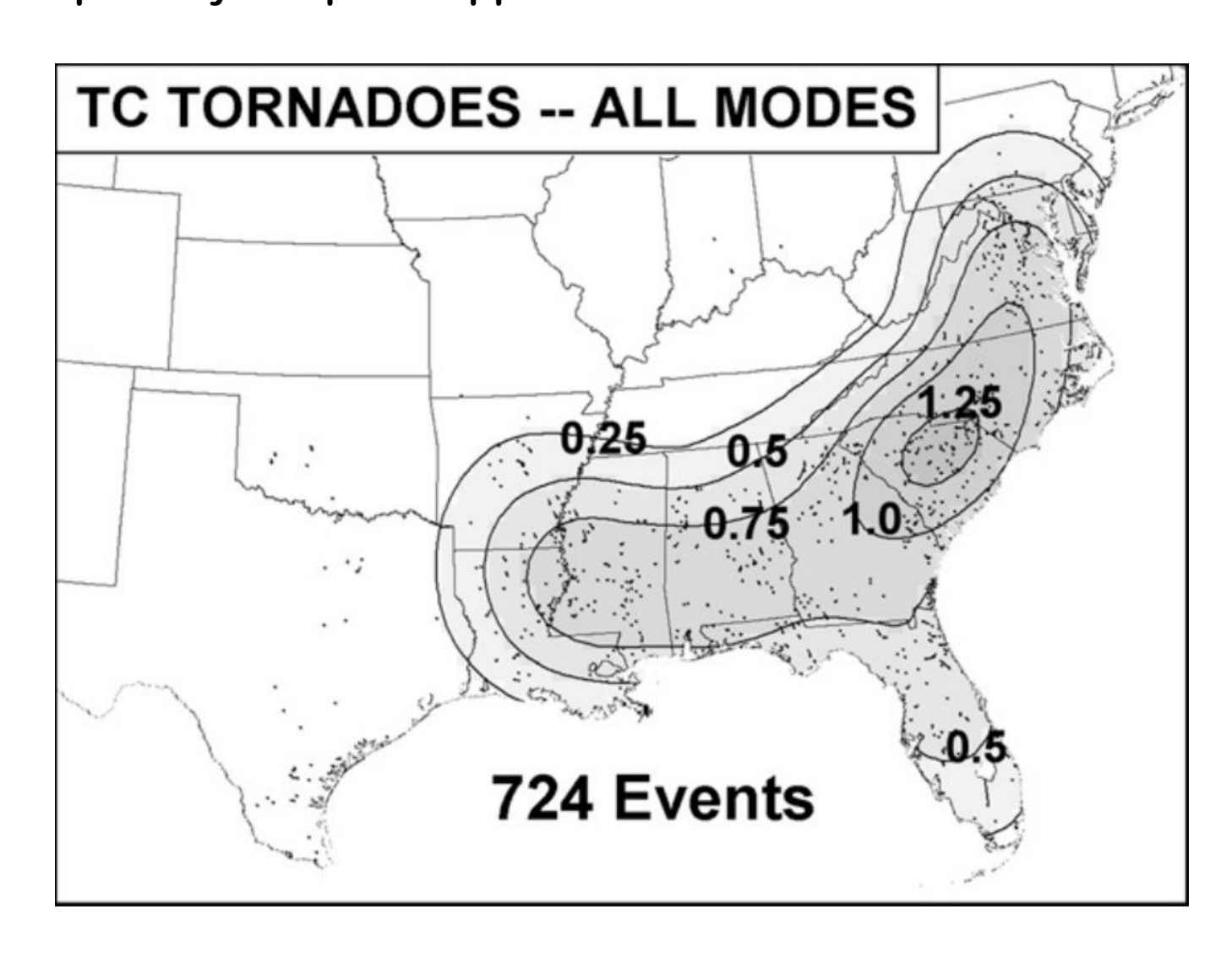
Cell in line: 2007 07 03 16:36 BJT Nanjing SA radar 0.5° elevation reflectivity and 0.5°, 1.5°, 2.4° elevation velocity.



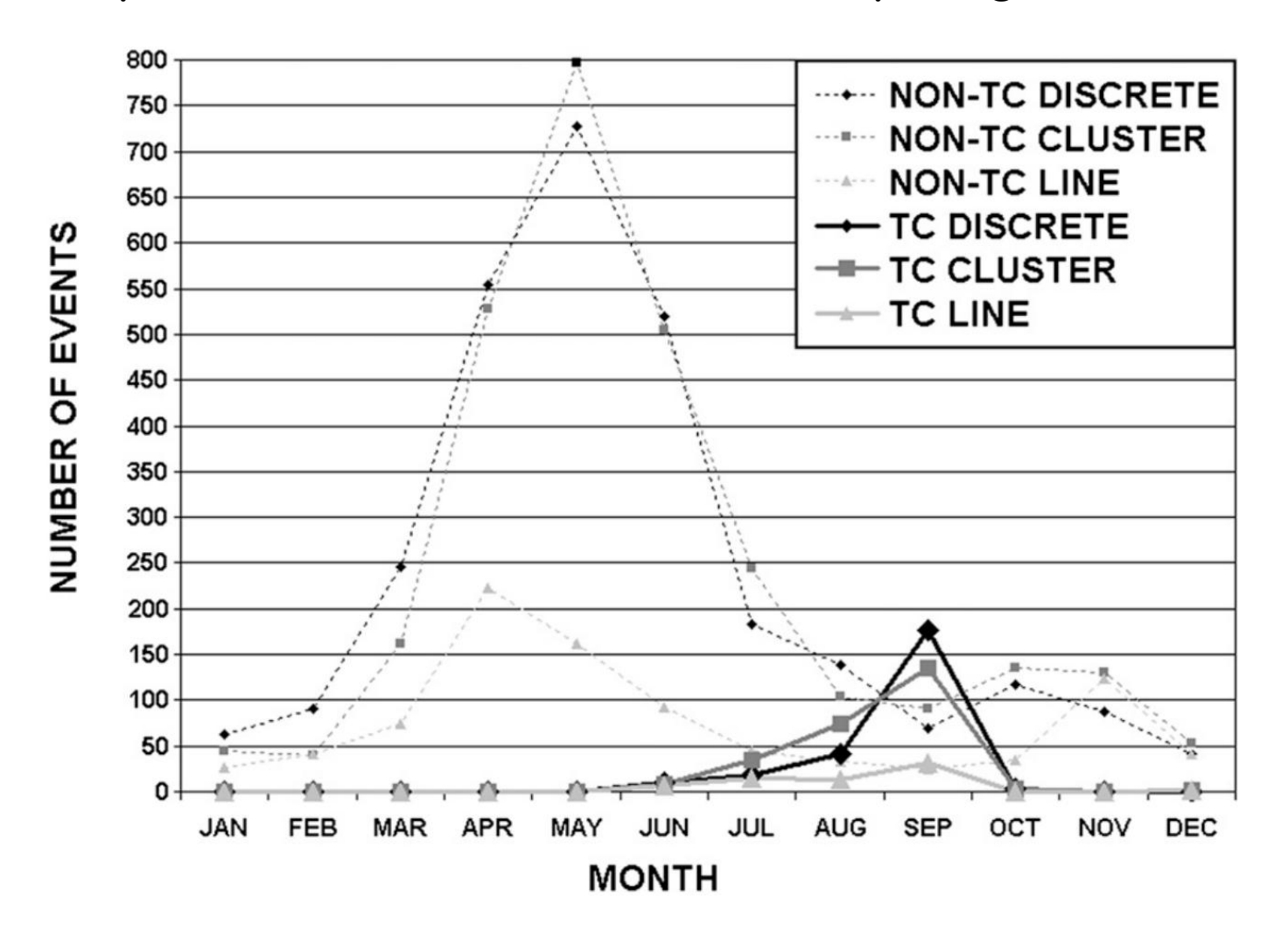
Kernel density estimate on a 40 km \times 40 km grid of filtered, continental U.S. tornado events in right-moving (RM) supercell modes: (a) non-TC in origin and (b) from TCs only. Sample sizes are given for each. Minimum contour is 0.5 events per 10 yr estimate based on 2003–11 data. Labeled contours begin at 1 event per 10 yr. Black dots represent events that formed the basis of the kernel density estimate, and the progressively darker gray fill represents a higher event estimate.



As in Figure b in the previous slide, but for all convective modes. Minimum contour is 0.25 events per 10 yr, based on 2003–11 data. Labeled contour intervals are 0.25 events per 10 yr. Map is cropped to affected areas of the United States.



Monthly graph of tornadic supercells, cumulatively for 2003–11, in three modes: discrete, embedded in a cluster, and embedded in a line. Dashed curves denote non-TC supercells; solid curves are TC events, per legend.



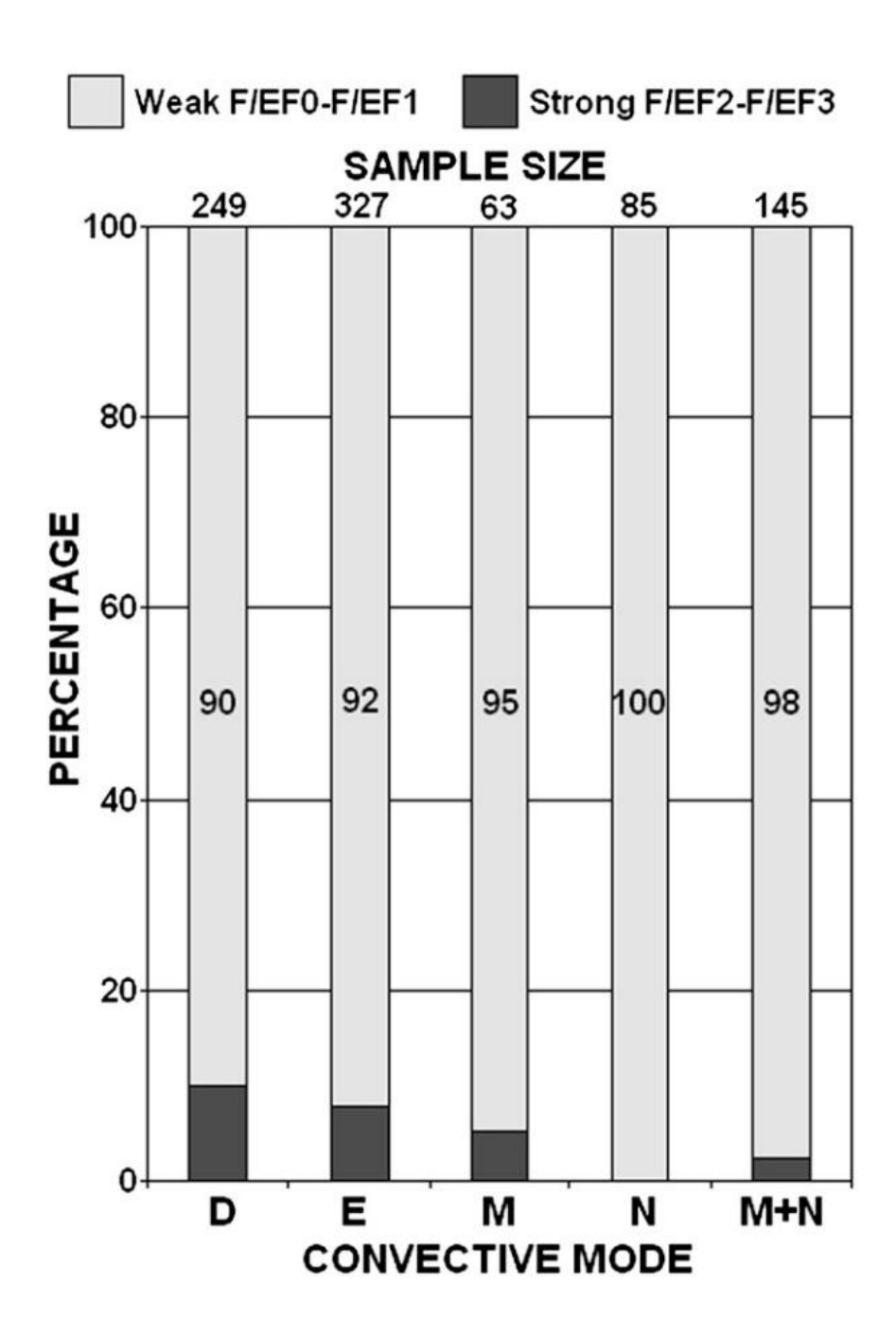
Tornadic supercells in TCs collectively accounted for 64% of all tornadic supercells in the conterminous United States during the month of September (2003–11), with the caveat that the two most prolific TC tornado seasons on record (2004 and 2005) are part of the analysis.

During an otherwise subdued interval from late summer into early autumn, the predominant source of supercell tornadoes nationally was the TC.

Overall, the gridfiltered number of TC tornado events in this 2003–11 dataset (730) was 7.3% of the number of gridfiltered non-TC tornado events (10023) or \approx 6.8% of the nationwide tornado event total (10753).

Storm-mode Analyses

- Of the storms responsible for TC tornadoes, 576 (79%) were unambiguously supercellular, 63 (9%) marginally supercellular, and the remaining 91 (12%) nonsupercellular.
- Among just the tornadic TC supercells, mesocyclone strength was classified as strong with 78 (14%), moderate with 134 (23%), and weak with 364 (63%).
- Thus, weak (strong) mesocyclones were far more (less) common with TC than nonTC events. The values for non-TC tornadic supercells from the corresponding dataset were 3077 (43%) strong, 1855(26%) moderate, and 3161 (30%) weak.
- Weak mesocyclones tended to be slightly more common in nondiscrete TC supercells (67%) compared to discrete (58%), while strong mesocyclones somewhat favored discrete supercell storms(16%) versus nondiscrete supercells (11%).
- In non-TC situations, nondiscrete supercells also carried a slightly higher percentage of weak mesocyclones (34%) than discrete supercells (30%).



Percentages of weak and strong tornadoes per mode bin, as labeled: D is discrete supercell, E is embedded supercell (collectively, all supercells in lines plus supercells in clusters), M is marginal (subcriteria) supercell, N is nonsupercell, and M+N combines all modes not meeting supercell criteria. Percentages of weak tornadoes are given in black integers, on bars. Sample size for each mode is given above each bar.

Only 54 (7%) of all TC tornado events overall were rated strong (EF2 or EF3). Strong tornadoes were far more common with supercells than with marginal or nonsupercells, and constituted a slightly higher share of tornadoes with discrete versus nondiscrete supercells. No NSTC tornadoes exceeded an EF1 rating.

Fraction of 2003–11 tornado damage rating occurrence for TCs and non-TC supercells.

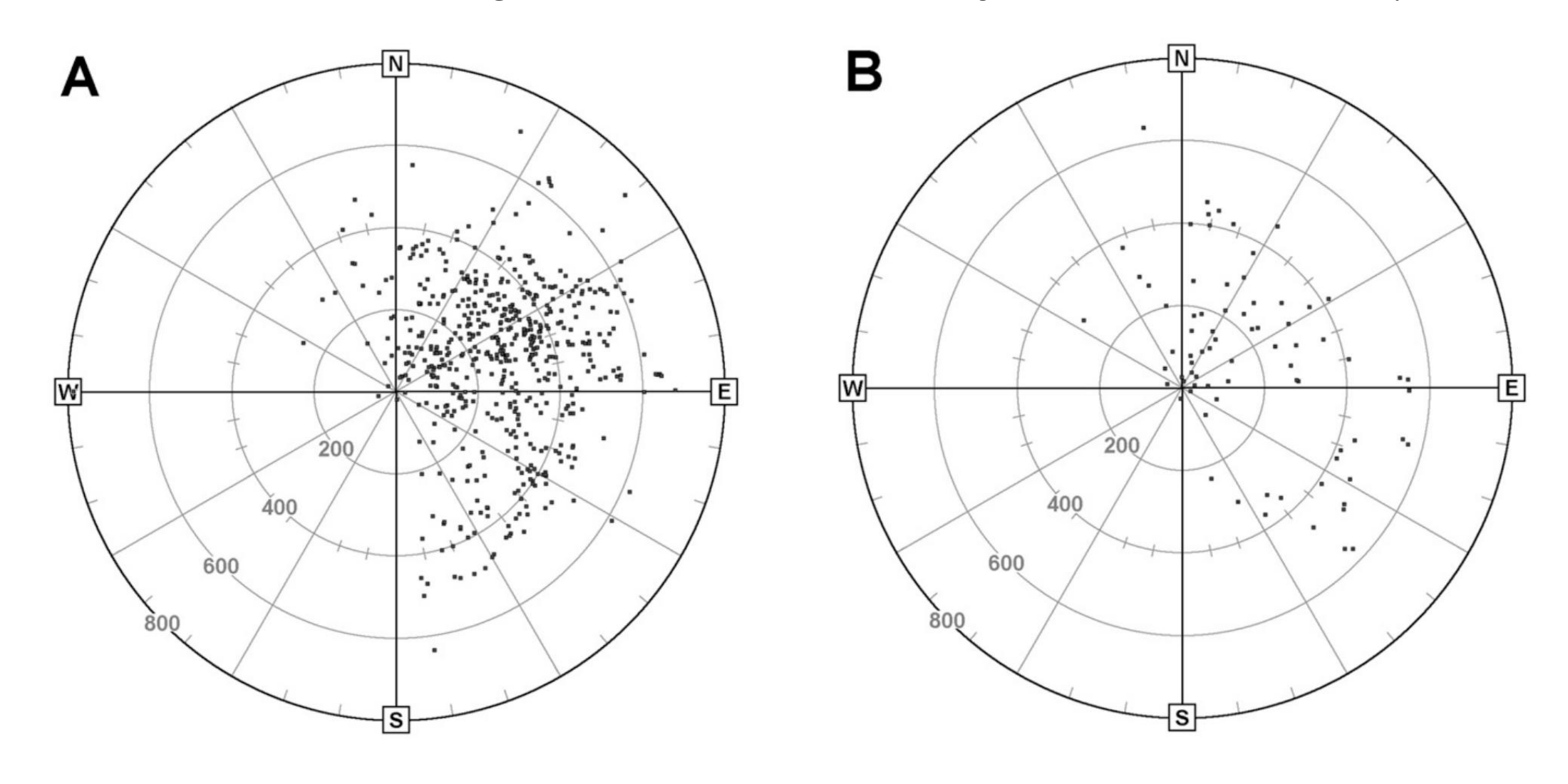
Damage (F/EF category)	TC	Non-TC
≥4	0.00	0.01
3	0.01	0.05
2	0.08	0.12
1	0.33	0.30
0	0.58	0.53

Comparisons of damage ratings with mid-latitude, non-tropical tornadic supercells (Table above) indicate that significant (≥EF2) tornadoes are somewhat more common with non-TC supercells, but not as much as the aforementioned difference in mesocyclone strength suggests.

As shown in next slide, NSTC tornadoes tended not only to yield weaker ratings than their supercellular counterparts, but also to occur closer to TC centers. The mean and median radii of NSTC tornadoes from center were 302 and 287 km, respectively, contrasted to the mean and median ranges for supercellular tornadoes of 341 and 342 km.

The supercell TC tornado distribution also stretched farther southward, largely because of both discrete and embedded supercells aligned with outer, trailing spiral bands.

The TC center-relative plots of 2003–11 TCTOR whole-tornado records (dots) corresponding to modal events classified as (a) fully supercellular and (b) nonsupercellular. Marginal supercells are not plotted. Events appear with respect to north-relative azimuth (tick marks and full radials at 10° and 30° intervals, respectively) and range (km as labeled) from center position, at the time of each tornado. Due to scaling effects, some tornadoes may obscure others in each panel.



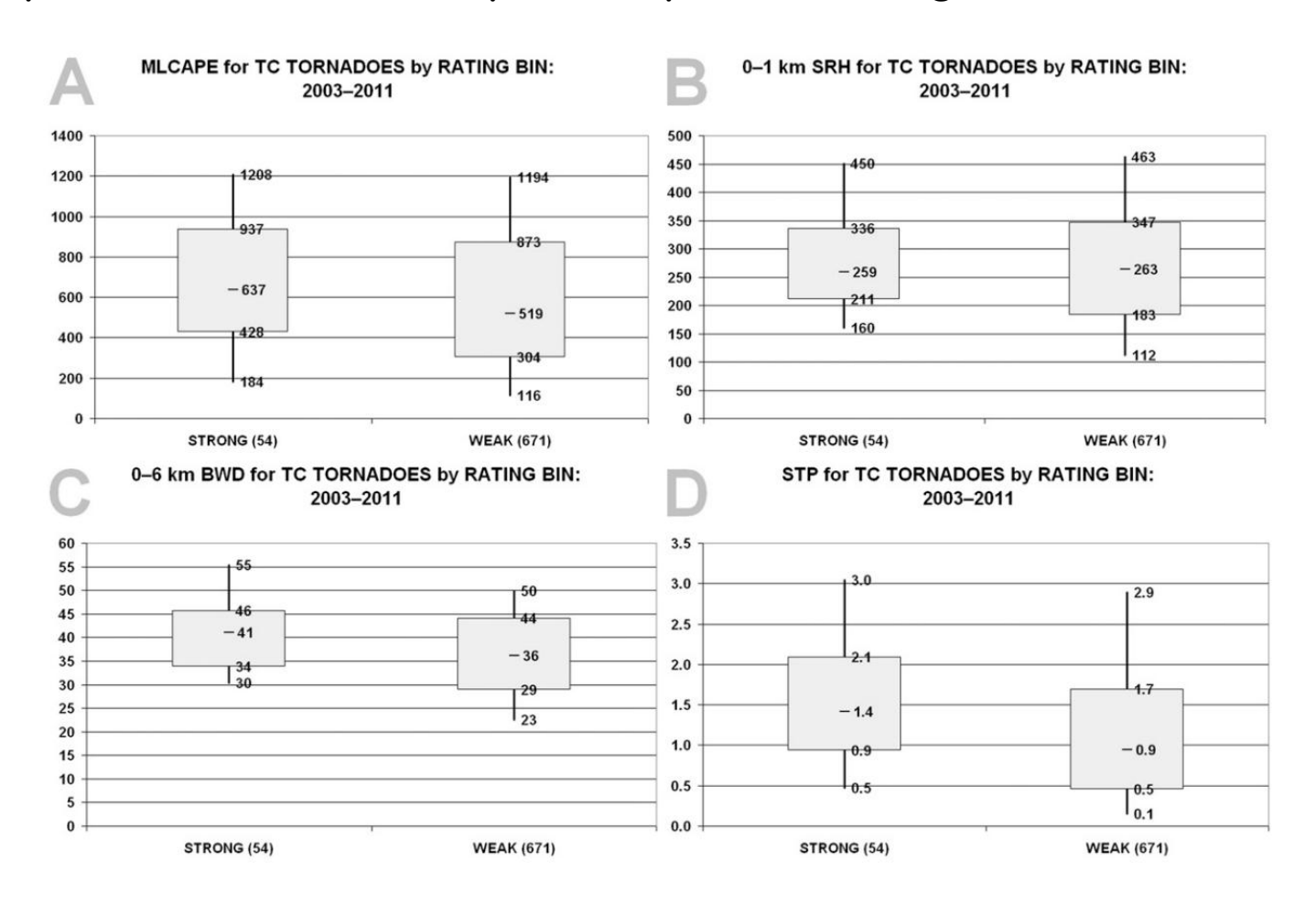
Environmental Results

- The main factor differentiating TC from non-TC tornado environments is much greater deep-tropospheric moisture, associated with reduced lapse rates, lower CAPE, and smaller and more compressed distributions of parameters derived from CAPE and vertical shear.
- For weak and strong TC tornado categories (EF0–EF1 and EF2–EF3 on the enhanced Fujita scale, respectively), little distinction is evident across most parameters.
- Supercellular TC tornadoes are accompanied by somewhat greater vertical shear than those occurring from other modes. Tornadoes accompanying nonsupercellular radar echoes tend to occur closer to the TC center, where CAPE and shear tend to weaken relative to the outer TC envelope, though there is considerable overlap of their respective radial distributions and environmental parameter spaces.

Some Abbreviation

- MLCAPE: lowest 100-hPa mean mixed layer (ML) CAPE
- MUCAPE: most unstable (MU) parcel CAPE
- EBWD: effective bulk wind difference (Thompson et al. 2007)
- BWD: bulk wind difference
- SRH: storm-relative helicity
- STP: fixed layer significant tornado parameter (Thompson et al. 2003).
- STP =(MLCAPE / 1000 J kg⁻¹)*(0-6 km vector shear / 20m s⁻¹)*(0-1 km SRH/100 m²s⁻²)
 ((2000 -MLLCL)/1500m)((150 MLCIN) /125 J kg⁻¹)
- SCP: supercell composite parameter
- SCP = $(MUCAPE / 1000 \text{ J kg}^{-1}) * (0-3 \text{ km SRH} / 150 \text{ m}^2\text{s}^{-2}) * (BRN denominator / 40 m}^2\text{s}^{-2})$
- BRN denominator = $0.5(\Delta u)^2$, Δu is defined to be the difference between the density weighted wind vector taken over the lowest 6km of the wind profile and an average surface wind vector taken over the lowest 500m of the profile.
- LR: Lapse rate

Box-and-whiskers diagrams, where percentile extents and corresponding values represent 25th–75th for boxes, 10th–90th for whiskers, and 50th at the inbox bar, for (a) MLCAPE (J kg⁻¹), (b) 0–1-km AGL SRH (m² s ⁻²), (c) 0–6-km AGL EBWD (kt), and (d) significant tornado parameter (fixed layer). Abscissa labels include sample size in parentheses; ordinate represents parameter magnitude.

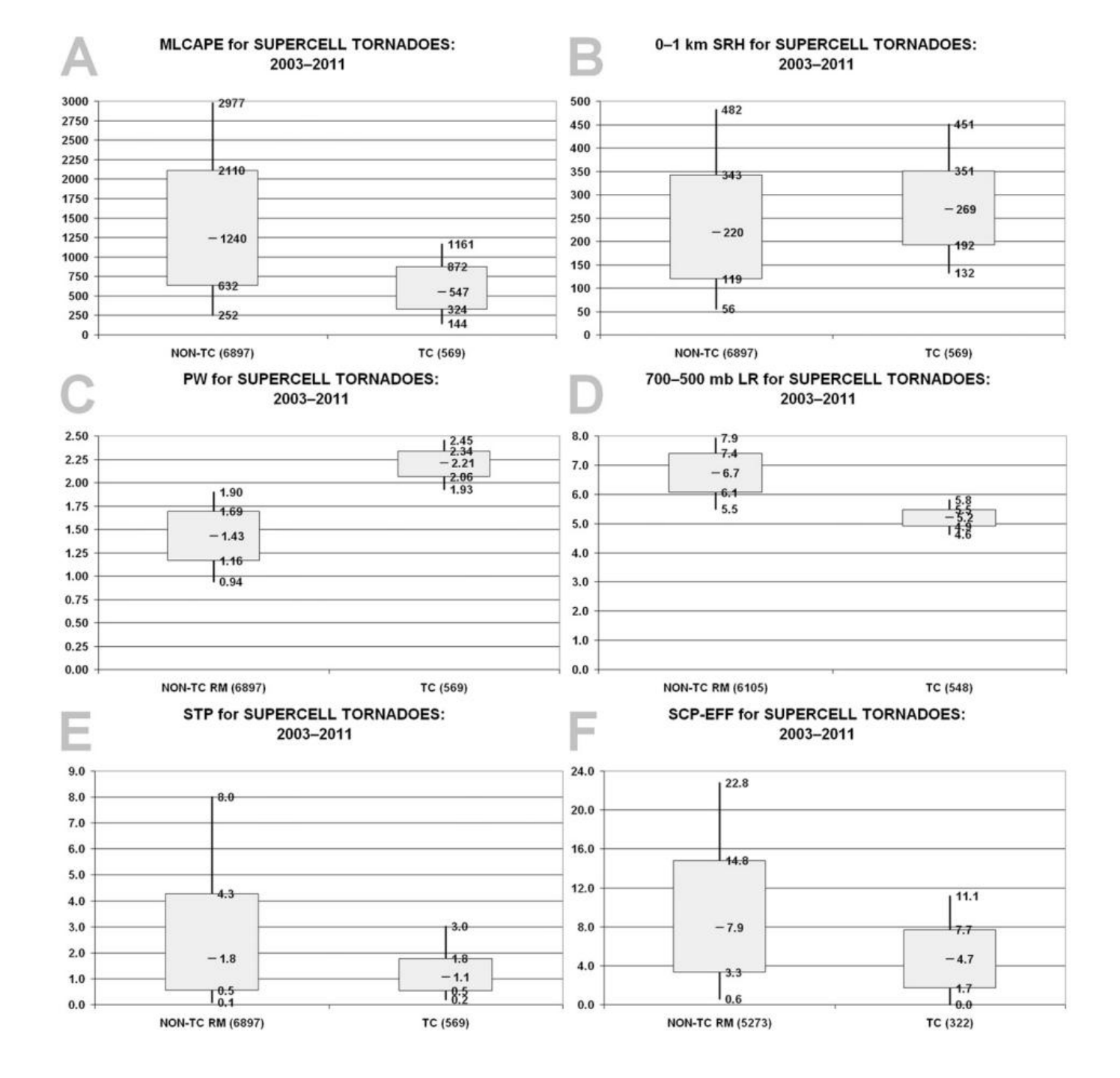


Values for the strong tornadoes tended to be somewhat larger for MLCAPE, fixed-layer BWD, and STP, but with considerable overlap. By contrast, the entire 10th–90th percentile range for 0–1-km SRH fit within the same distribution for weak tornadoes.

Some compression of the middle 50% of the distributions also was evident in most variables and parameters for strong TC tornadoes; It is unknown if this is a function of actual meteorological distribution or of the sample size being an order of magnitude smaller for strong tornadoes.

Box-and-whiskers diagrams, where percentile extents and corresponding values represent 25th–75th for boxes, 10th–90th for whiskers, and 50th at the inbox bar, for the following parameters in TC and non-TC tornadic supercell datasets:

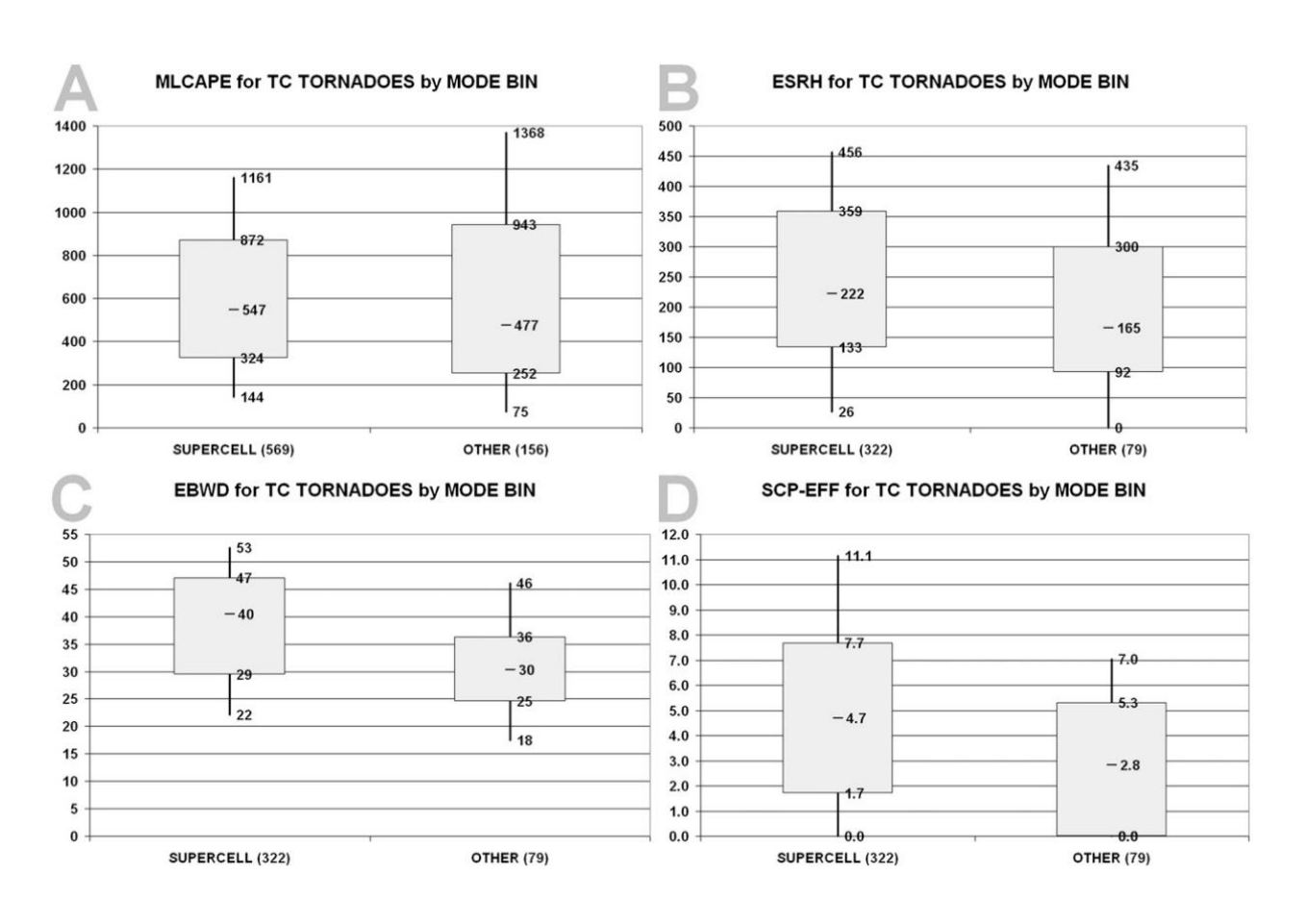
- (a) MLCAPE ($J kg^{-1}$),
- (b) $0-1-km AGL SRH (m^2 s^{-2}),$
- (c) precipitable water (in.),
- (d) 700–500-hPa lapse rate (°C km⁻¹),
- (e) significant tornado parameter (fixed layer),
- (f) supercell composite parameter (effective layer).



Some facts from the previous slide

- Environmental parameters previously examined for mid-latitude, supercellular tornado environments were analyzed for the TC cases, and compared with up to 6897 non-TC tornado events associated with right-moving supercells.
- Similarly to the intensity category analyses, the smaller sample sizes of the TC subset is associated with compression in the quartile distributions.
- In general, thermodynamic variables (e.g., Fig. a) differentiated the tropical and nontropical tornado environments better than the kinematic ones.
- Shear-based parameters for TC events did show slightly tighter distributions on the margins (exemplified by 0–1-km SRH in Fig.b), but otherwise were similar to their non-TC counterparts.
- The primary difference between midlatitude and TC tornado situations in this study centers on moisture, as indicated by total precipitable water (PW; Fig. c). The 10th percentile of the PW distribution for TCs exceeded the 90th percentile for nontropical tornadoes, with the middle 50% being well separated. This reflects the characteristic thermodynamic environment of TCs, which are very rich indeep-tropospheric moisture.
- TC supercell environments were decidedly weaker in middle-level lapse rates (e.g., Fig. d), which contributed to smaller overall CAPE and a more compressed distribution of the latter (e.g., Fig. a).
- This extended to composite parameters such as SCP and STP (Figs. e,f) that substantially incorporate CAPE as part of their formulation.

Box-and-whiskers diagrams, where percentile extents and corresponding values represent 25th–75th for boxes, 10th–90th for whiskers, and 50th at the inbox bar, for the following parameters in TC supercells and in the remainder of TC tornadic storm modes ("other"): (a) MLCAPE (J kg⁻¹), (b) effective SRH (m² s ⁻²), (c) EBWD (kt), (d) supercell composite parameter (effective layer).



Most kinematic and thermodynamic variables, along with the STP, exhibited little if any meaningful discrimination between supercells and the other modes (e.g., Figs. a,b). Exceptions (Figs. c,d) were noted in the distributions of the EBWD (Thompson et al. 2007) and, in turn, the effective-layer version of the SCP, given the latter's dependence on EBWD.

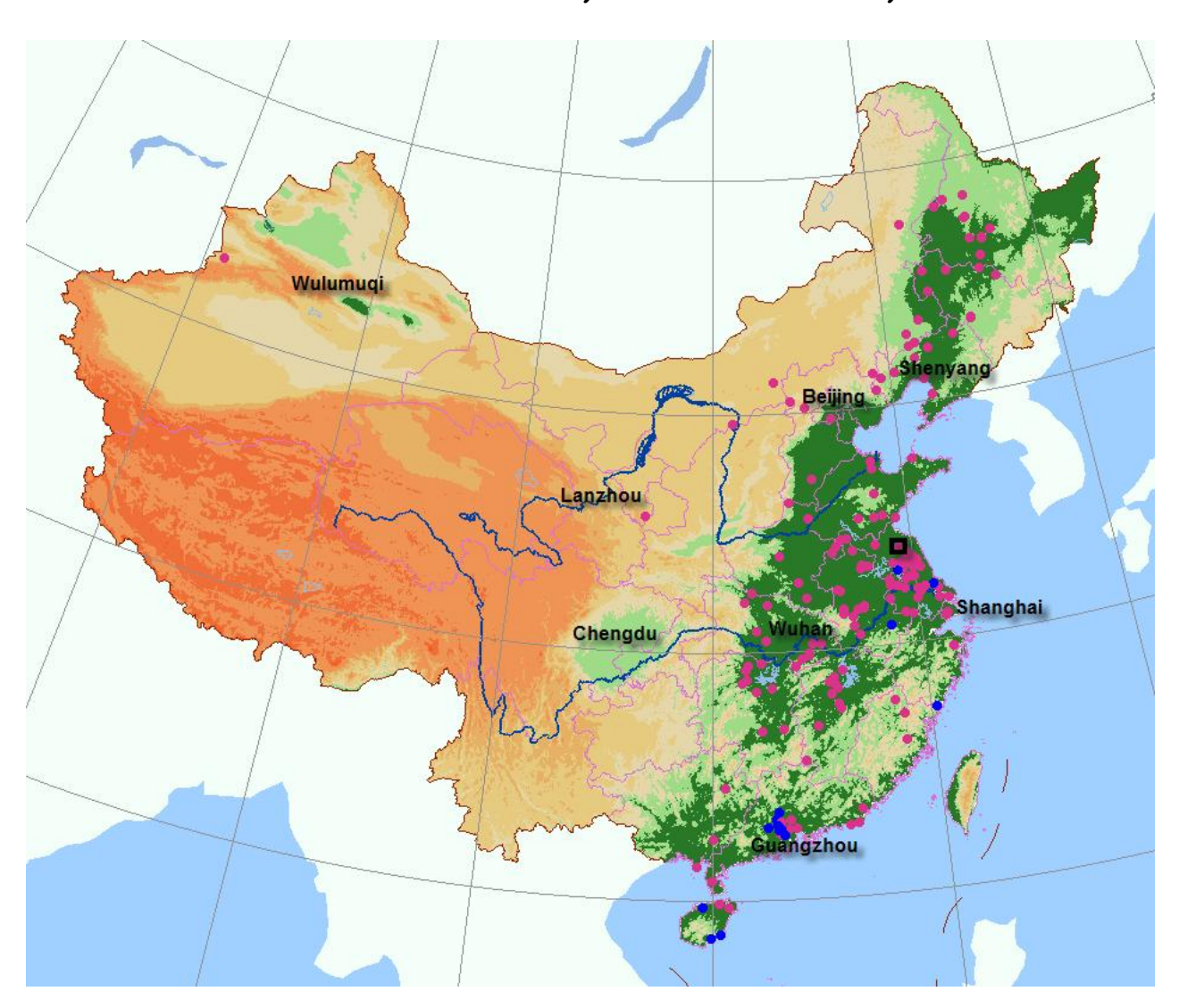
Summary (Edwards et al.,2012)

- Examination of associated storm modes indicates that TC tornadoes are far more common with supercells, with a steadily greater potential for stronger (EF1 and EF2) events as convective organization goes from nonsupercell to discrete supercell.
- However, the mesoscale environments of strong and weak tornadoes in TCs often are very similar, based on the results of this study.
- The great relative abundance of moisture in the TC setting, far more so than kinematic measures, seems to account for most of the difference between TC and midlatitude tornado environments.

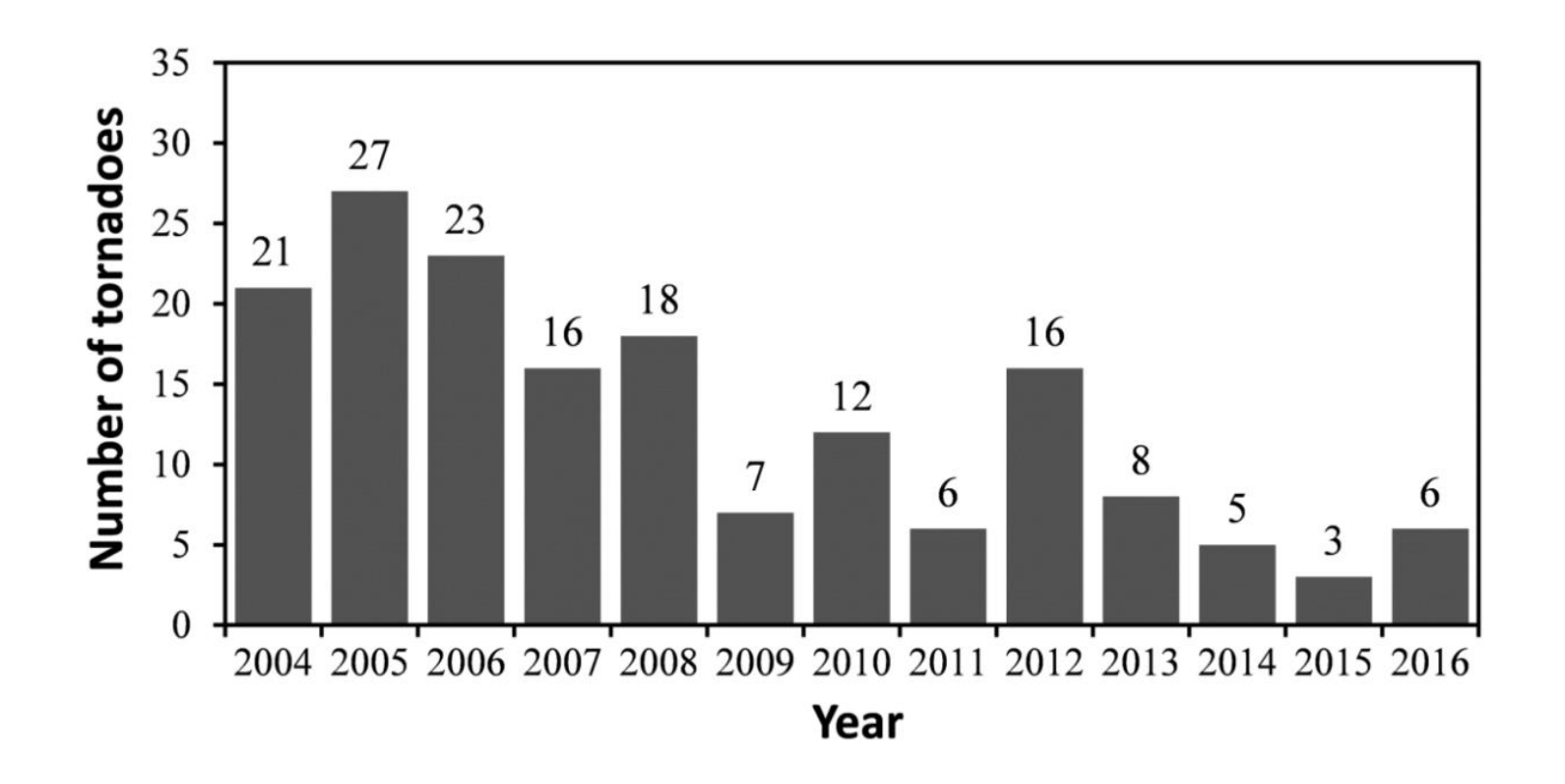
Climatology of tropical cyclone tornadoes in China(2006-2018)

- Based on the work of Bai et al., 2020;
- Climatological statistics for TC tornadoes in China: A total of 64 TC tornadoes were cataloged for these 13 years, with a mean of five per year.
- TC tornadoes in 2018
- Key environmental parameters of TC tornadoes in China
- Summary

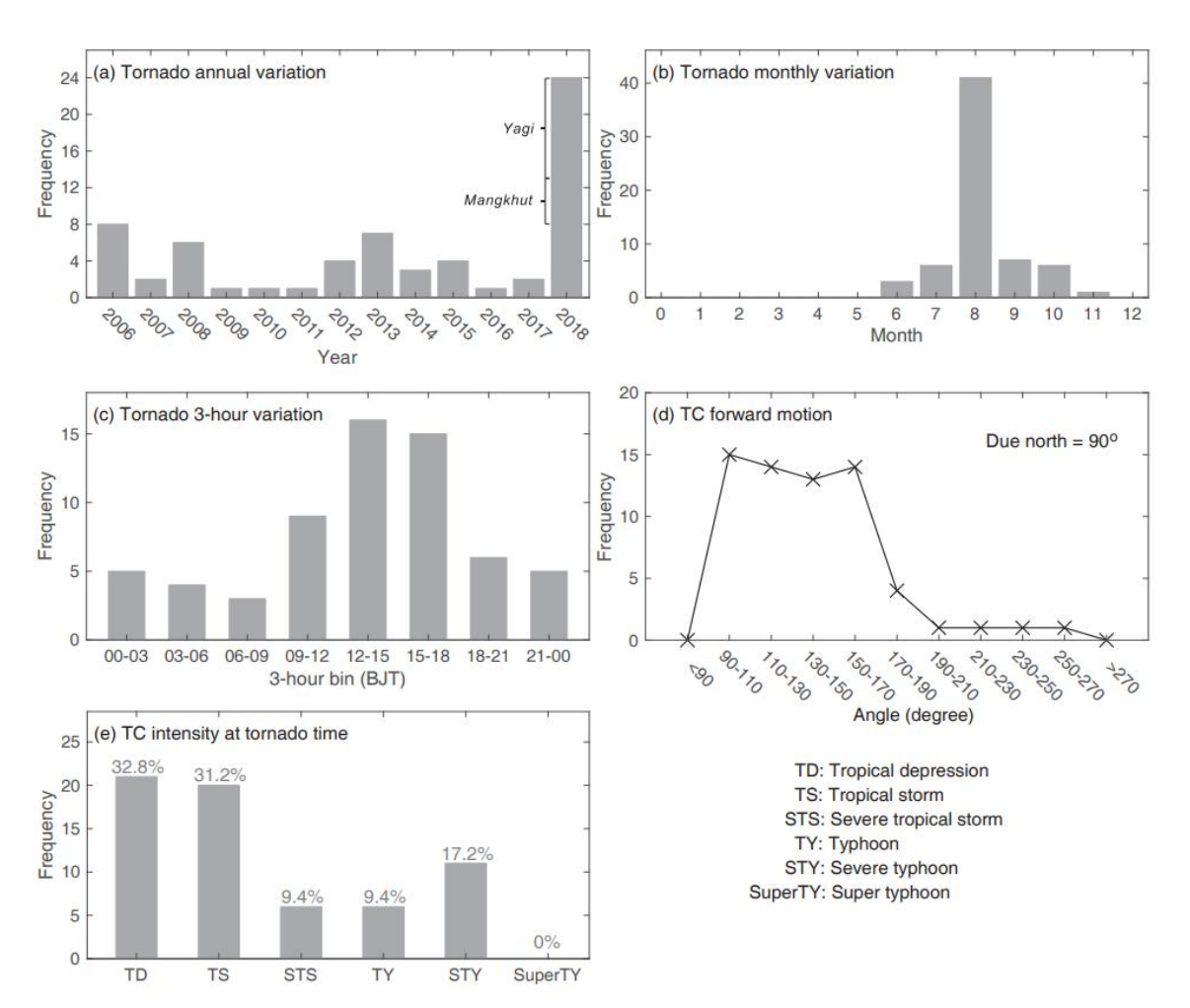
EF1 or stronger tornadoes spatial distribution in China from 2004-2016. (pink dot represents non-TC tornadoes, blue dot represents the TC tornadoes), from Yu et al., 2021.



EF1 or stronger tornado annual variation for the period of 2004-2016 in China. The total tornadoes number is 168, while the number of TC tornadoes is 14, ~8.3 % of the total. From Yu et al., 2021.



Statistics for TC tornadoes in China from 2006 to 2018, including the variation in the annual (a), monthly (b) and daily (c) occurrence frequency. The forward motion (d) and intensity of the TC (e) at the time of the tornado are also shown. From Bai et al.,2020.



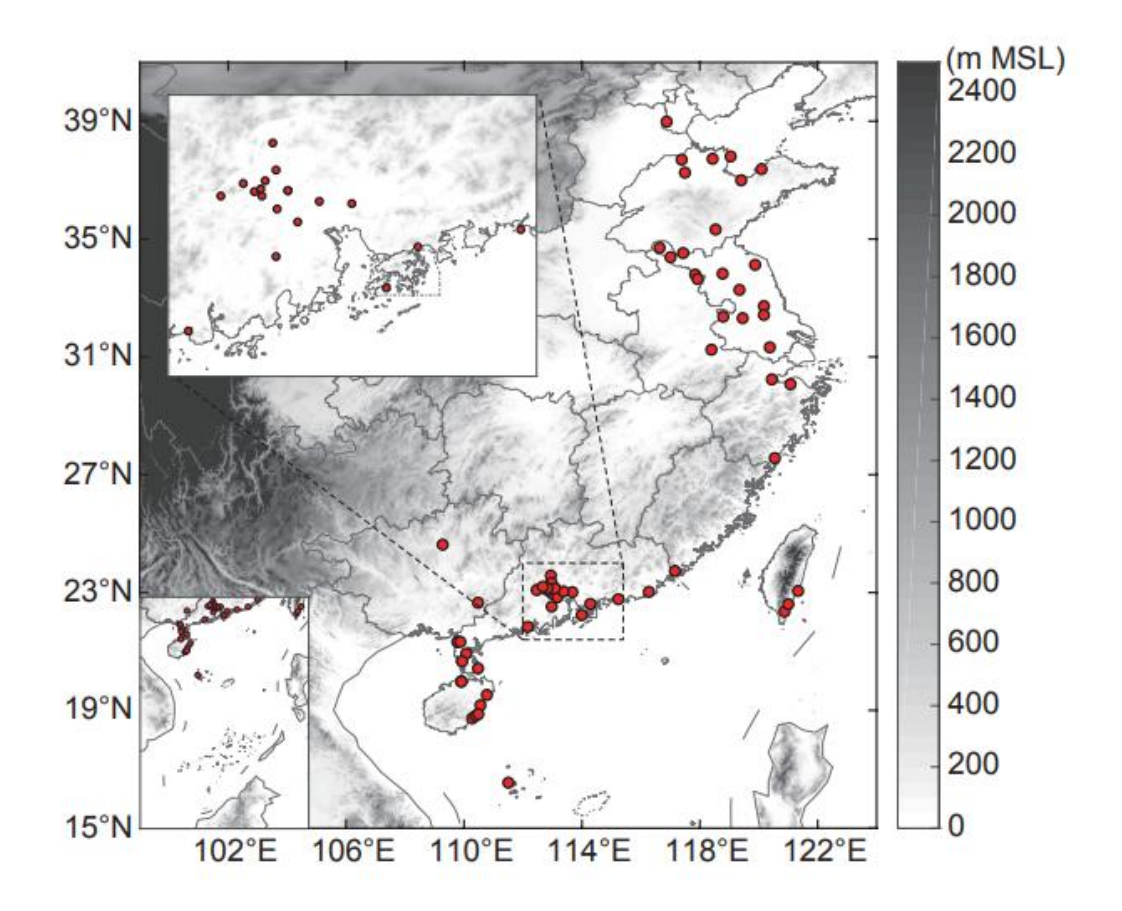
In 2018, TCs Yagi and Mangkhut spawned 11 and 5 tornadoes, respectively. There was no noticeable trend in the annual occurrence of TC tornadoes (Figure a).

TC tornadoes primarily occurred in August (63%), the month with the maximum number of TCs in the northwest Pacific basin (Figure b).

The occurrence of TC tornadoes showed a clear diurnal variation, with a high frequency in the afternoon (Figure c); 50% of TC tornadoes occurred between 12:00 and 18:00 BJT.

About 94% of the TC translational motions were toward the northwest at the time of the tornado (Figure d).

Locations of TC tornadoes (red dots) in China from 2006 to 2018. The region around the Pearl River Delta is enlarged in the upper-left corner. Terrain heights (shaded) are also shown for reference. From Bai et al. 2020.

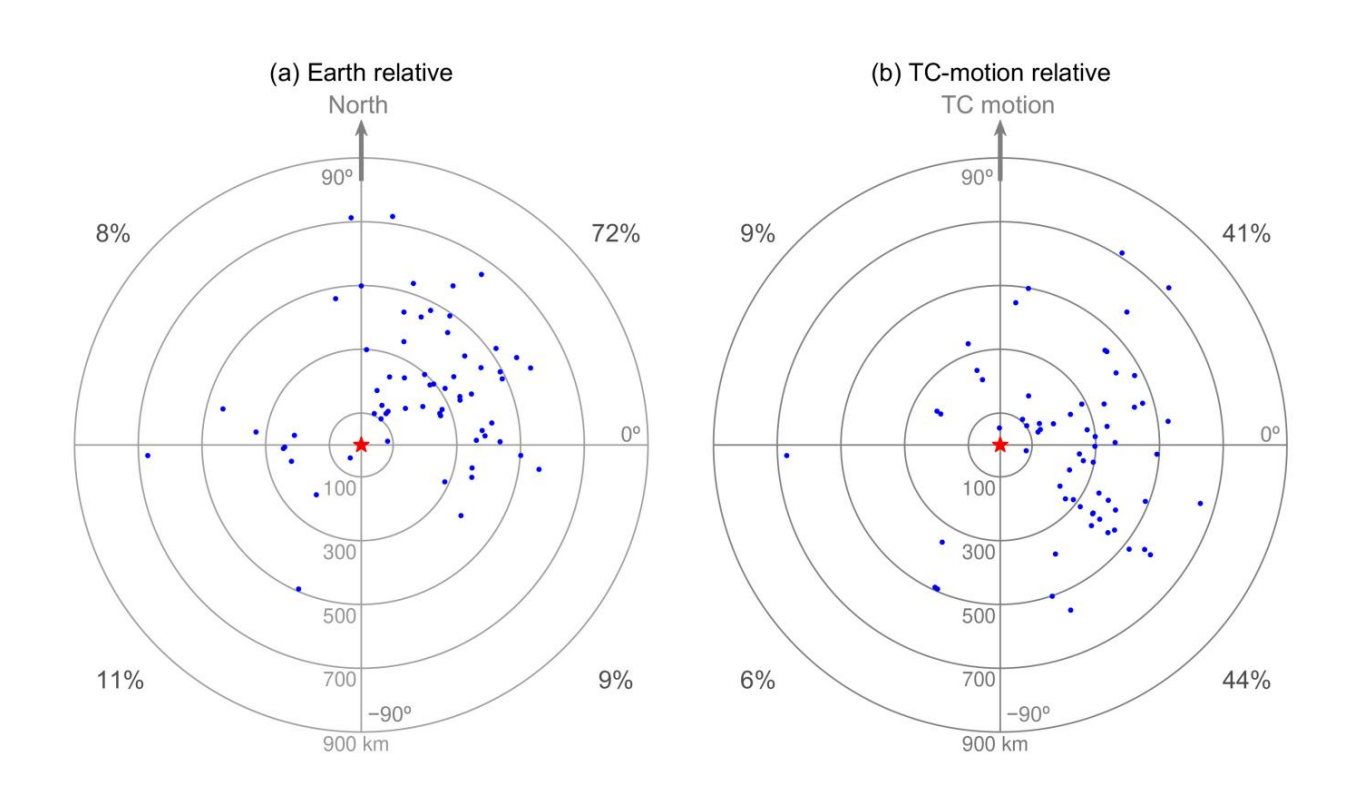


There were two preferred geographical regions for the occurrence of TC tornadoes: coastal areas in the tropics and coastal areas in the mid-latitudes.

Guangdong and Jiangsu provinces had the highest occurrences of TC tornadoes, where there are also the most records of non-TC tornadoes.

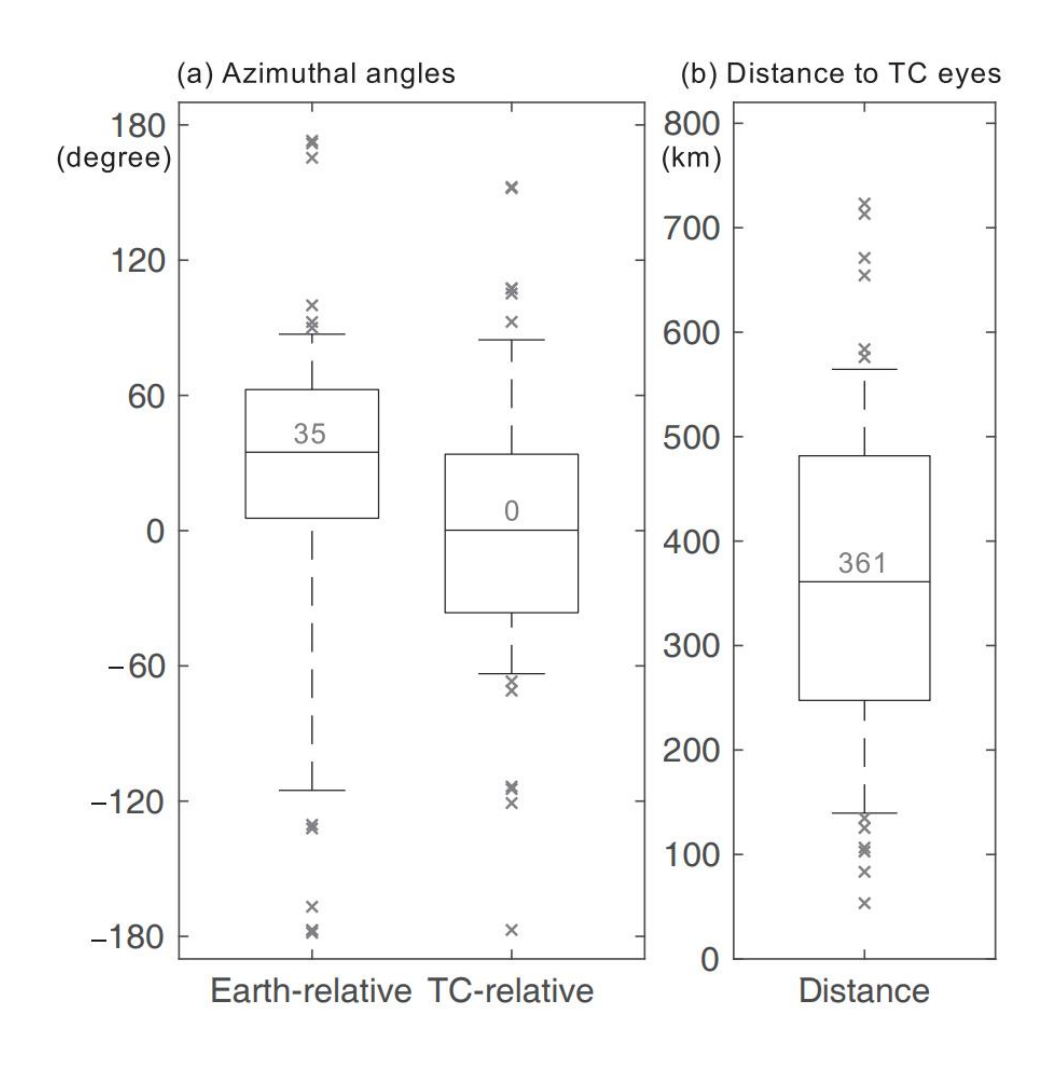
The TC tornadoes mainly occurred in areas with relatively flat topography. About 95% of the TC tornadoes occurred within 250 km of the coastline. Remarkably, 16 tornadoes (25% of the total) occurred in the Pearl River Delta region (inset), where there are large urban agglomerations with dense populations.

Locations of TC tornadoes (dots) relative to the eye of their parent TC (star) at the time of each tornado in China from 2006 to 2018 shown on Earth-relative (a) and TC motion-relative coordinates (b). From Bai et al., 2020.



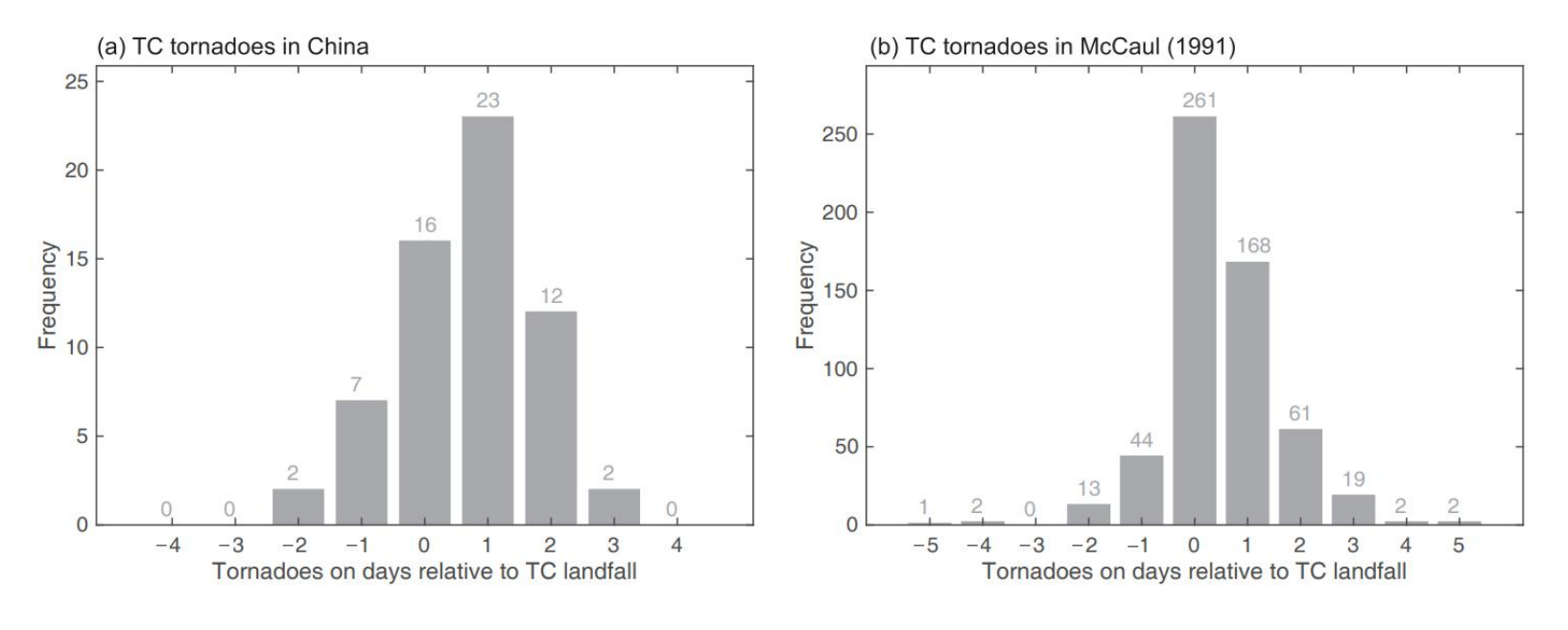
TC tornadoes mainly occurred in the northeast quadrant with respect to the TC center, rather than the right-front quadrant relative to the TC motion. Using Earth-relative coordinates, a large fraction of the tornadoes (72%) occurred in the northeast quadrant of their parent TCs (Figure a) with a median azimuthal angle of 35° (next slide). Using TC motion-relative coordinates, however, about 41% of the tornadoes occurred in the rightfront quadrant and a similar percentage occurred in the right-rear quadrant (Figure b). The median azimuthal angle was approximately 0°(next slide).

Box-and-whisker diagrams for the azimuthal angles (units: degree) (a) and distances (units: km) (b) of the tornado locations relative to the eyes of their parent TC at the time of each tornado in China from 2006 to 2018. In (a), the due north in the Earth-relative (left) coordinate and the TC forward motion in the TC motion-relative (right) coordinate are 90° as shown in Figure of the previous slide. In the box-and-whisker diagrams, the percentile extents and corresponding values represent the 25–75th percentiles for the boxes, the 10–90th percentiles for whiskers and the 50th percentiles for the lines in boxes. Values greater/smaller than the 90th/10th percentile are shown by crosses.



The distances between the TC center and the corresponding tornado primarily ranged from 250 to 500 km with a median of 361 km (Figure b). About 94% of the TC translational motions were toward the northwest at the time of the tornado.

Temporal distribution of TC tornadoes in China from 2006 to 2018 (a) and TC tornadoes in the United States from 1948 to 1986 (b) (adapted from the Figure 15 in McCaul 1991) relative to the day of TC landfall. Day 0 means that the tornado was spawned within 12 h of landfall of the TC and day 1 means that the tornado was spawned from 12 to 36 h after landfall of the TC.



More specifically, many TC tornadoes in China occurred 12–36 h after landfall, accounting for 36% of the tornadoes.

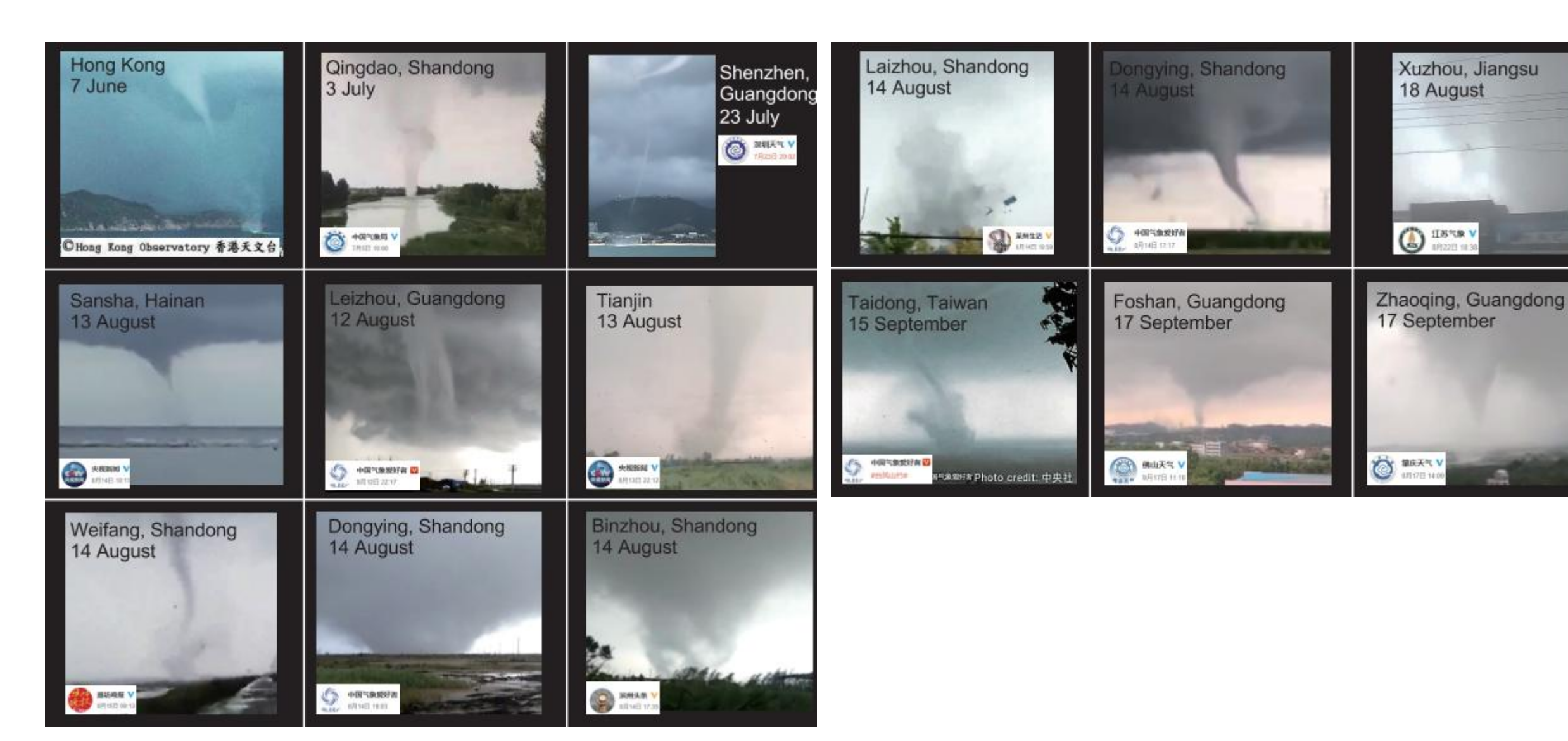
The surveyed tornadoes were spawned by 32 TCs, including 30 that made landfall. For reference, 110 TCs landed in China (including the islands of Hainan and Taiwan) during the time period 2006–2018. Therefore about 27% of the TCs that made landfall spawned tornadoes.

The variation in the time of TC tornadoes with respect to the landfall of the TCs was generally identical to that surveyed in the United States. About 67% of all the surveyed TC tornadoes occurred after the TC had made landfall. The tornado activity primarily occurred within a period from –12 to 36 h relative to the landfall of the TC, encompassing 63% of the tornadoes (Figure a), in contrast with 75% of the tornadoes in the United States (Figure b; McCaul Jr, 1991).

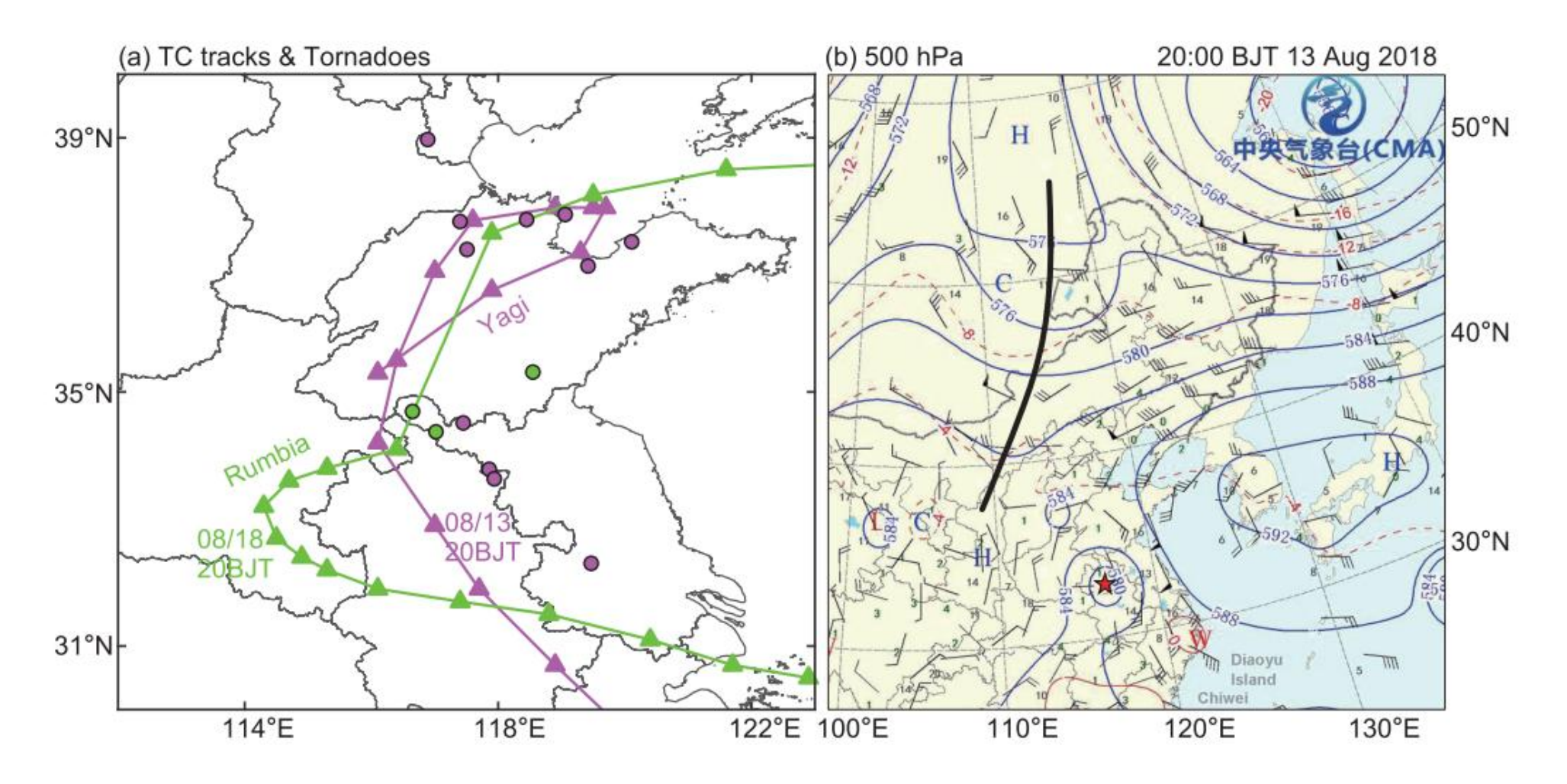
TC tornadoes in 2018

- TC tornadoes in 2018 was active in China, contributing 37.5% of the TC tornadoes in the previous 13 years. Eleven TCs landed in China (including the islands of Hainan and Taiwan) and seven spawned at least one tornado. The first tornado outbreak event in the modern history of China was recorded in 2018 and remains the only recorded outbreak event up to now.
- TC Yagi (2018) spawned at least 11 tornadoes within a 20-h period in central eastern China.
 Most of these tornadoes occurred one day after rather than on the day of the landfall of the parent TC.
- The Foshan city of Guangdong Province is one of the most tornado-prone areas in China. It was hit by two TC tornadoes in 2018. The first occurred in TC Ewiniar (2018) on the afternoon of 8 June 2018. The other TC tornado was spawned on the morning of 17 September by TC Mangkhut(2018). TC Mangkhut (2018) produced another tornado in Zhaoqing city (neighboring Foshan).

Gallery of the TC tornadoes photographed in China in 2018 and available online at https://weibo.com. The credits for these photographs is indicated in each panel.



(a) Best tracks of TCs Yagi (magenta) and Rumbia (green) in 2018. The locations of tornado (dots) are shown in the corresponding colors. The TC centers (triangles) are plotted every 6 h. The data for the track of Rumbia were obtained from the National Meteorological Center of China Meteorological Administration (http://typhoon.nmc.cn/web.html). (b) Synoptic chart provided by the China Meteorological Administration with geopotential heights (blue contours; units: dagpm), horizontal winds and temperature (red contours; units: °C) at 500 hPa at 20:00 BJT on 13 August 2018. The half-barb, full-barb and pennant symbols represent wind speeds of 2, 4 and 20 m s⁻¹, respectively. The location of TC Yagi is shown by the red star.



Tropical cyclone tornadoes recorded in China in 2018^{a)}

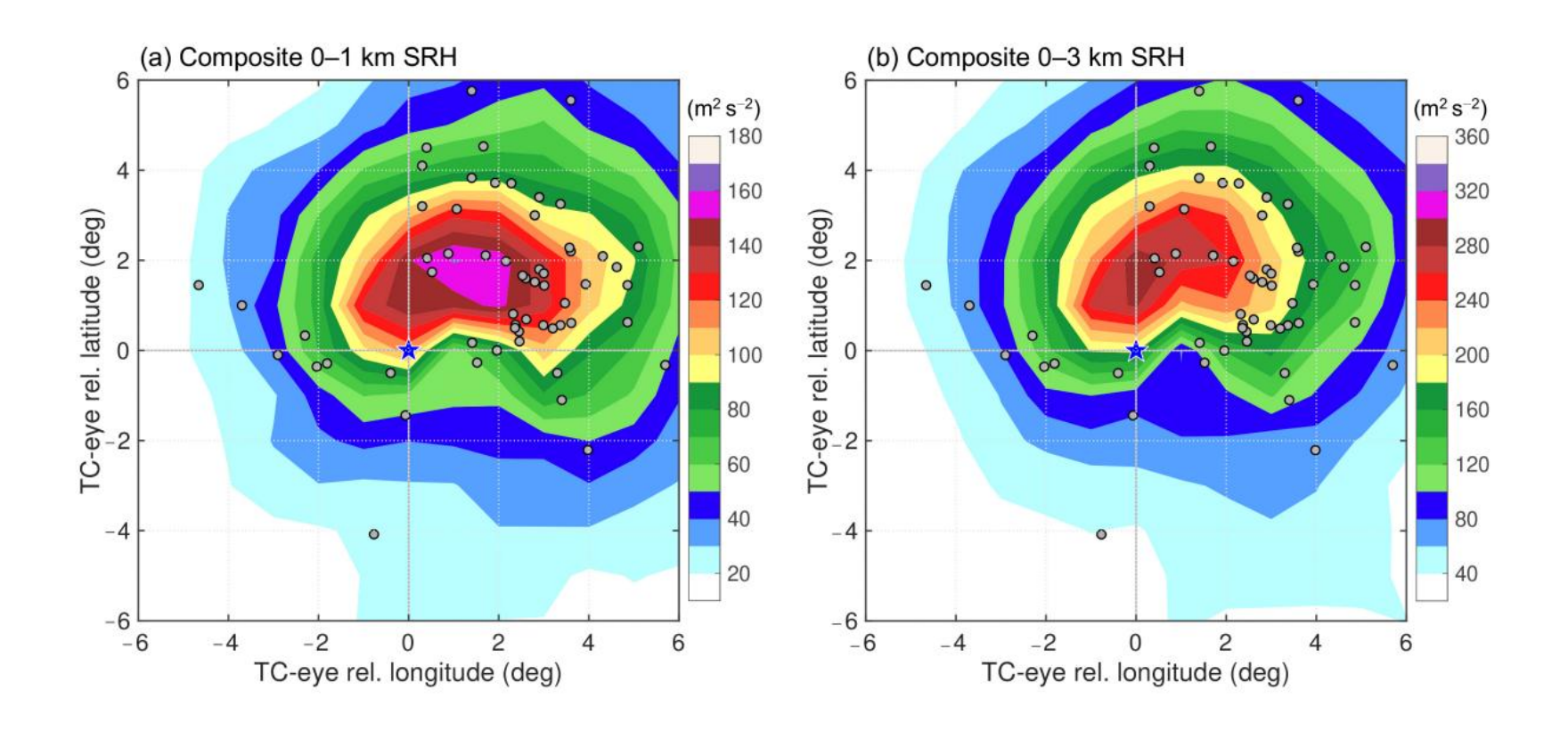
No.	TC	Intensity	Tornado date	Location
1	Ewiniar	TS	7 June	Hong Kong
2	Ewiniar	TS	8 June	Foshan, Guangdong
3	Nameless	TD	23 July	Shenzhen, Guangdong
4	Bebinca	TS	12 August	Leizhou, Guangdong
5	Bebinca	TS	13 August	Sansha, Hainan
6	Yagi	TS	13 August	Tianjin
7	Yagi	TS	13 August	Xuzhou, Jiangsu
8	Yagi	TS	13 August	Suzhou, Anhui
9	Yagi	TD	13 August	Zaozhuang, Shandong
10	Yagi	TD	14 August	Yizheng, Jiangsu
11	Yagi	TD	14 August	Weifang, Shandong
12	Yagi	TD	14 August	Dongying, Shandong
13	Yagi	TD	14 August	Laizhou, Shandong
14	Yagi	TD	14 August	Binzhou, Shandong
15	Yagi	TD	14 August	Dongying, Shandong
16	Yagi	TD	14 August	Dezhou, Shandong
17	Rumbia	TD	18 August	Xuzhou, Jiangsu
18	Rumbia	TD	18 August	Xuzhou, Jiangsu
19	Rumbia	TD	19 August	Linyi, Shandong
20	Mangkhut	STY	15 September	Taidong, Taiwan
21	Mangkhut	STY	15 September	Taidong, Taiwan
22	Mangkhut	STY	16 September	Taidong, Taiwan
23	Mangkhut	TS	17 September	Foshan, Guangdong
24	Mangkhut	TS	17 September	Zhaoqing, Guangdong

a) Nameless means that the tropical cyclone was not given a name because it did not reach the intensity of tropical storm. The date of the tornado is given in Beijing time (BJT=UTC+8 h).

Key environmental parameters of TC tornadoes in China

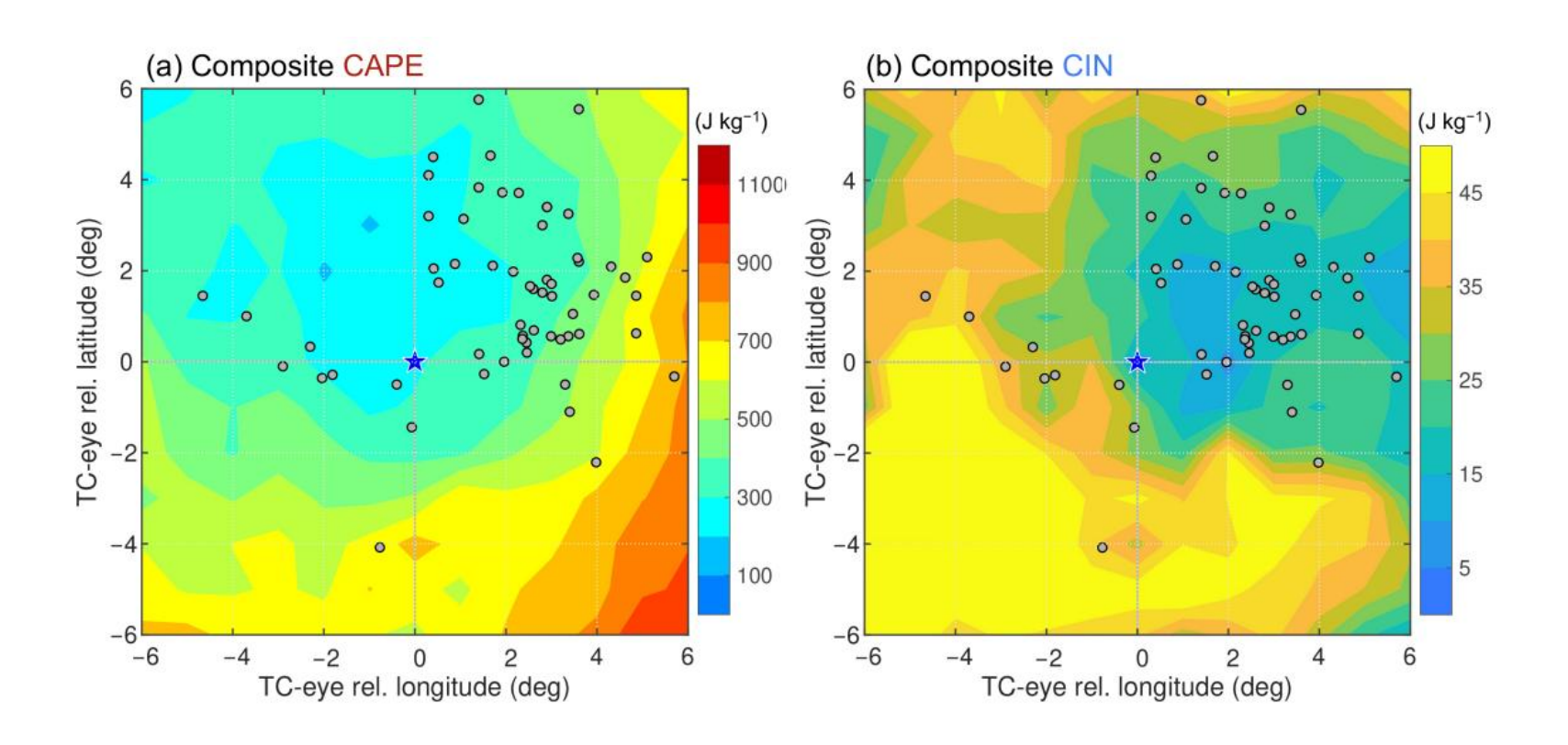
- SRH :The SRH is a measure of the potential for cyclonic updraft rotation in rightmoving supercells.
- CAPE
- In the present study, we used the National Centers for Environmental Prediction (NCEP) Final Operational Global Analysis (NCEP FNL) which has been demonstrated having the best performance in representing the TC intensity and warm-core structure.
- The representative environment of a tornado was determined using the NCEP FNL data at the hour closest to the time of the tornado. The composite of an environmental parameter was obtained by simply superposing the TC centers and calculating the average value.
- the spatial distribution of these parameters relative to the occurrence of TC tornadoes was examined to determine the principal environmental conditions that favor TC tornadogenesis.

Composite horizontal distributions of the (a) 0–1 km and (b) 0–3 km SRH around the TC eyes (blue stars). The solid gray circles represent the locations of TC tornadoes in 2006–2018 relative to the eye of their parent TC. The X (Y) axis is arranged in the TC eye relative longitude (latitude) for convenience.



Consistent with the results in Sueki and Niino (2016), the composite SRH peaked in the northeast quadrant relative to the TC center. Large SRH values were primarily located within about 600 km of the TC center.

Composite horizontal distributions of the (a) CAPE and (b) CIN around the eyes of the TC (blue stars). The solid gray circles represent the locations of TC tornadoes in 2006–2018 relative to the eye of their parent TC. The X(Y) axis is arranged in the TC eye relative longitude (latitude) for convenience.



Similar to the results of Sueki and Niino (2016), most of the tornadoes were located in a region with a moderate CAPE, whereas the area with a large value of CAPE was located to the southeast of the TC center (Figure a). The median value of CAPE was 401 J kg⁻¹, which was comparable with the average CAPE (253 J kg⁻¹) for the TC tornado environment in the United States (McCaul, 1991).

Case study

- TC tornado at Foshan City on the 4th October 2015.
- TC tornadoes at Foshan City on 4th August 2006.

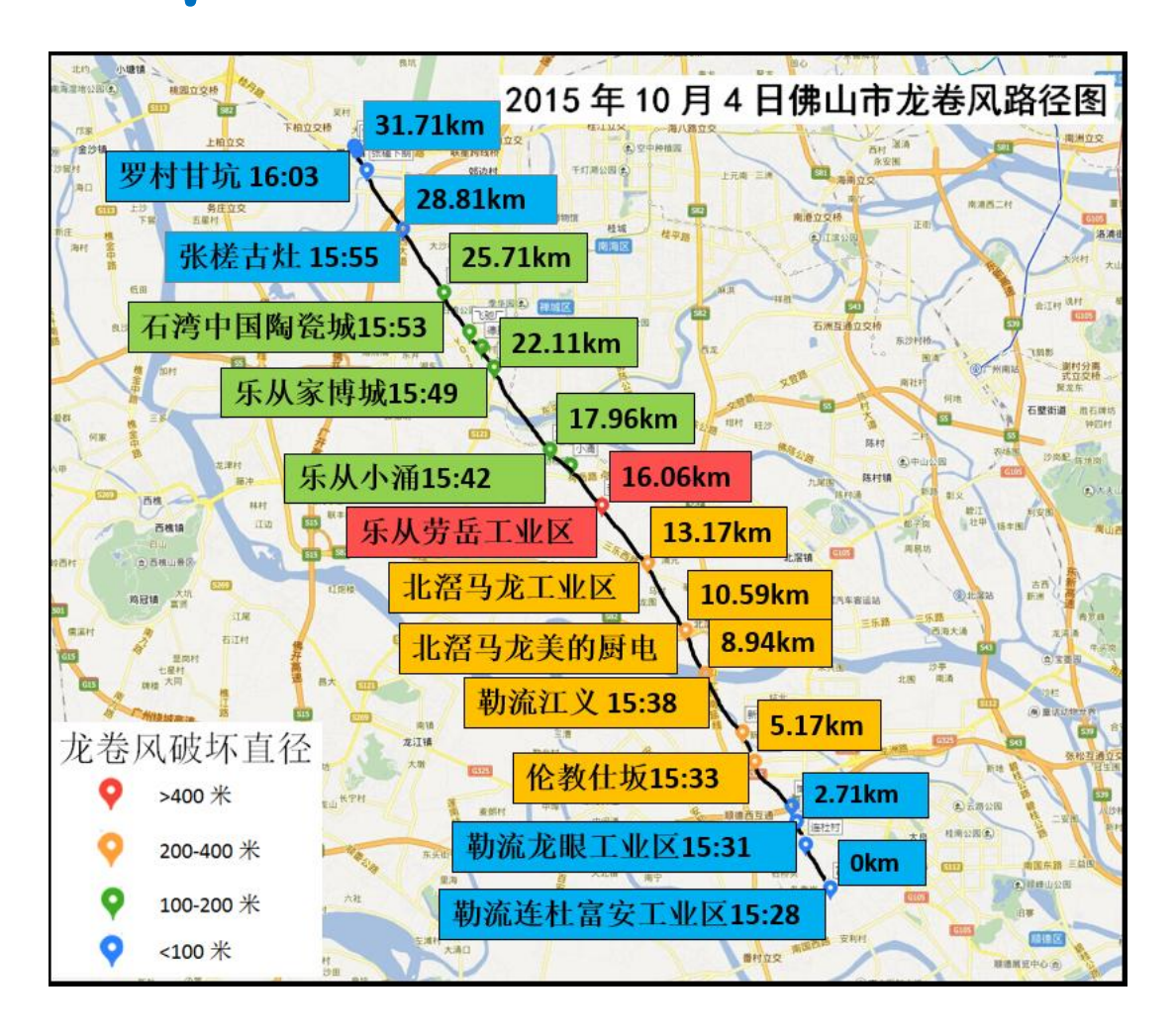
Case 01 TC tornado at Foshan City on the 4th October 2015.

- Ground truth
- Weather pattern and key environmental parameters
- Satellite images
- Characteristics of Doppler weather radar echoes
- Summary

Ground truth

- A tornado, rated as a category 3 on the Enhanced Fujita Scale(EF3), occurred at Foshan City (Guangdong Province) within the mini-supercell embeded in the spiral rain belt of the landed Typhoon "Mujigae" between 15:28 and 16:00 BJT on the 4th October 2015. The Typhoon "Mujigae" landed on Zhanjiang city (Guangdong province) around 14:00 BJT on the 4th October 2015.
- This strong tornado lasted 32 minutes, killed 4 people, wounded over 80 people, and destroyed a large number of factories and houses.
- This tornadoes swath was 31.7 km long, and the largest tornado swath diameter is 580m. Photos and videos of the tornado were collected during the damages survey.

Tornado path



Photos of the tornado







Damages made by the tornado







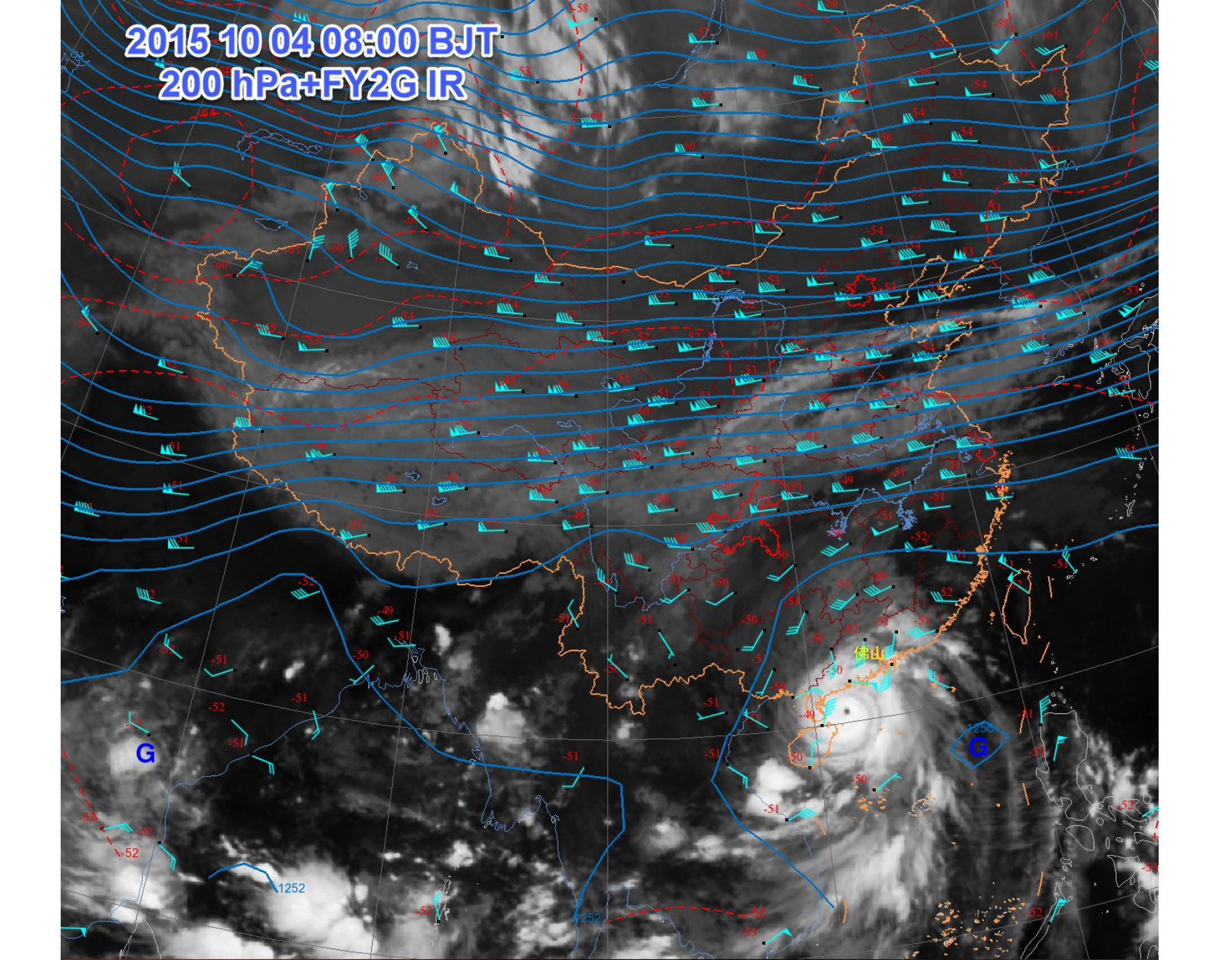


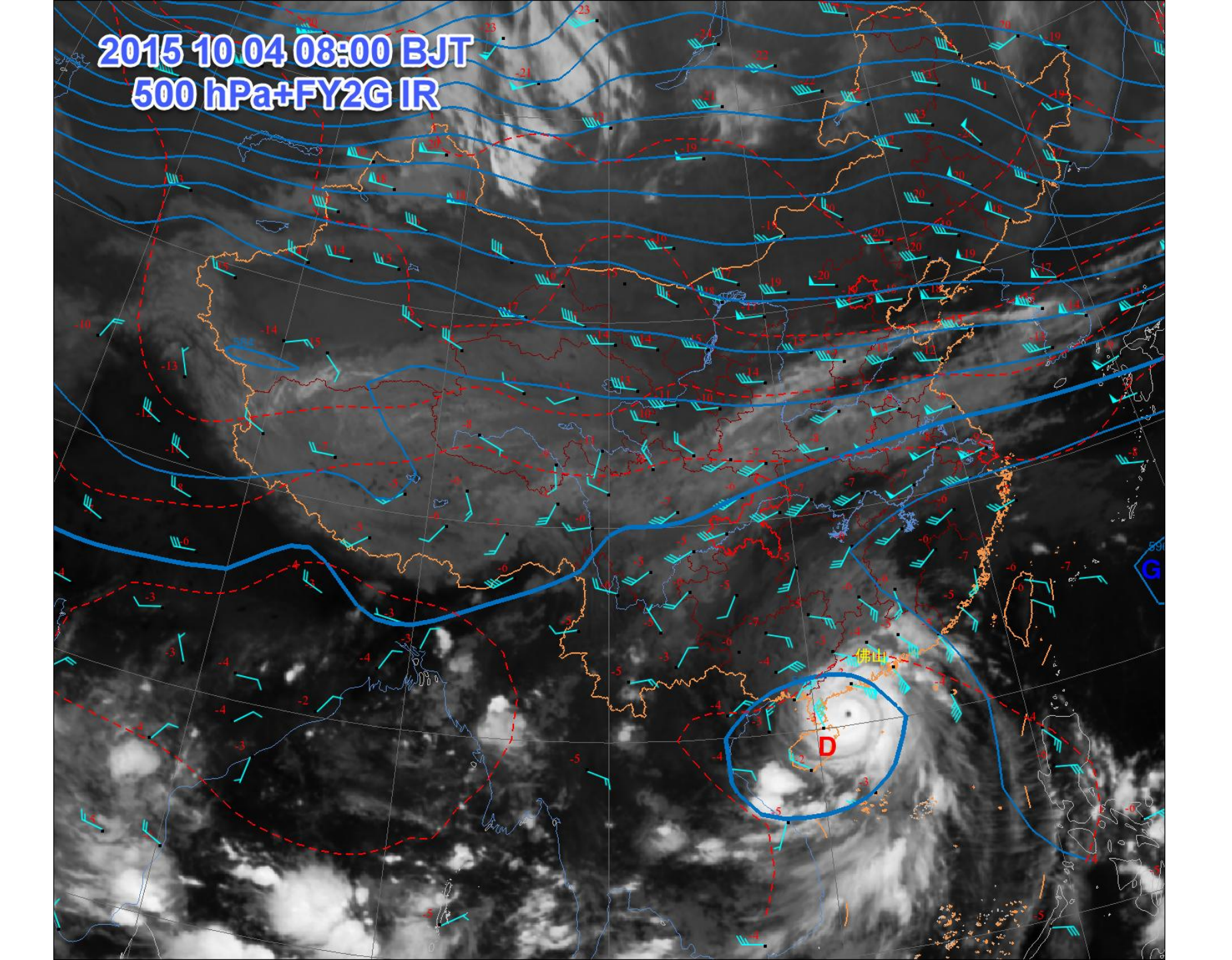


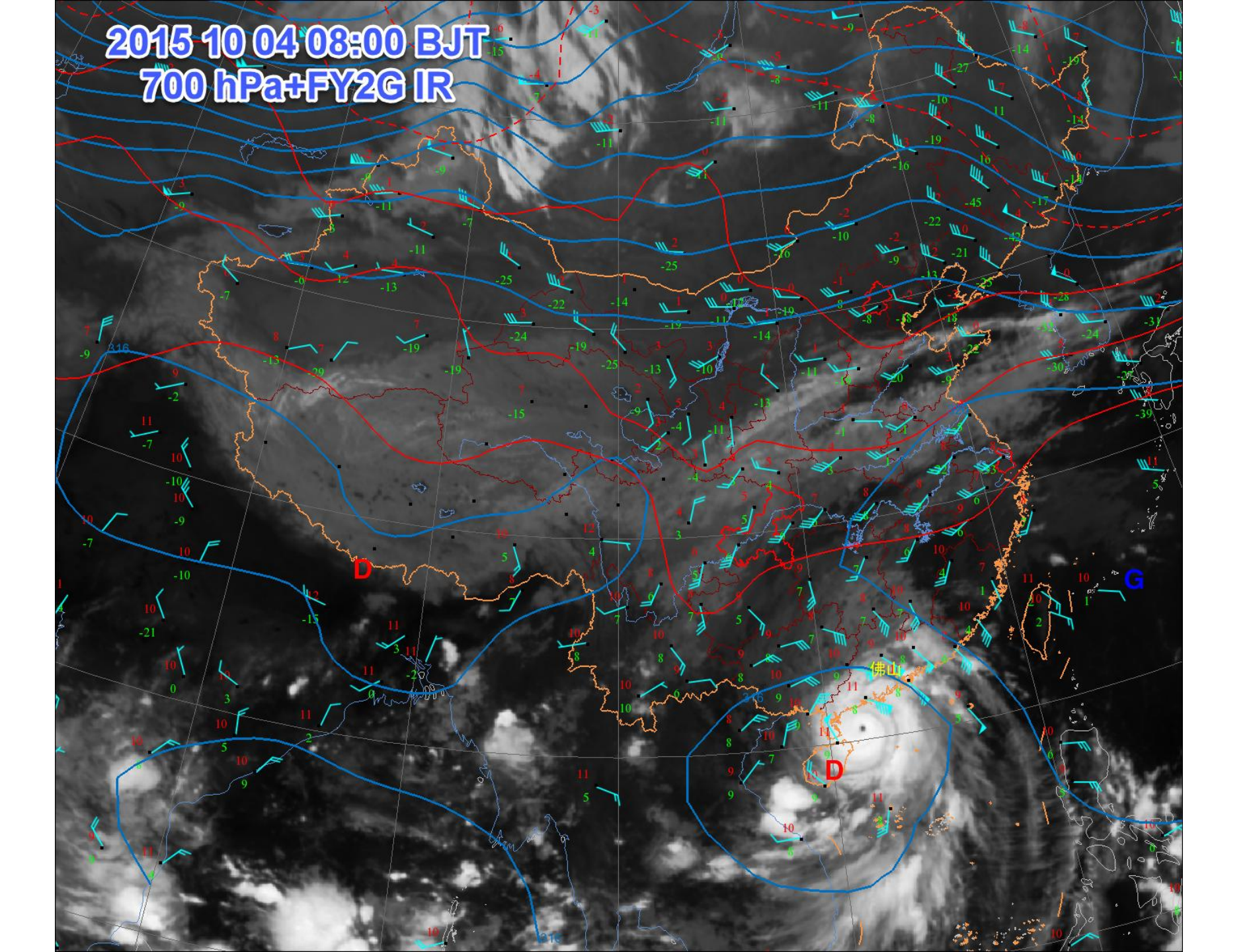


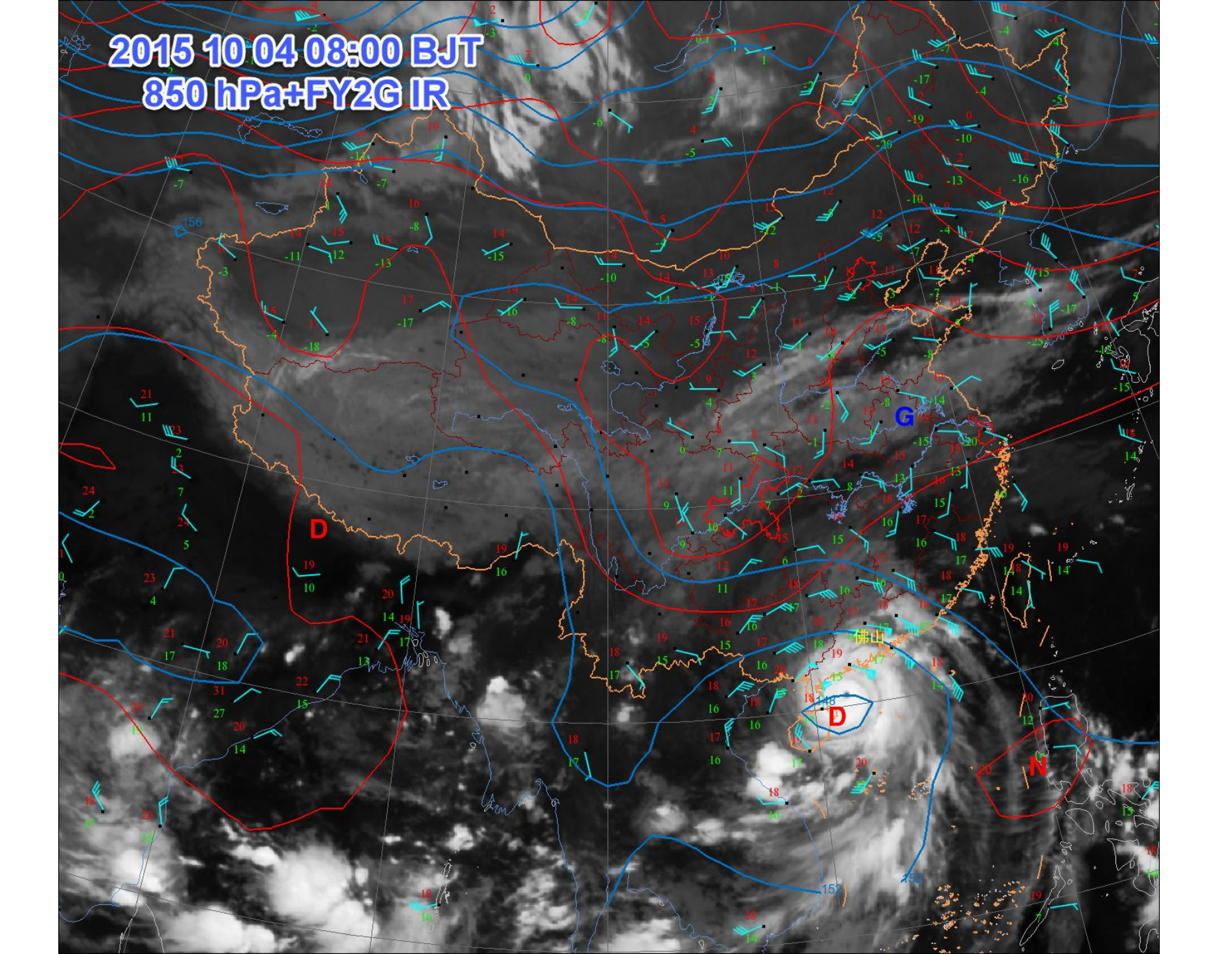
Weather patterns and key environmental parameters

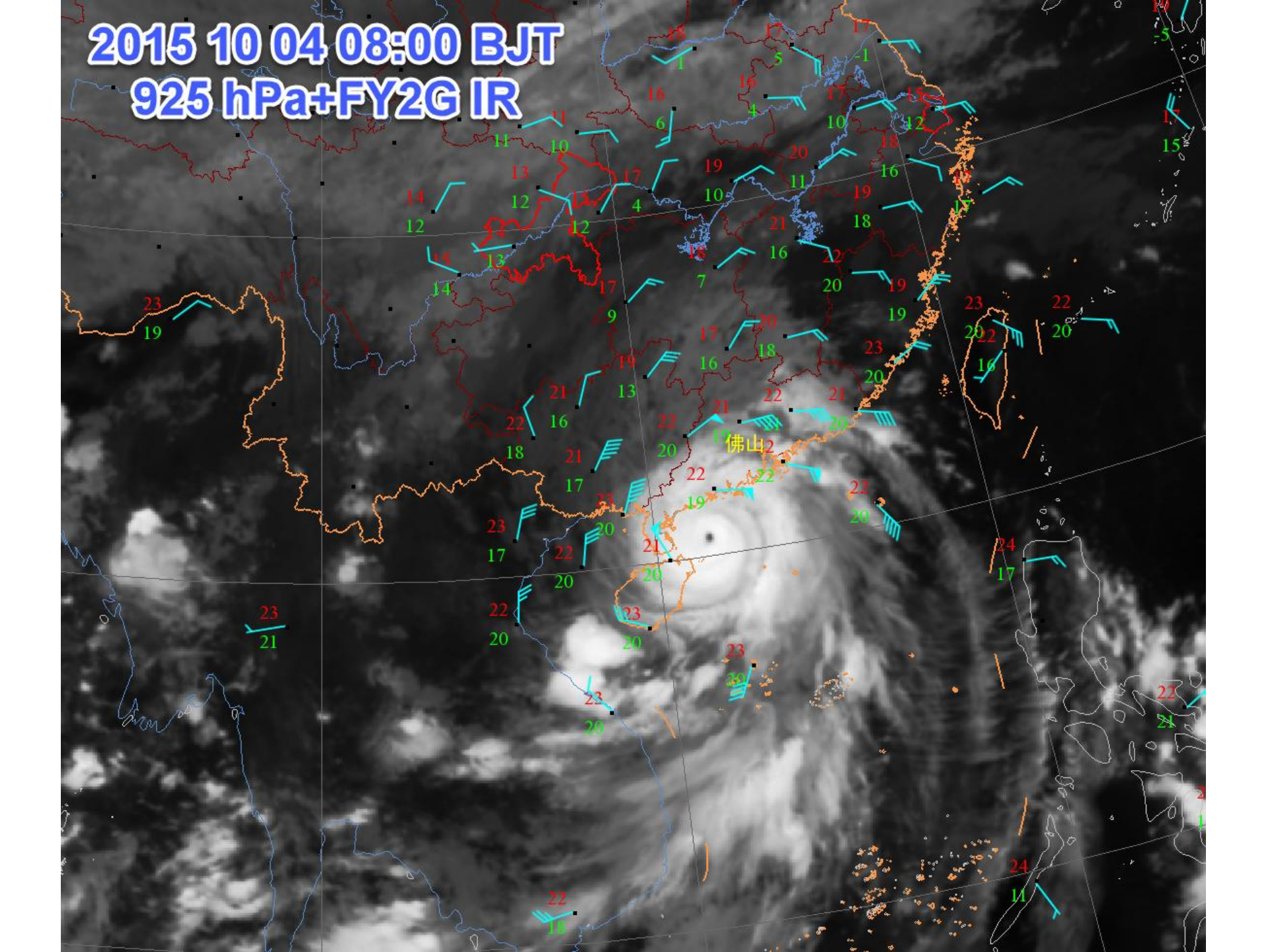
- Upper-air weather maps
- T-Log P diagram
- Satellite images
- Dense surface observations





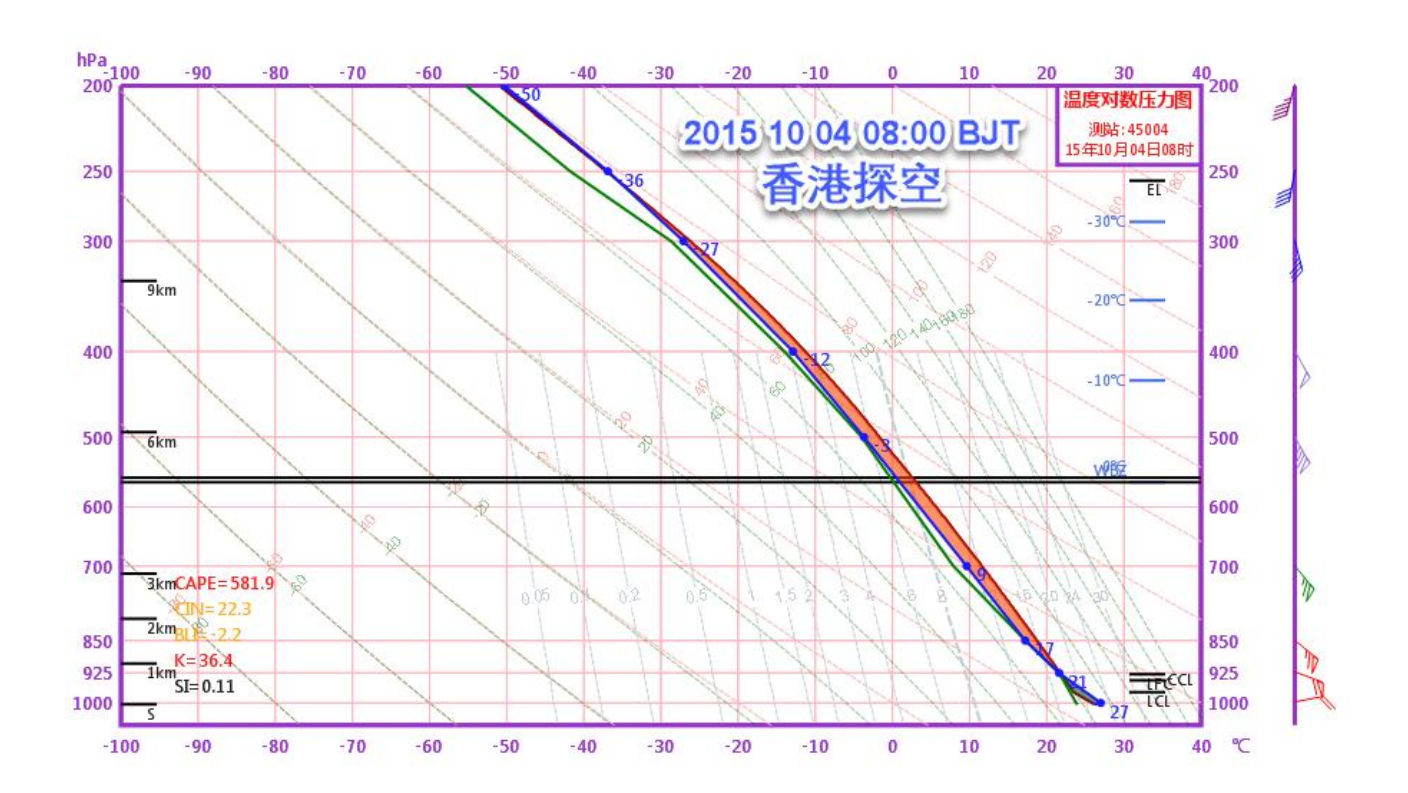




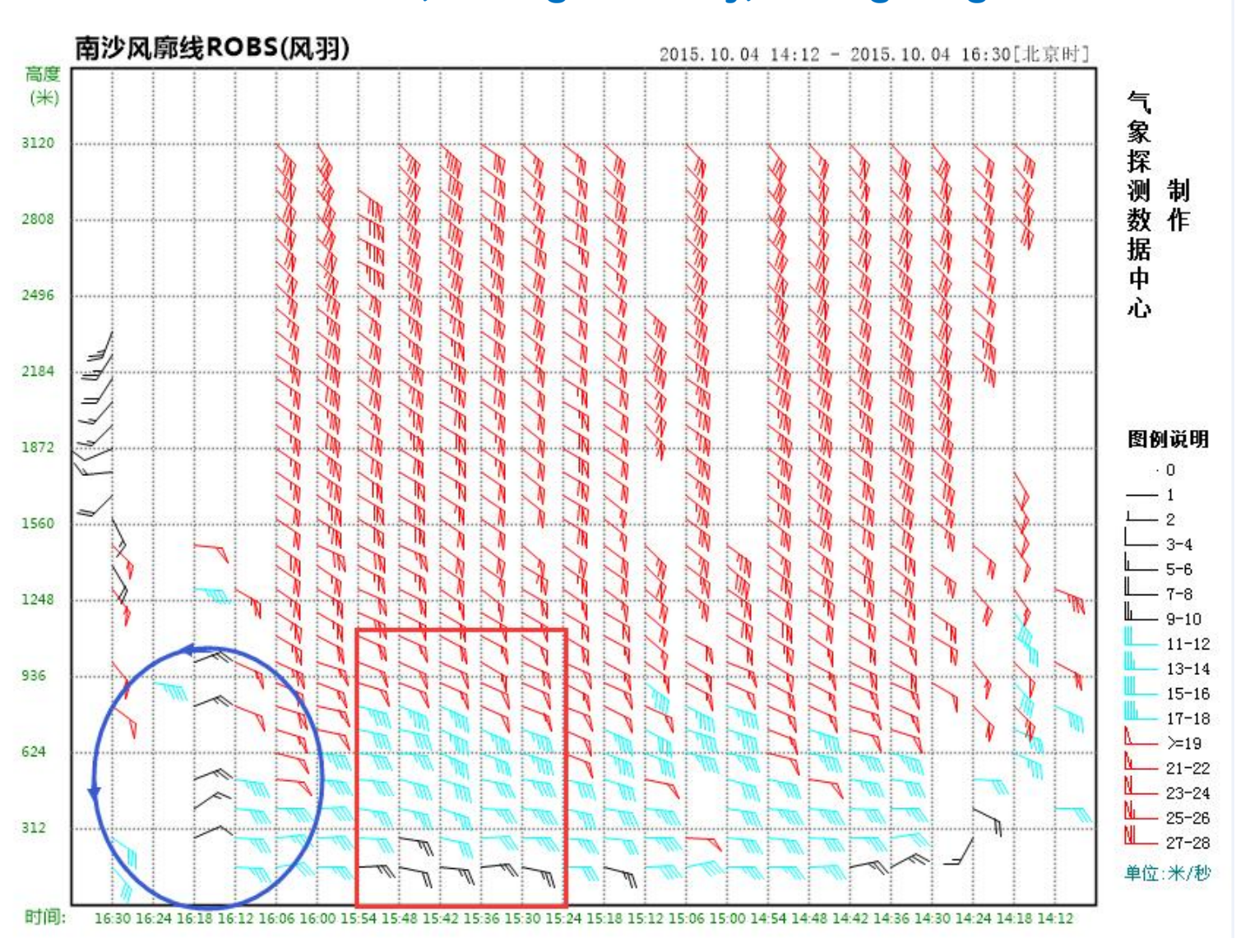


Proximity sounding

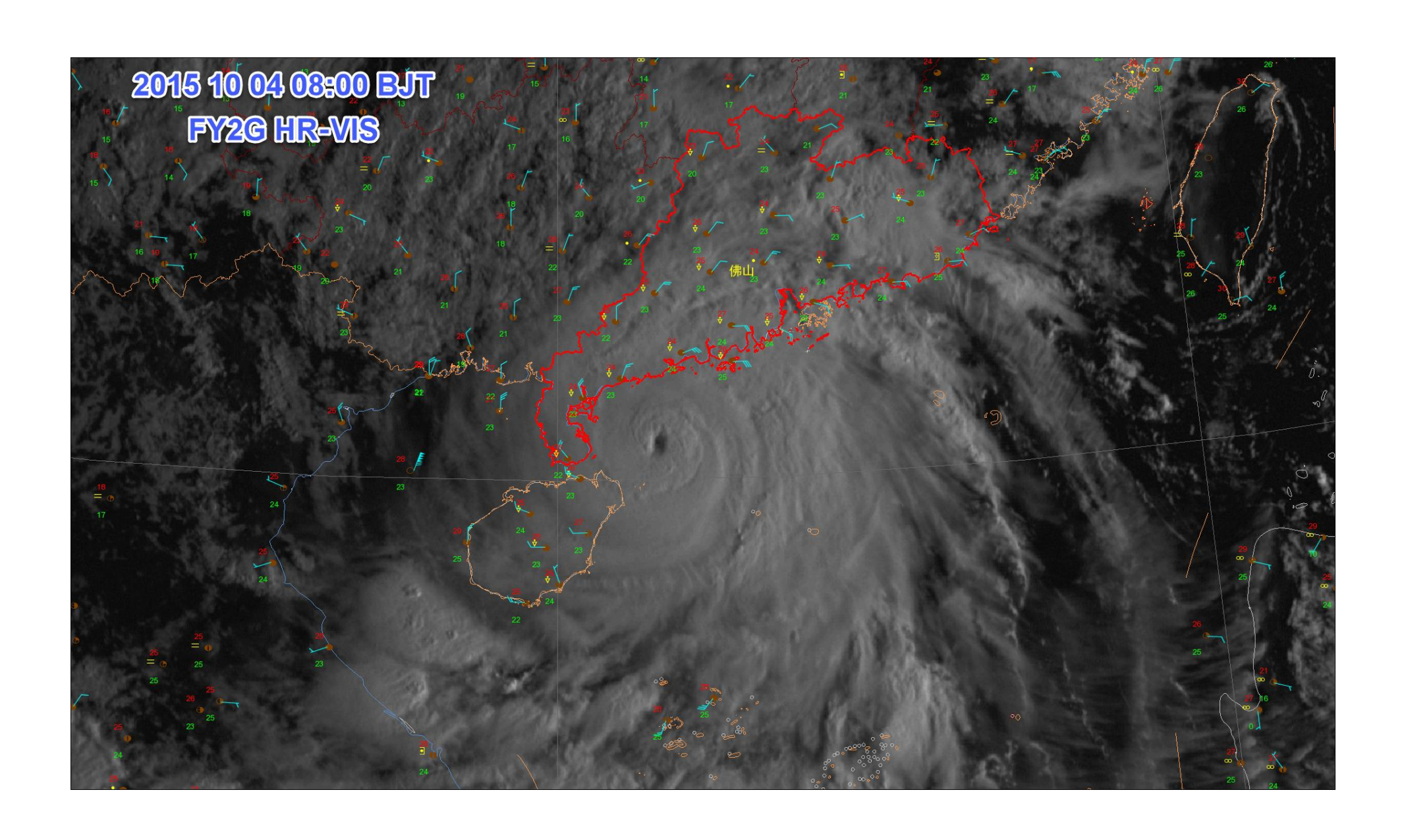
T850-T500=21°C, Td-sur=24°,
PW=67mm;
CAPE=580J/kg, CIN=22J/kg;
DCAPE=170J/kg;
0-6km shear=22m/s,
0-3km shear=20m/s,
0-1km shear=16m/s,
SRH3=430m²/s²;
LCL=350m, LFC=760m,
EL=10.8km;
WBZ=5.0km;
ZH=5.1km, -20°C H=8.7km;

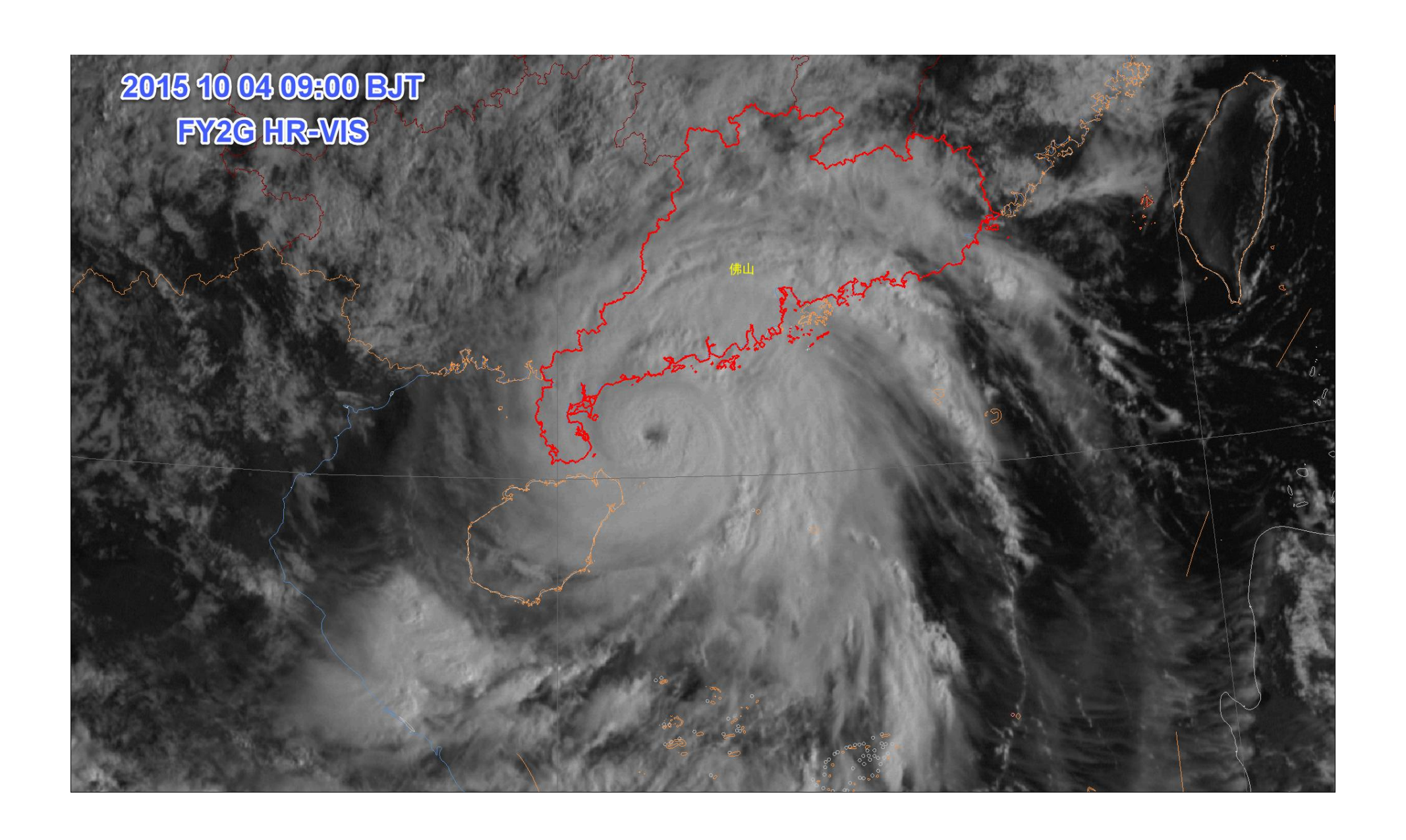


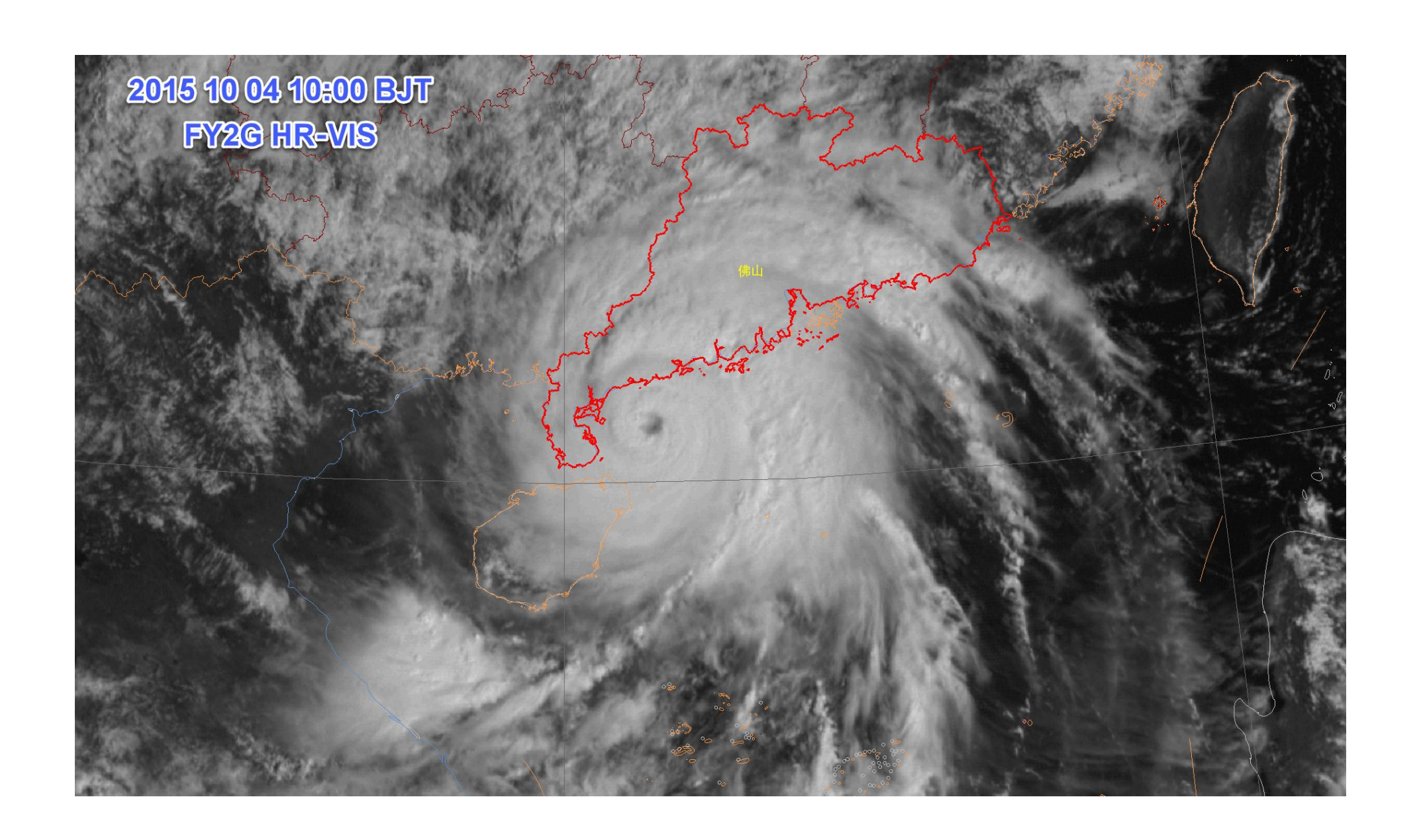
2015 10 04 14:12 – 16:30 BJT boundary layer profiler's observation in Nansha district, Guangzhou City, Guangdong Province.

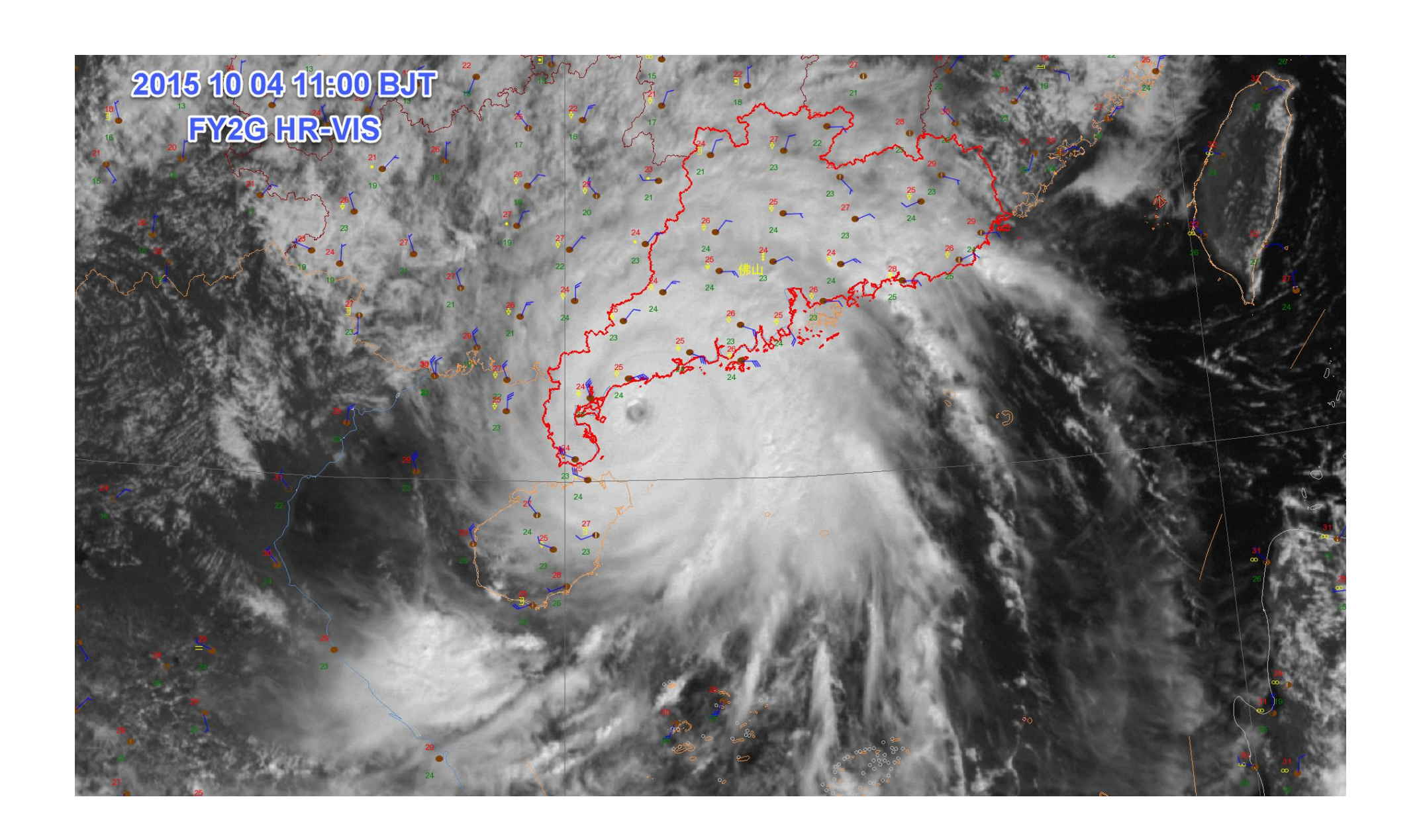


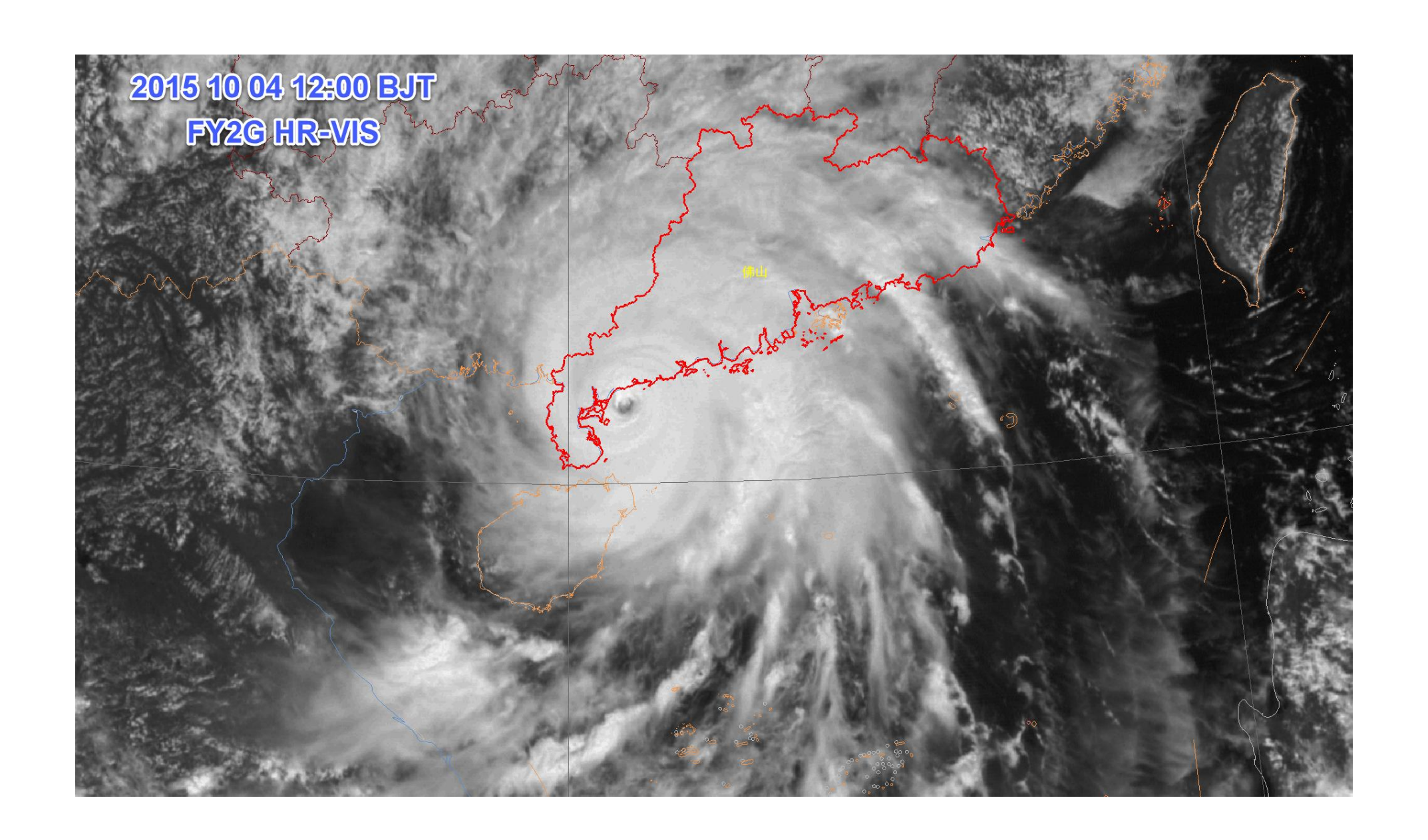
FY2G visible channel satellite images and dense surface observations

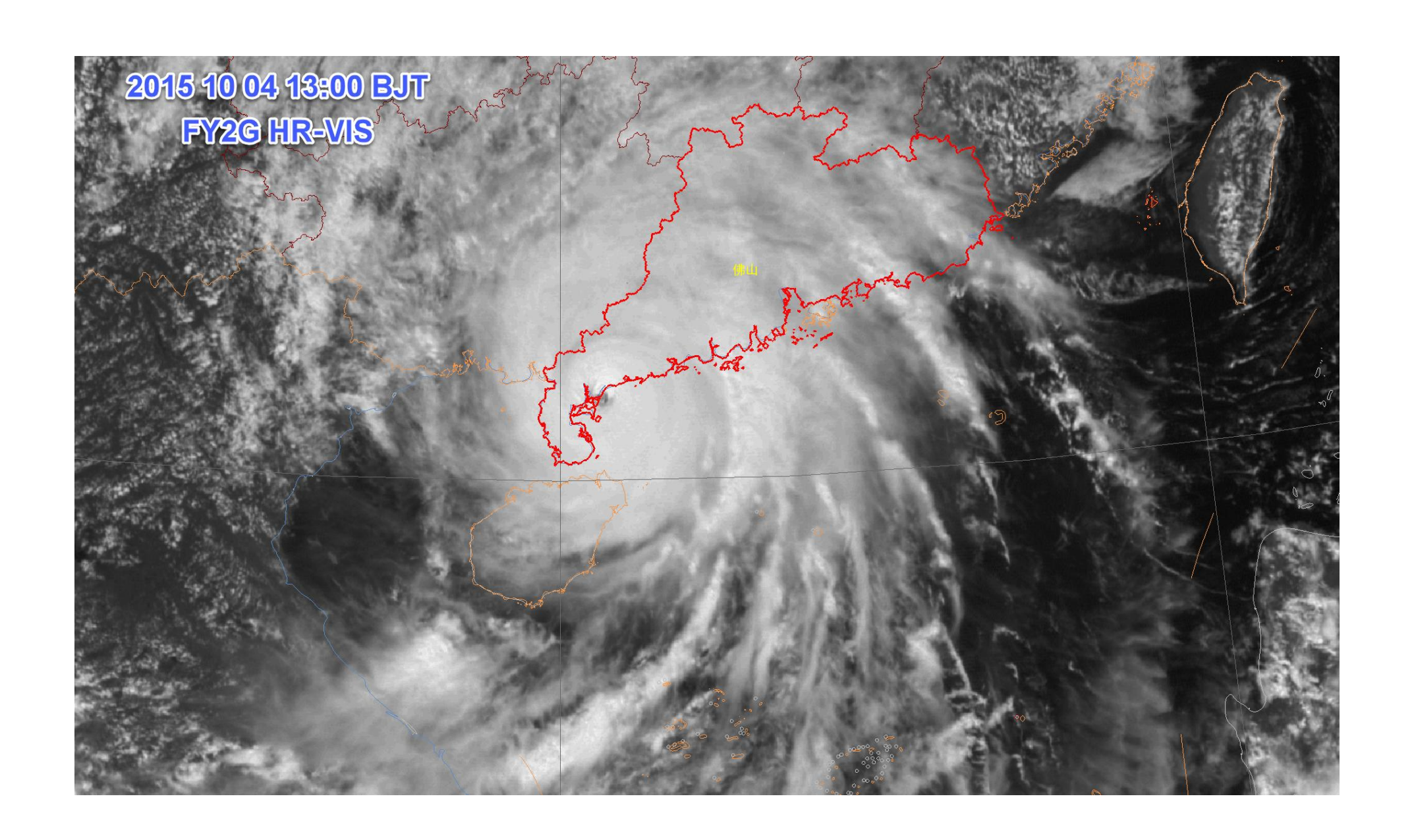


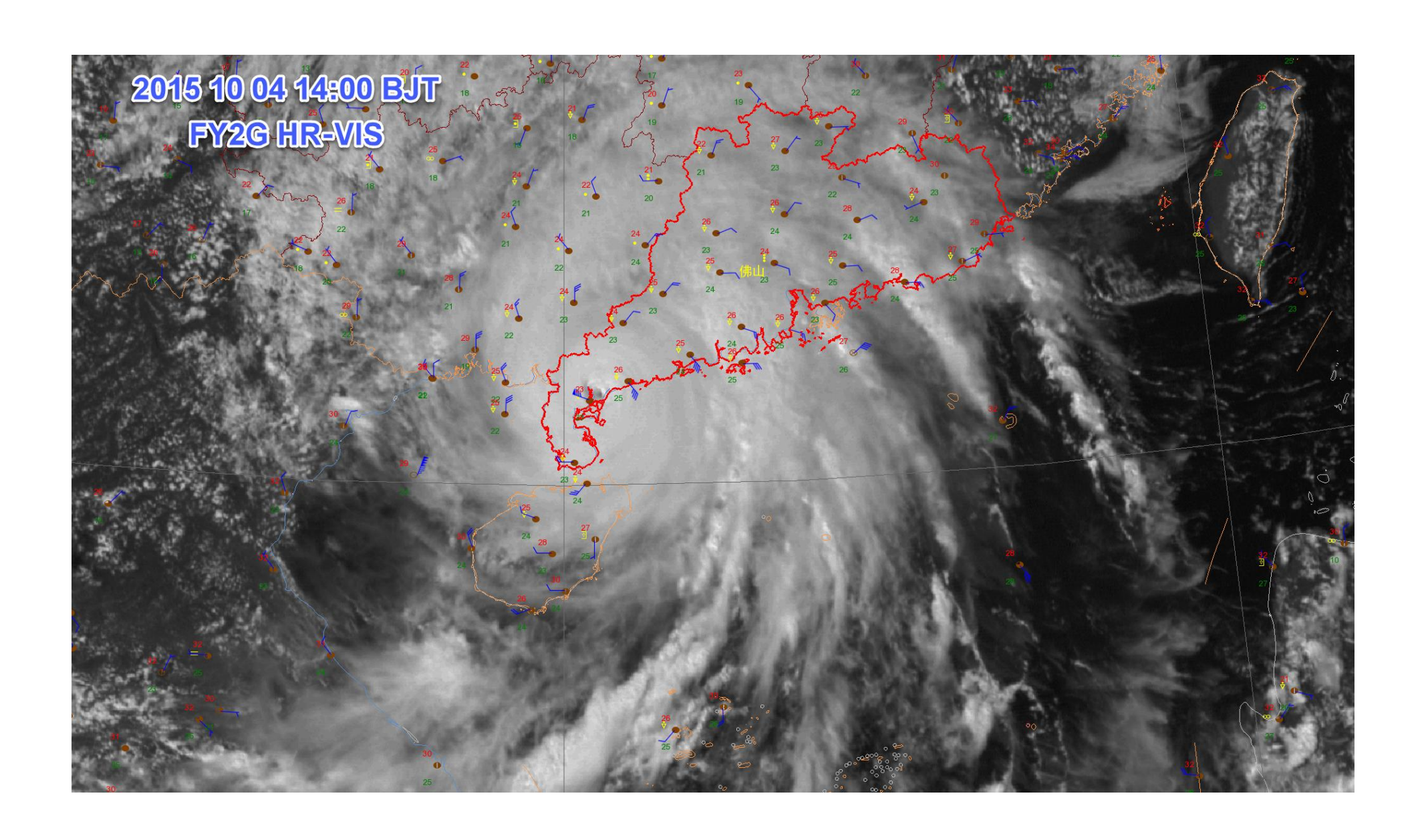




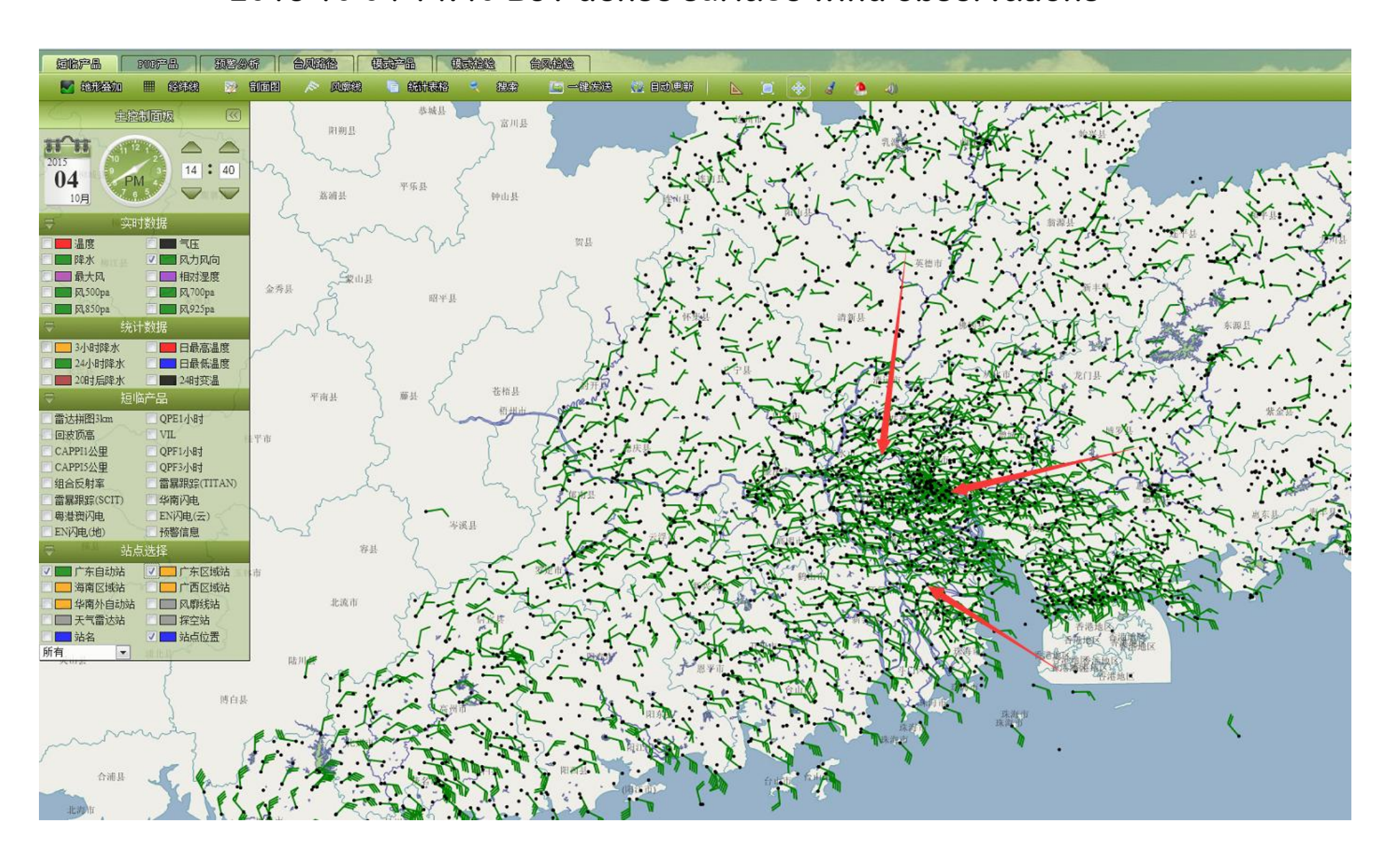


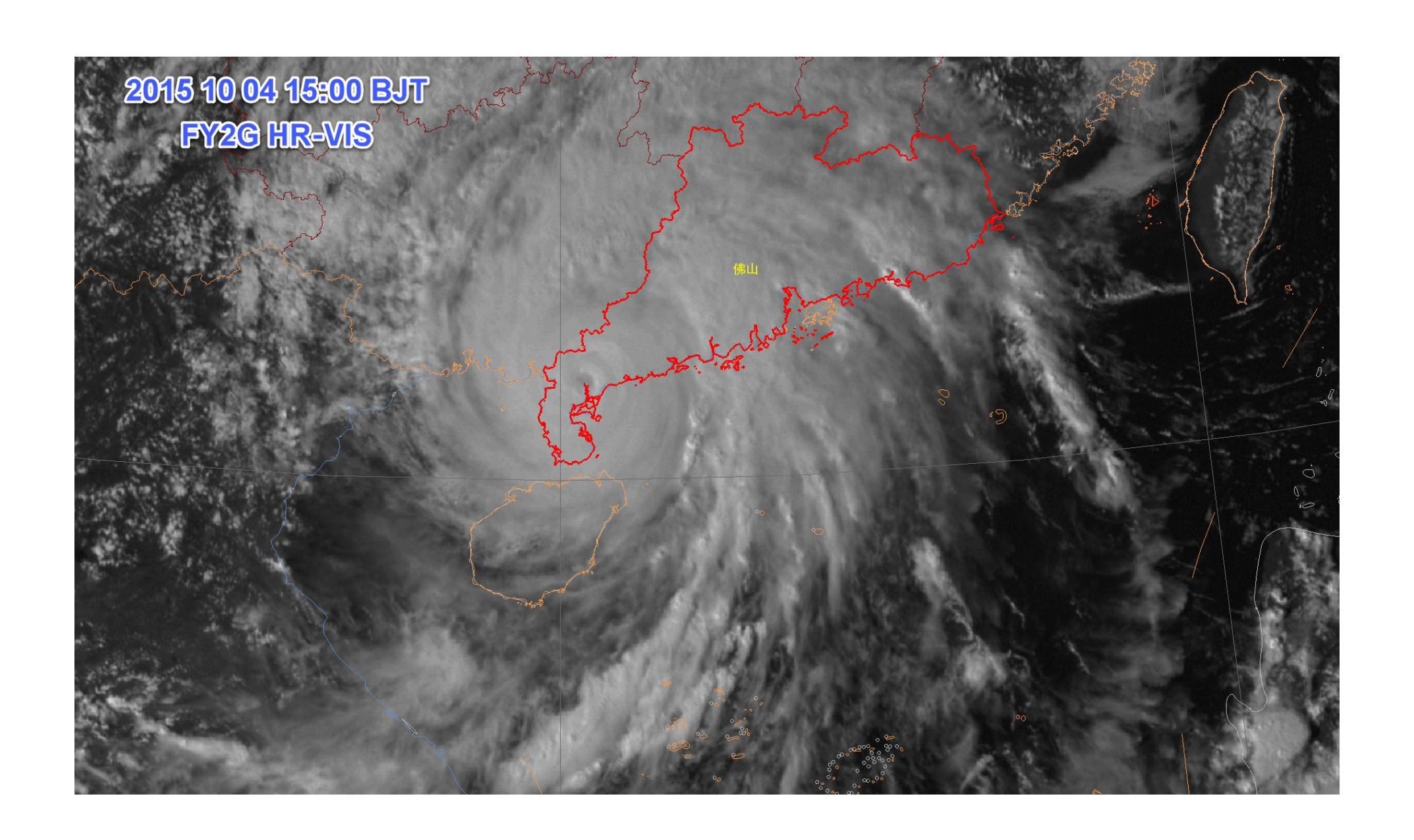


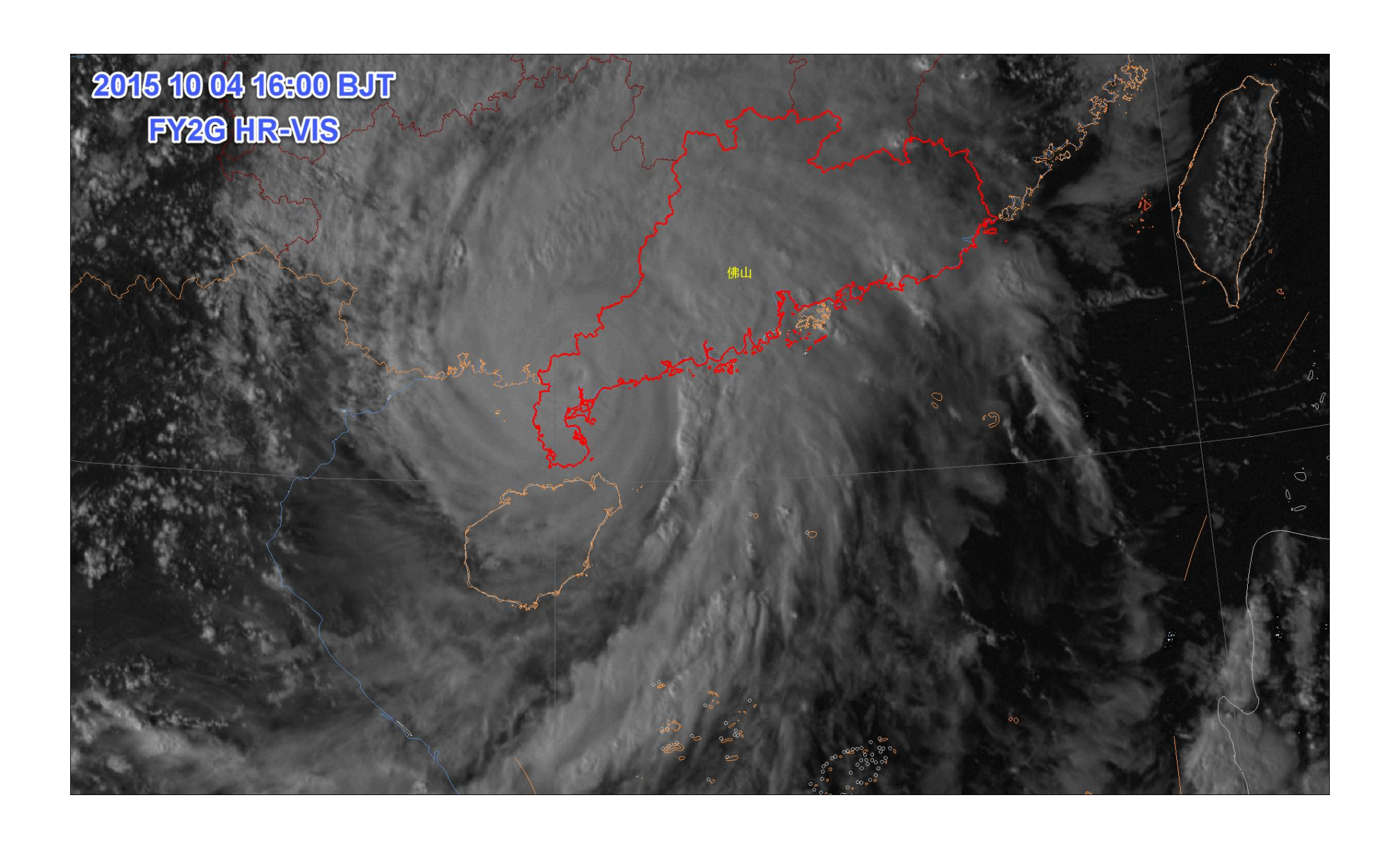


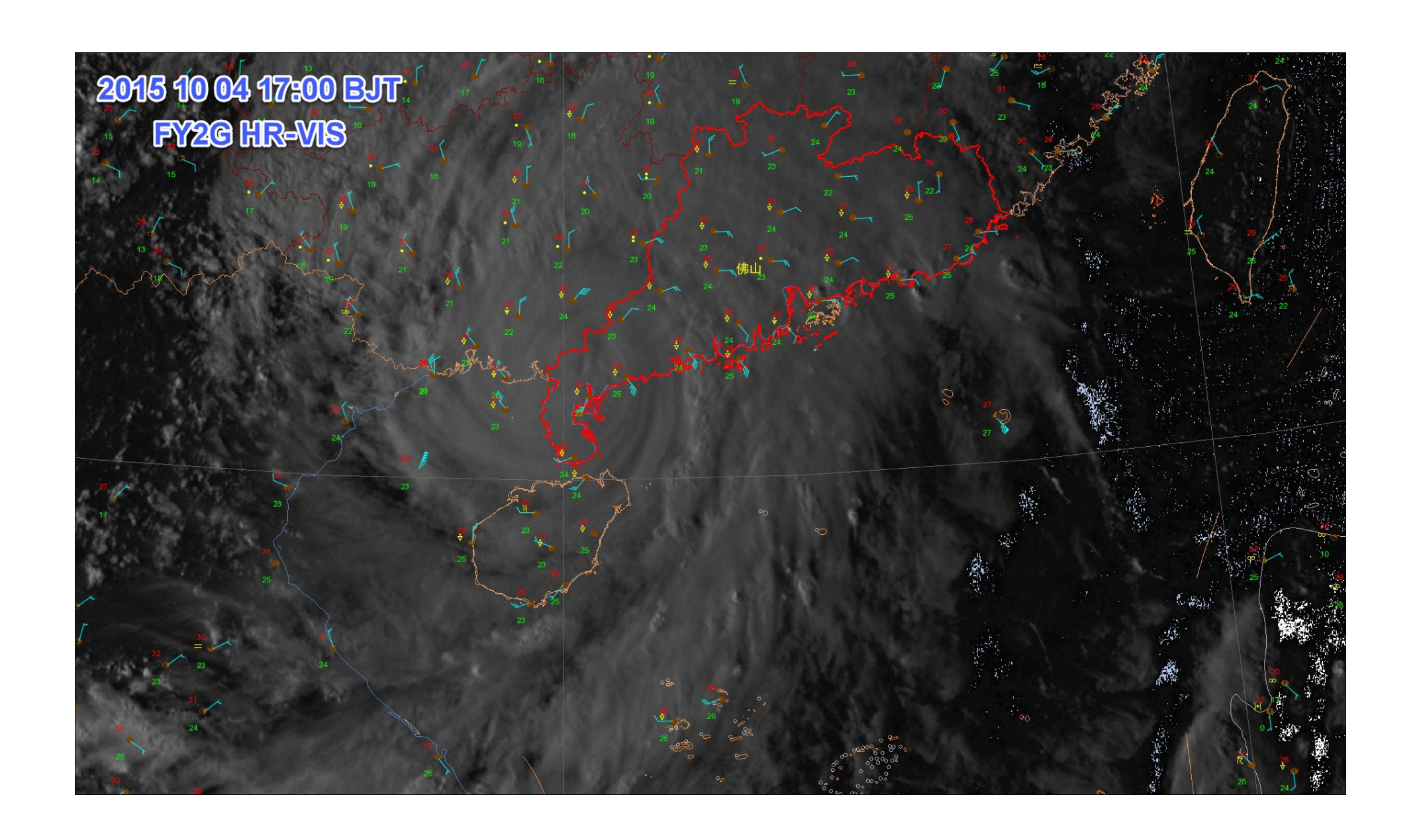


2015 10 04 14:40 BJT dense surface wind observations



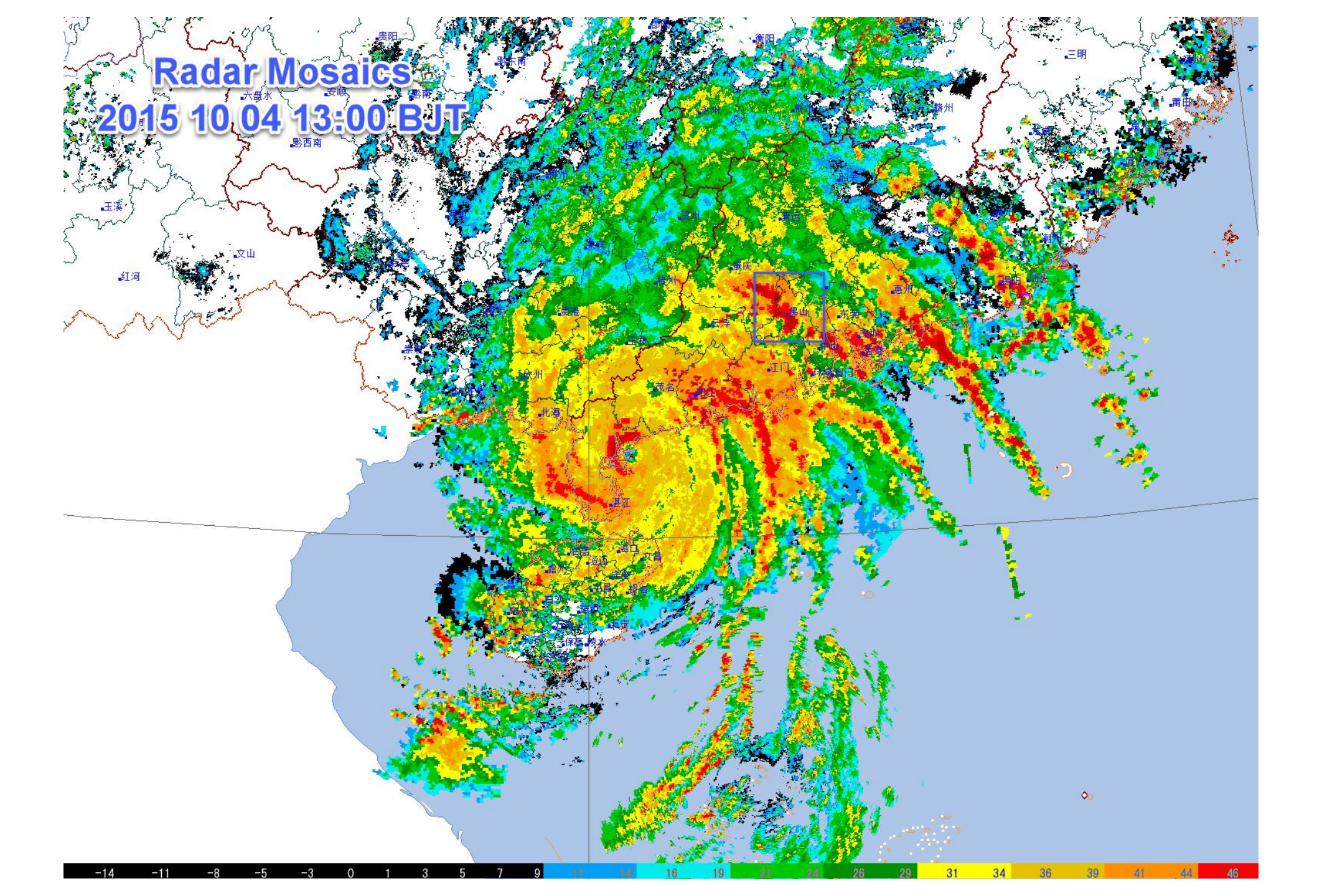


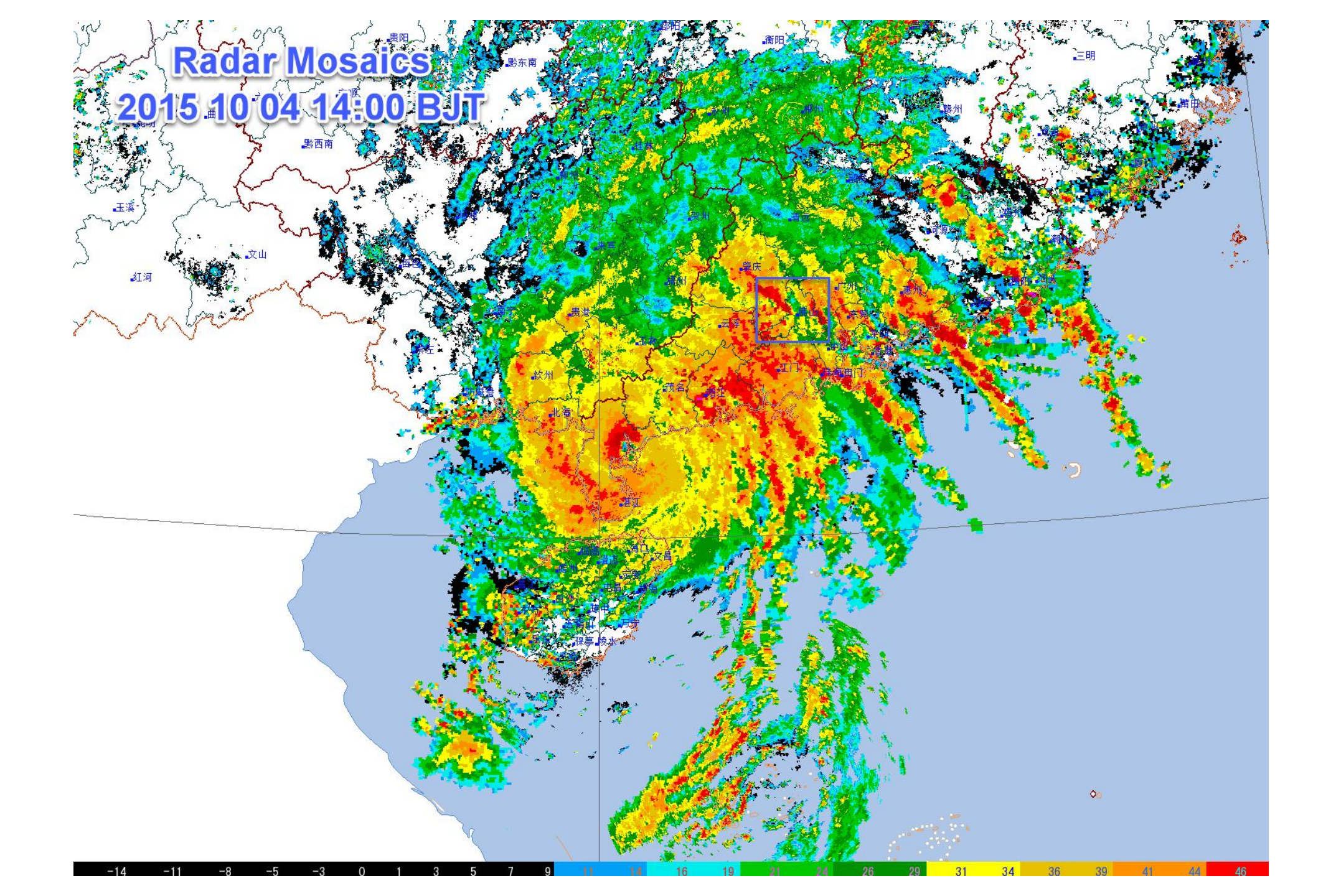


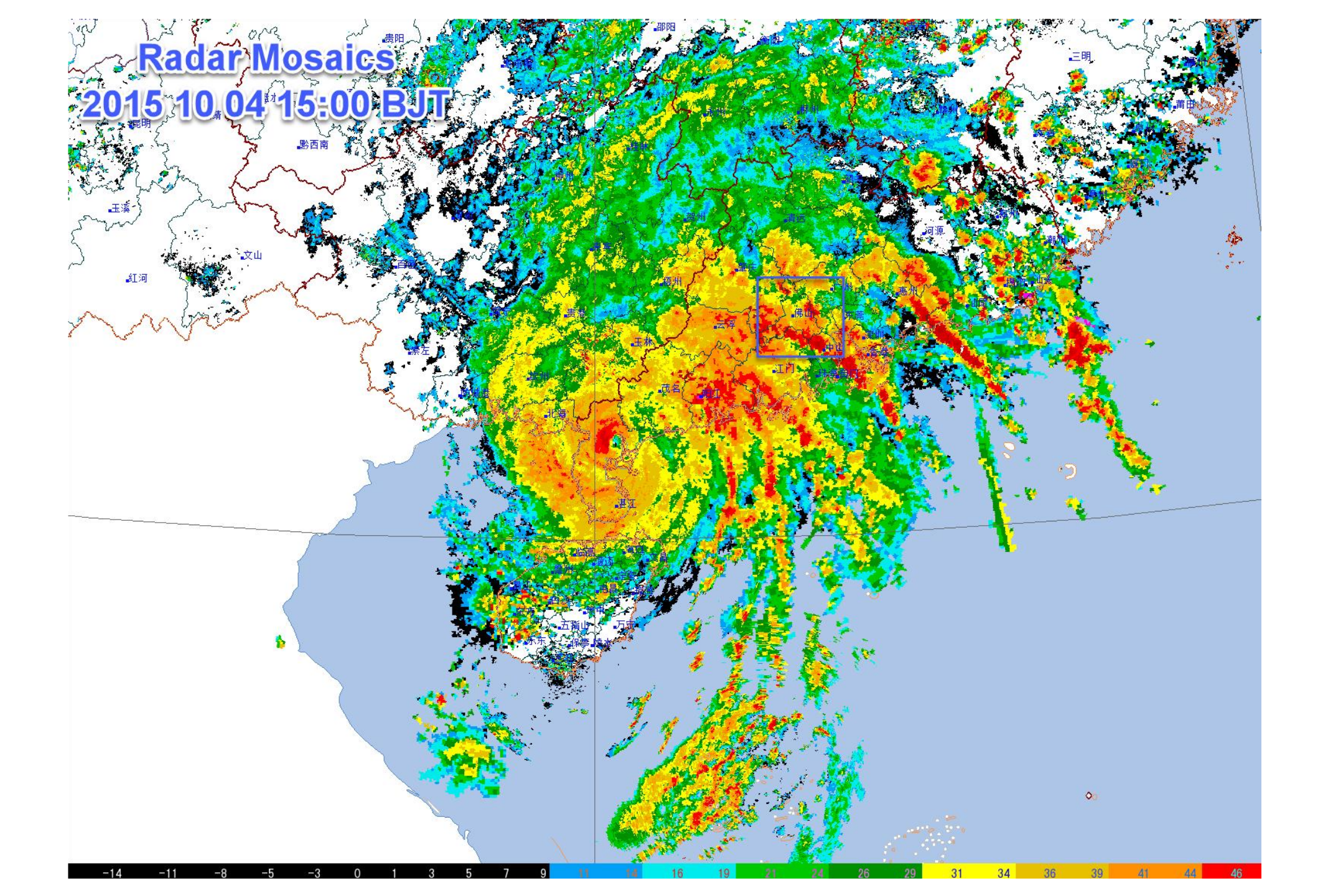


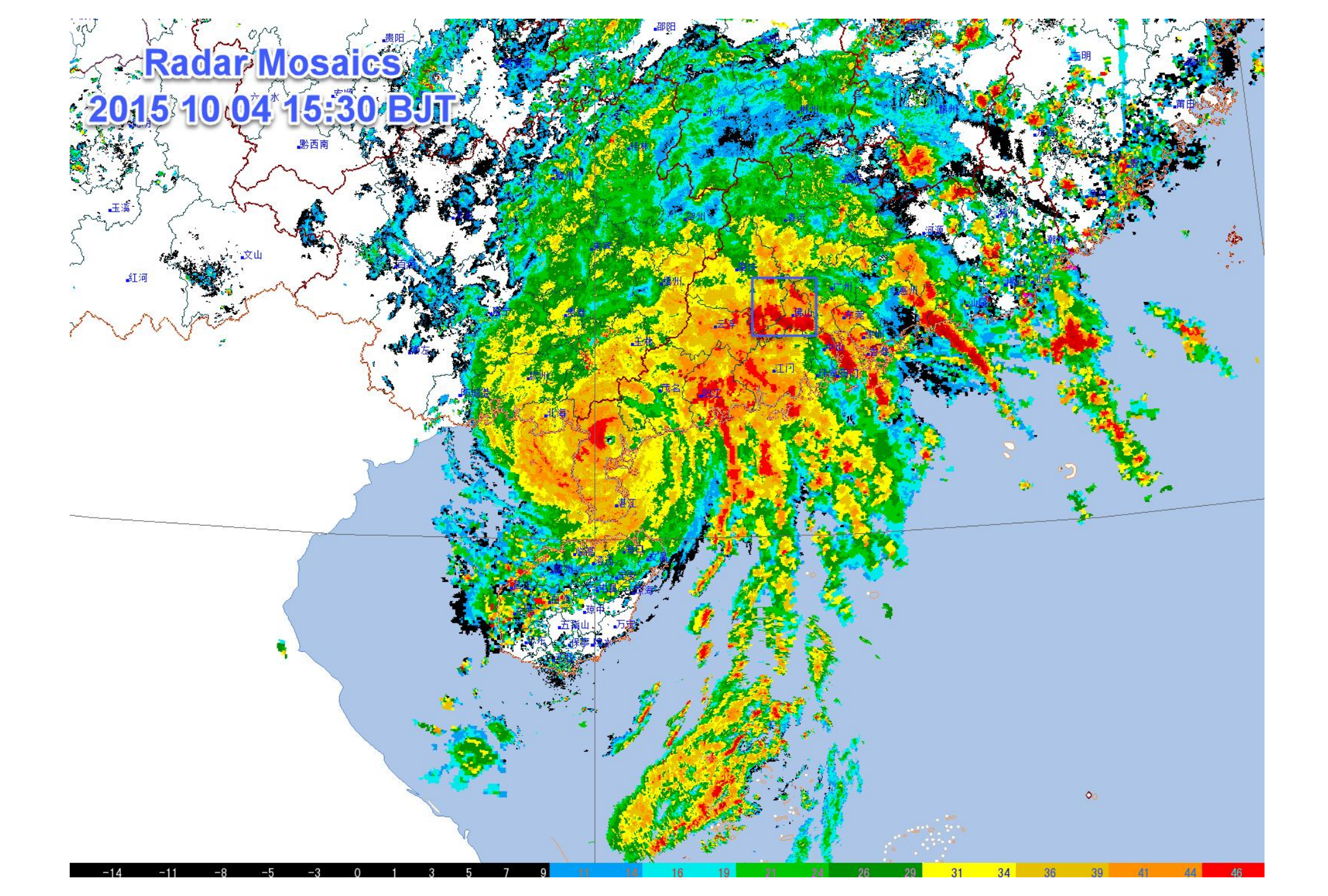
Characteristics of Doppler weather radar echoes

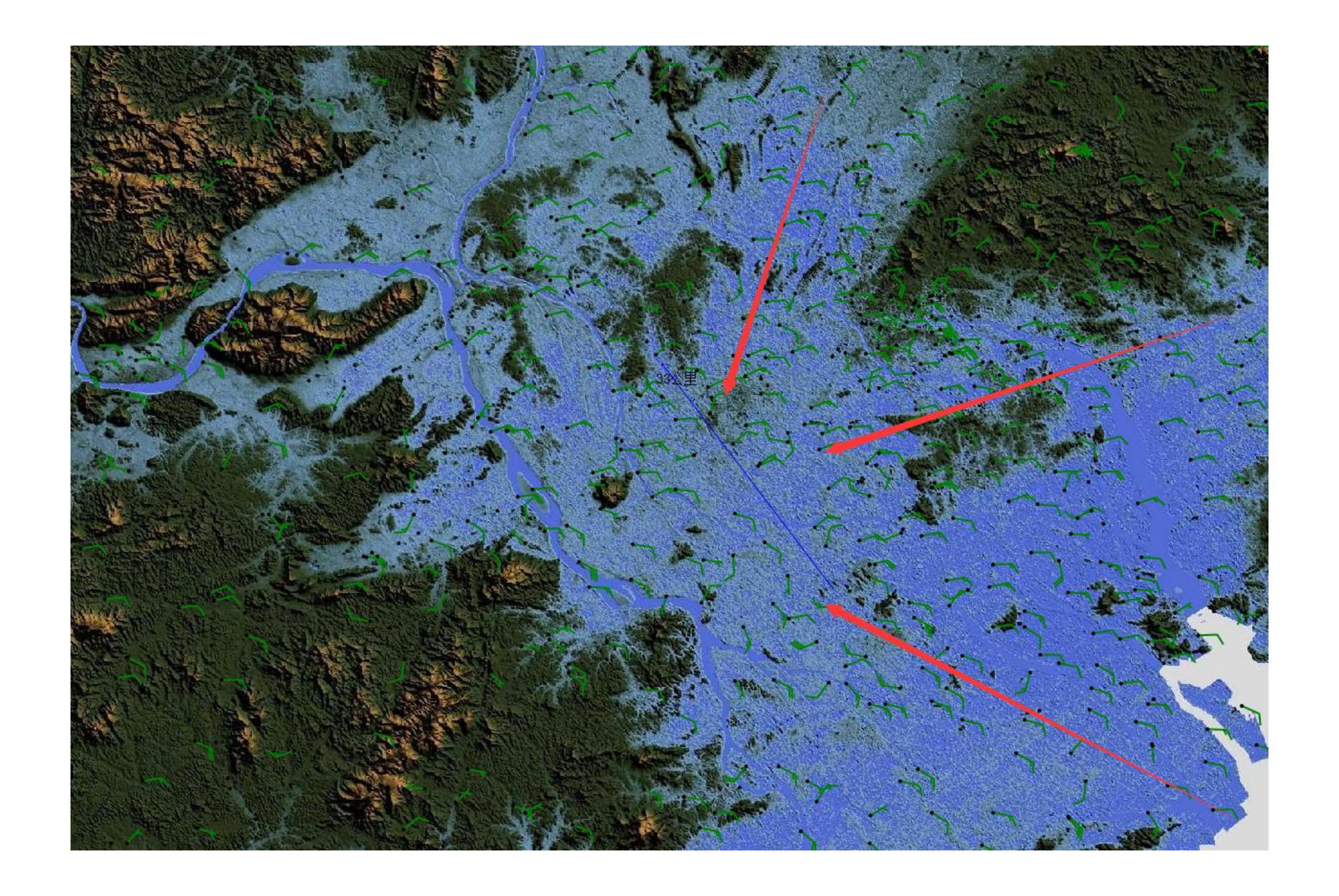
- Radar mosaics
- Single radar echoes

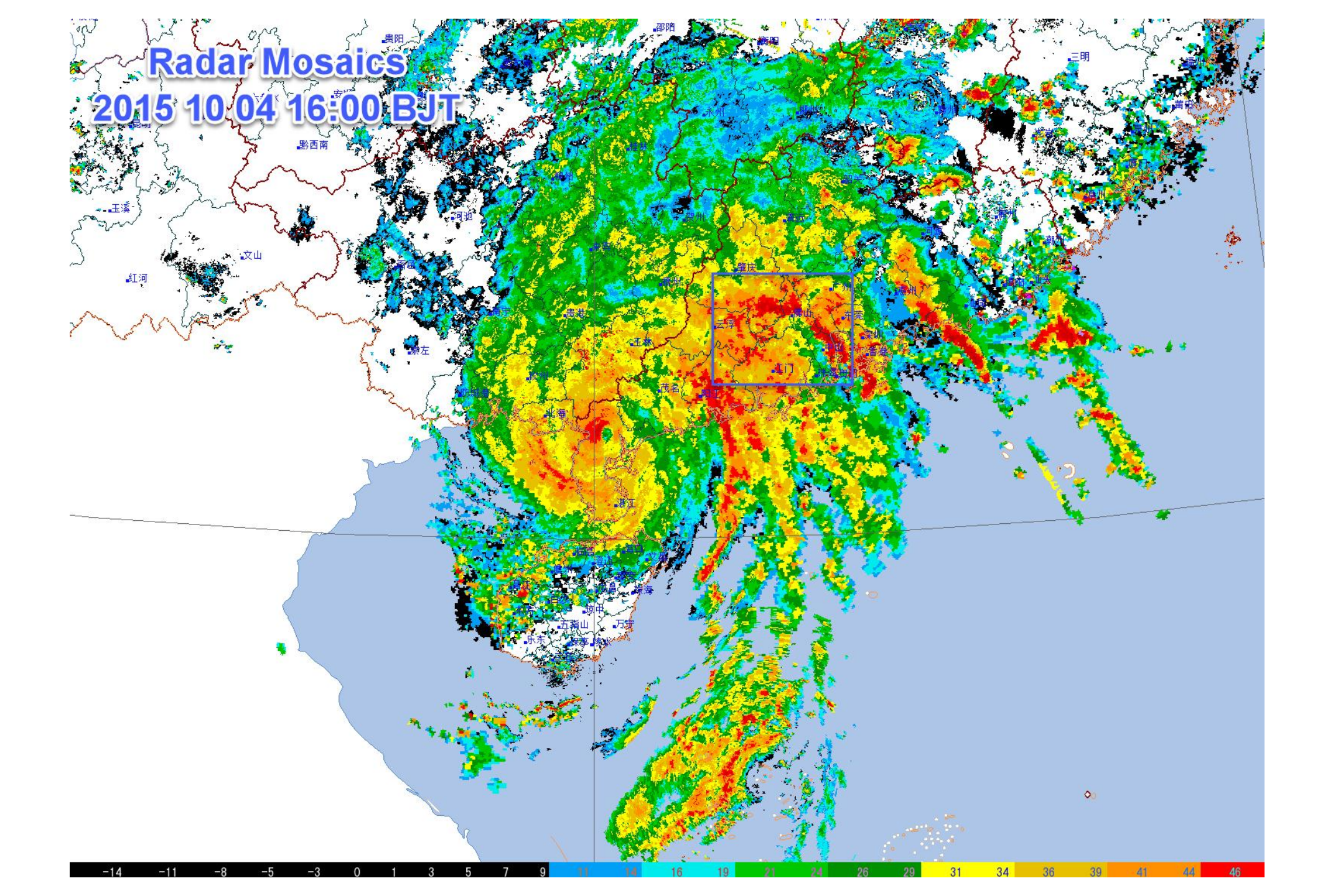


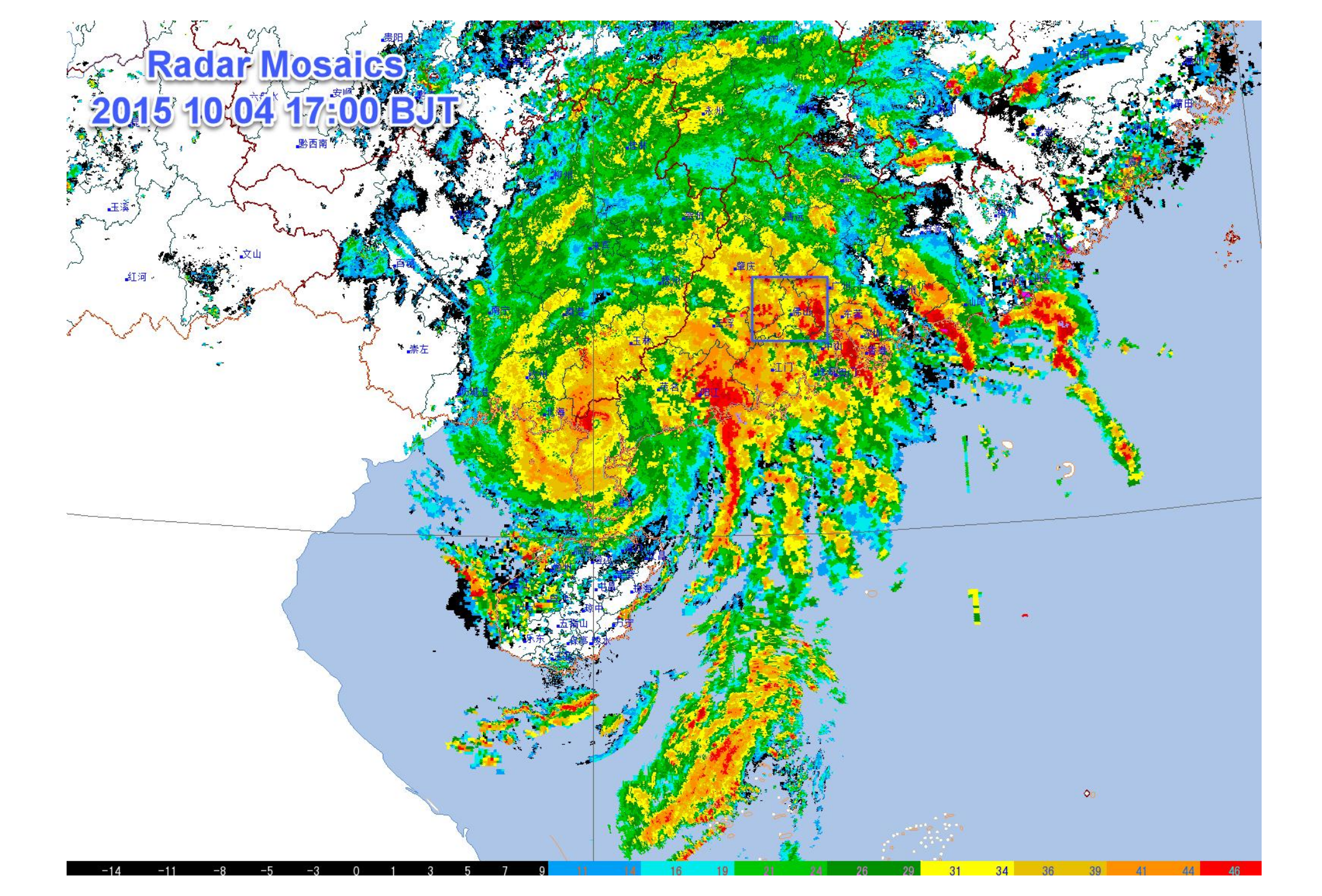




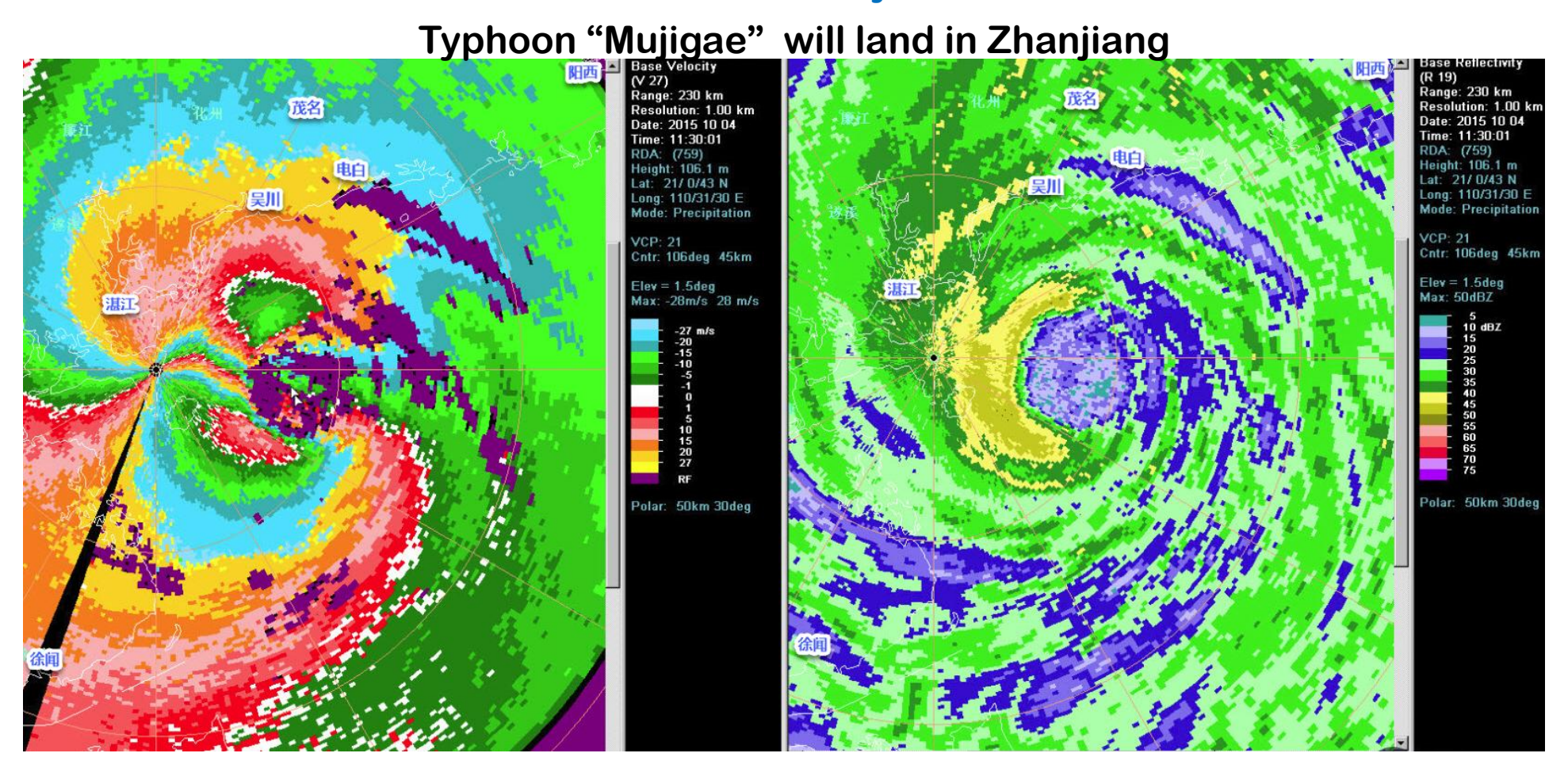




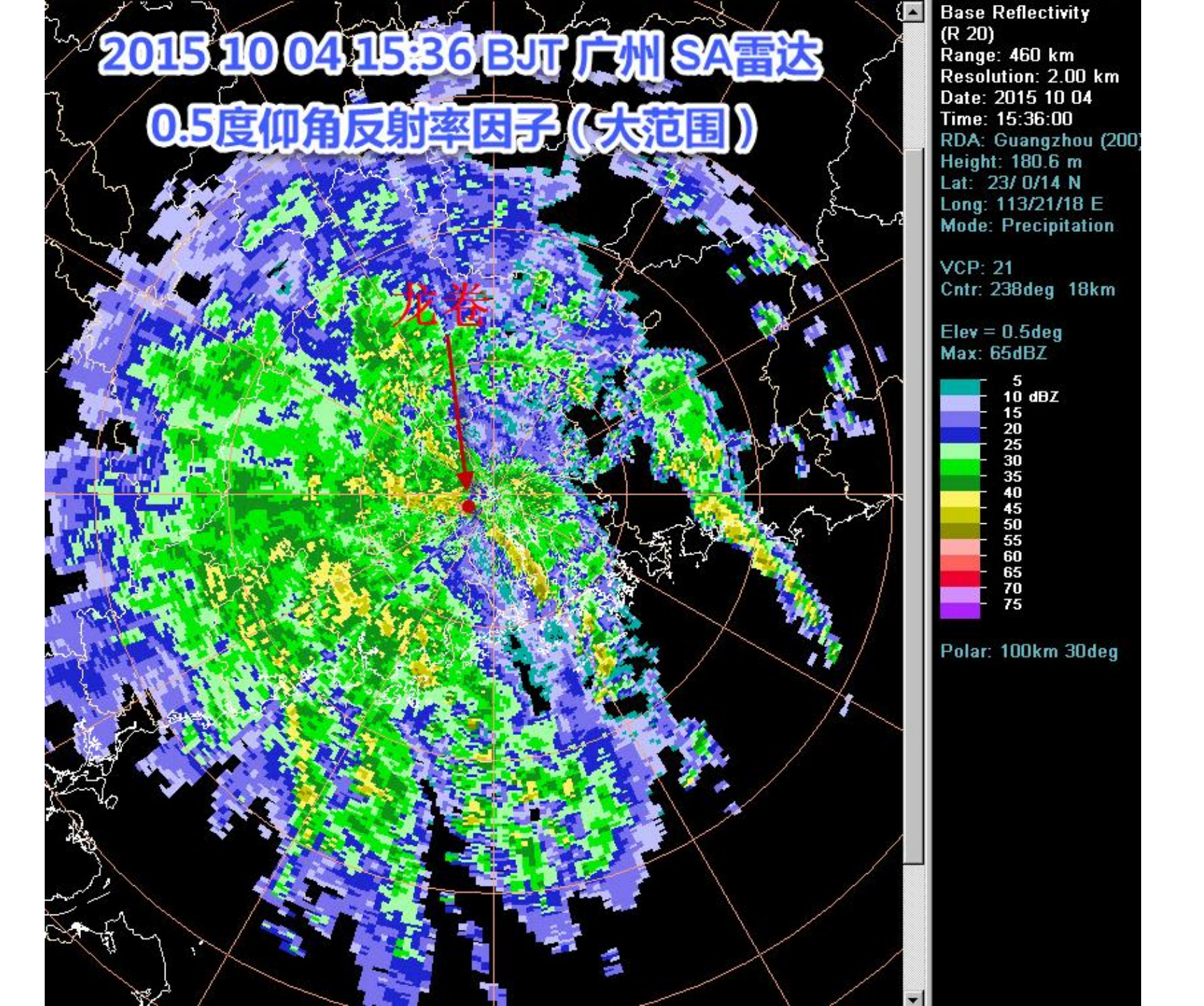




2015 10 04 11:30 BJT Zhanjiang SA radar 1.5° elevation velocity and reflectivity

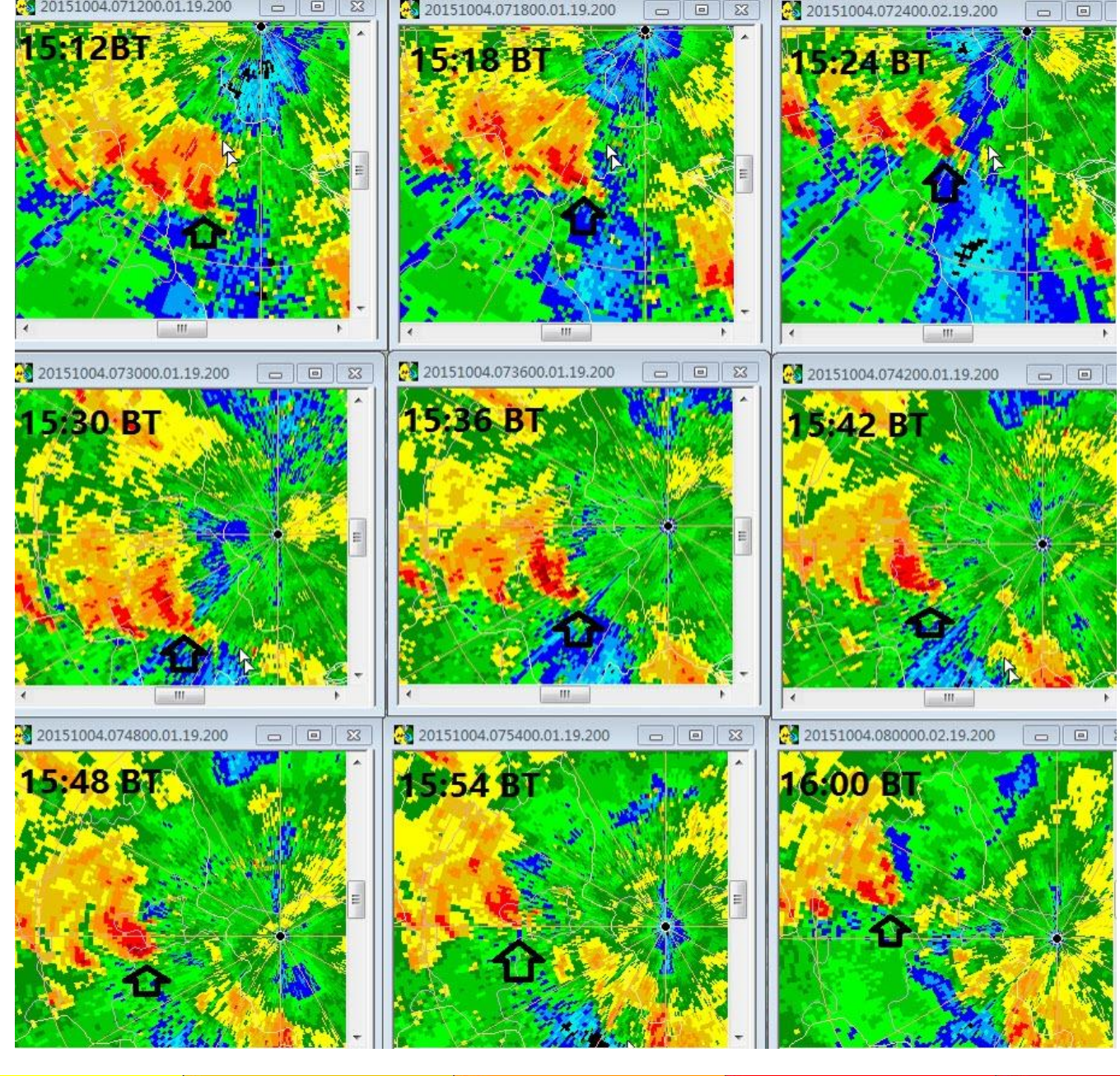


Maximum outbound velocity 70m/s, maximum inbound velocity -66m/s, rotational speed=68m/s; diameter of the TC eye vortex is 32km, the vertical vorticity is 0.85×10^{-2} s⁻¹



2015 10 04 15:36 BJT Guangzhou SA 0.5° elevation reflectivity.

The red arrow points to the position of the tornado.

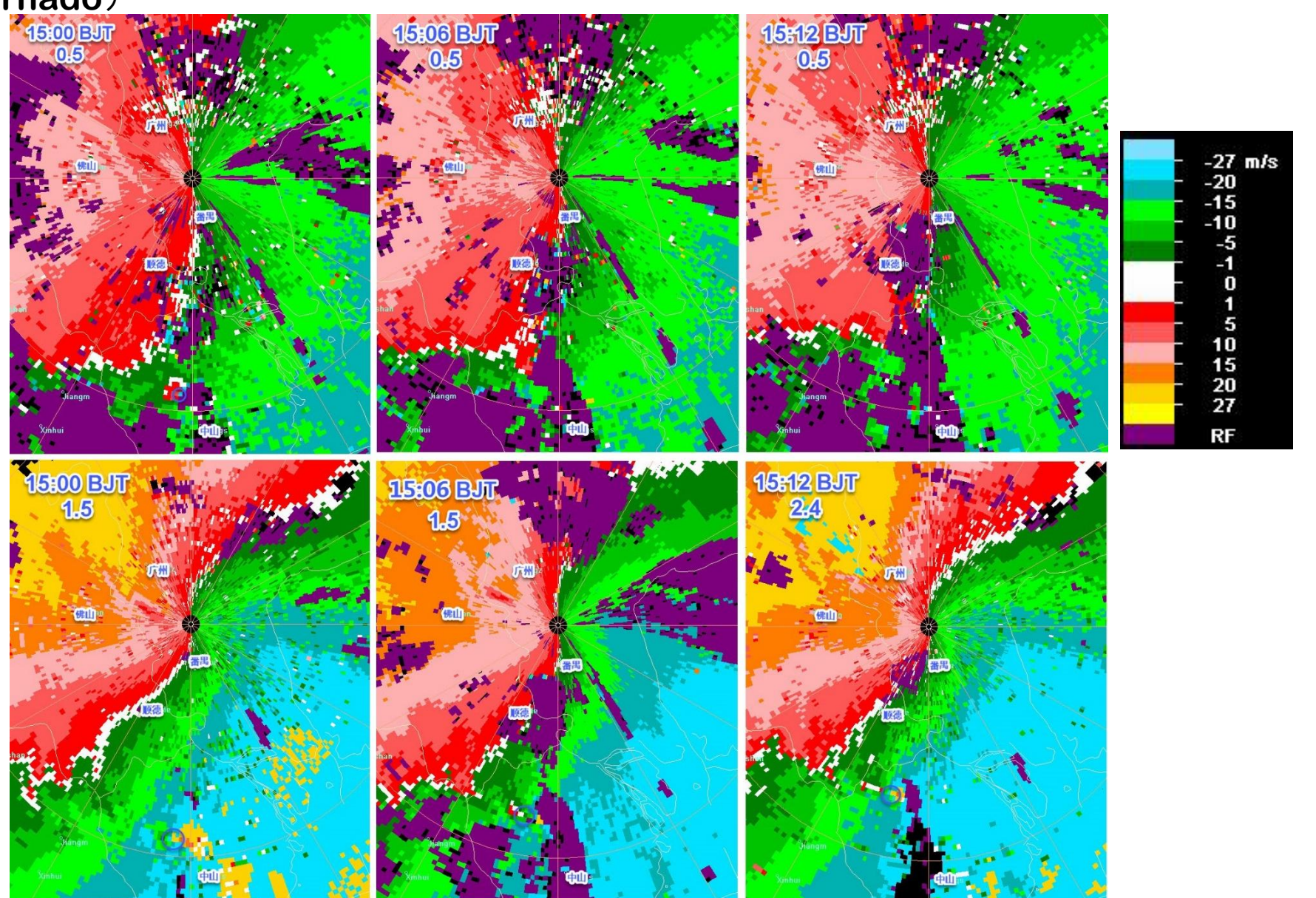


2015 10 04 15:12-16:00 BJT Guangzhou SA radar 05° elevation reflectivity evolution: the black arrow points to the minisupercell producing the tornado.

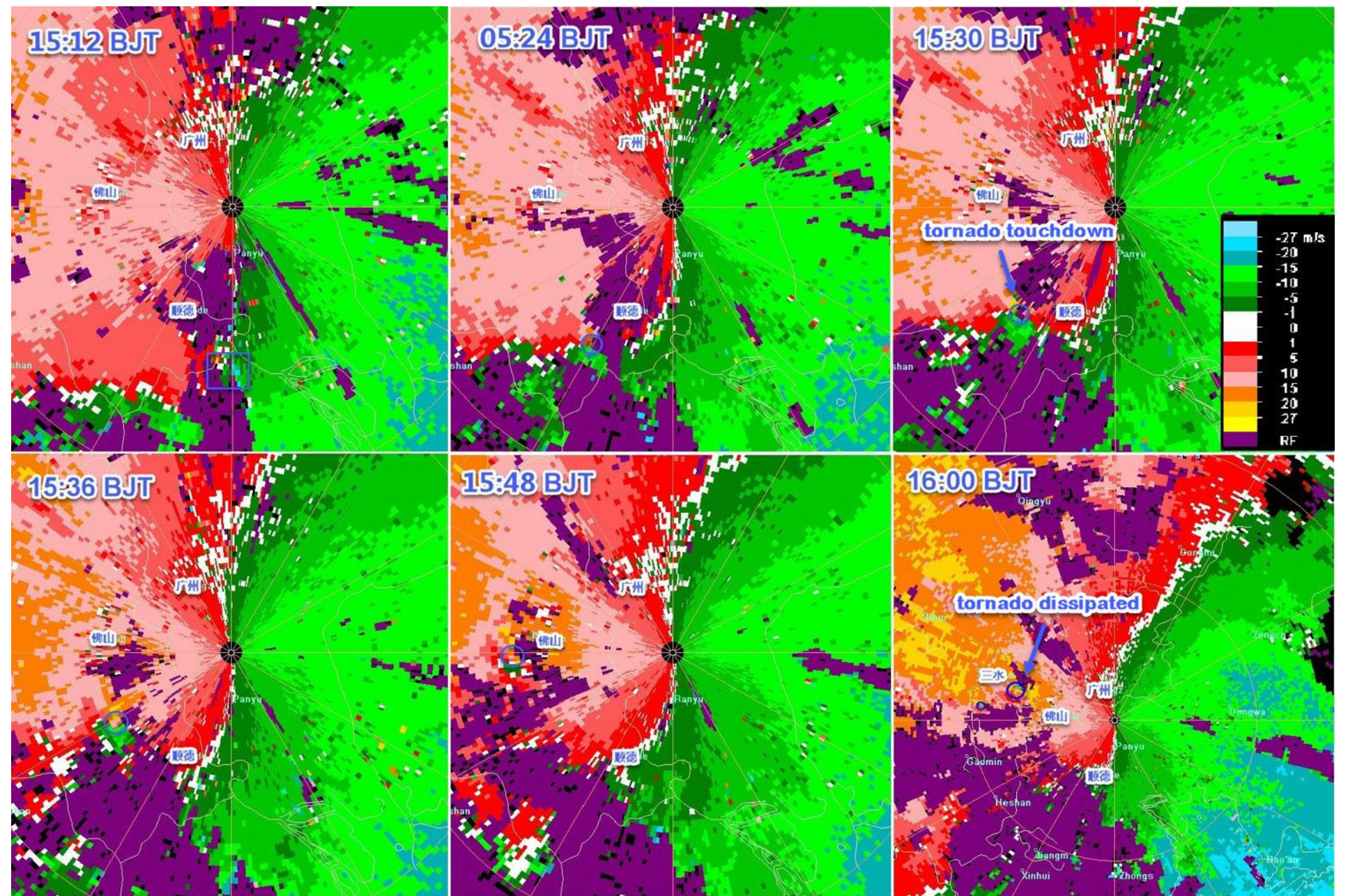
From Li et al., 2016

30 45 50 55

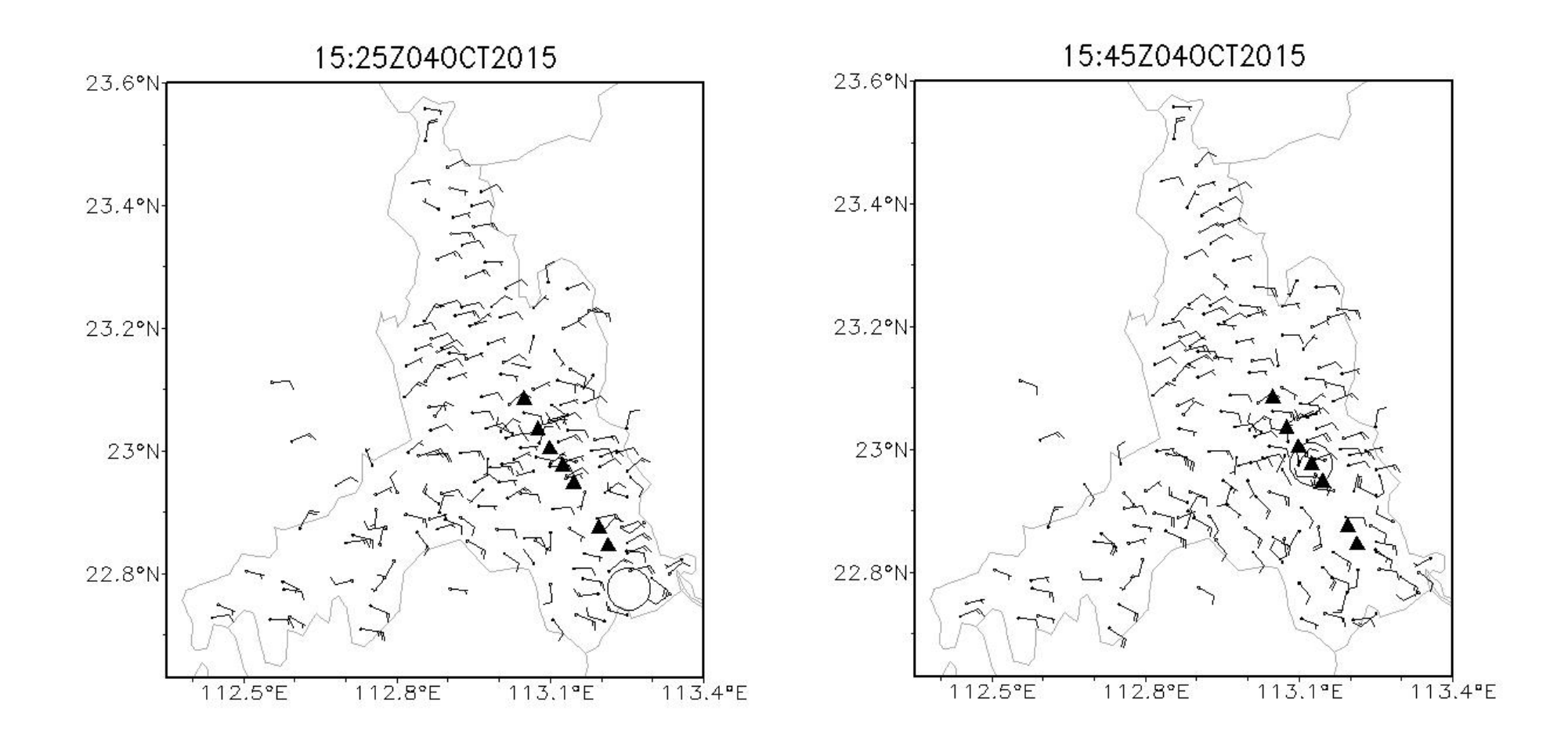
2015 10 04 15:00-15:12 BJT Guangzhou SA radar 0.5° and 1.5° or 2.4° elevation velocity (small blue circle refers to mesocyclone leading to the tornado)

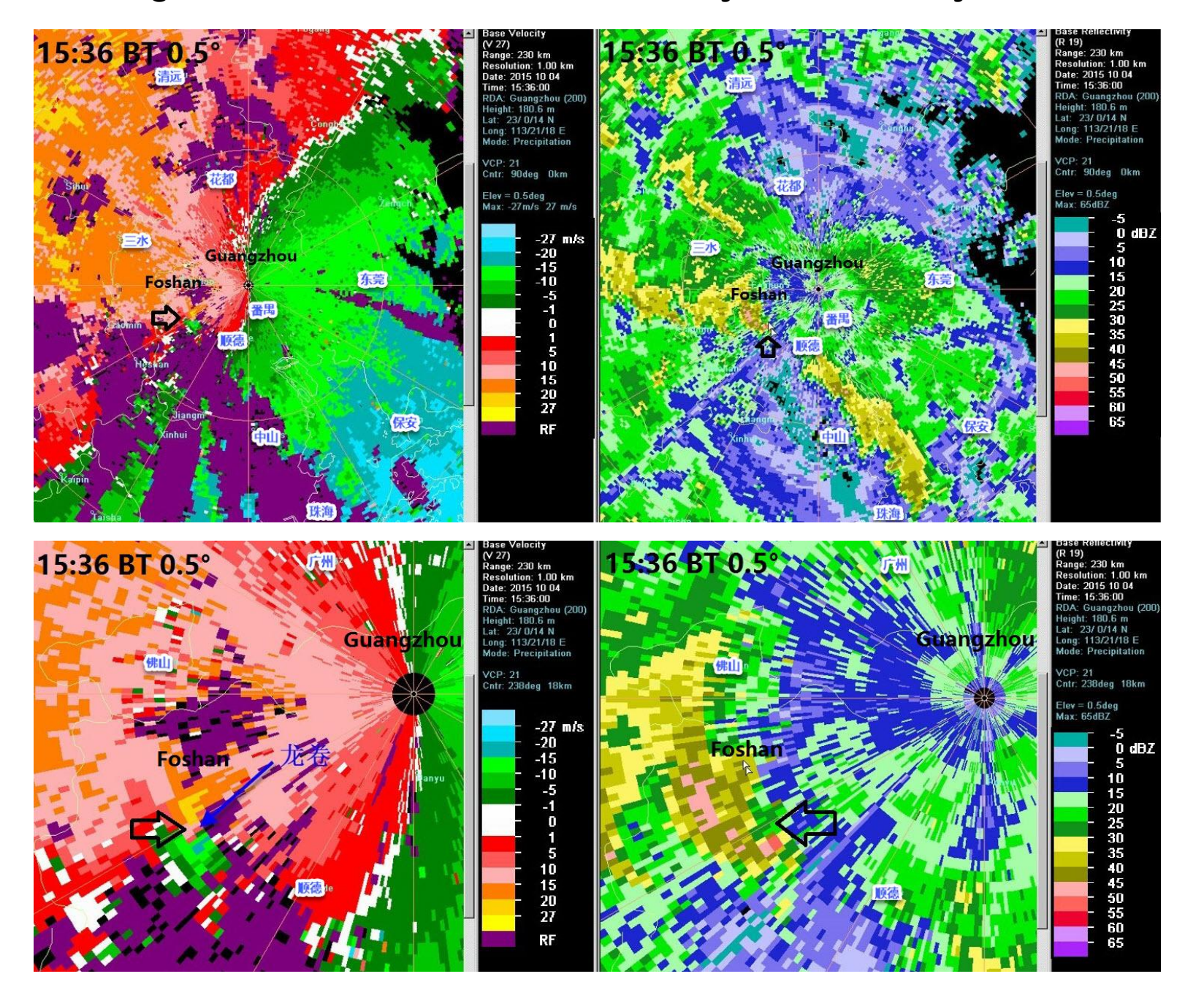


2015 10 04 15:12-16:00 BJT Guangzhou SA radar 0.5° elevation velocity evolution (small blue circle refers to mesocyclone leading to the tornado)

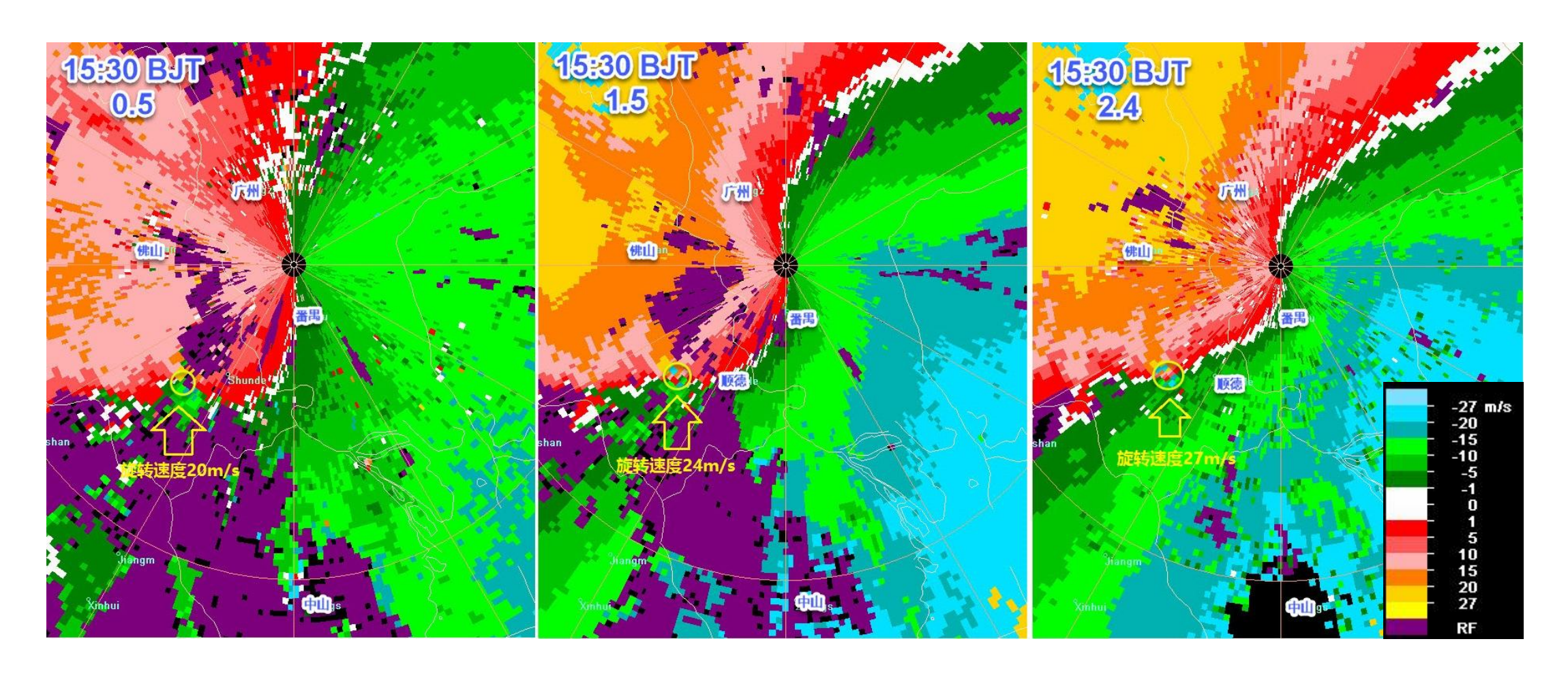


2015 10 04 15:25 and 15:45 BJT surface 2-minute mean wind observations (▲ refer to tornado path)

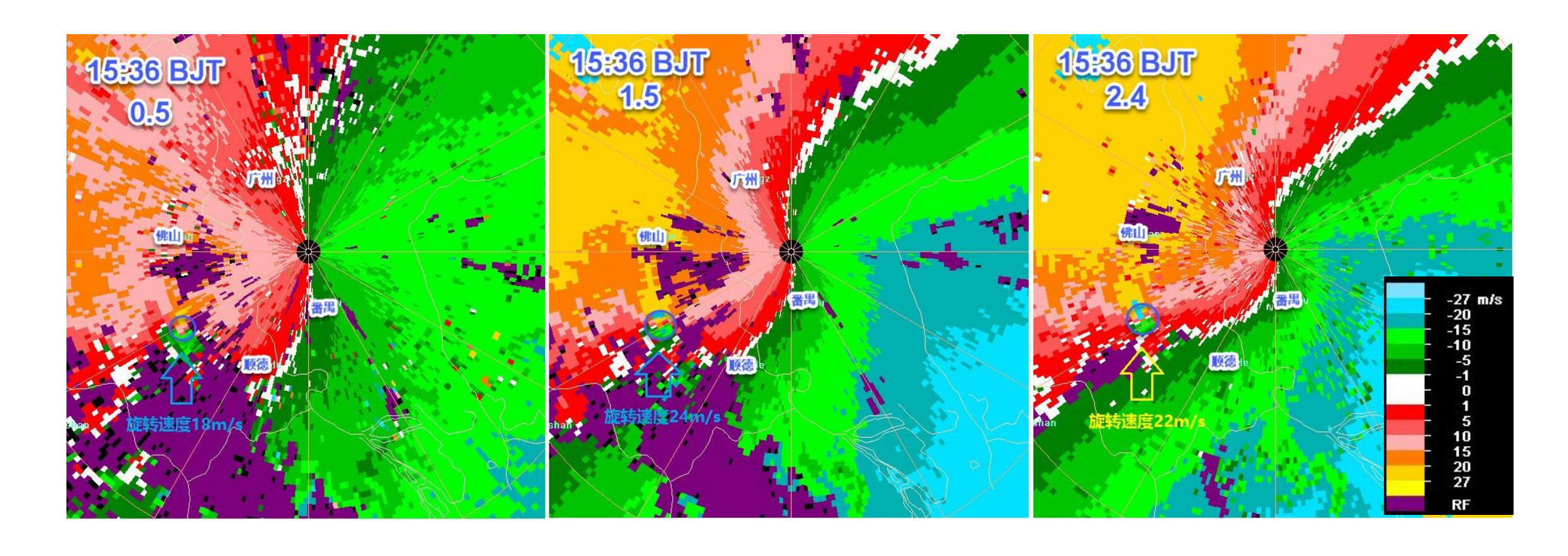




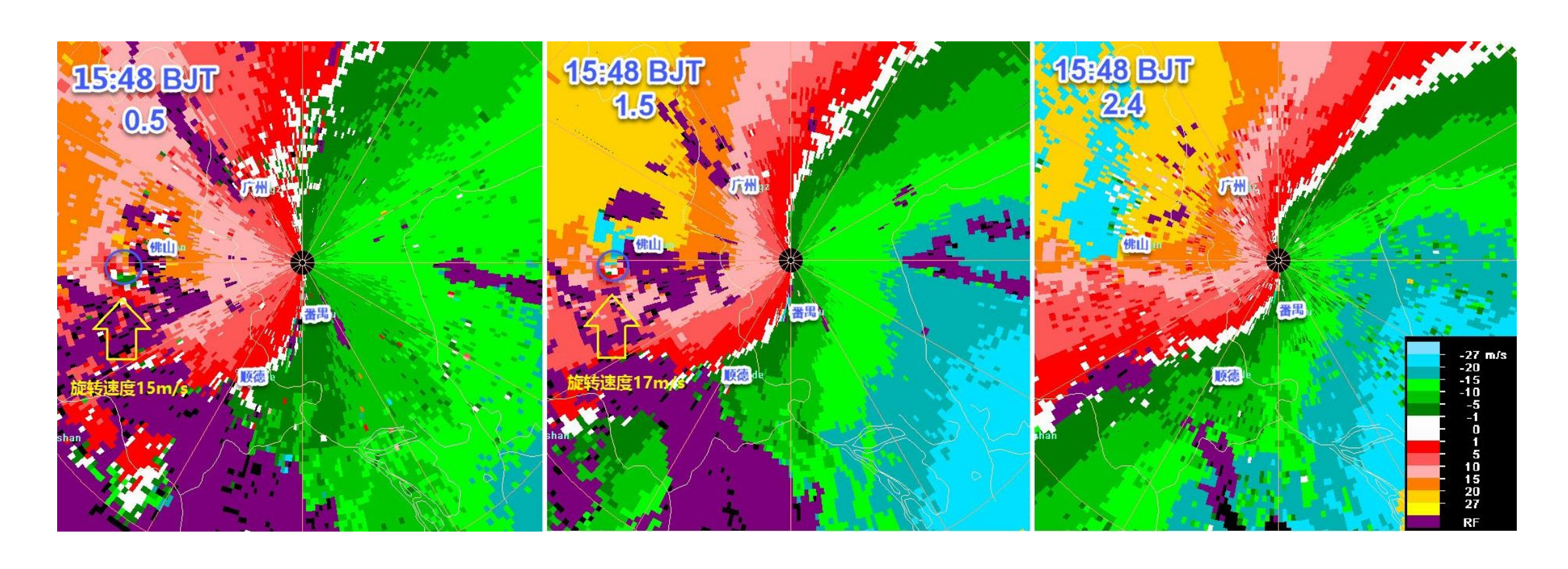
2015 10 04 15:30 BJT Guangzhou SA radar 0.5, 1.5 and 2.4° elevation velocity, the small yellow circles refer to the mesocylones leading to the tornado



2015 10 04 15:36 BJT Guangzhou SA radar 0.5, 1.5 and 2.4° elevation velocity, the small blue circles refer to the mesocylones leading to the tornado



2015 10 04 15:48 BJT Guangzhou SA radar 0.5, 1.5 and 2.4° elevation velocity, the small blue circles refer to the mesocylones leading to the tornado



Case01 summary

- 2015 10 04 13:00 BJT, Typhoon "Mujigae" landed on Zhanjiang City, Guangdong Province. two and a half hour later, from 15:28 BJT to 16:00 BJT, a mini-supercell embedded in the spiral rain belt of this Typhoon, 200km northeast from the Typhoon center, produced a EF3 tornado.
- Based on the Hongkang sounding at 08:00 BJT on the 4th October 2015, it shows weak conditional instability in the lower troposphere, with the temperature difference between 850 and 500 hPa being 21° C; There is abundant water vapor in lower troposphere, with surface dew point being 24° C, and precipitable water being 67mm; The weak conditional instability and abundant water vapor in the lower troposhere give a relative weak CAPE (580J/kg) and CIN(22J/kg); The 0-6km and 0-1km wind vector difference are 20m/s and 14m/s, respectively, with 0-3km SRH being 450m²s⁻² and LCL being 350m. These conditions are favorable the supercell tornadoes.
- Around 15:00 BJT on 4th October 2015, The Guangzhou SA radar began to detect a mini-supercell with mesocyclone embedded in the spiral convective rainbelt, 200km to northeast of TC center, the mesocyclone located in Zhongshan City at the moment, Guangdong Province. Afterwards, the mesocyclone moved northward into the Shunde town of Foshan City, Guangdong Province. The tornado touched down within the mesocyclone around 15:28 BJT, eventually moved to the City center, and dissipated at 16:00 BJT.
- During the evolution of the tornado, the parent mesocyclone attains its maximum intensity at 15:30 and 15:36 BJT, with 1.5° elevation rotational speed being 24m/s, mesocyclone diameter being 3.5km, the corresponding vertical vorticity being 2.7×10-2s-1°.

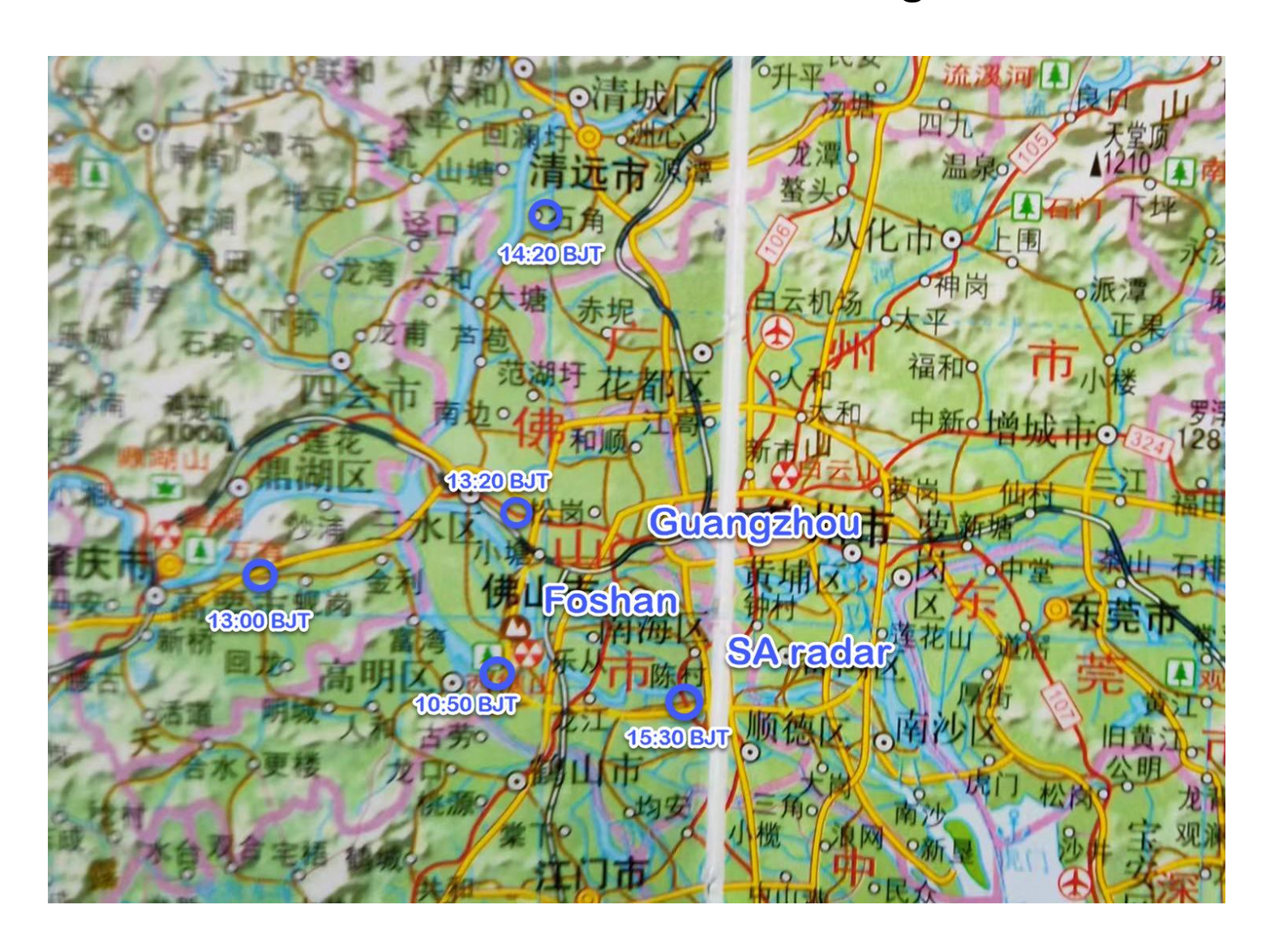
Case02 2006 08 04 Guangdong Pearl River Delta region TC Tornadoes

- Ground truth
- Weather pattern and environmental conditions
- Satellite Images
- Characteristics of Doppler weather radar echoes
- Summary

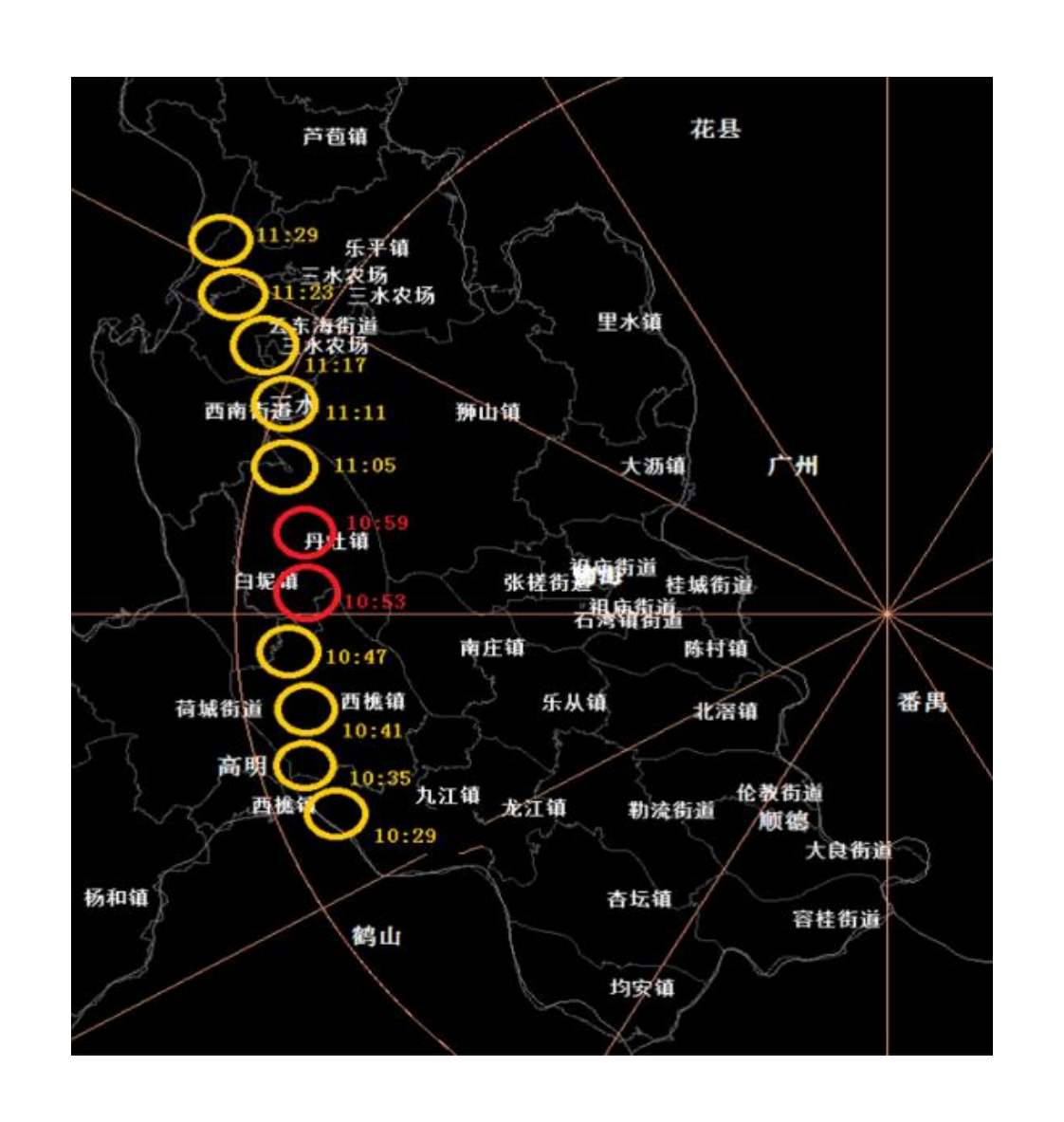
Ground truth

 On the 4th August 2006, five tornadoes produced by the mini-surpercells embeded in the outer spiral rain belts of Typhoon "Prapiroon" hit Danzao town, Baini town, Dali town of Foshan city, Jindu town of Zhaoqing city, and Shijiao town of Qingyuan city, 9 people were killed. The first tornado (10:50 BJT Danzao town) was considered EF2 rank based on the damage survey, no damage survey have been done for other four tornadoes.

The five TC tornadoes on the 4th August 2006



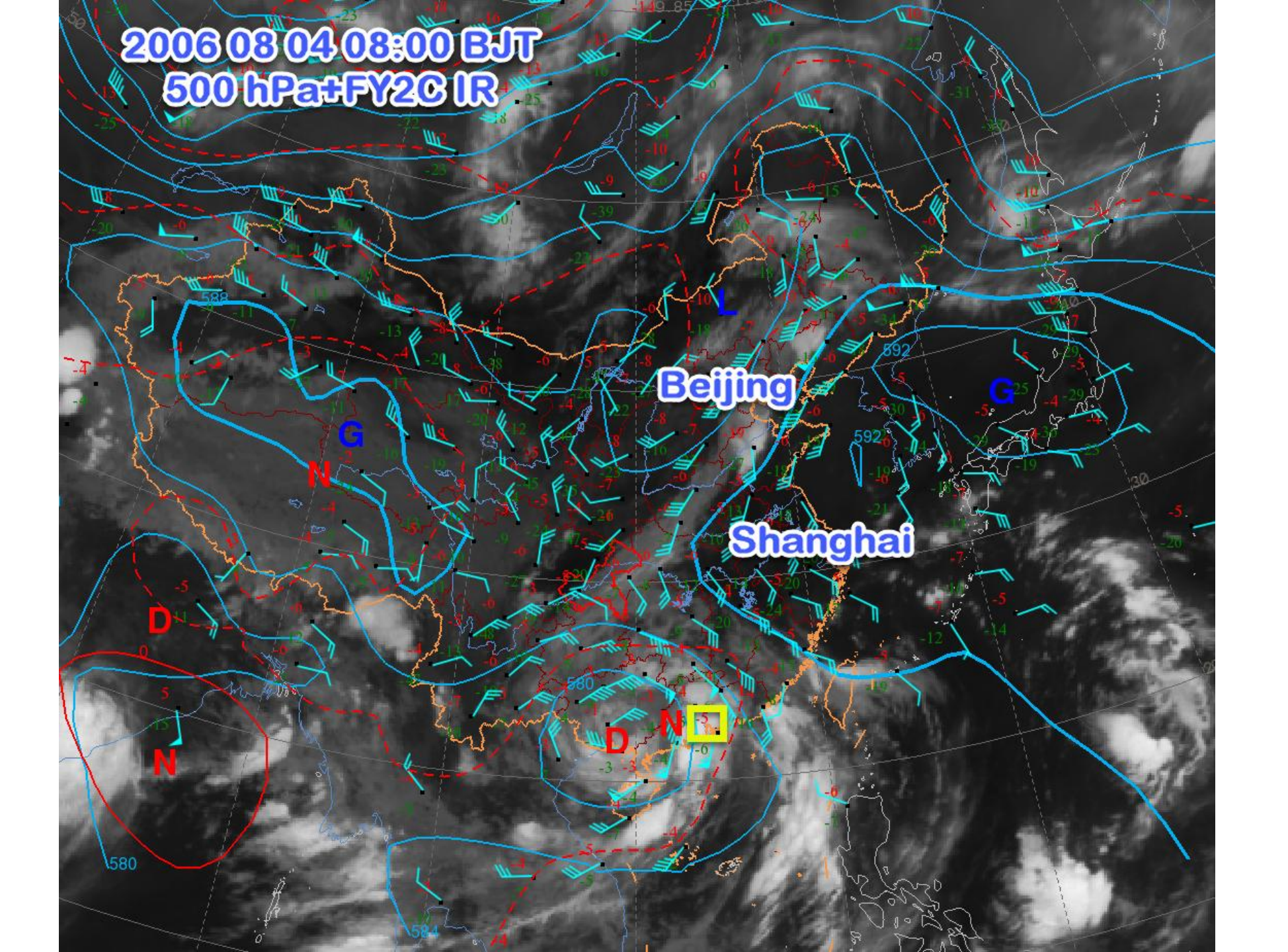
The Danzao town tornado, 10:50 BJT, the path and photo.

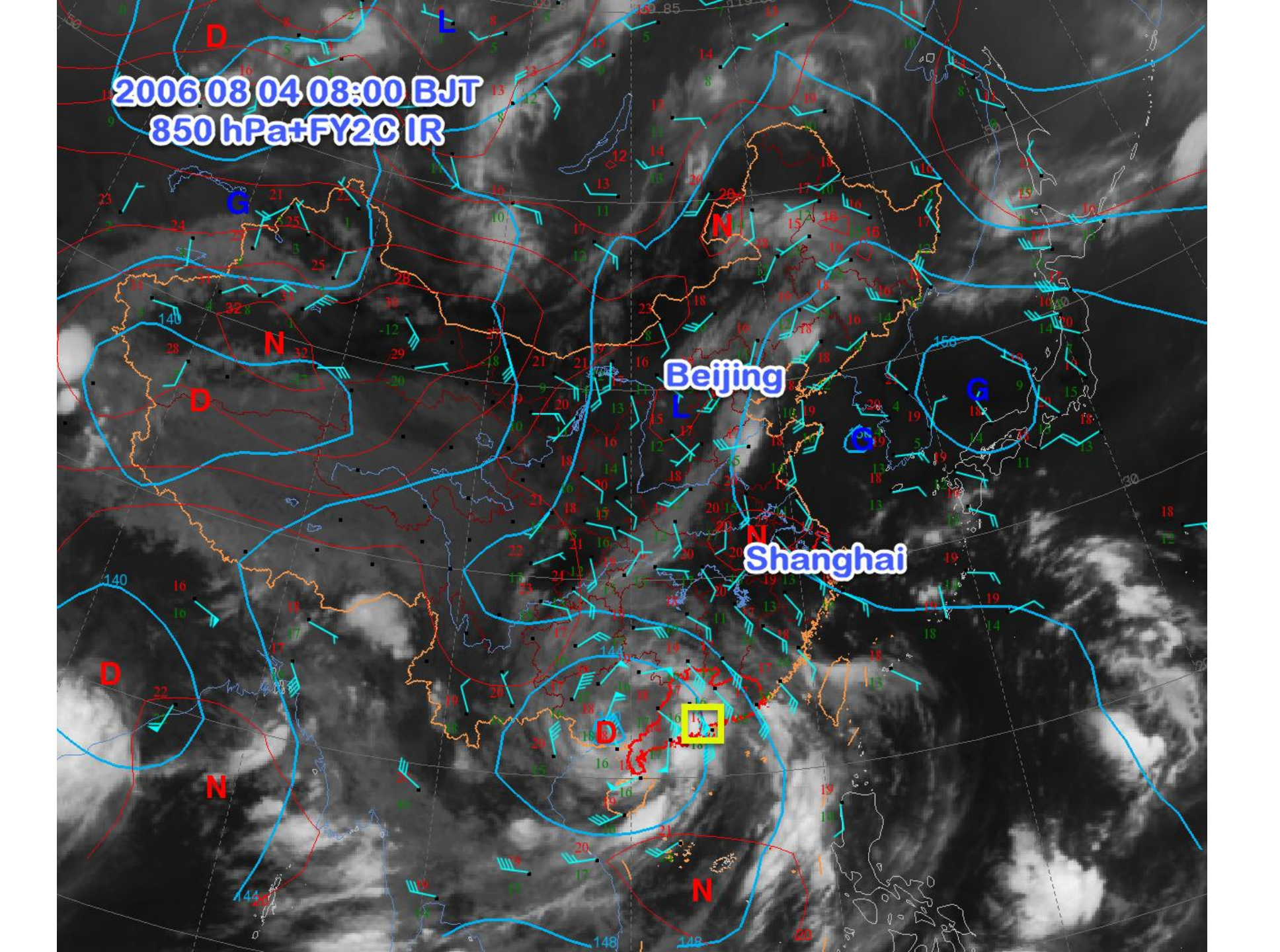


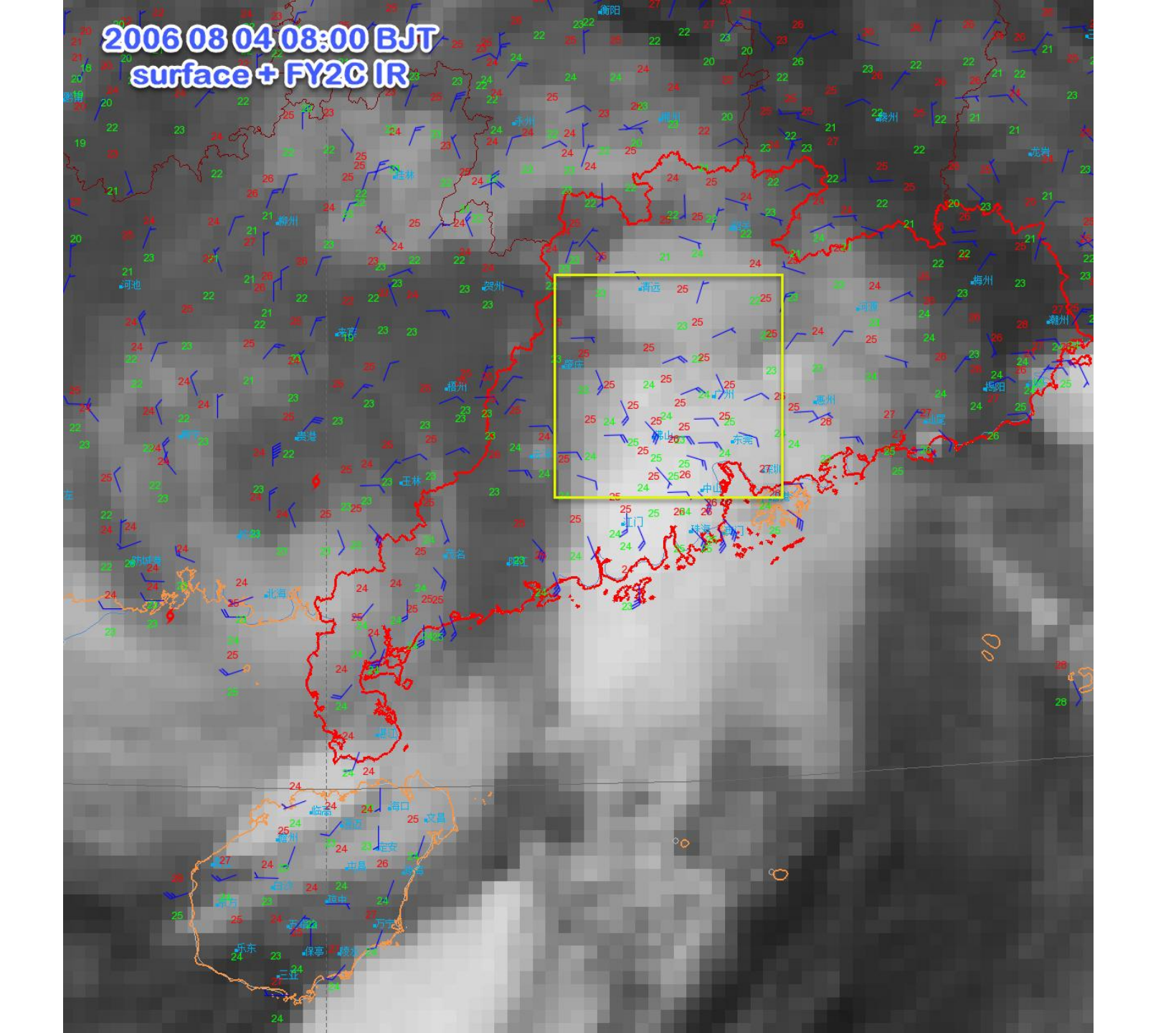


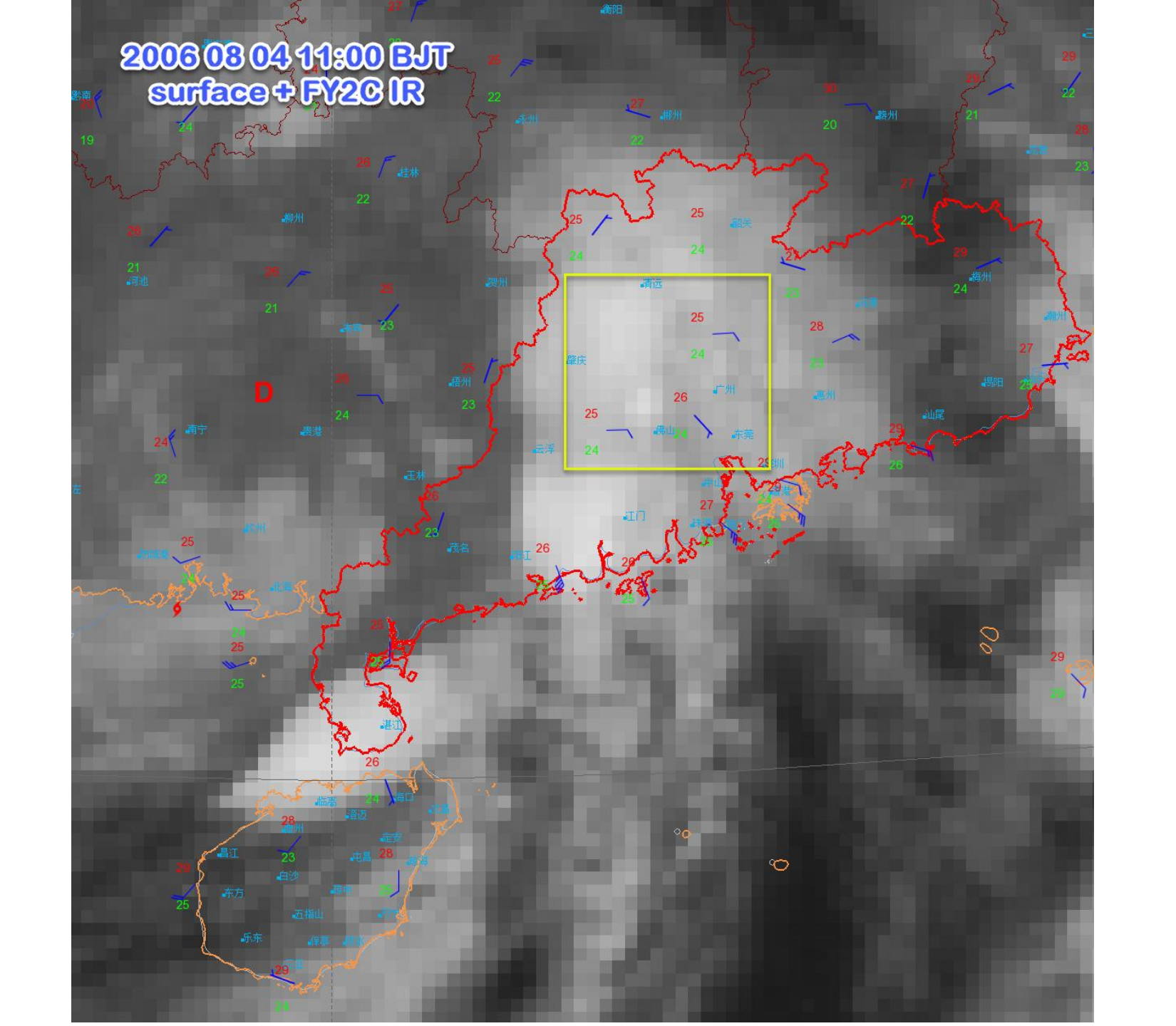
Weather pattern and environmental conditions

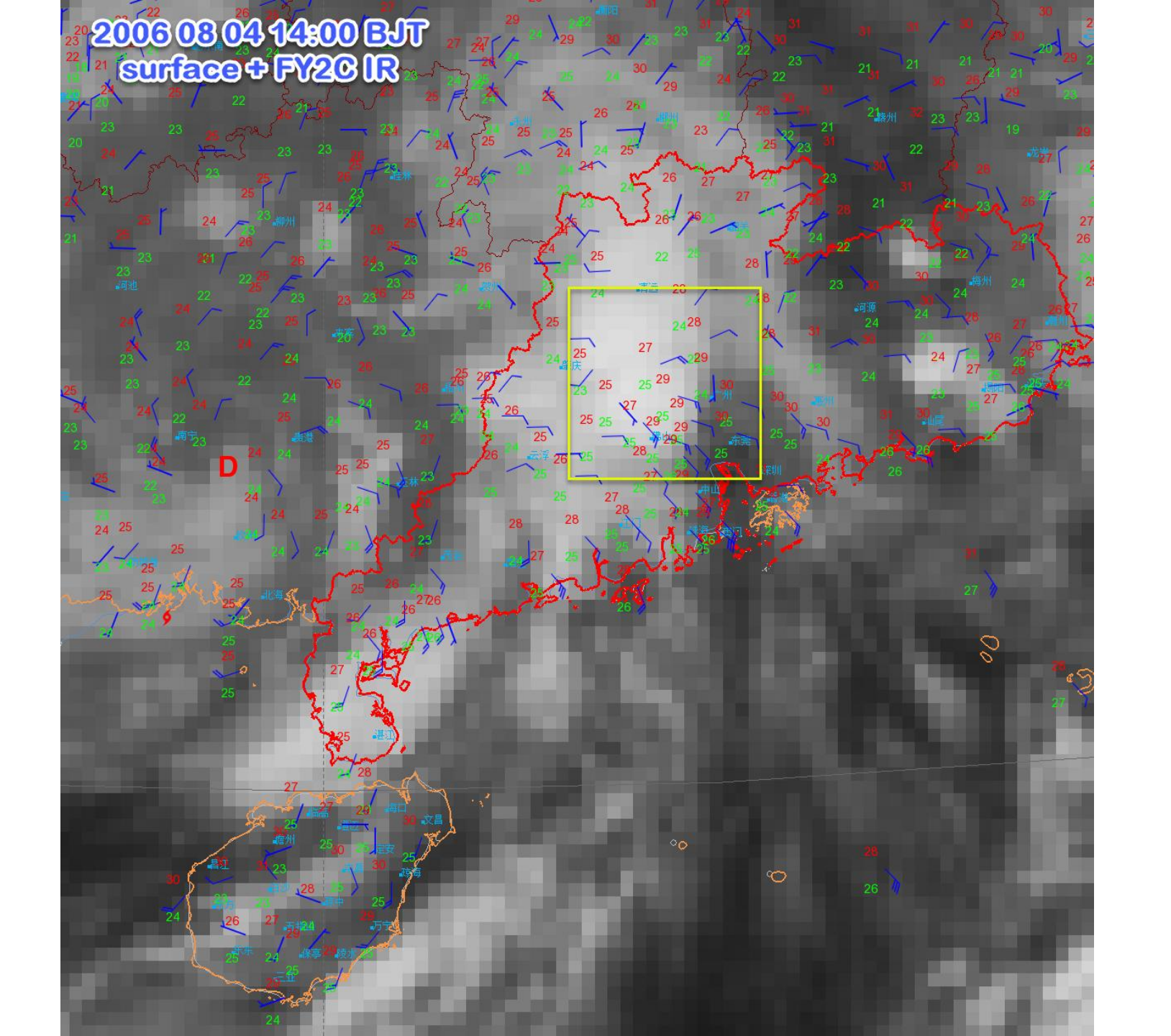
- Upper-air maps
- Surface maps
- Satellite images

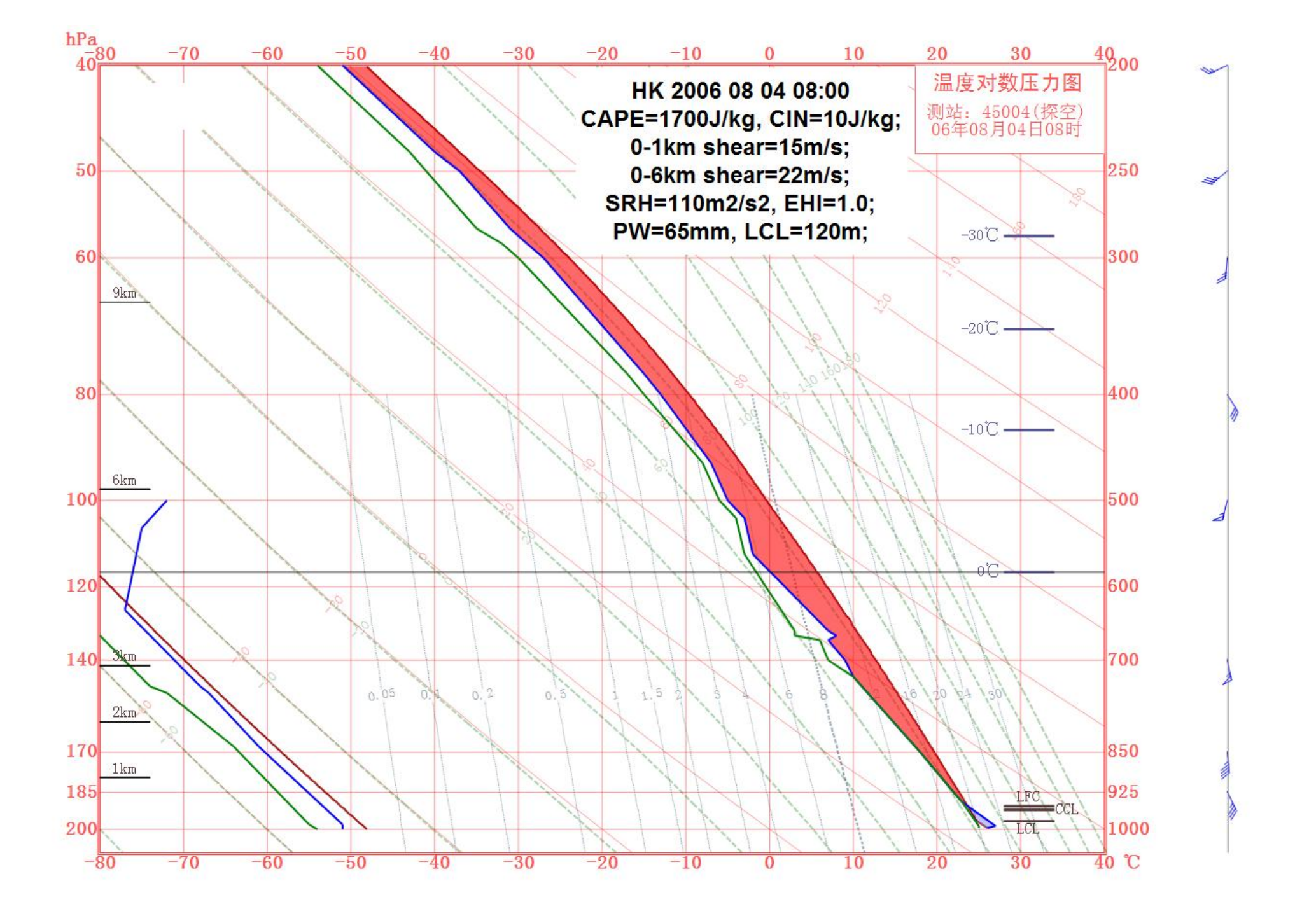






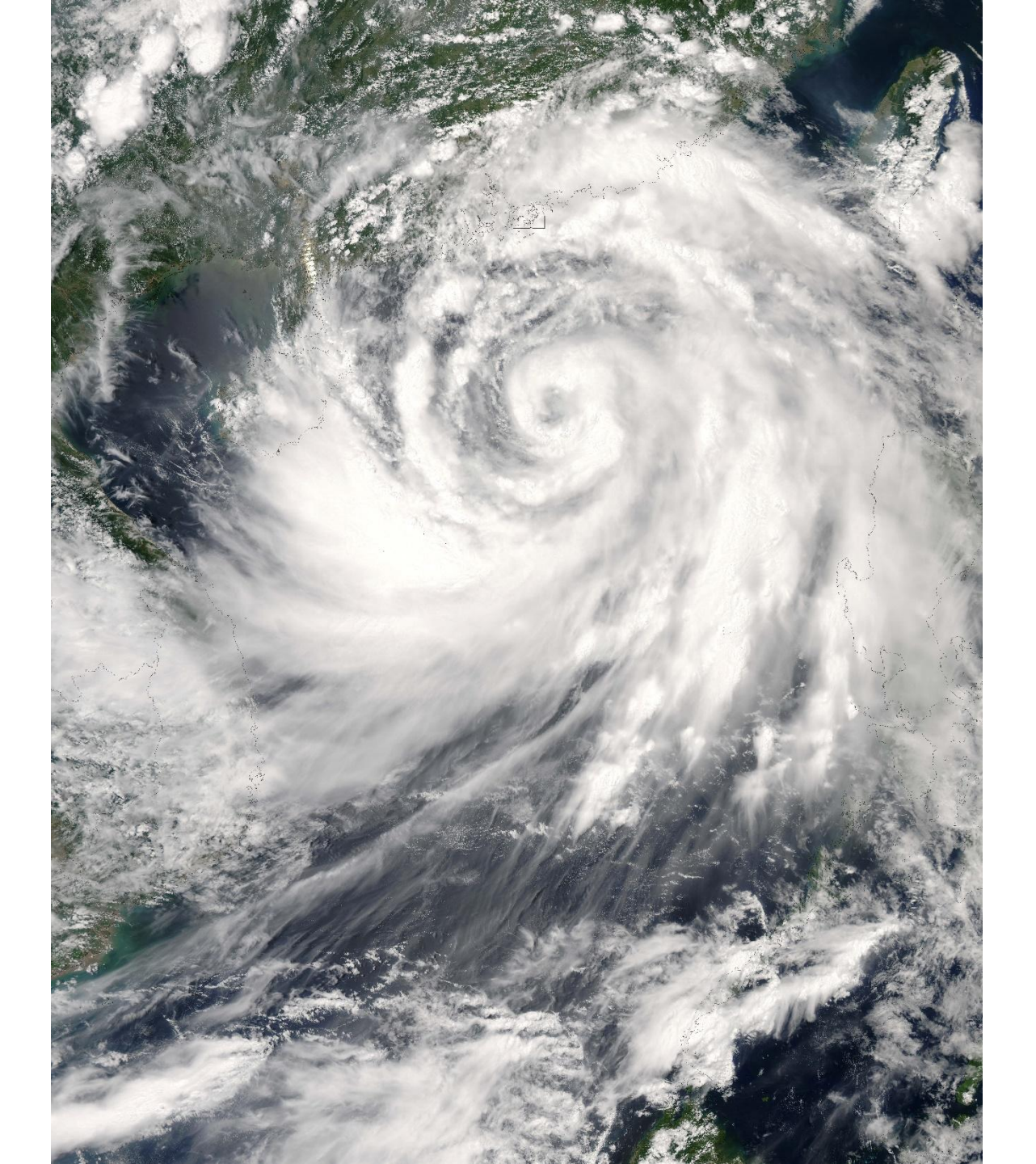






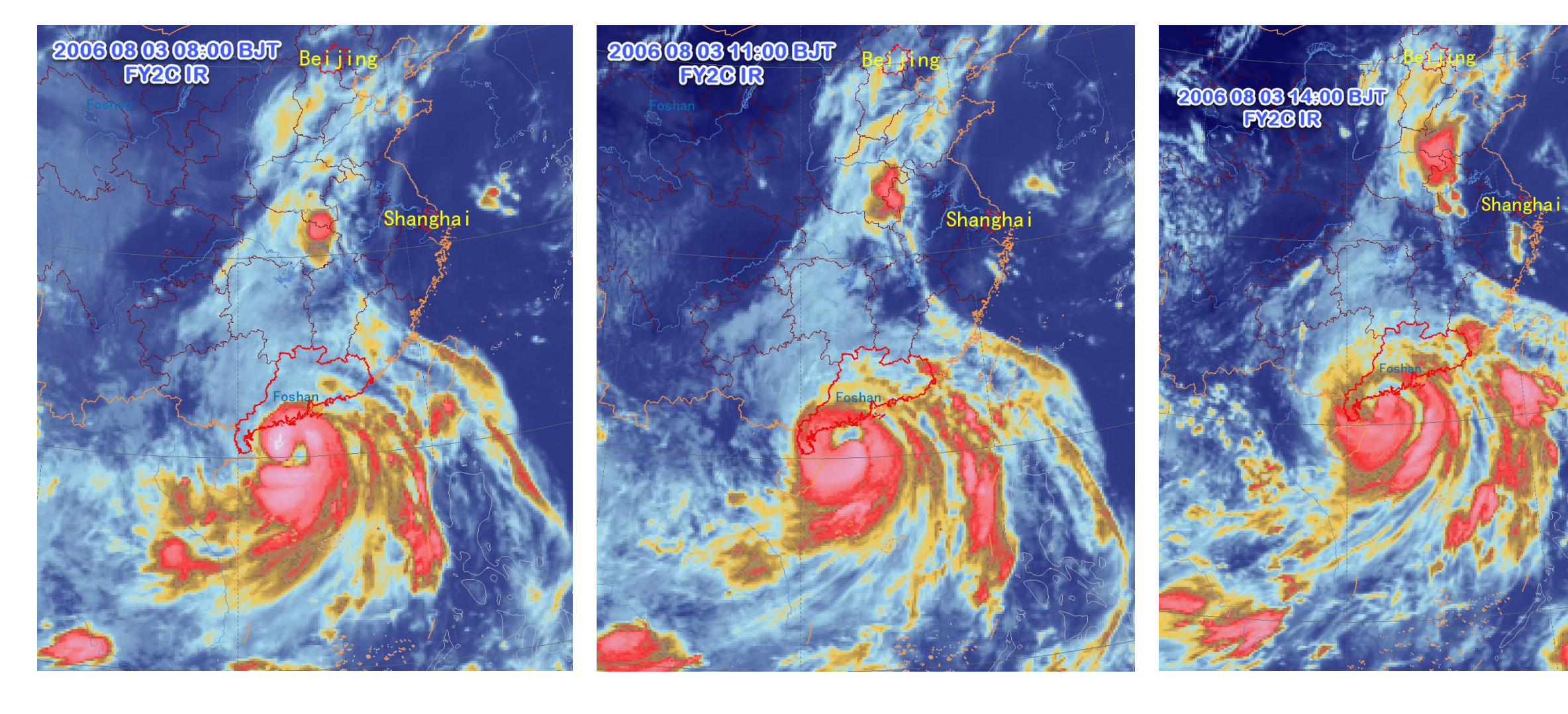
Satellite Images of Typhoon "Prapiroon"

- EOS aqua MODIS visible channel
- FY2C IR images
- FY2C Visible images

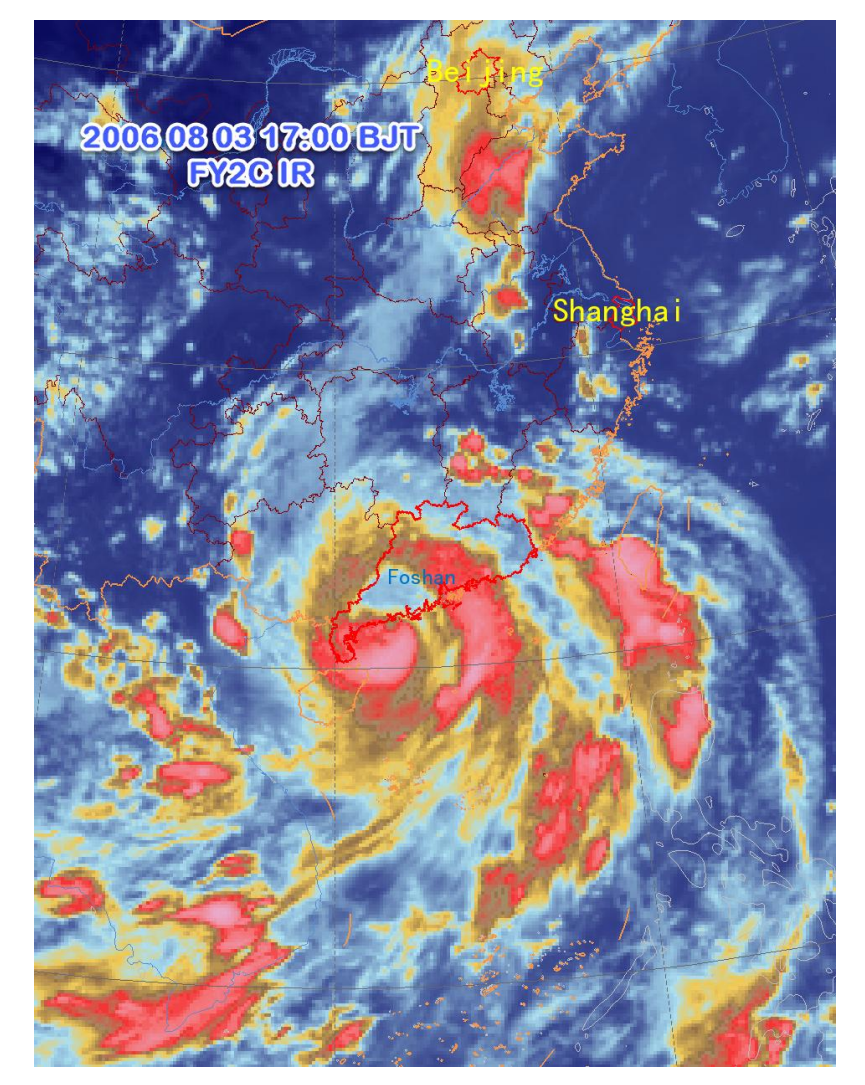


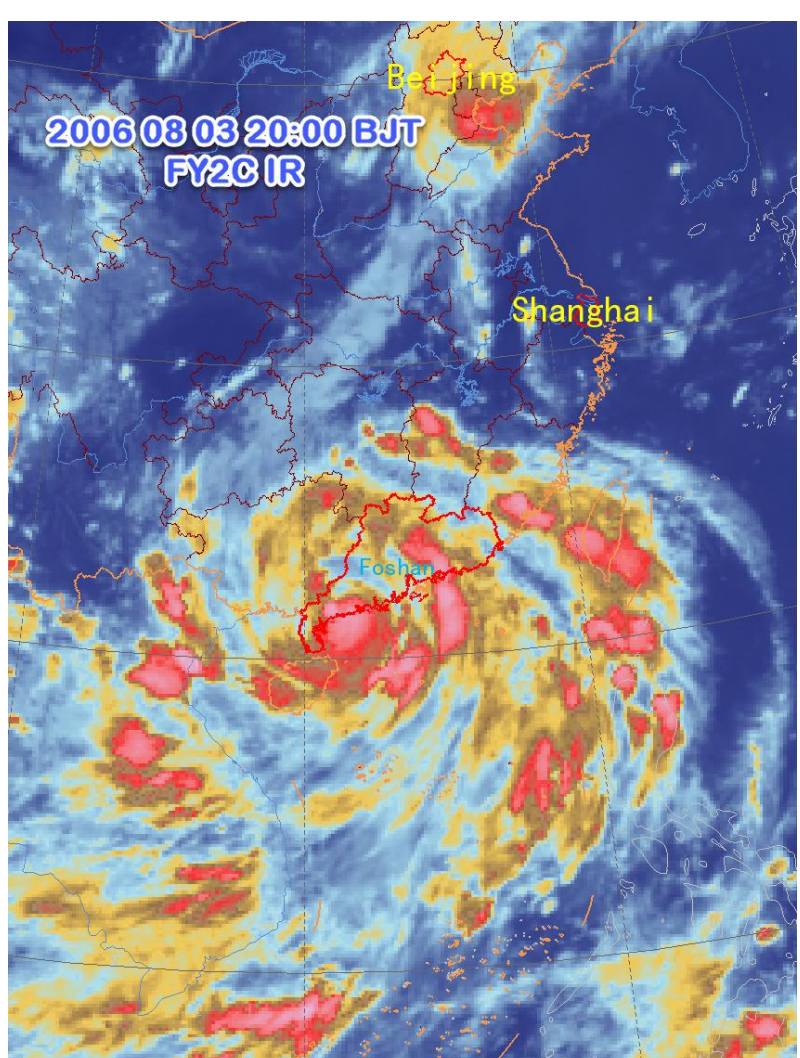
EOS Aqua MODIS 2006 08 02 13:50 BJT

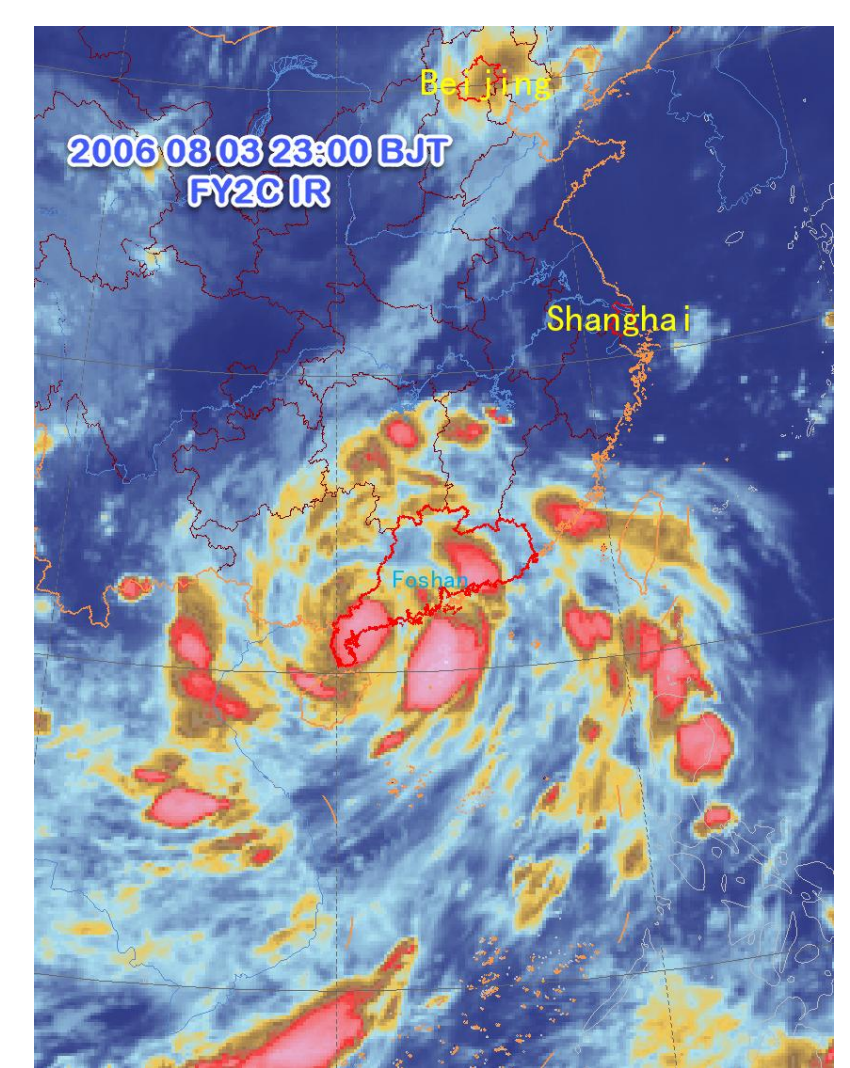
Typhoon "Prapiroon"

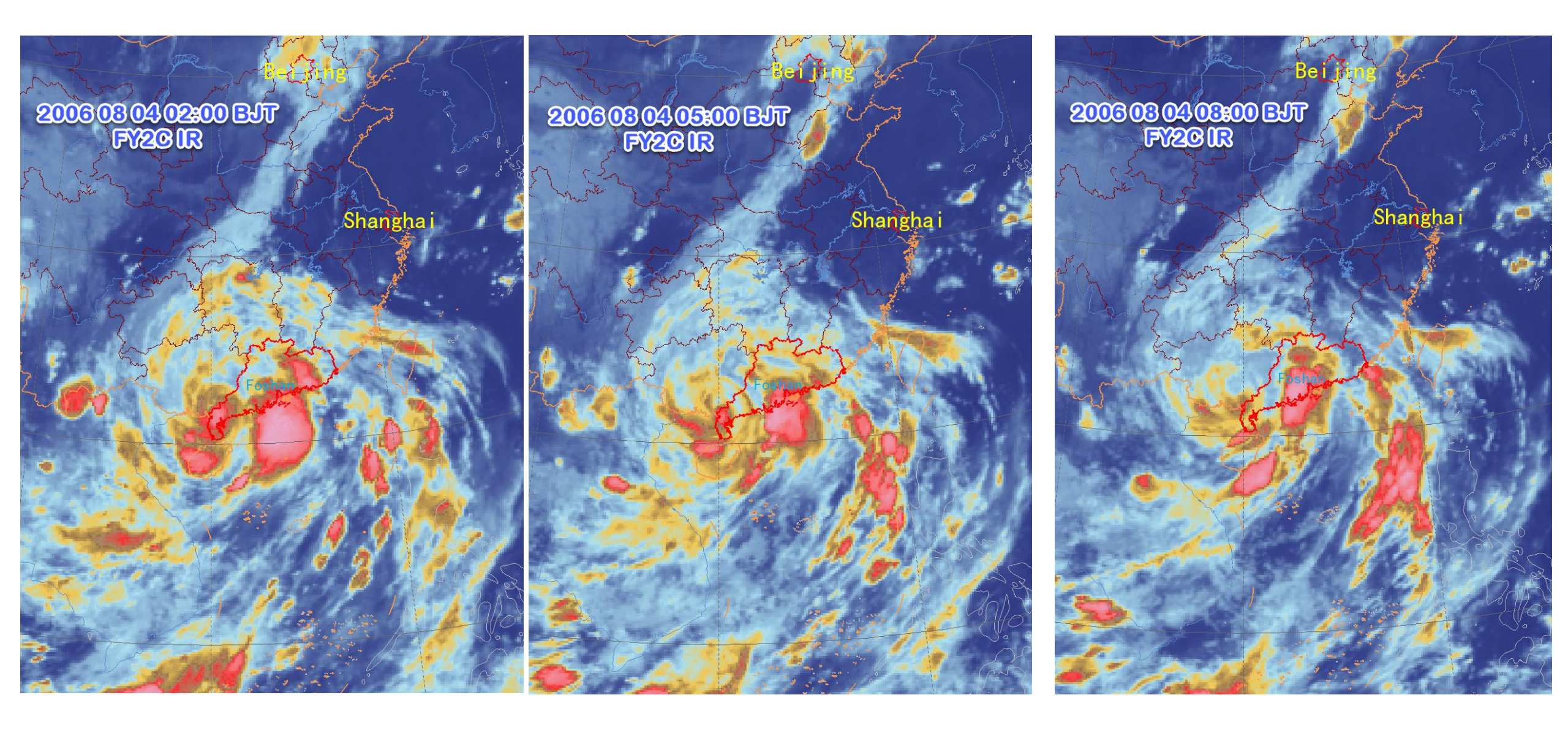


Typhoon "Prapiroon"

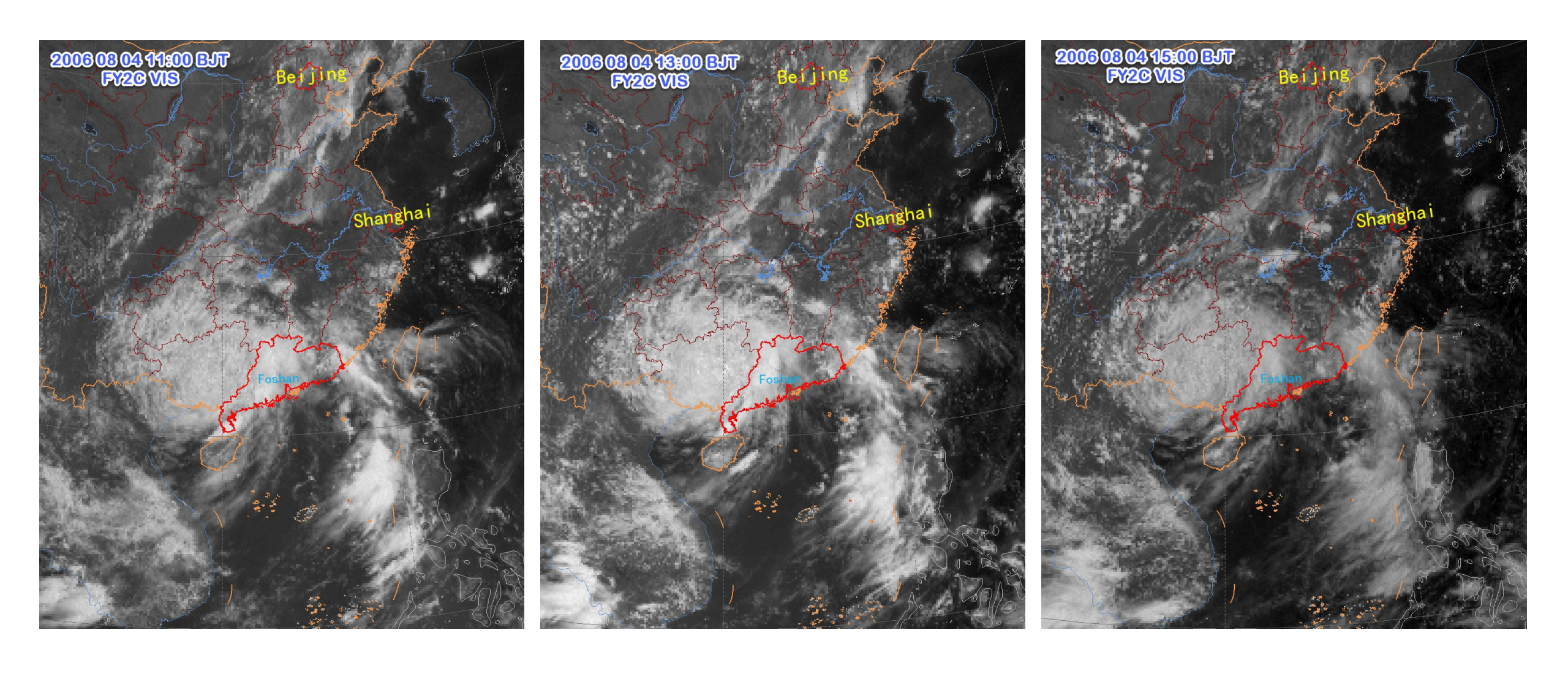








Typhoon "Prapiroon"



Typhoon "Prapiroon"

Characteristics of Doppler weather radar echoes

• Tornado 1: Danzao town, Foshan city, around 10:50 BJT on the 4th October 2015

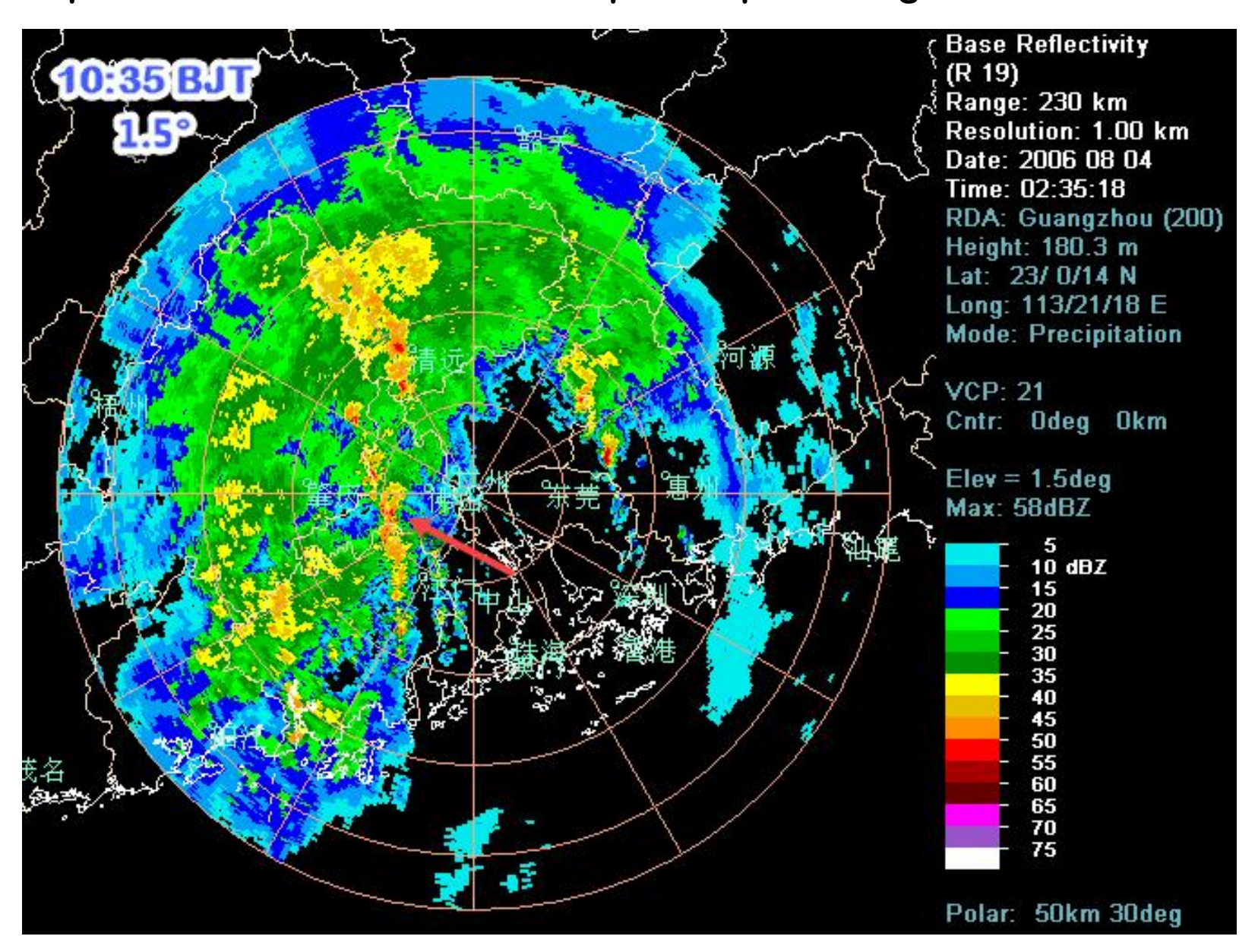
Tornado 1: Danzao town, Foshan city, around 10:50 BJT on the 4th October 2015



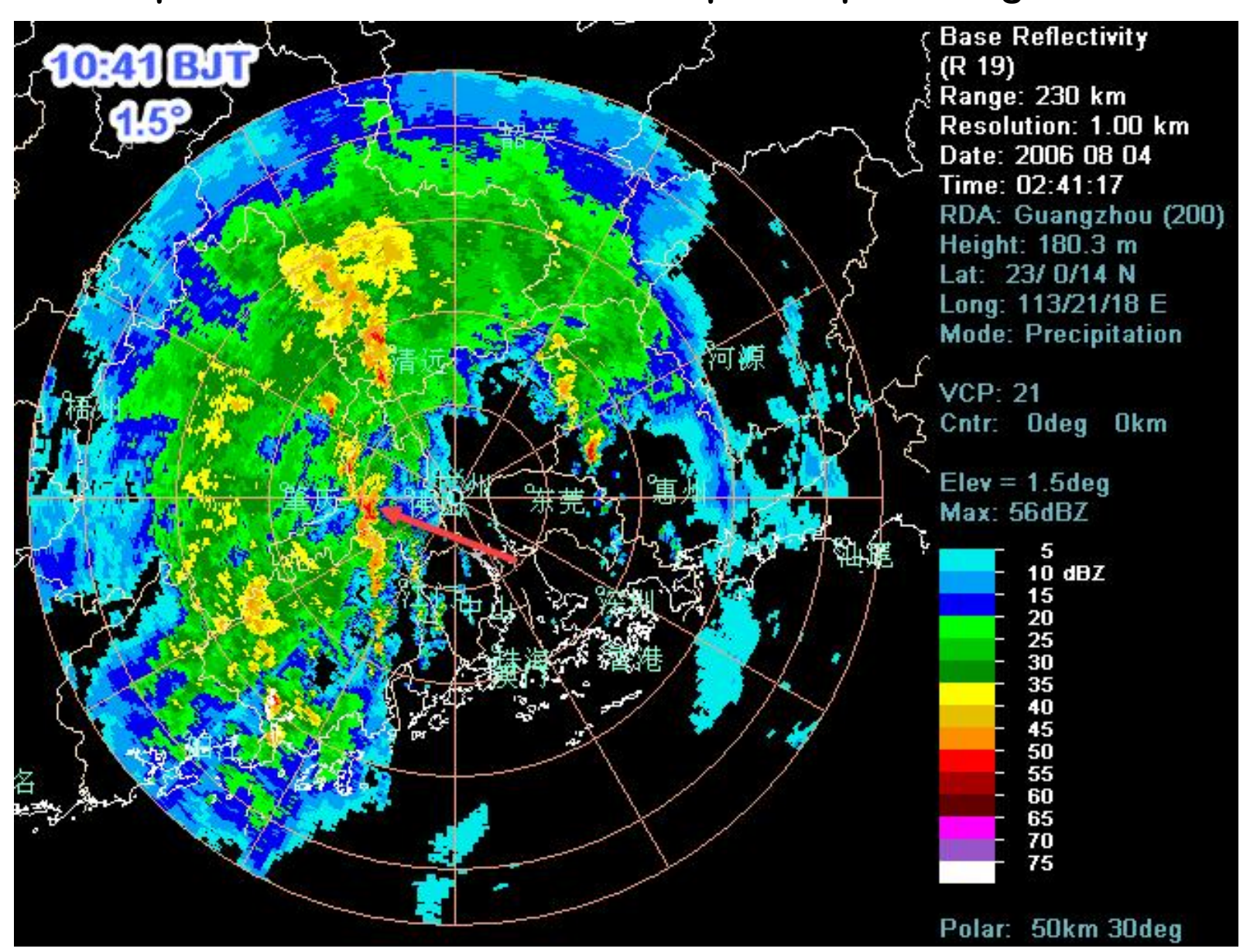
30-22℃ ◆天津 雷阵雨 32-25℃

GIMES 呼和浩特 阵雨

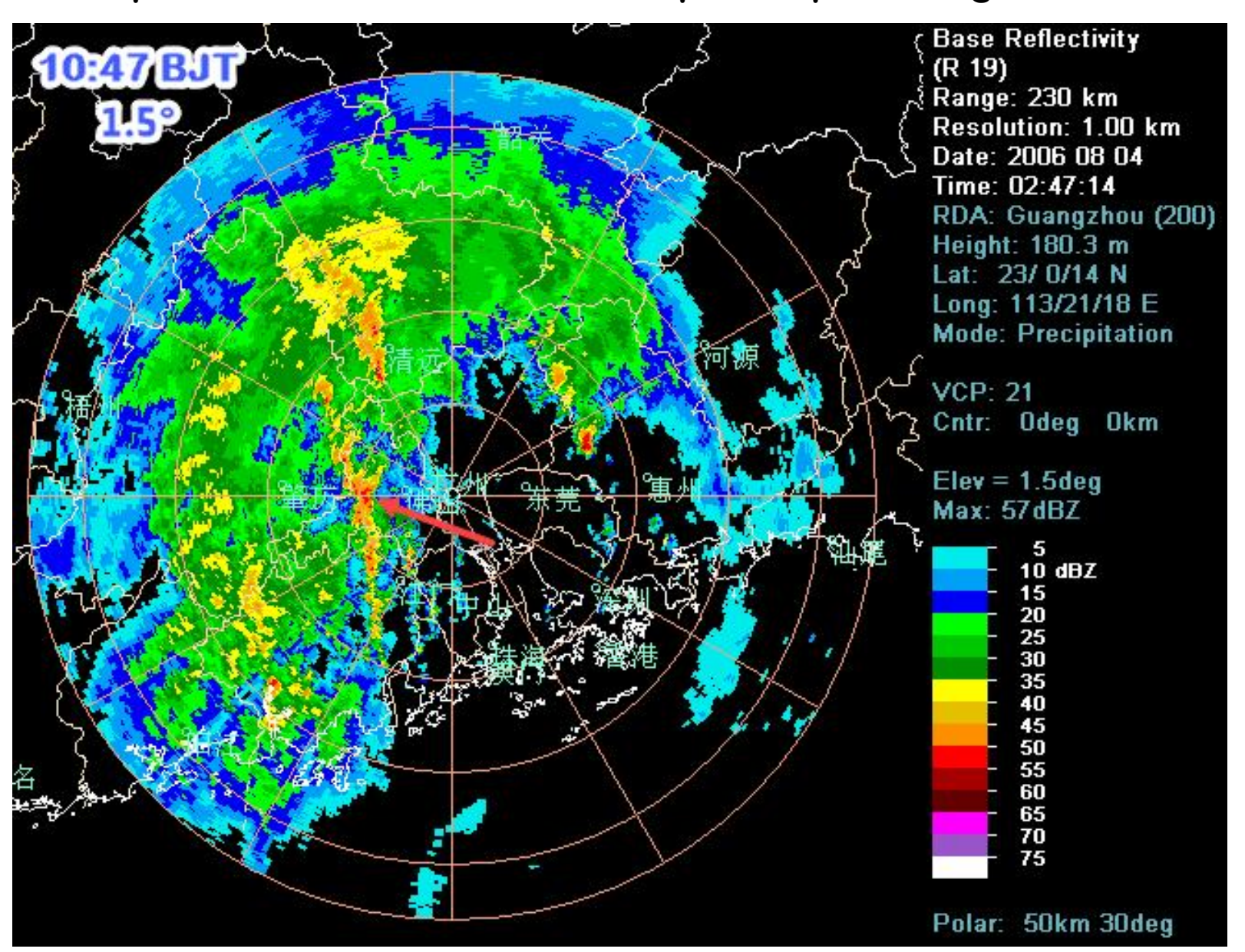
2006 08 04 10:35 BJT Guangzhou SA radar 1.5° elevation reflectivity, the red arrow points to the embodied mini-supercell producing the tornado.



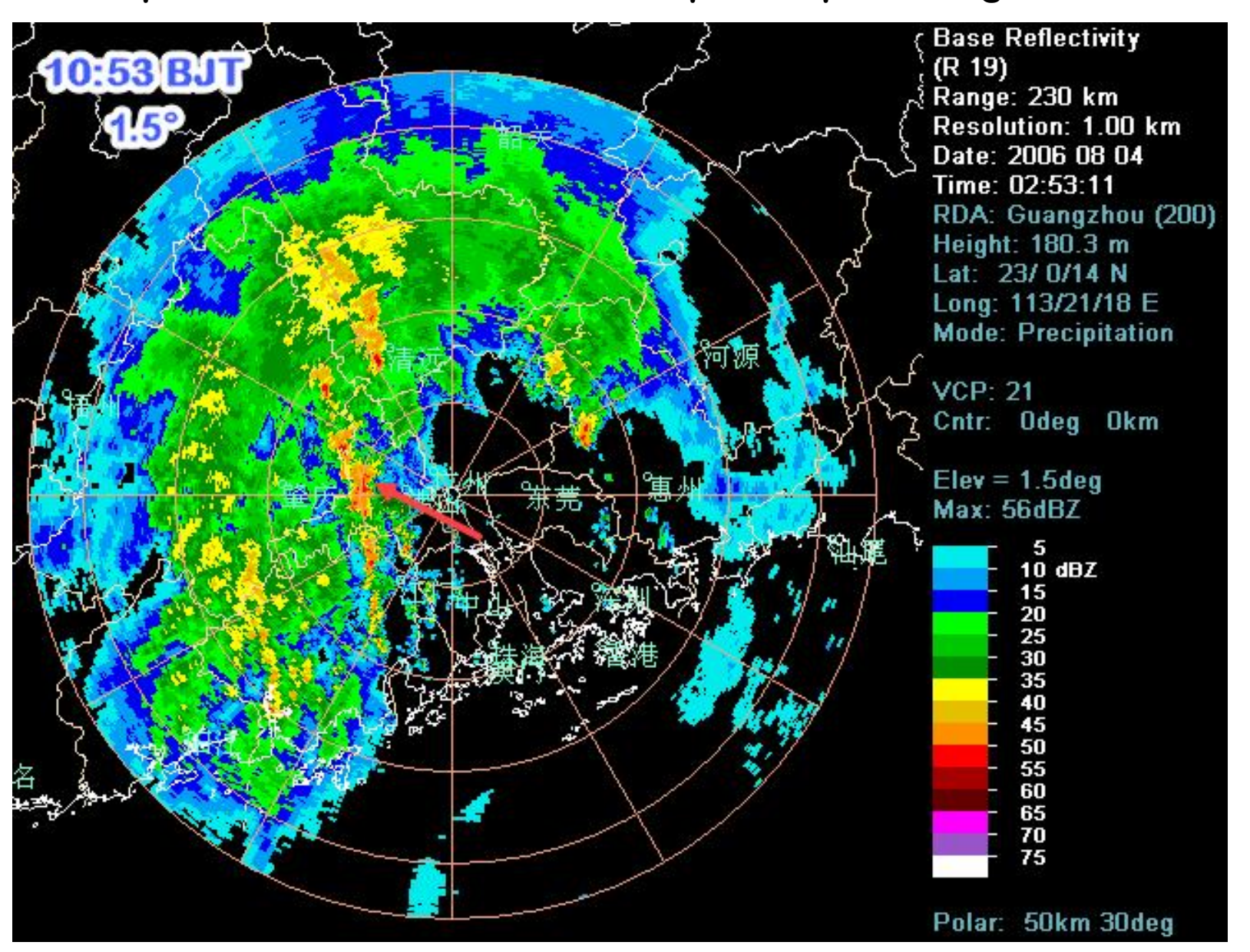
2006 08 04 10:41 BJT Guangzhou SA radar 1.5° elevation reflectivity, the red arrow points to the embodied mini-supercell producing the tornado.

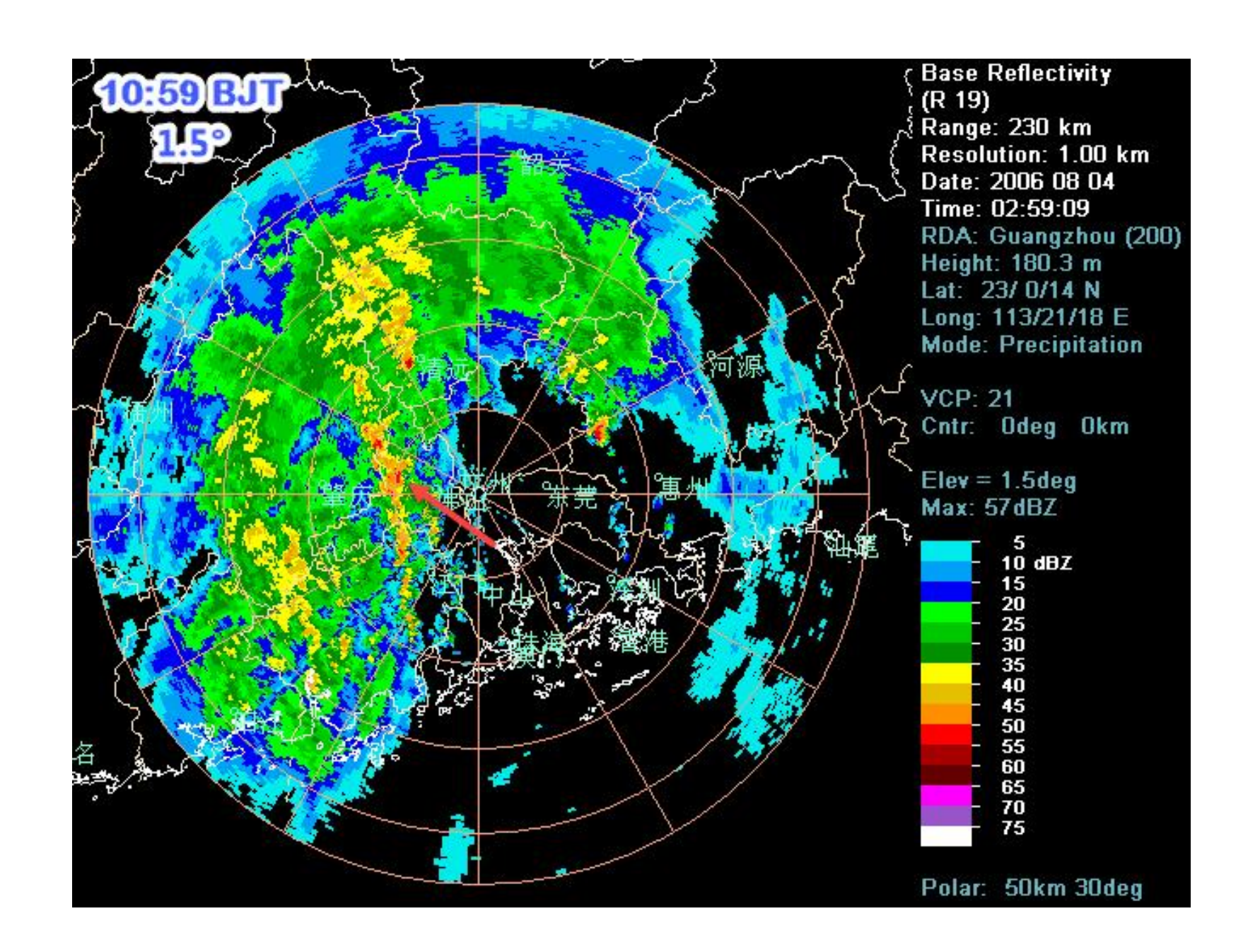


2006 08 04 10:47 BJT Guangzhou SA radar 1.5° elevation reflectivity, the red arrow points to the embodied mini-supercell producing the tornado.

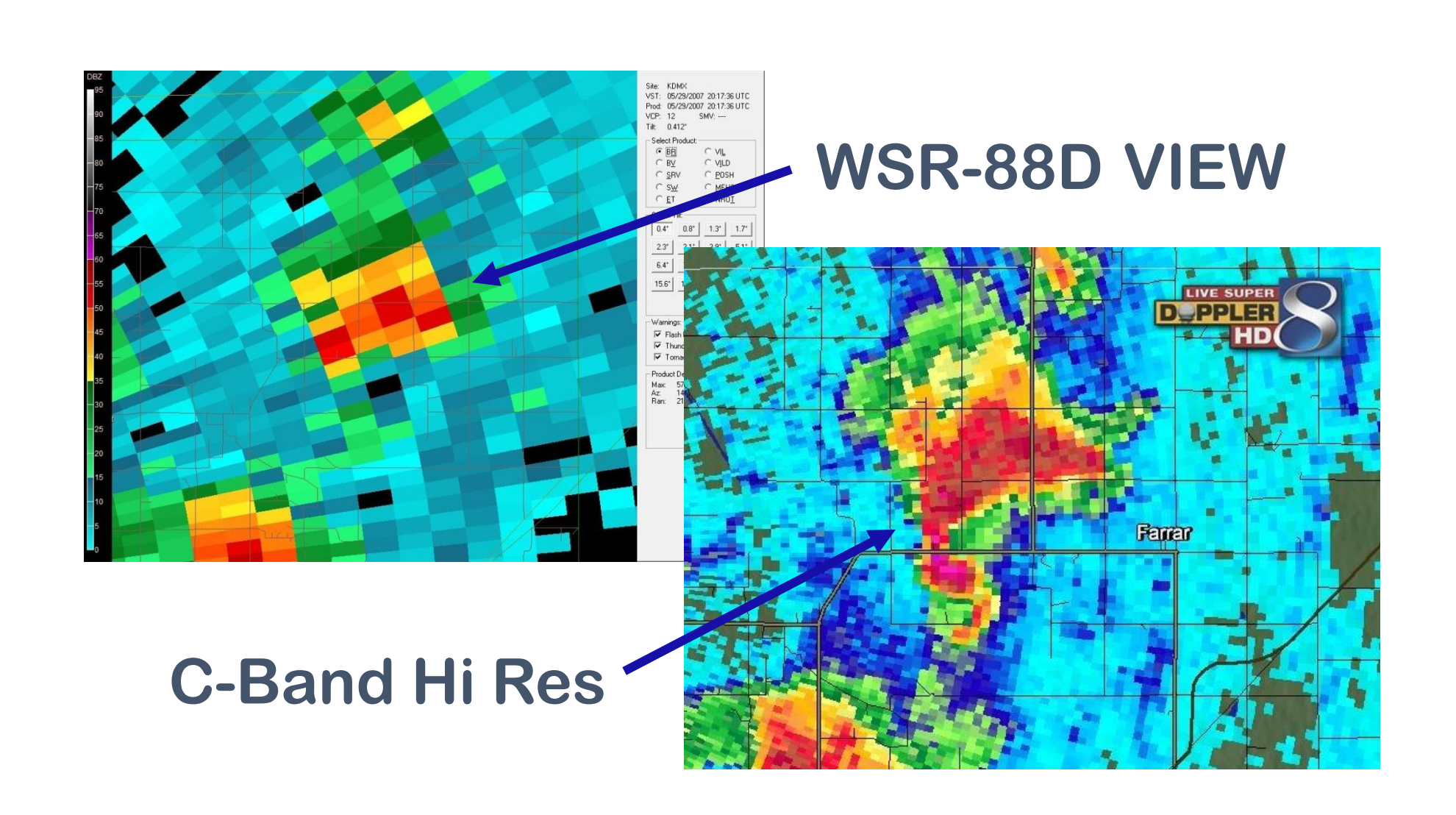


2006 08 04 10:53 BJT Guangzhou SA radar 1.5° elevation reflectivity, the red arrow points to the embodied mini-supercell producing the tornado.

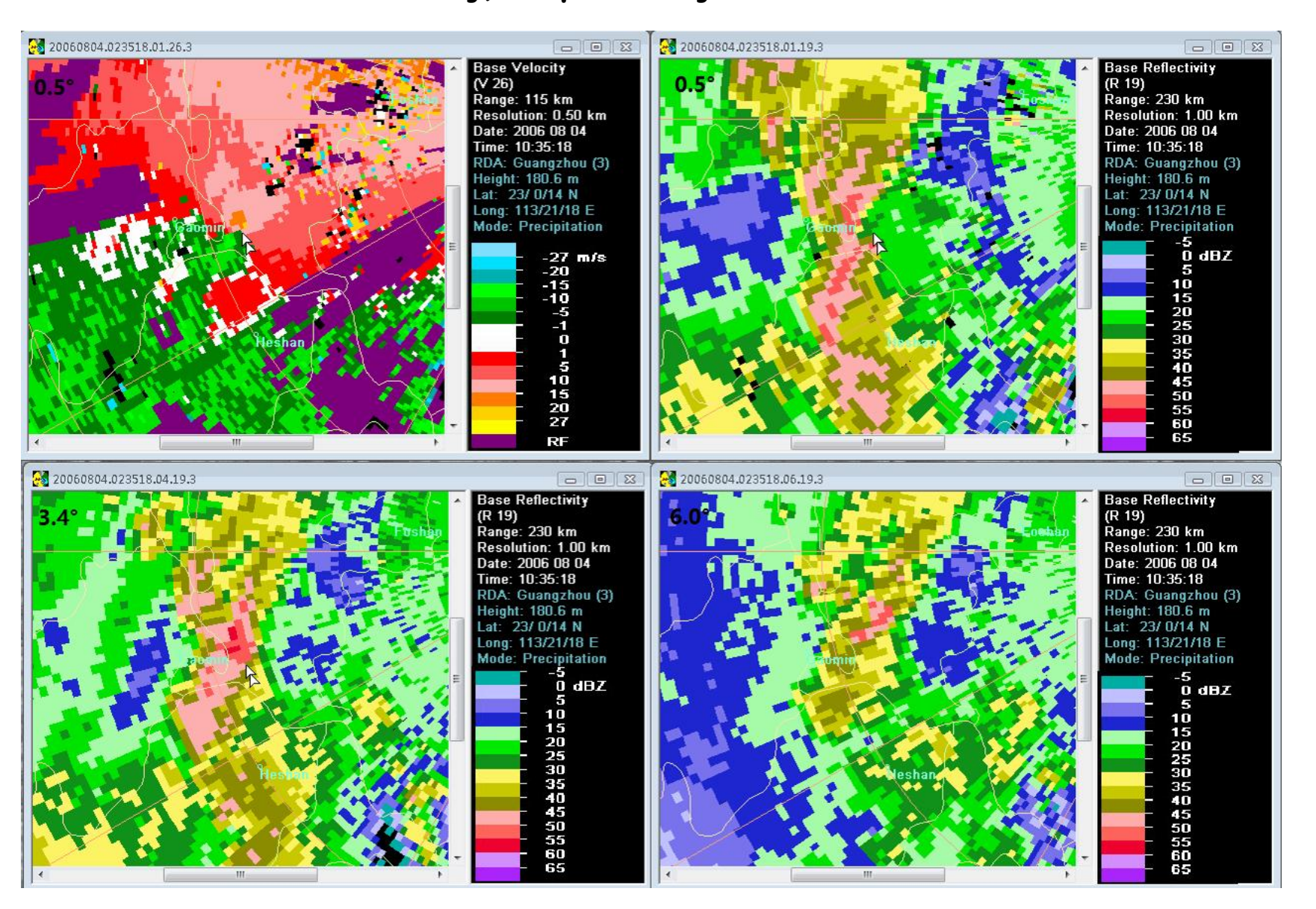




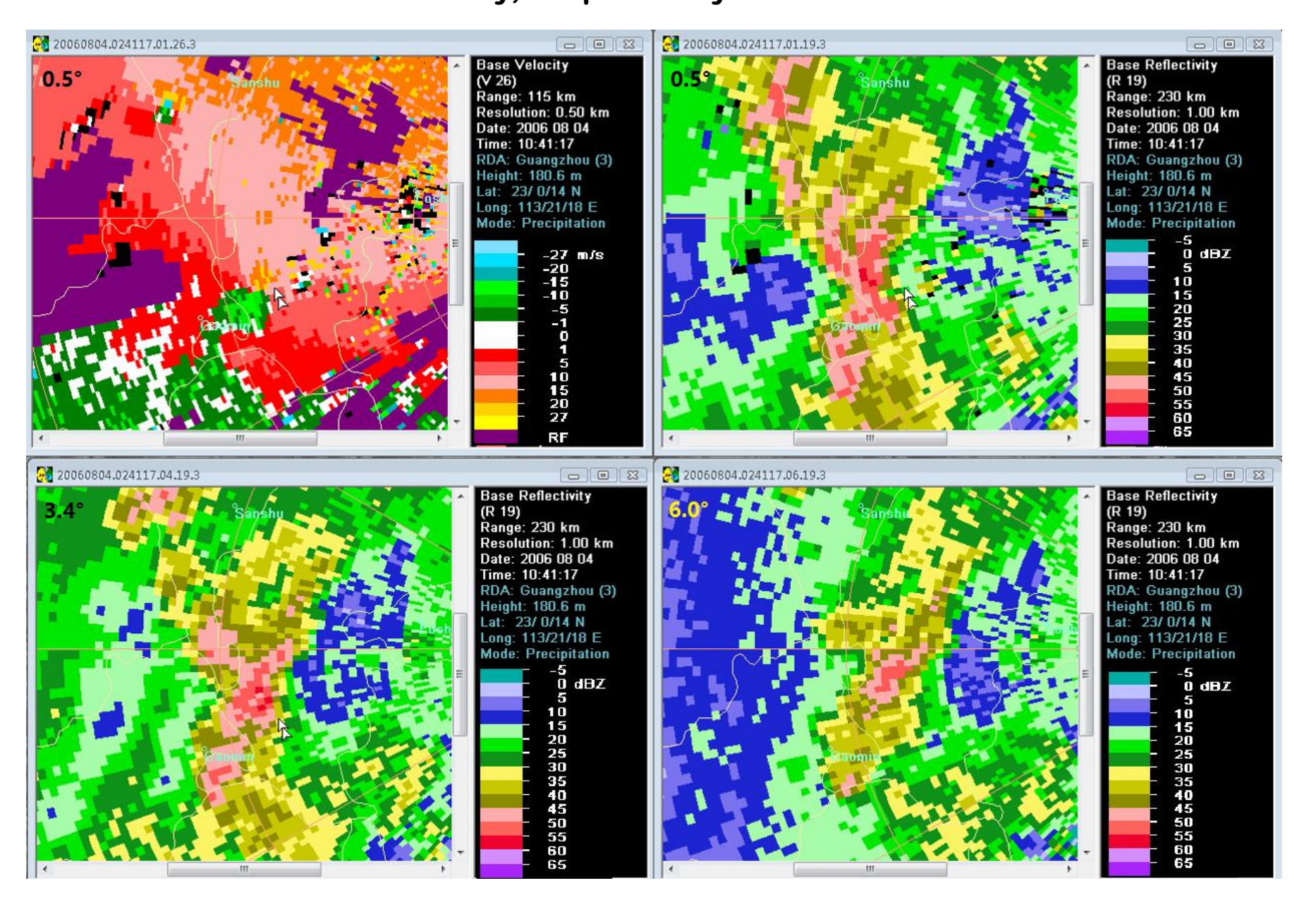
Mini Supercell View: Two Different Radars



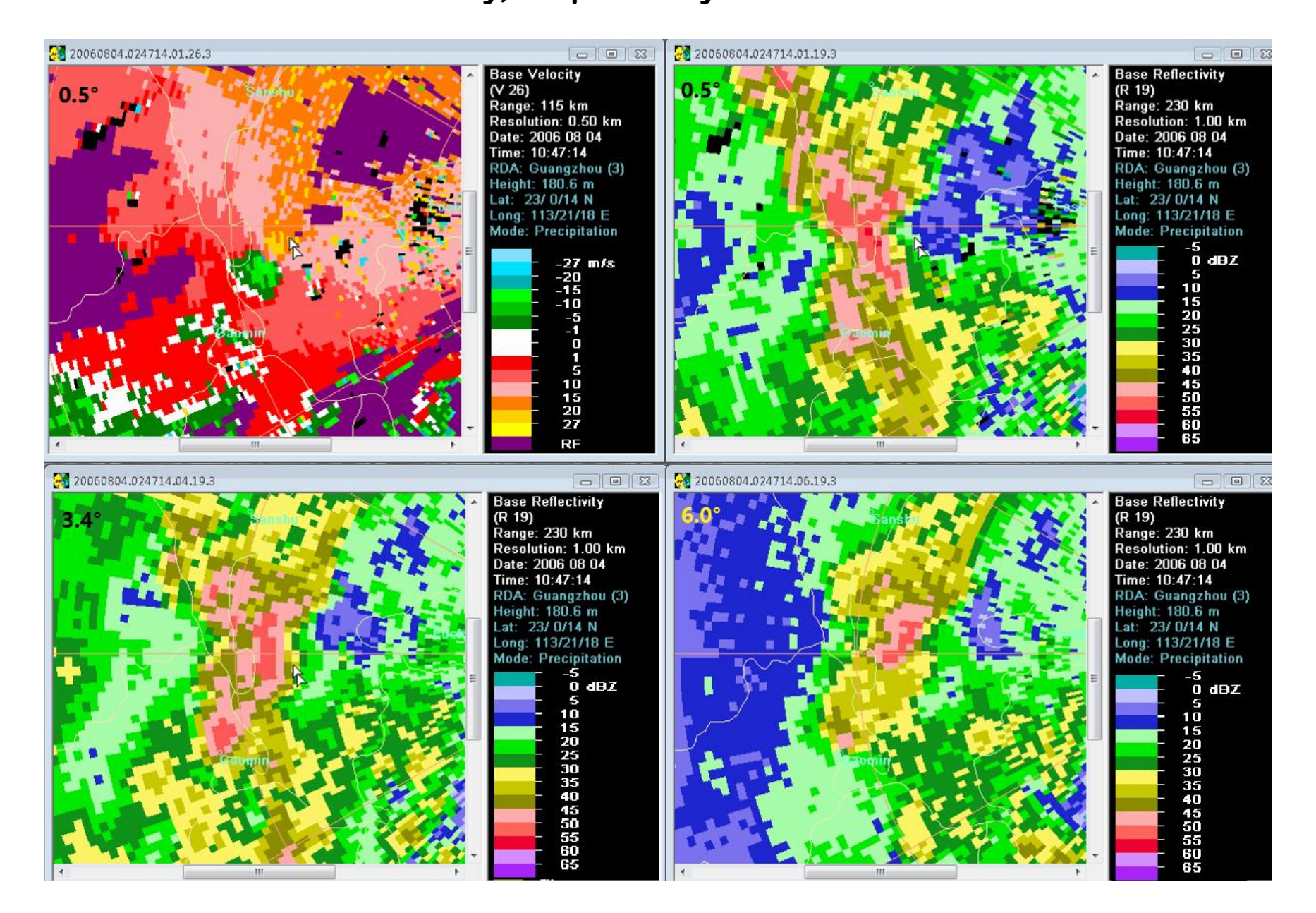
2006 08 04 10:35 BJT Guangzhou SA radar 0.5° elevation velocity, 0.5°, 3.4°, and 6.0° elevation reflectivity, respectively.



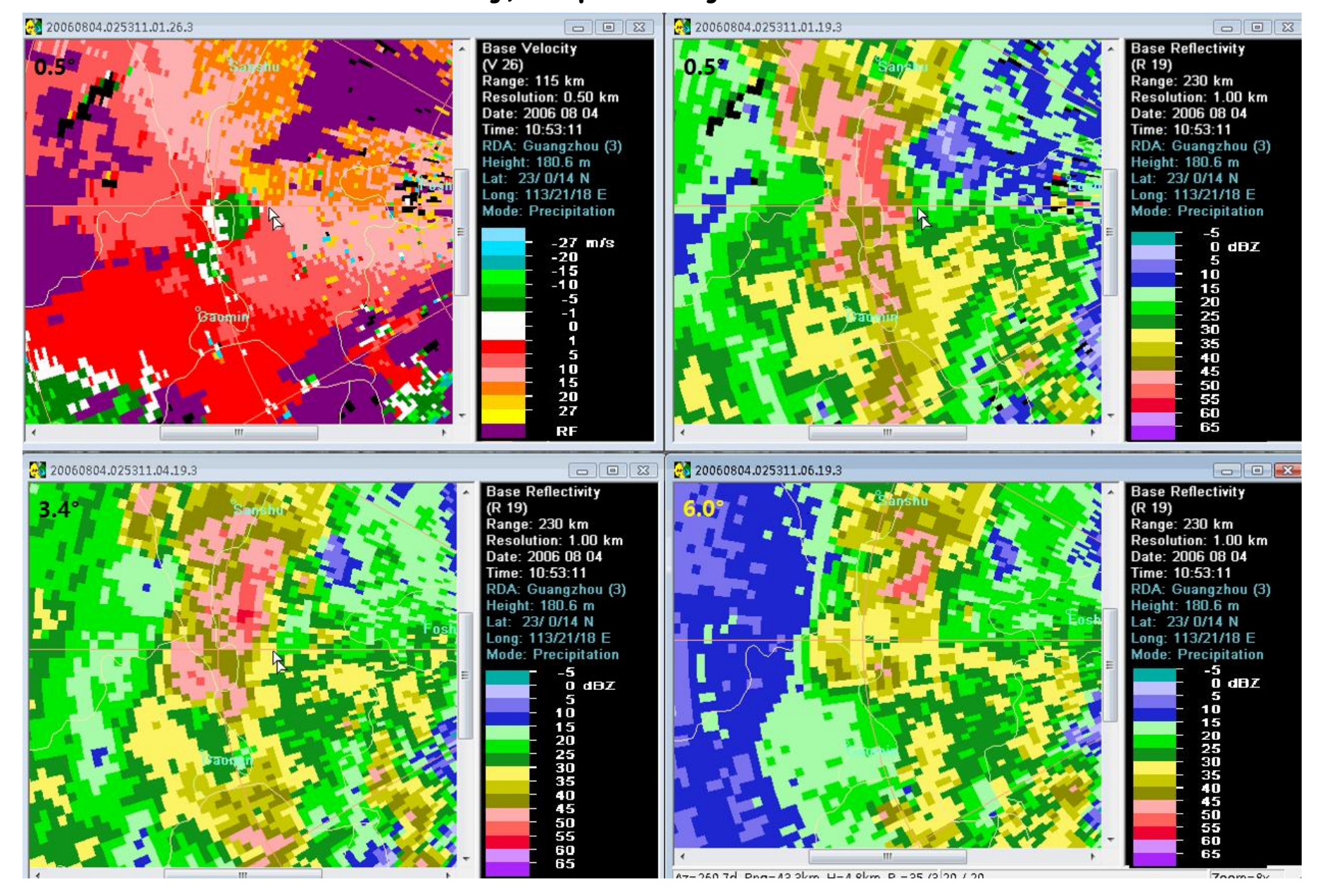
2006 08 04 10:41 BJT Guangzhou SA radar 0.5° elevation velocity, 0.5°, 3.4°, and 6.0° elevation reflectivity, respectively.



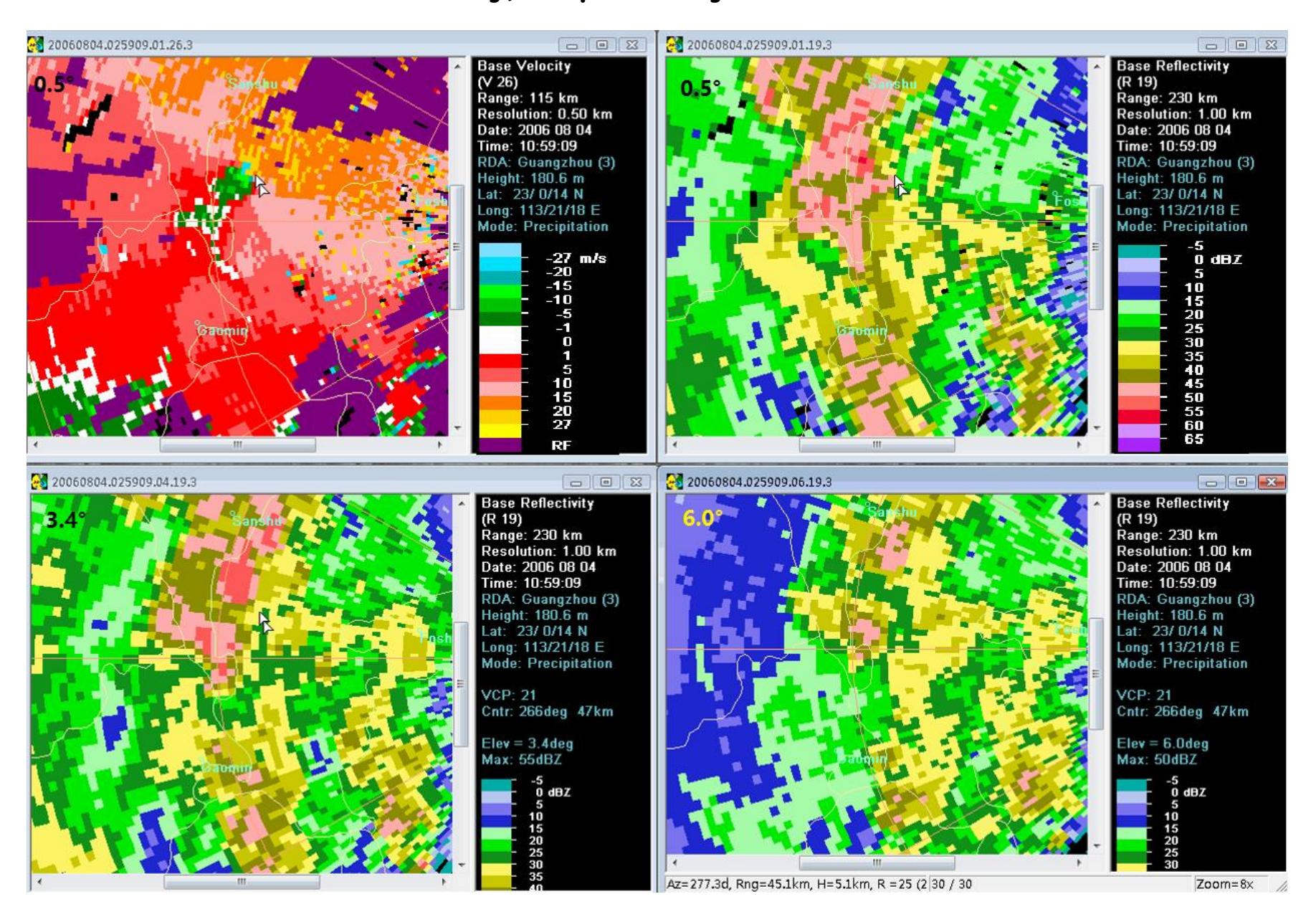
2006 08 04 10:47 BJT Guangzhou SA radar 0.5° elevation velocity, 0.5°, 3.4°, and 6.0° elevation reflectivity, respectively.



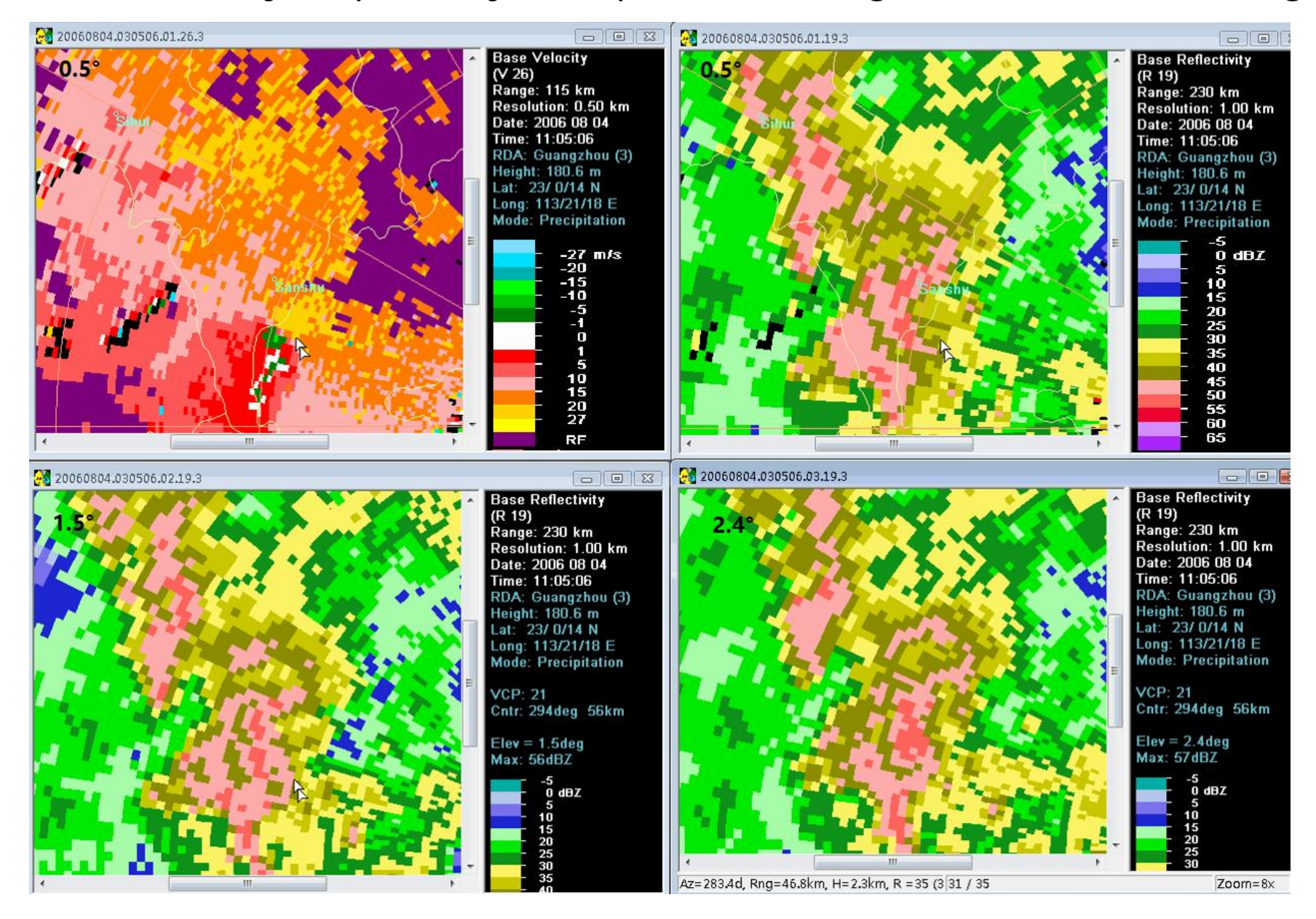
2006 08 04 10:53 BJT Guangzhou SA radar 0.5° elevation velocity, 0.5°, 3.4°, and 6.0° elevation reflectivity, respectively.



2006 08 04 10:59 BJT Guangzhou SA radar 0.5° elevation velocity, 0.5°, 3.4°, and 6.0° elevation reflectivity, respectively.

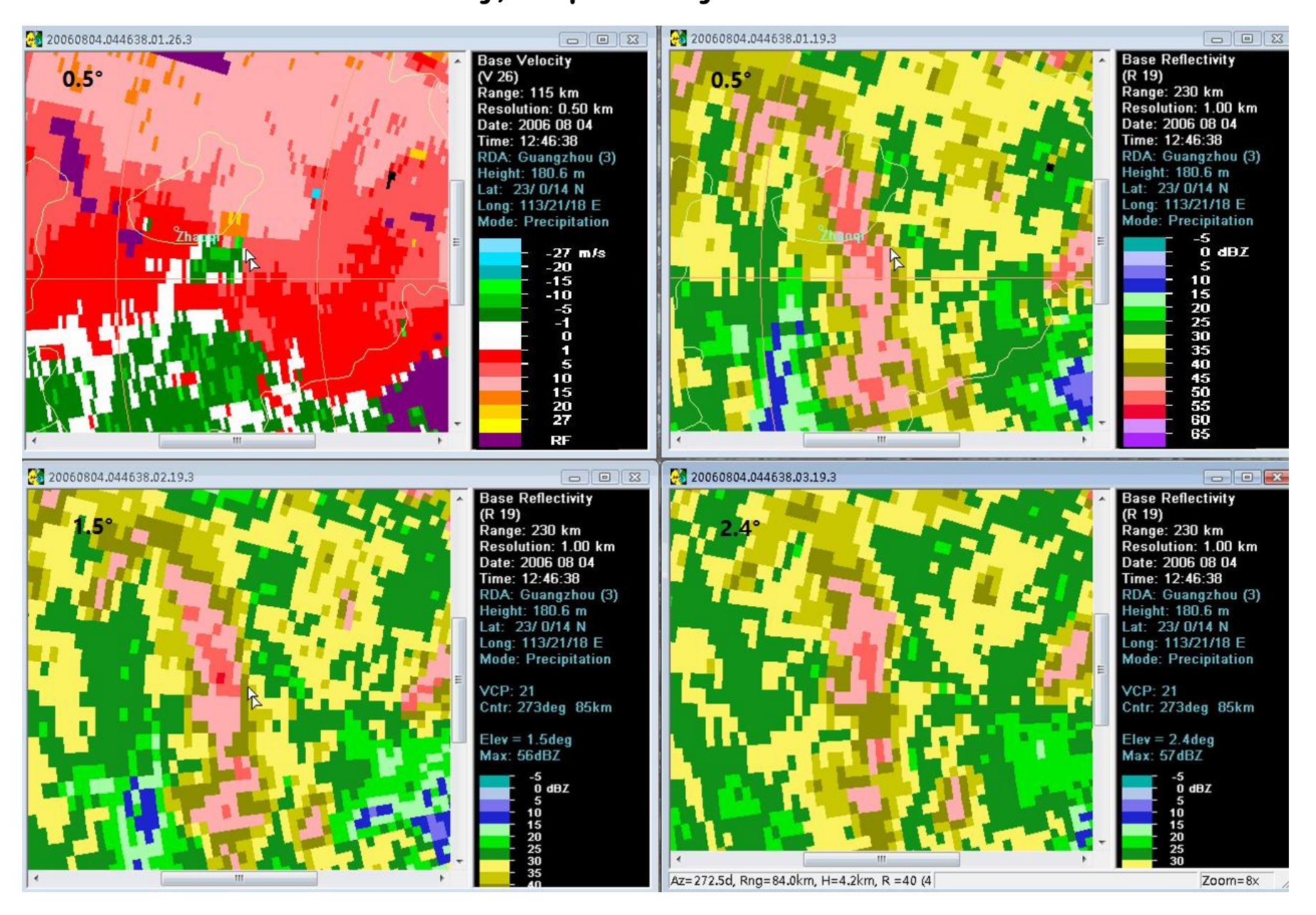


2006 08 04 11:05 BJT Guangzhou SA radar 0.5° elevation velocity, 0.5°, 1.5°, and 2.4° elevation reflectivity, respectively. The position of image center has been changed.

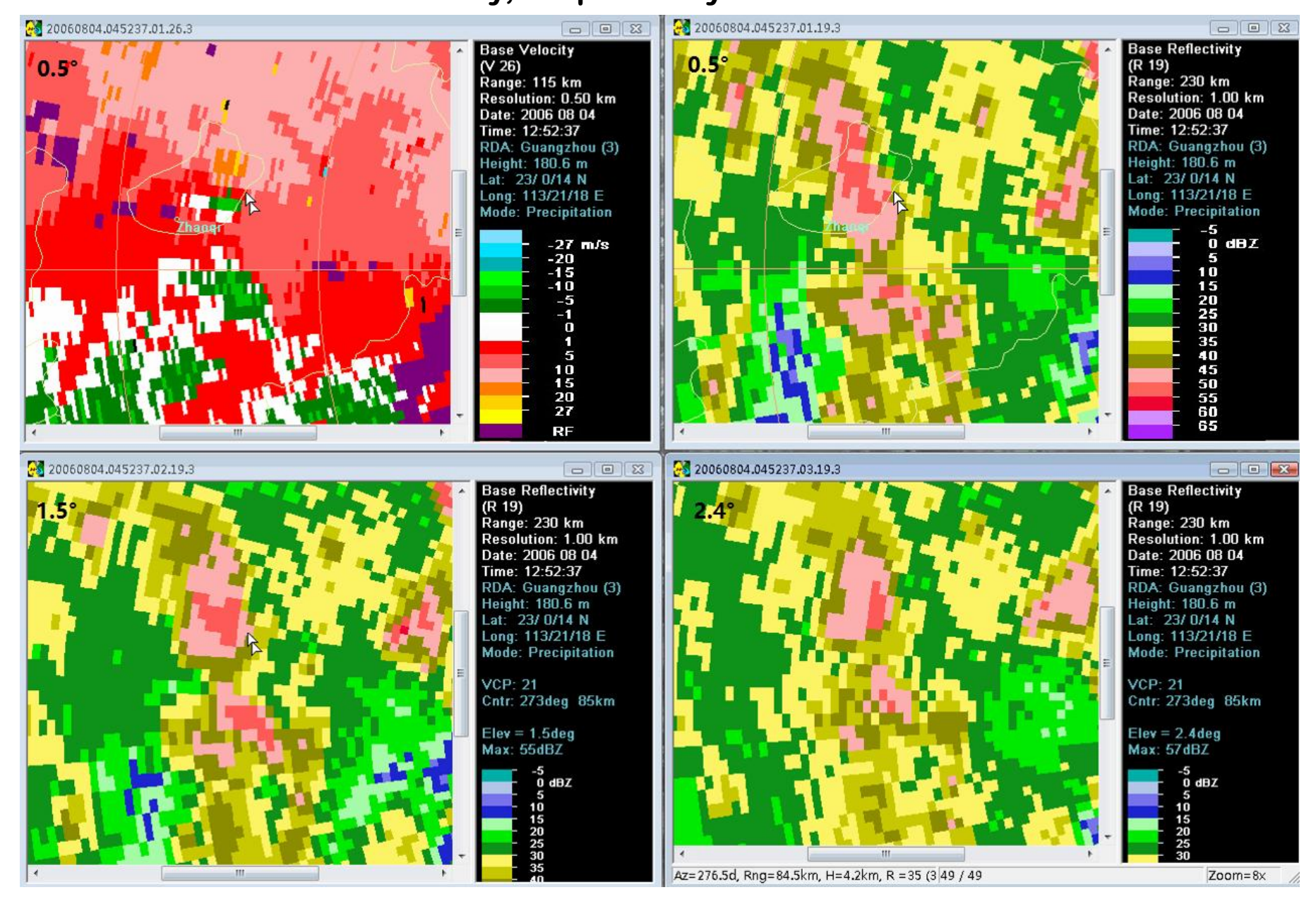


Tornado 2: Jindu town, Zhaoqing city, around 13:00 BJT on the 4th October 2015

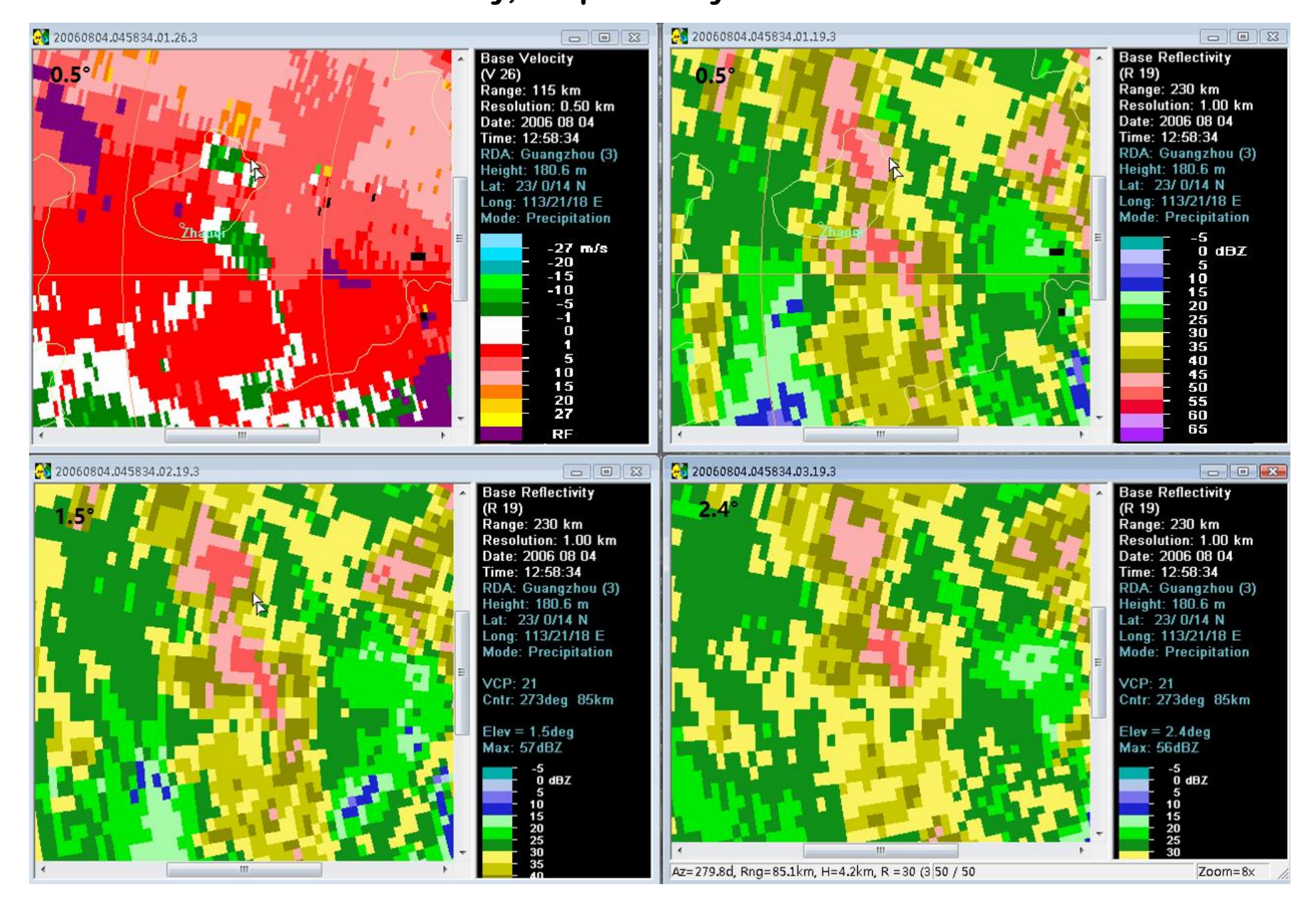
2006 08 04 12:46 BJT Guangzhou SA radar 0.5° elevation velocity, 0.5°, 1.5°, and 2.4° elevation reflectivity, respectively.



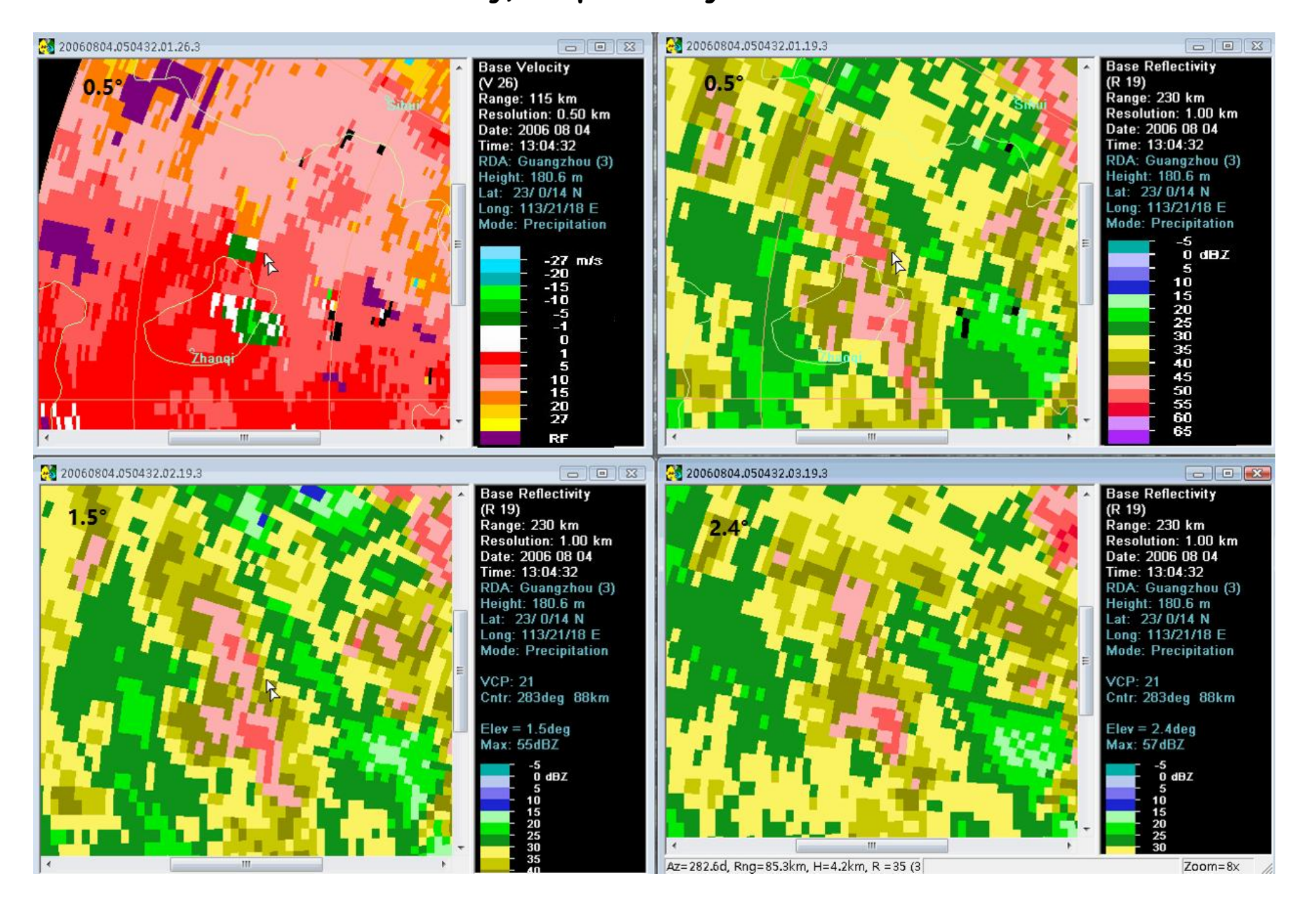
2006 08 04 12:52 BJT Guangzhou SA radar 0.5° elevation velocity, 0.5°, 1.5°, and 2.4° elevation reflectivity, respectively.



2006 08 04 12:58 BJT Guangzhou SA radar 0.5° elevation velocity, 0.5°, 1.5°, and 2.4° elevation reflectivity, respectively.

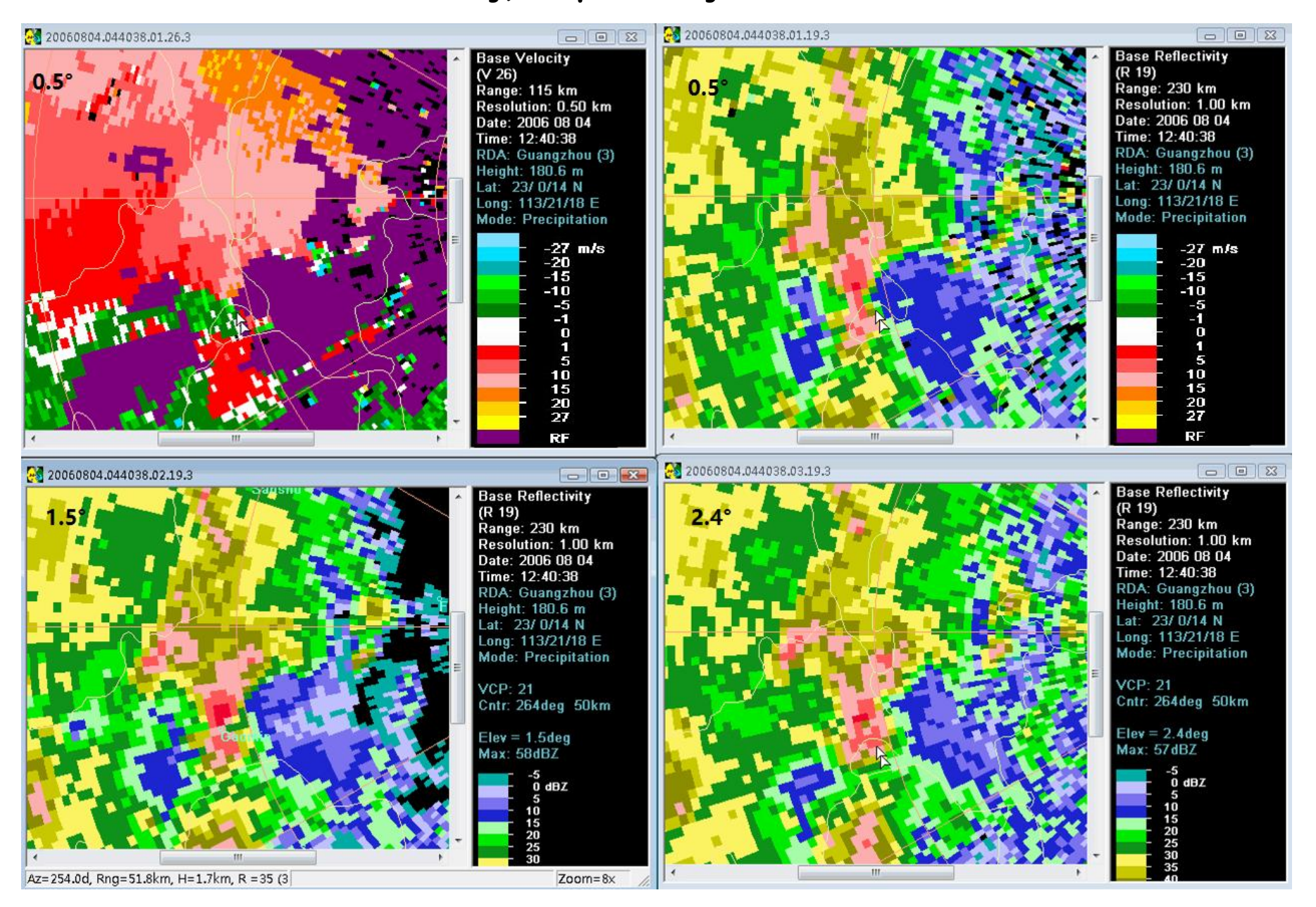


2006 08 04 13:04 BJT Guangzhou SA radar 0.5° elevation velocity, 0.5°, 1.5°, and 2.4° elevation reflectivity, respectively.

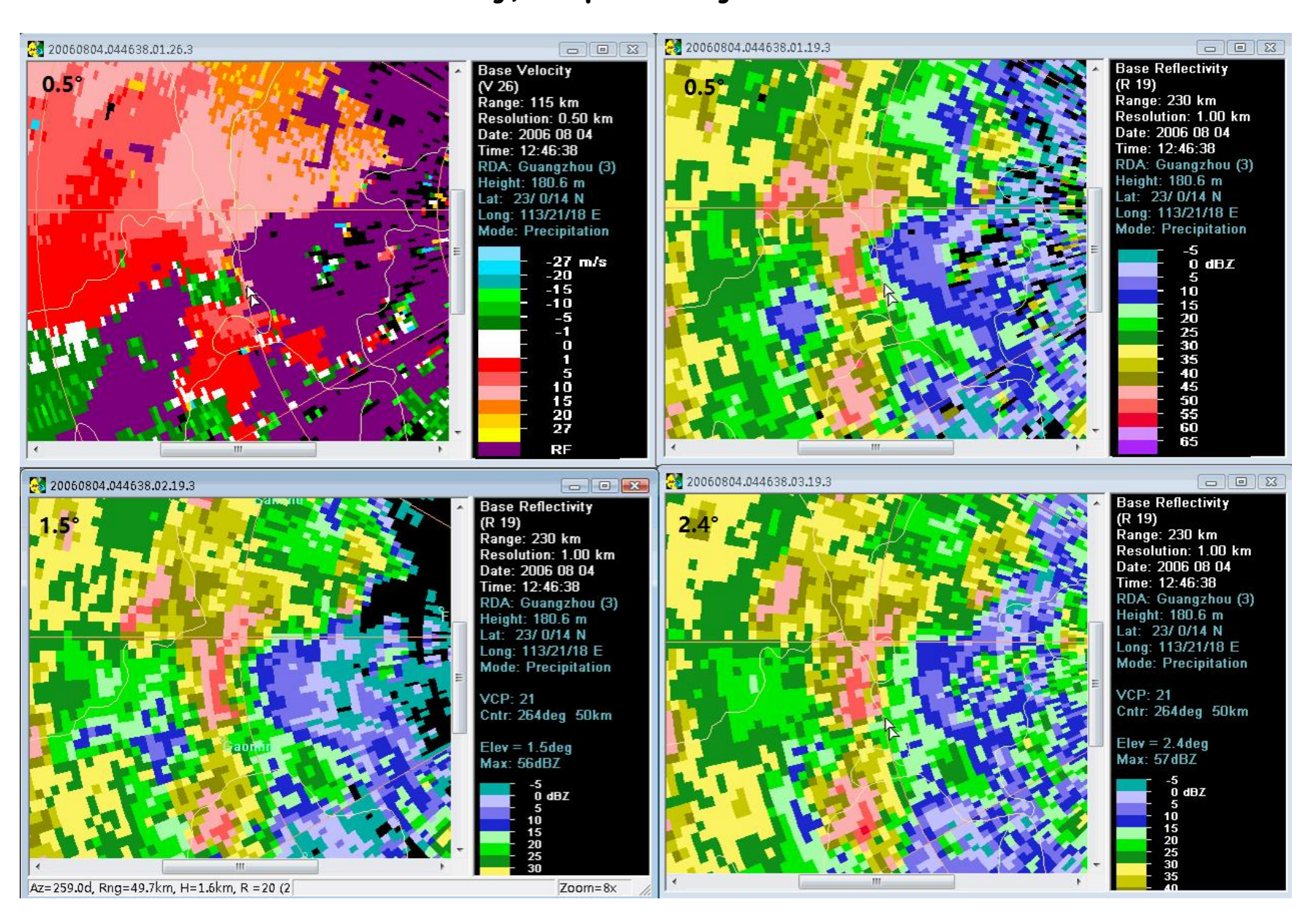


Tornado 3: Baini town, Foshan city, around 13:20 BJT on the 4th October 2015

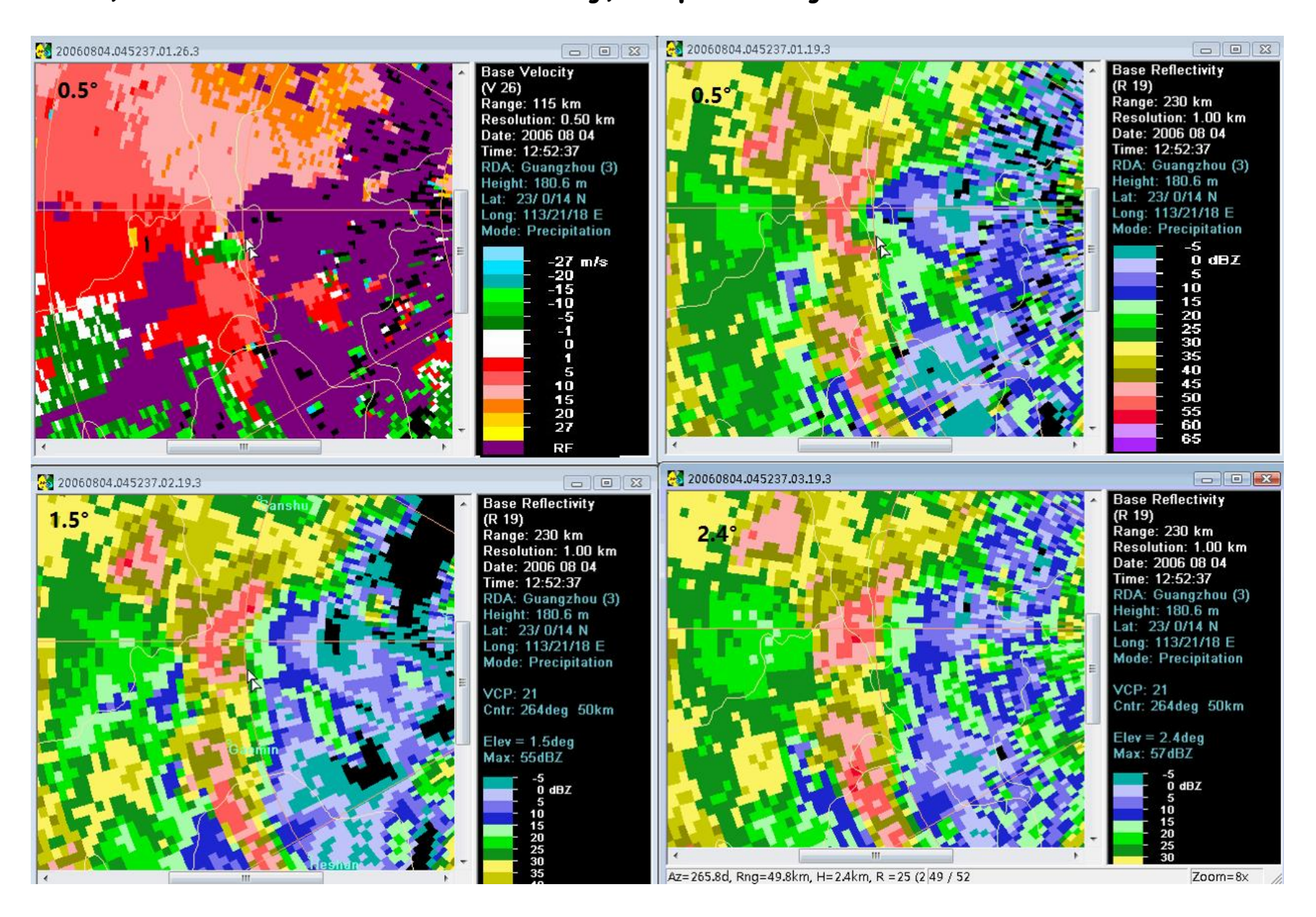
2006 08 04 12:40 BJT Guangzhou SA radar 0.5° elevation velocity, 0.5°, 1.5°, and 2.4° elevation reflectivity, respectively.



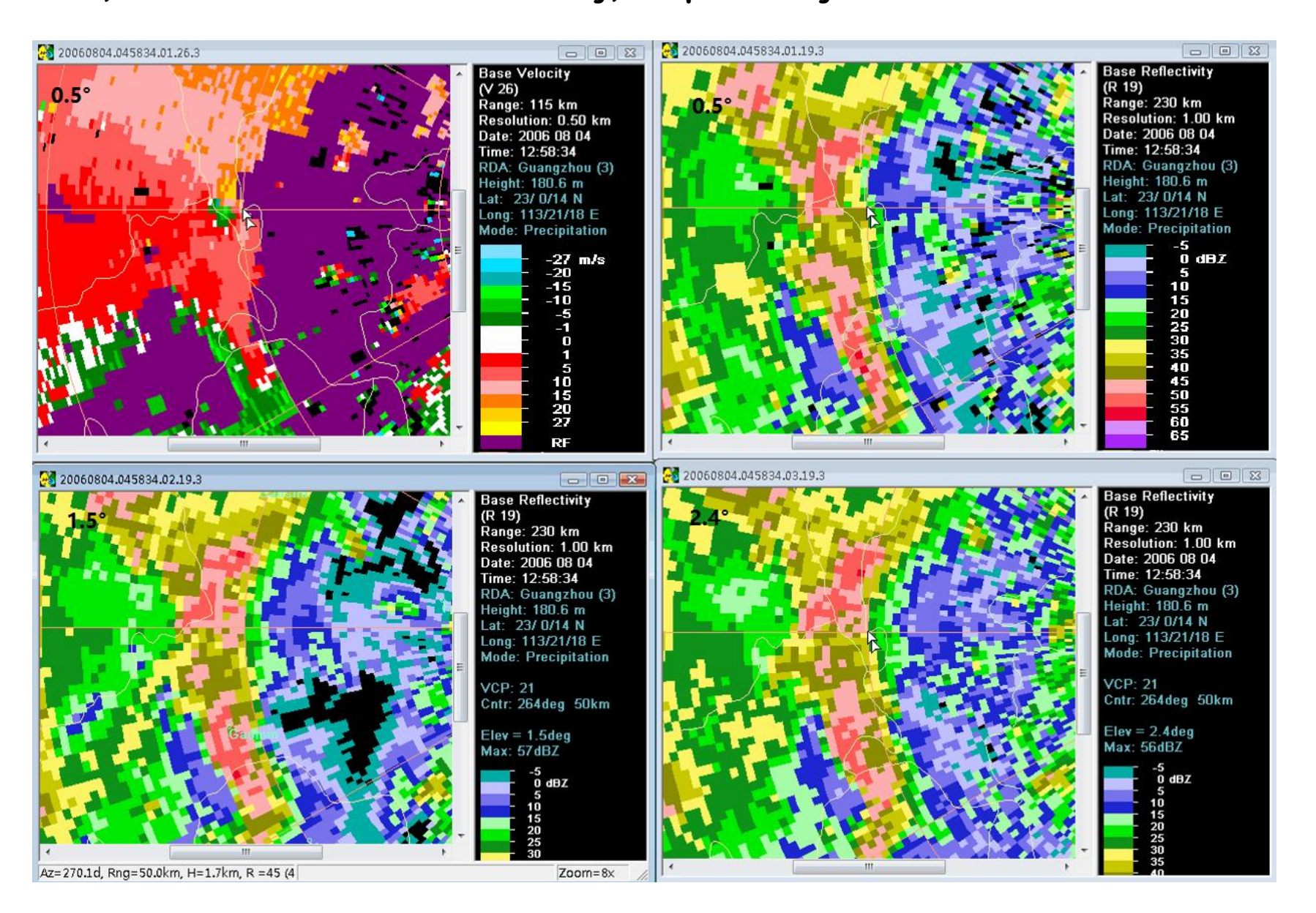
2006 08 04 12:46 BJT Guangzhou SA radar 0.5° elevation velocity, 0.5°, 1.5°, and 2.4° elevation reflectivity, respectively.



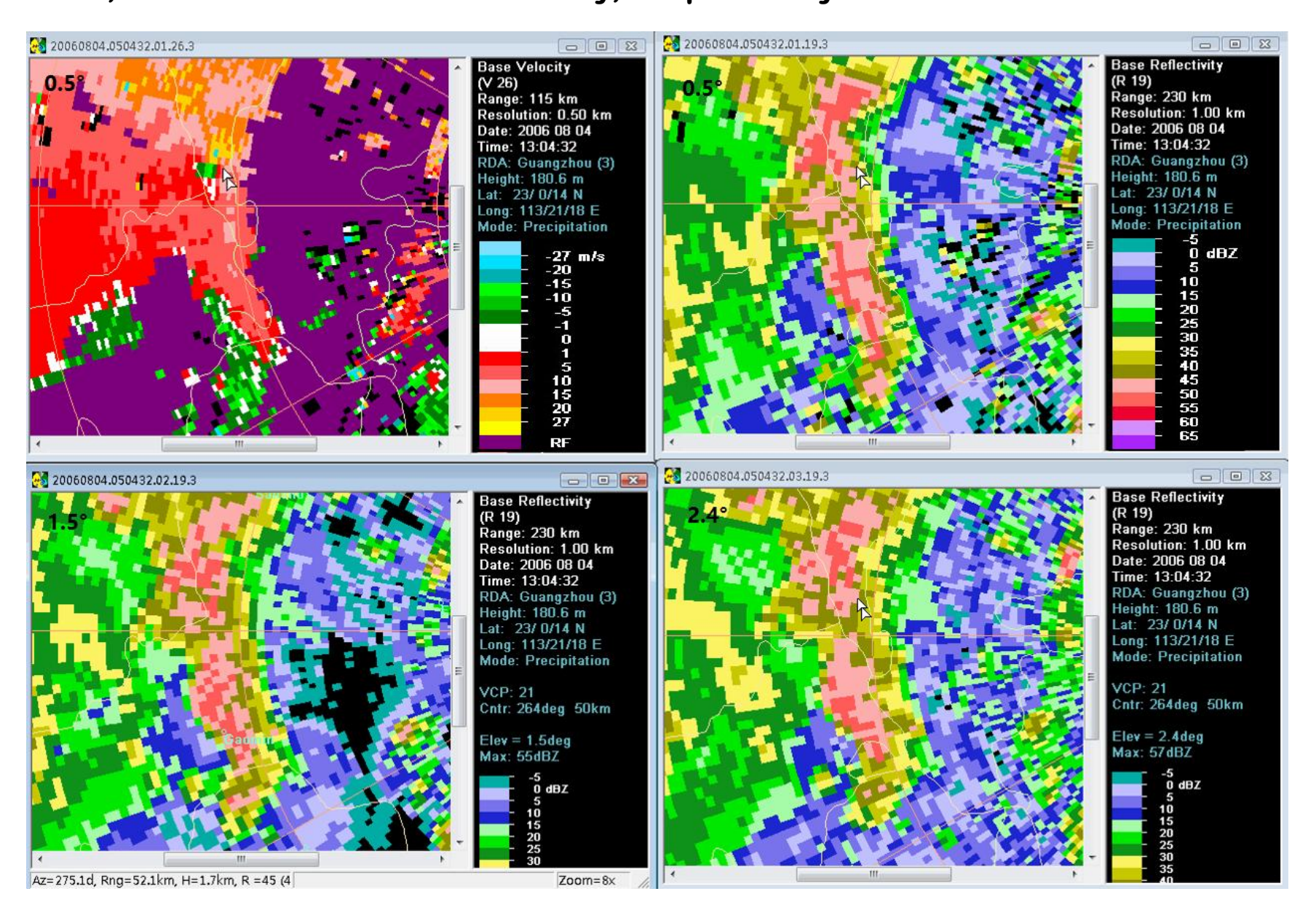
2006 08 04 12:52 BJT Guangzhou SA radar 0.5° elevation velocity, 0.5°, 1.5°, and 2.4° elevation reflectivity, respectively.



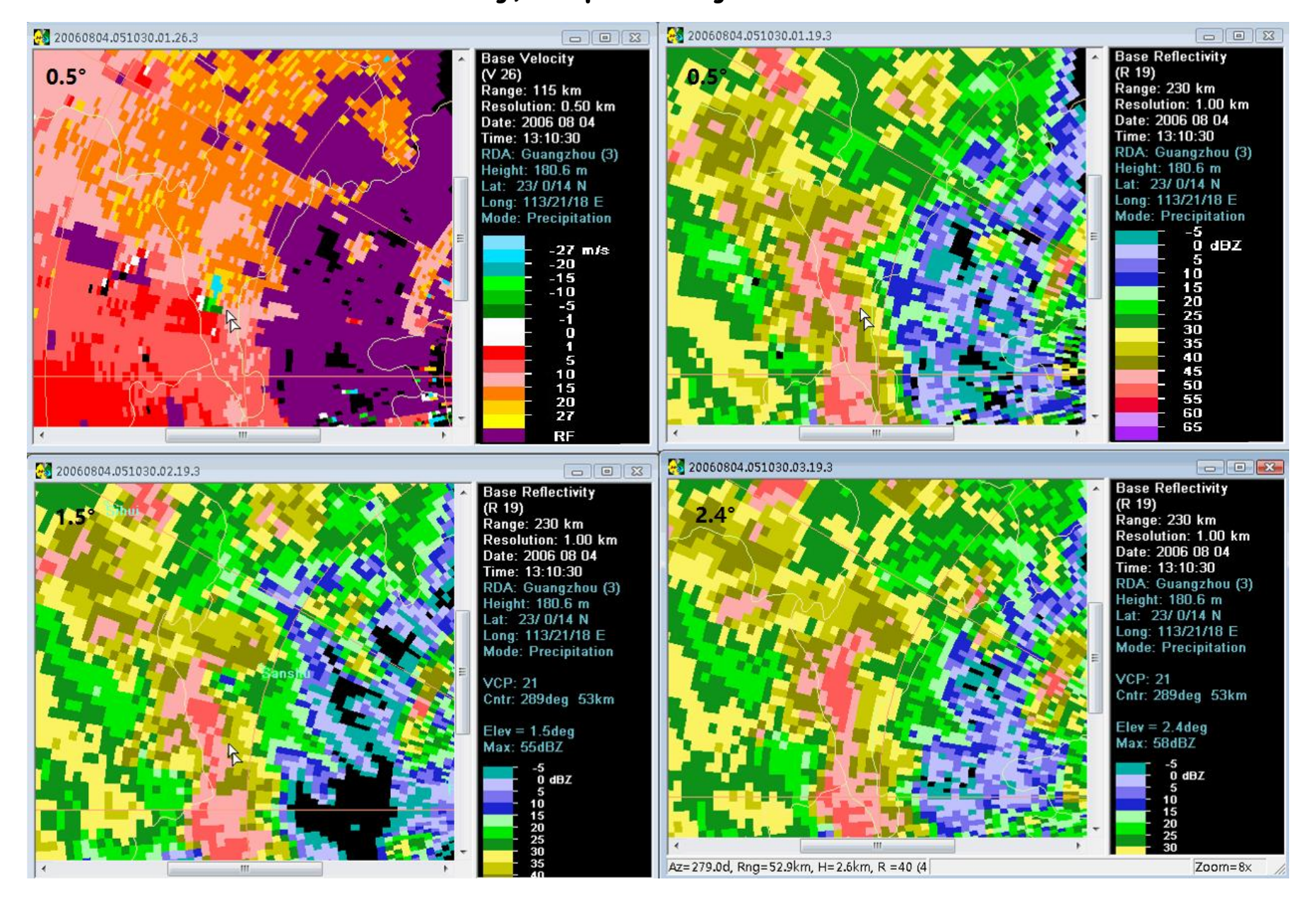
2006 08 04 12:58 BJT Guangzhou SA radar 0.5° elevation velocity, 0.5°, 1.5°, and 2.4° elevation reflectivity, respectively.



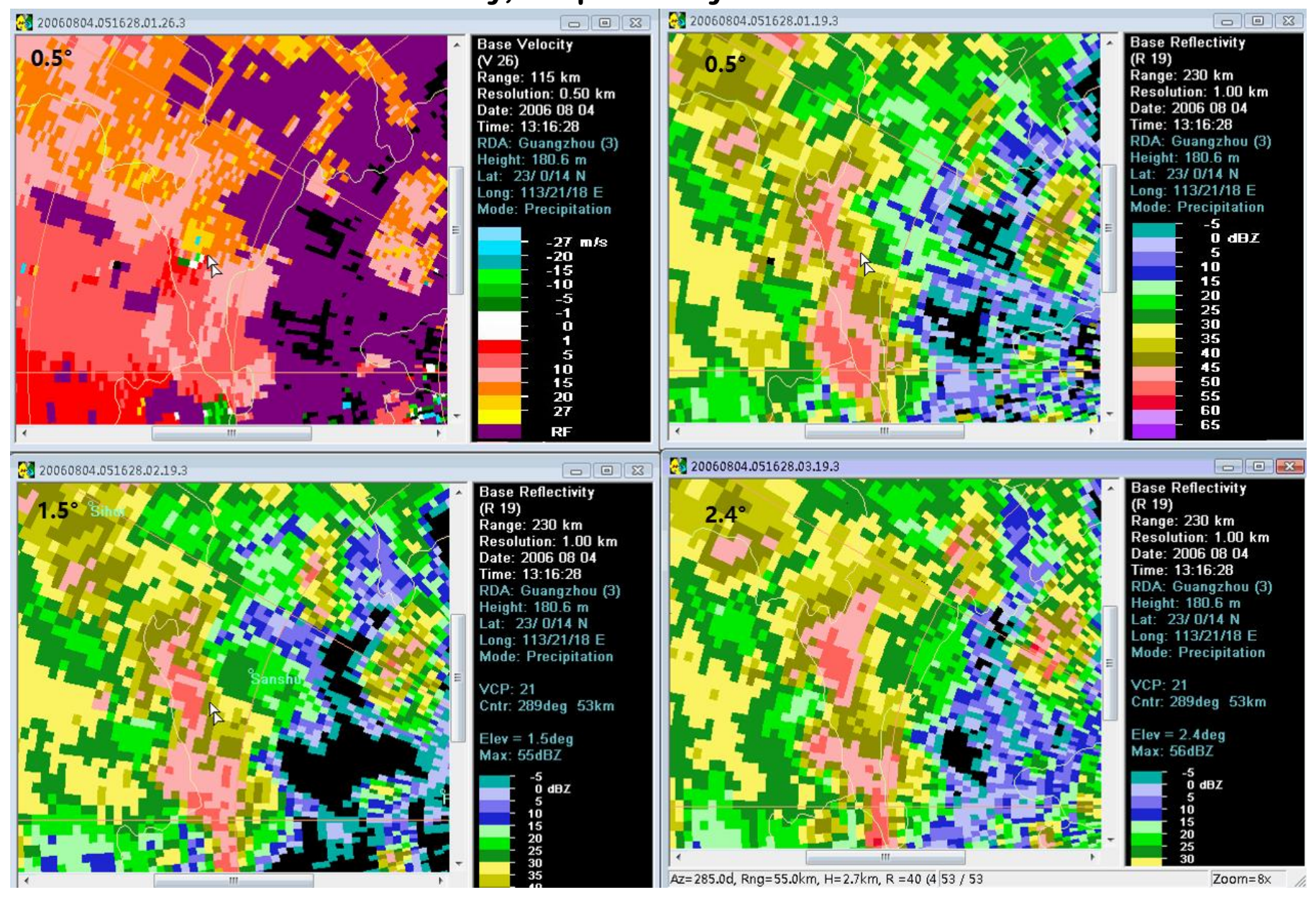
2006 08 04 13:04 BJT Guangzhou SA radar 0.5° elevation velocity, 0.5°, 1.5°, and 2.4° elevation reflectivity, respectively.



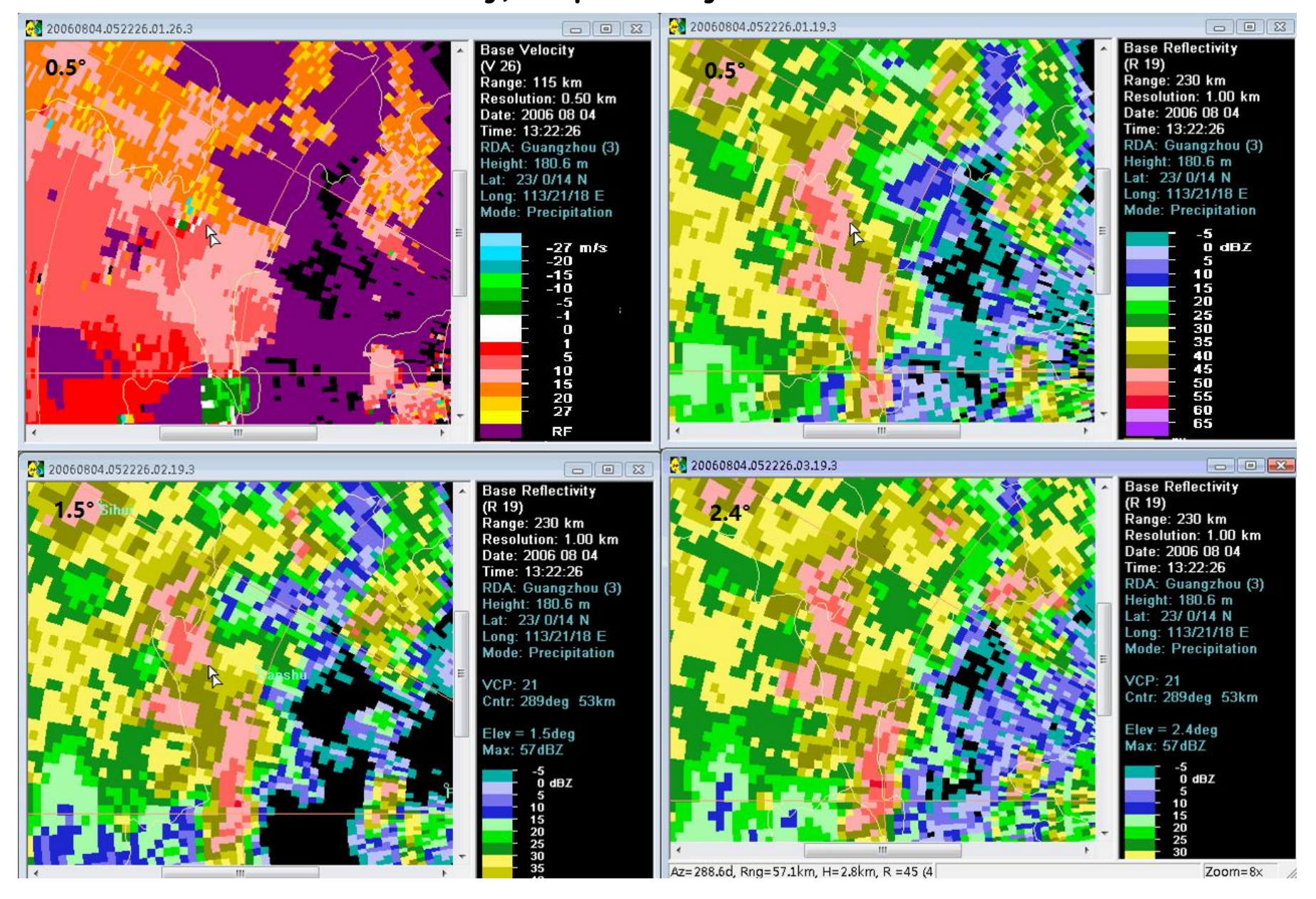
2006 08 04 13:10 BJT Guangzhou SA radar 0.5° elevation velocity, 0.5°, 1.5°, and 2.4° elevation reflectivity, respectively.



2006 08 04 13:16 BJT Guangzhou SA radar 0.5° elevation velocity, 0.5°, 1.5°, and 2.4° elevation reflectivity, respectively.

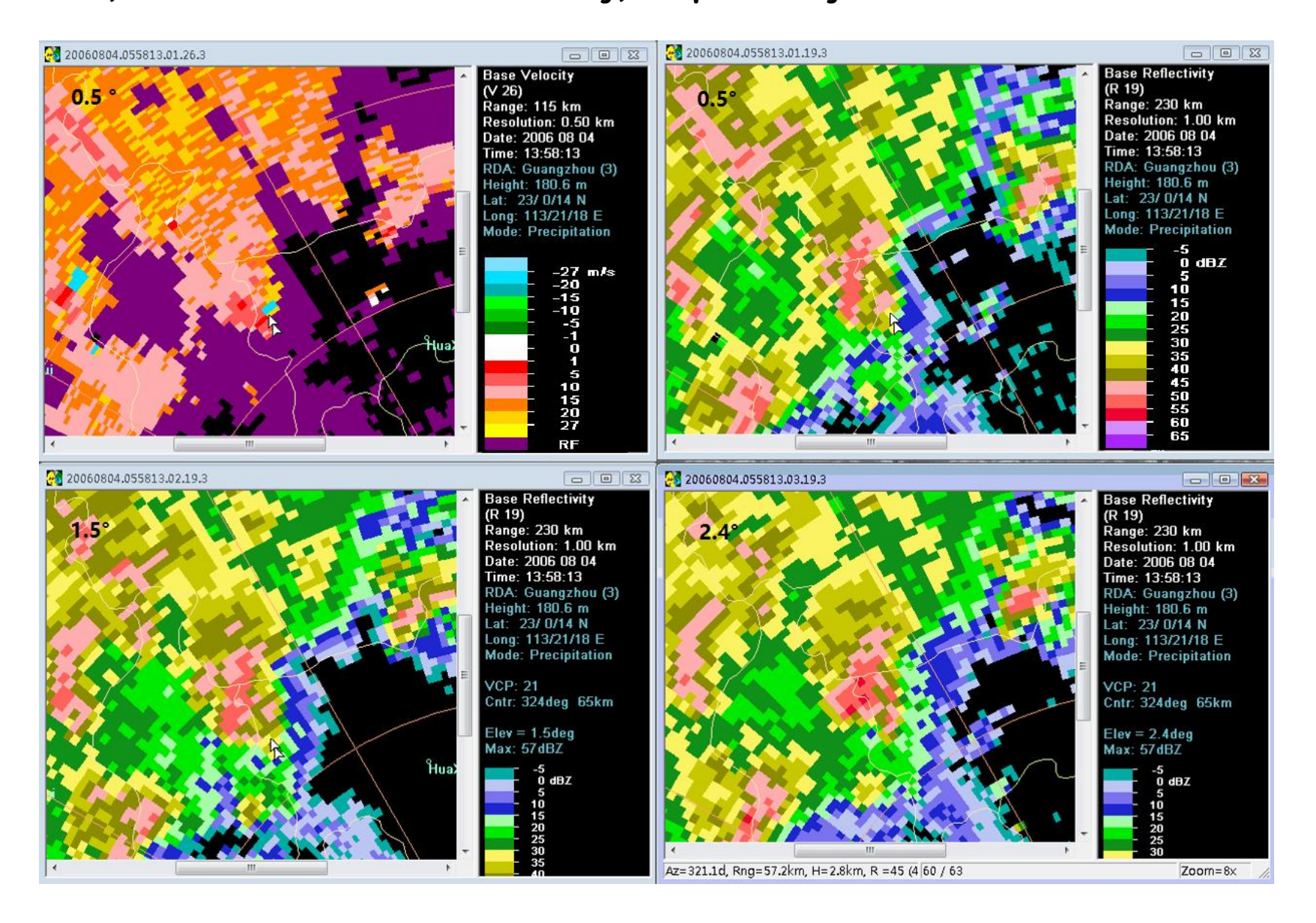


2006 08 04 13:22 BJT Guangzhou SA radar 0.5° elevation velocity, 0.5°, 1.5°, and 2.4° elevation reflectivity, respectively.

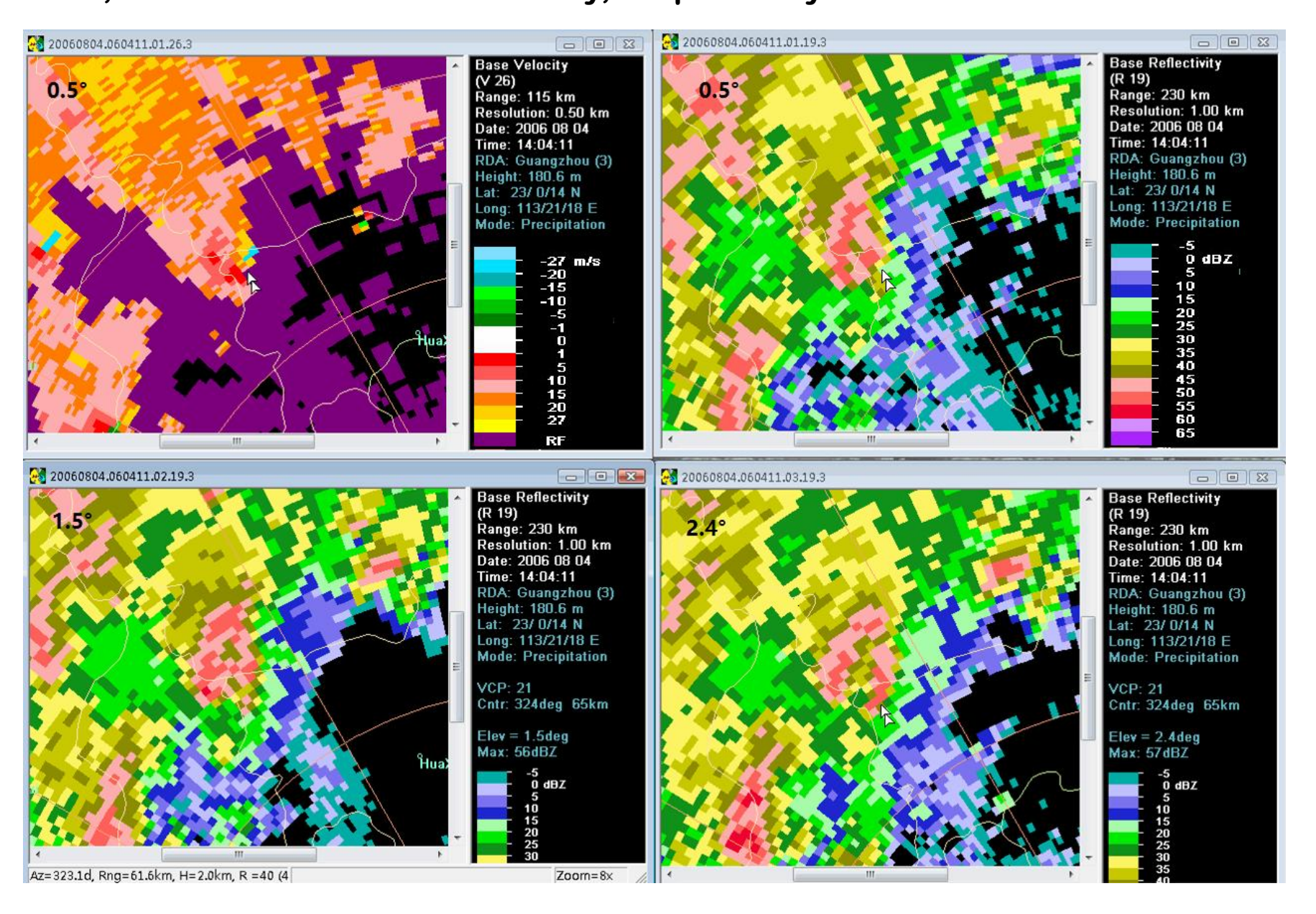


Tornado 4: Shijiao town, Qingyuan city, around 14:30 BJT on the 4th October 2015

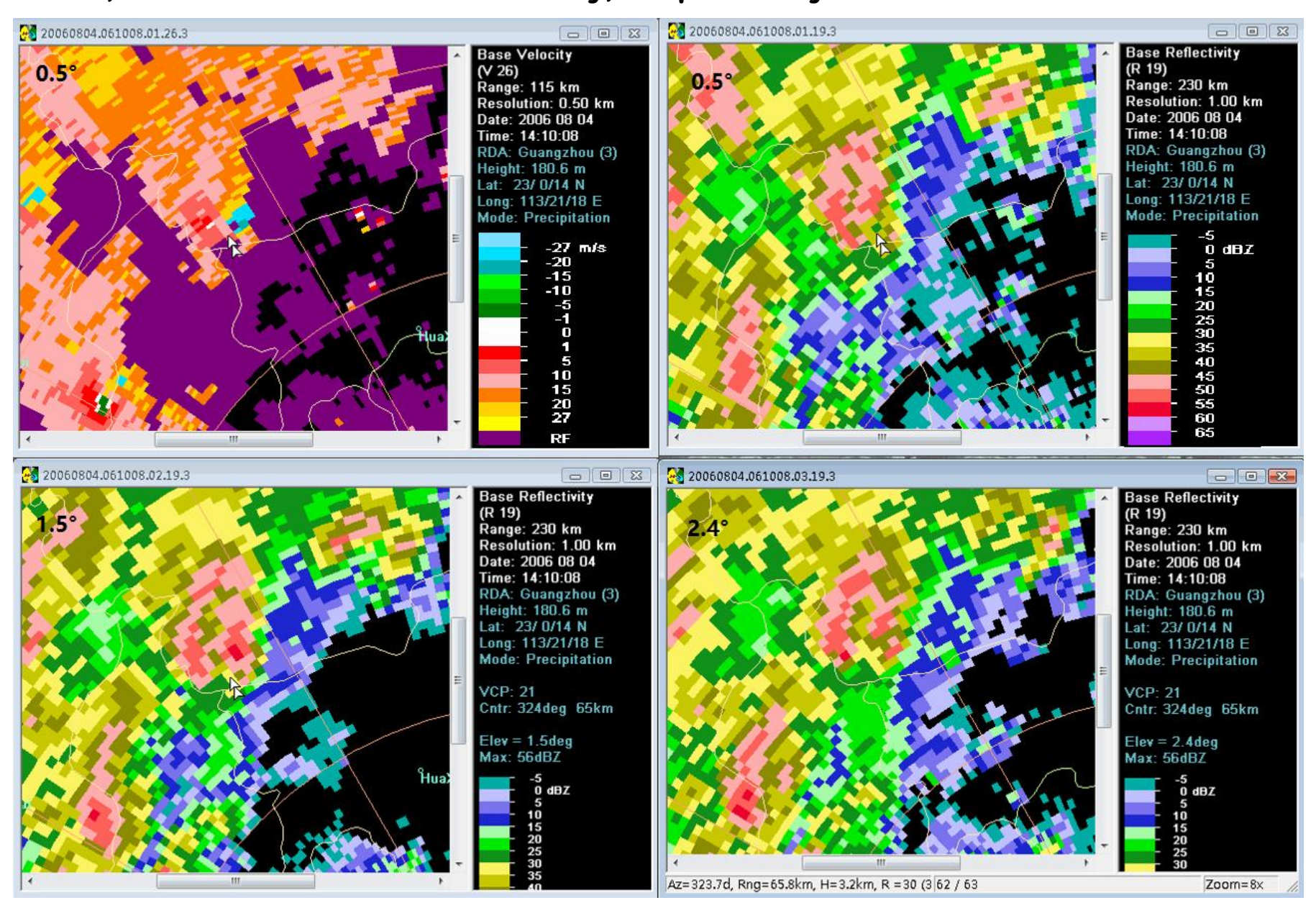
2006 08 04 13:58 BJT Guangzhou SA radar 0.5° elevation velocity, 0.5°, 1.5°, and 2.4° elevation reflectivity, respectively.



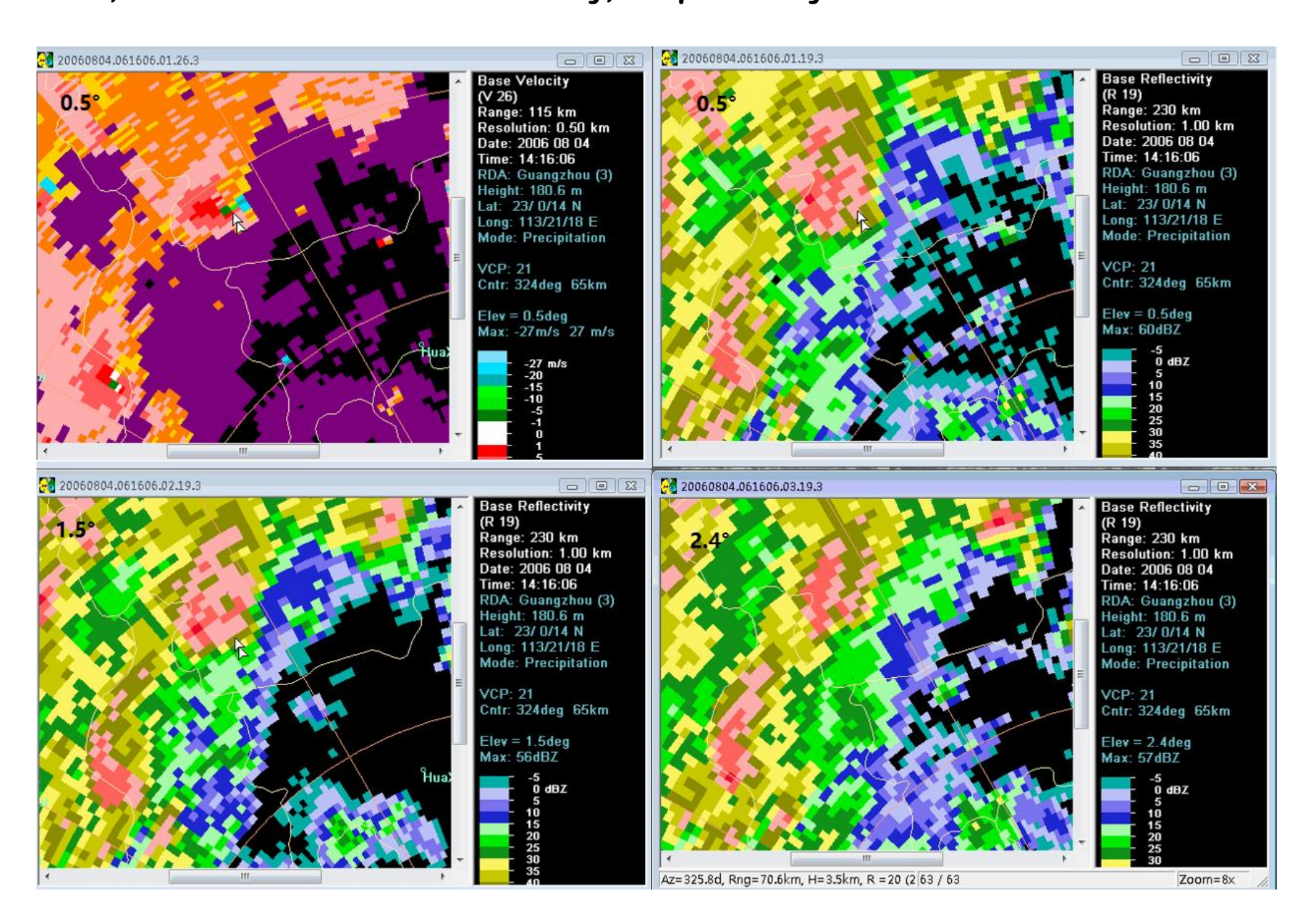
2006 08 04 14:04 BJT Guangzhou SA radar 0.5° elevation velocity, 0.5°, 1.5°, and 2.4° elevation reflectivity, respectively.



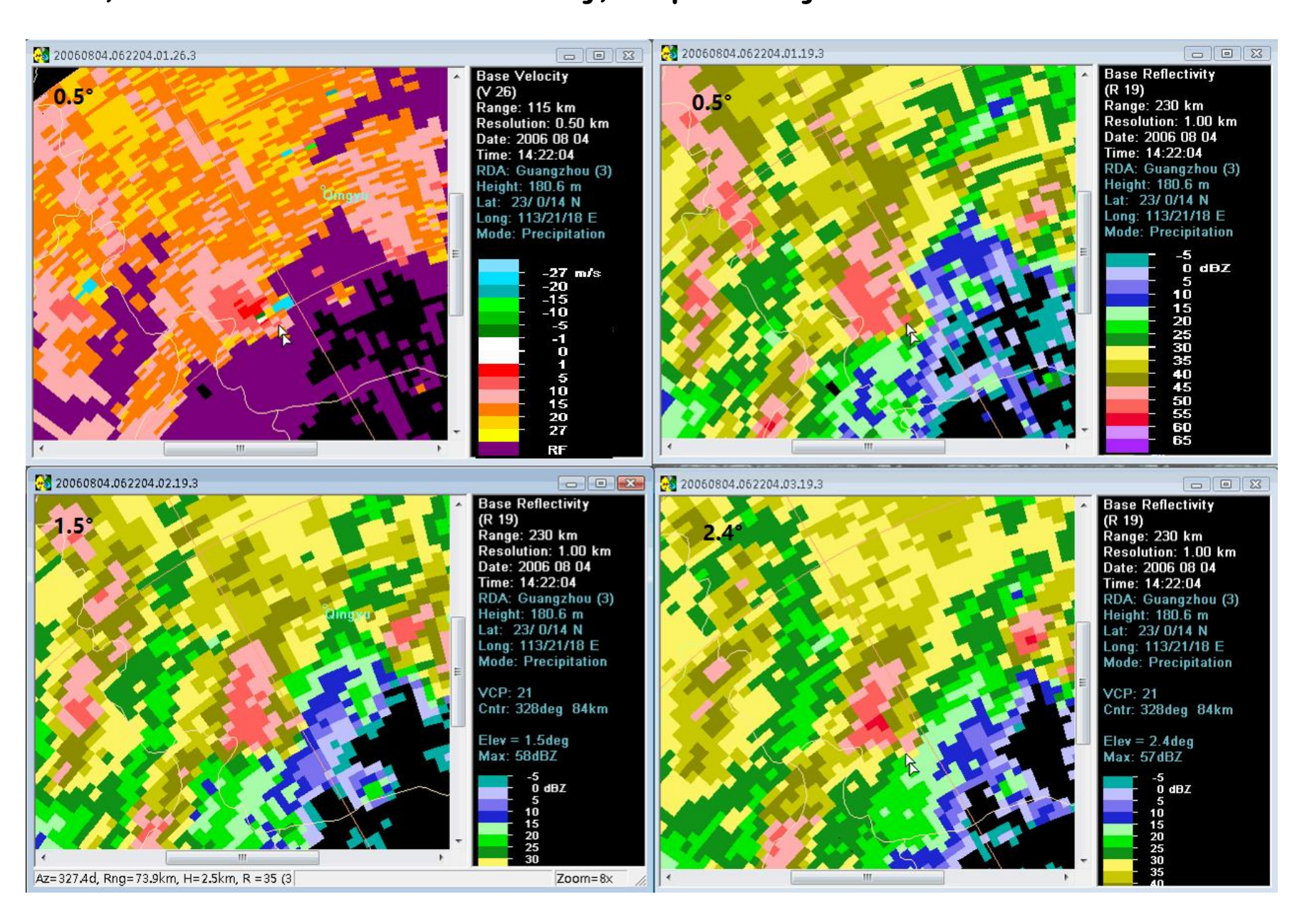
2006 08 04 14:10 BJT Guangzhou SA radar 0.5° elevation velocity, 0.5°, 1.5°, and 2.4° elevation reflectivity, respectively.



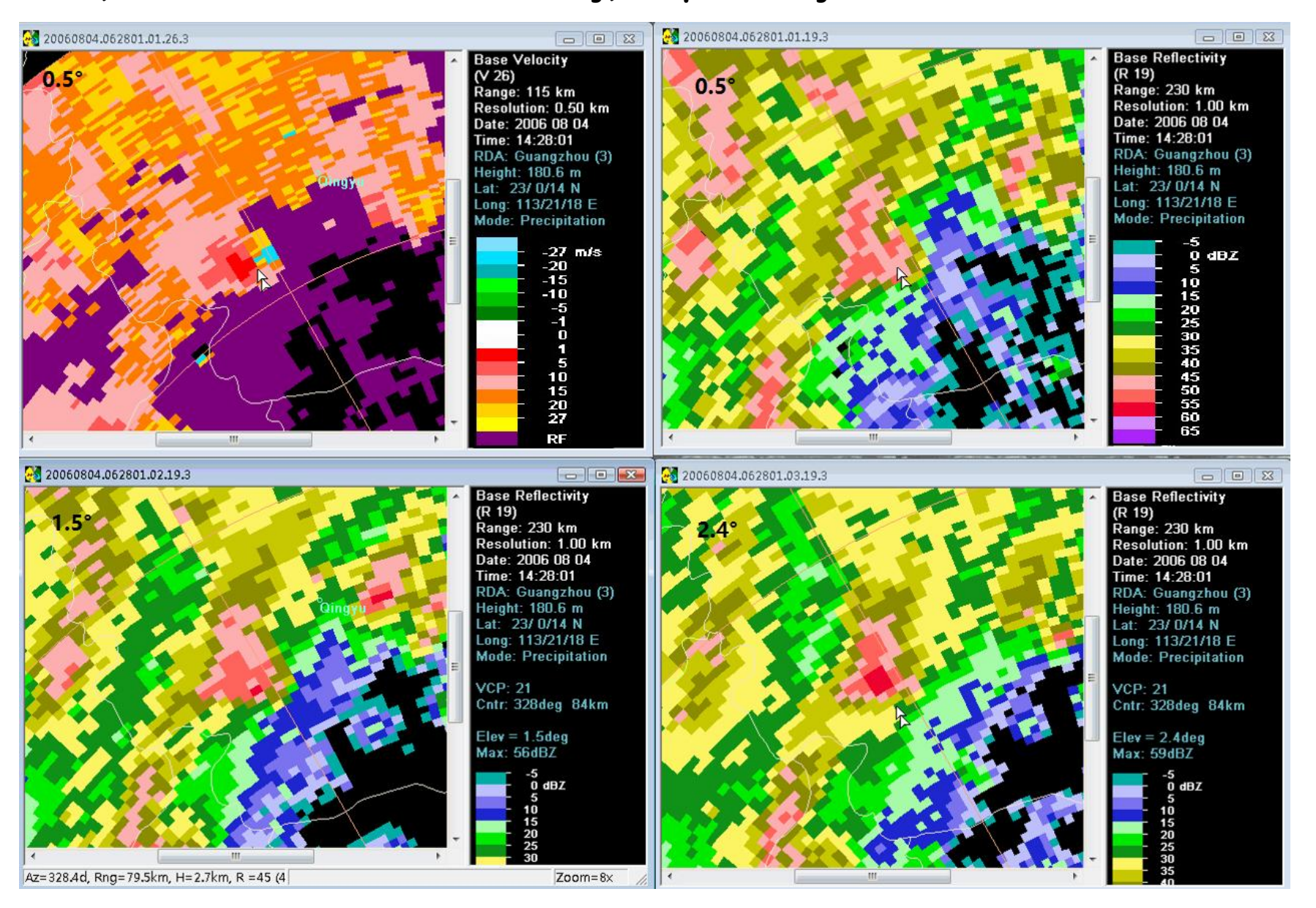
2006 08 04 14:16 BJT Guangzhou SA radar 0.5° elevation velocity, 0.5°, 1.5°, and 2.4° elevation reflectivity, respectively.



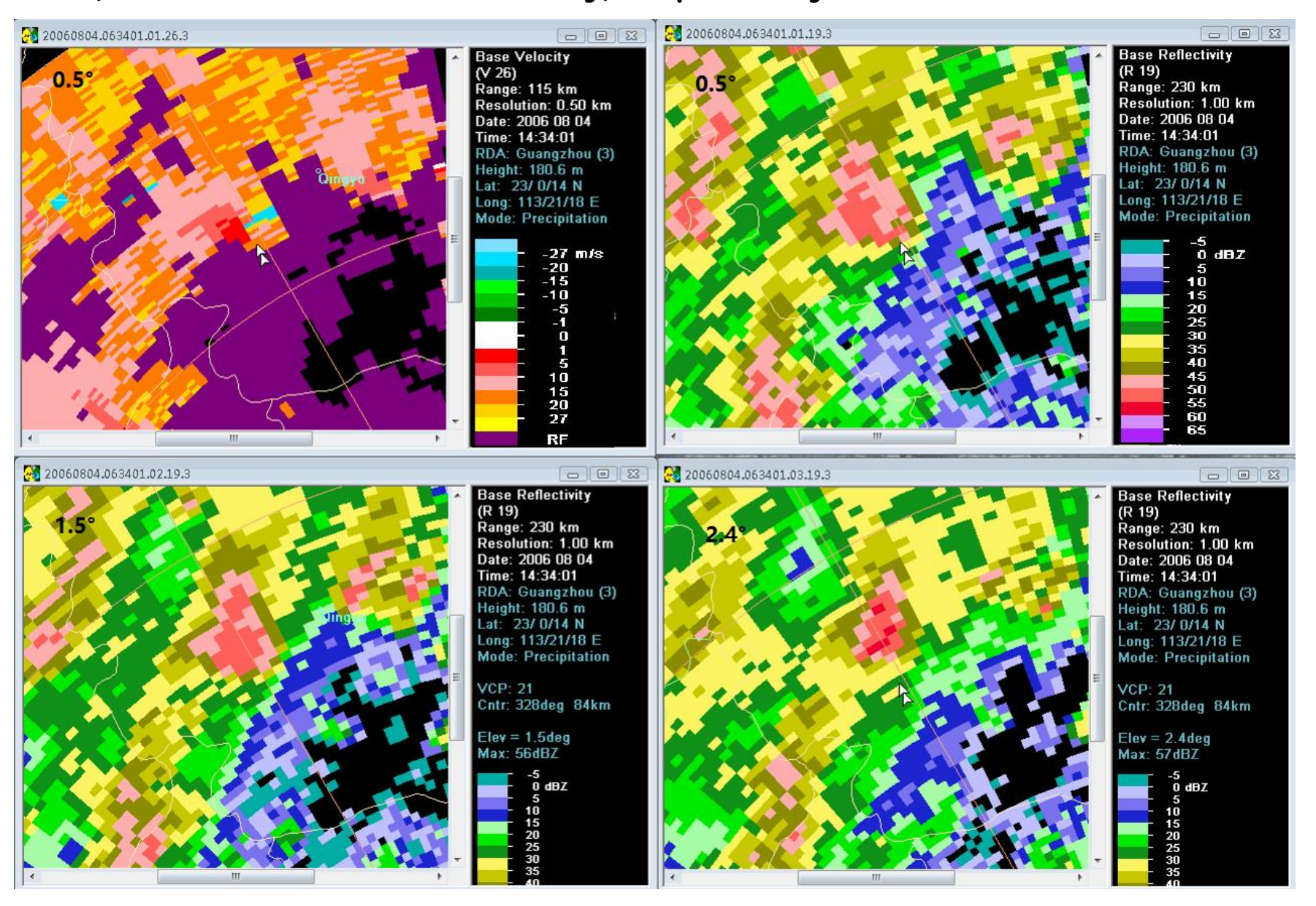
2006 08 04 14:22 BJT Guangzhou SA radar 0.5° elevation velocity, 0.5°, 1.5°, and 2.4° elevation reflectivity, respectively.



2006 08 04 14:28 BJT Guangzhou SA radar 0.5° elevation velocity, 0.5°, 1.5°, and 2.4° elevation reflectivity, respectively.

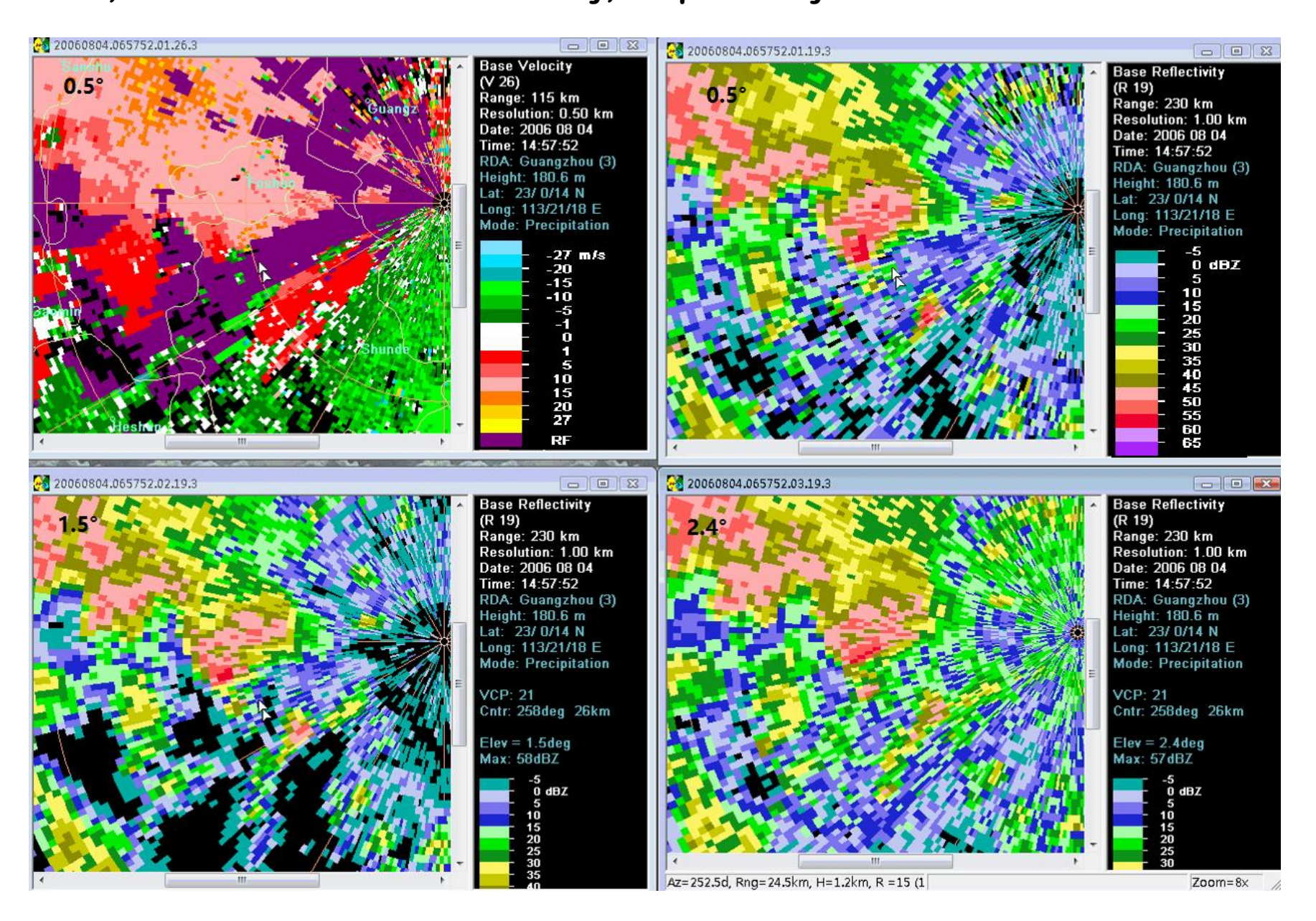


2006 08 04 14:34 BJT Guangzhou SA radar 0.5° elevation velocity, 0.5°, 1.5°, and 2.4° elevation reflectivity, respectively.

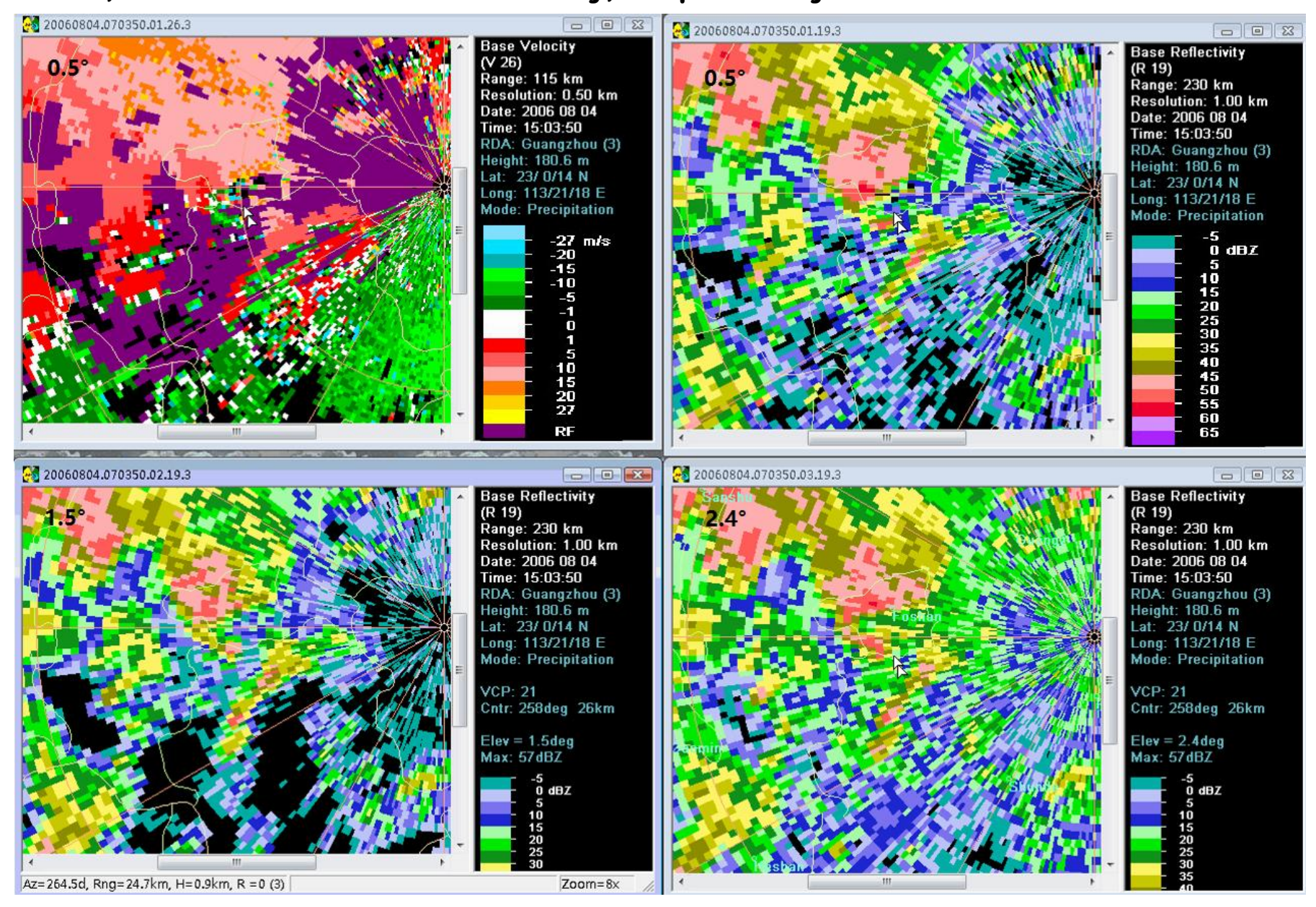


Tornado 5: Dali town, Foshan city, around 15:30 BJT on the 4th October 2015

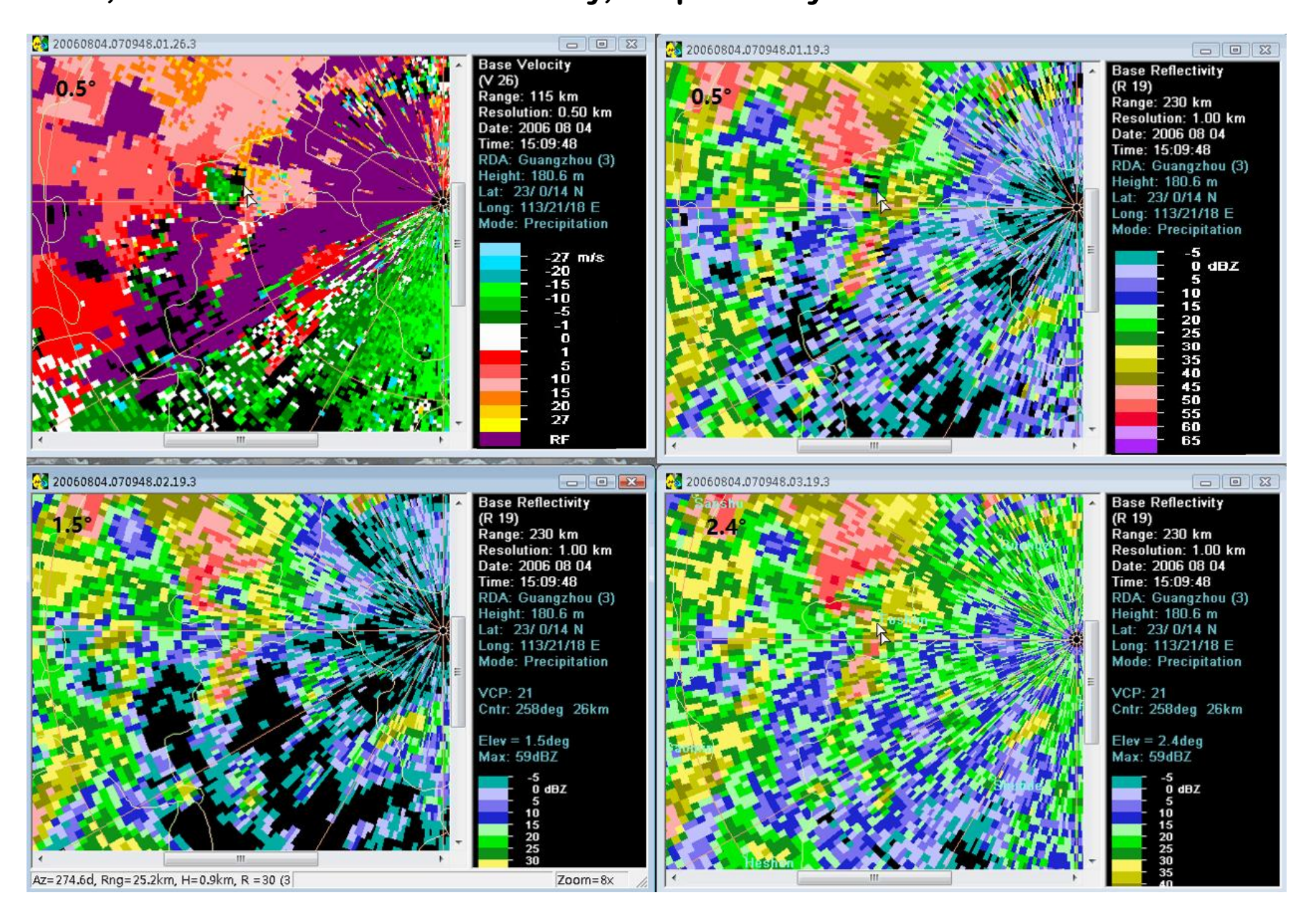
2006 08 04 14:58 BJT Guangzhou SA radar 0.5° elevation velocity, 0.5°, 1.5°, and 2.4° elevation reflectivity, respectively.



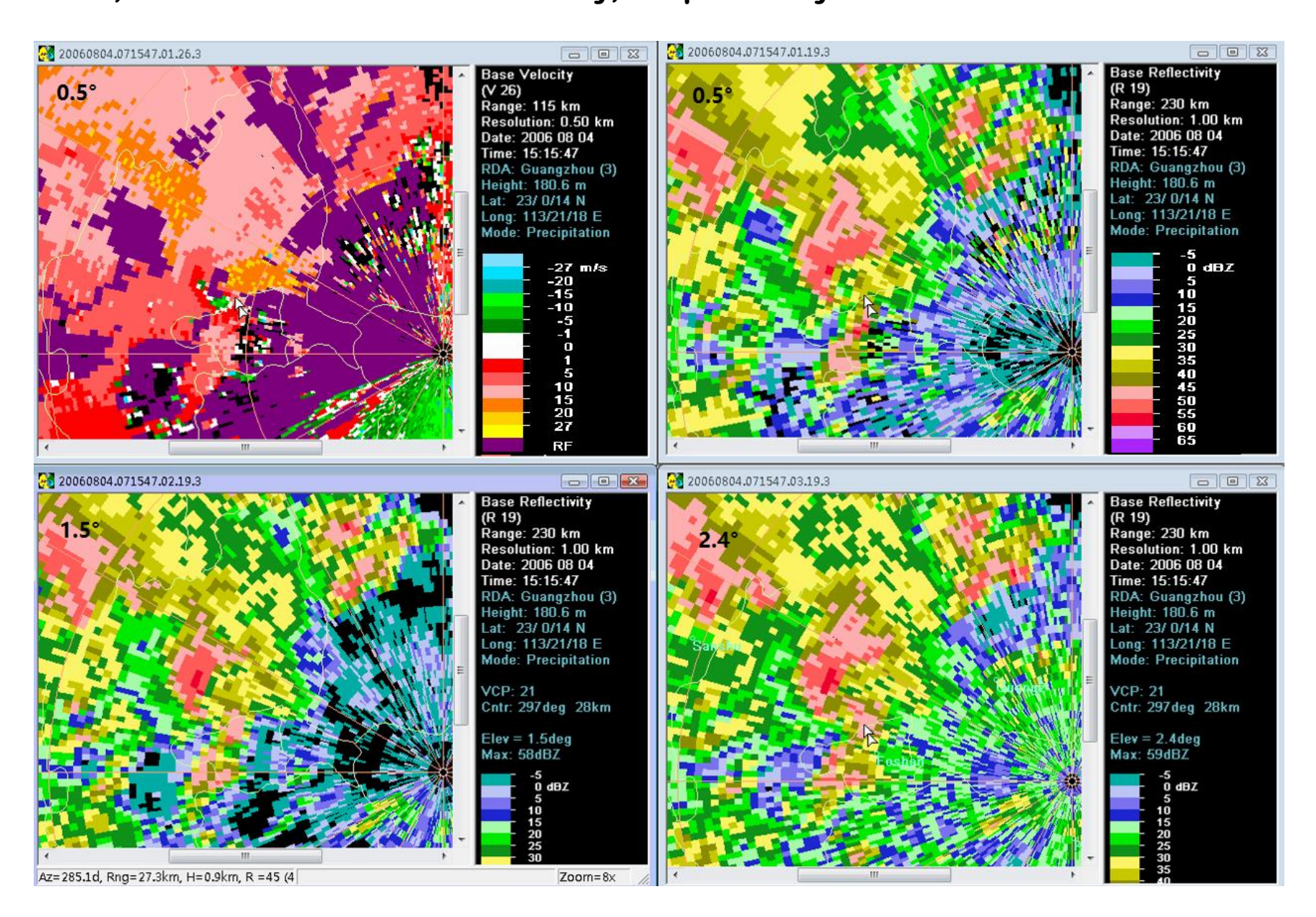
2006 08 04 15:04 BJT Guangzhou SA radar 0.5° elevation velocity, 0.5°, 1.5°, and 2.4° elevation reflectivity, respectively.



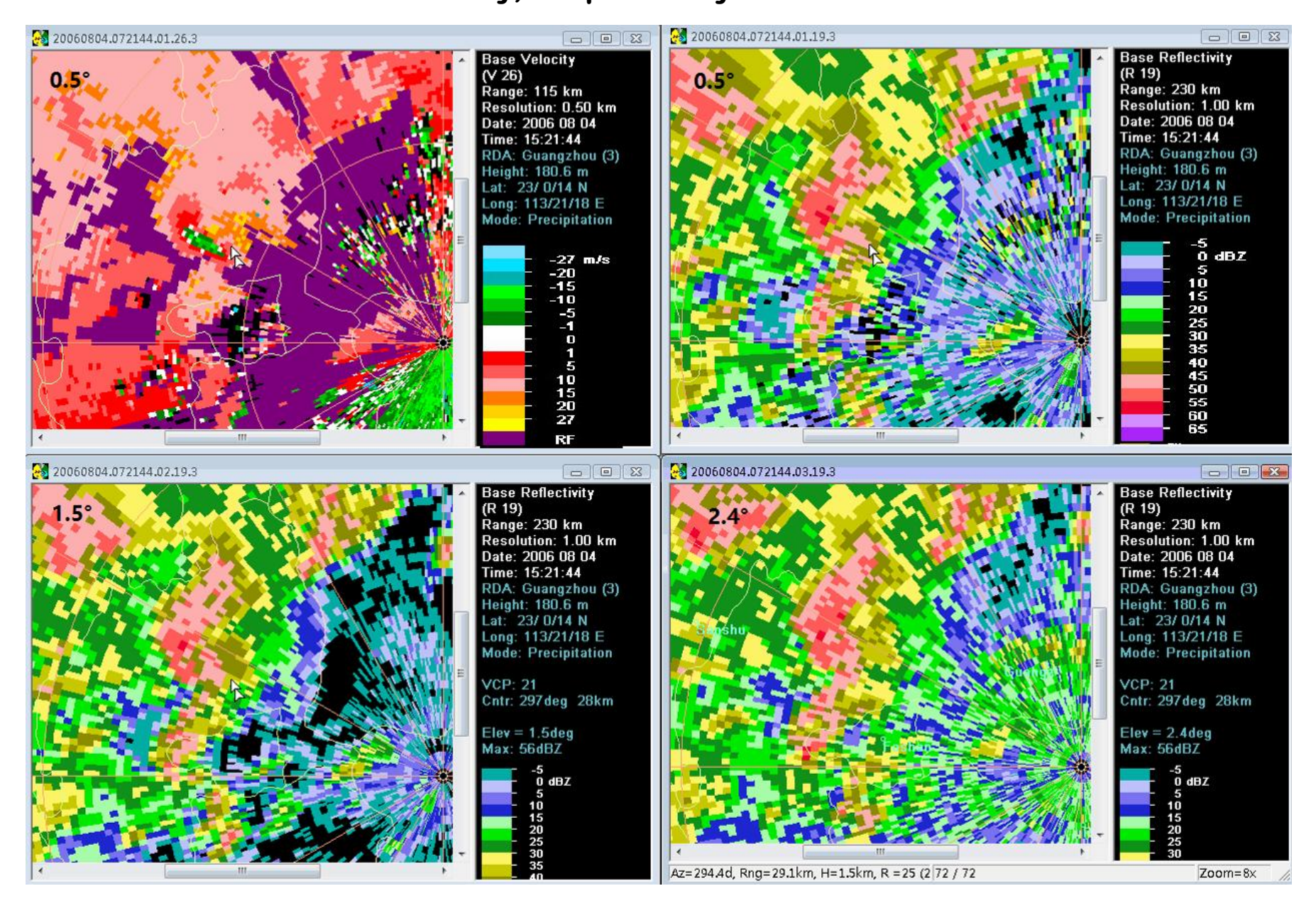
2006 08 04 15:10 BJT Guangzhou SA radar 0.5° elevation velocity, 0.5°, 1.5°, and 2.4° elevation reflectivity, respectively.



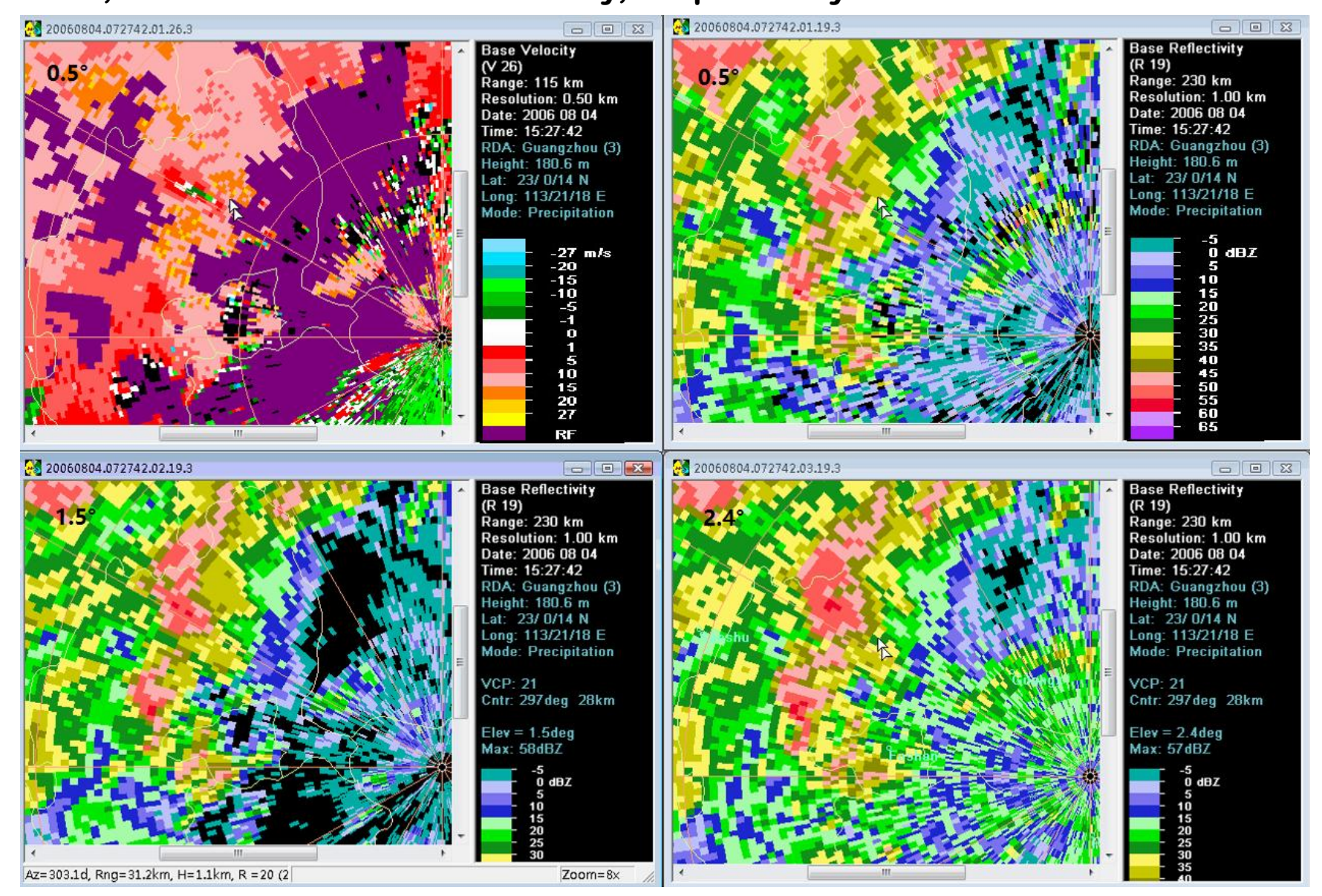
2006 08 04 15:16 BJT Guangzhou SA radar 0.5° elevation velocity, 0.5°, 1.5°, and 2.4° elevation reflectivity, respectively.



2006 08 04 15:22 BJT Guangzhou SA radar 0.5° elevation velocity, 0.5°, 1.5°, and 2.4° elevation reflectivity, respectively.



2006 08 04 15:28 BJT Guangzhou SA radar 0.5° elevation velocity, 0.5°, 1.5°, and 2.4° elevation reflectivity, respectively.

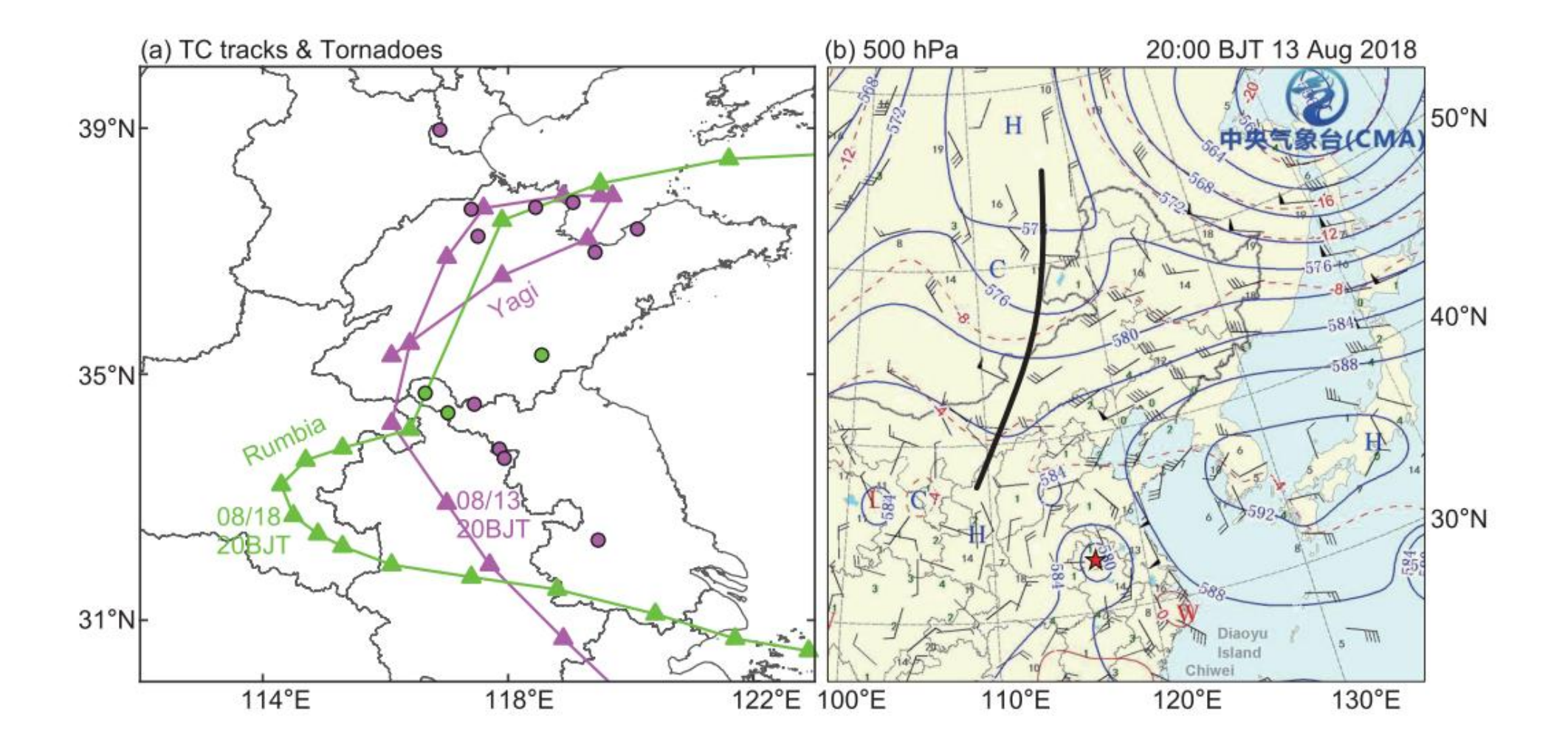


Case02 summary

- On the 4th August 2006, five tornadoes produced by the mini-surpercells embeded in the outer spiral rain belts of Typhoon "Prapiroon" hit Danzao town(10:50 BJT) of Foshan city, Jindu town (13:00 BJT) of Zhaoqing city, Baini town (13:20 BJT) of Foshan city, Shijiao town (14:30 BJT) of Qingyuan city, and Dali town (15:30 BJT) of Foshan city, 10 people were killed, over 100 people wounded. The first tornado (10:50 BJT Danzao town) was considered EF2 rank based on the damage survey, no damage survey have been done for other four tornadoes. The Typhoon "Prapiroon" landed between Maoming city and Yangjiang city (Guangdong province) around 19:00 BJT on 3rd August 2006.
- Based on the Hongkang sounding at 08:00 BJT on the 4th August 2006, it shows moderate conditional instability in the lower troposphere, with the temperature difference between 850 and 500 hPa being 23°C; There is abundant water vapor in lower troposphere, with surface dew point being 25°C, and precipitable water being 65mm; The moderate conditional instability and abundant water vapor in the lower troposhere give a moderate CAPE (1700J/kg) and weak CIN(10J/kg); The 0-6km and 0-1km wind vector difference are 22m/s and 15m/s, respectively, with LCL being 120 m. These conditions are favorable the supercell tornadoes.
- The maximum rotational speed of the mesocyclones of the first to fifth tornadoes are 18.0 m/s, 15.5 m/s, 18.0 m/s, 18.5 m/s and 18.0 m/s, respectively, with diameter being 3.5km, 4.3km, 3.6km, 4.6km, and 3.5 km, corresponding vertical vorticity being 2.1×10⁻²s⁻¹, 1.4×10⁻²s⁻¹, 2.0×10⁻²s⁻¹, 1.6×10⁻²s⁻¹, and 2.1×10⁻²s⁻¹.

2018 08 13 and 08 14 TC Yagi tornadoes

- TC Yagi produced 11 tornadoes in Jiangsu, Shandong provinces and Tianjin City;
- Two of them are EF2 tornadoes, one occurs in Tjianjin city, another in Shandong province, we will analyze the two EF2 TC tornadoes.



TC Yagi EF2 tornado around 17:30 BJT on 13 August 2018 in Jinghai county, Tianjin city

- Ground truth
- Weather patterns
- Radar echoes

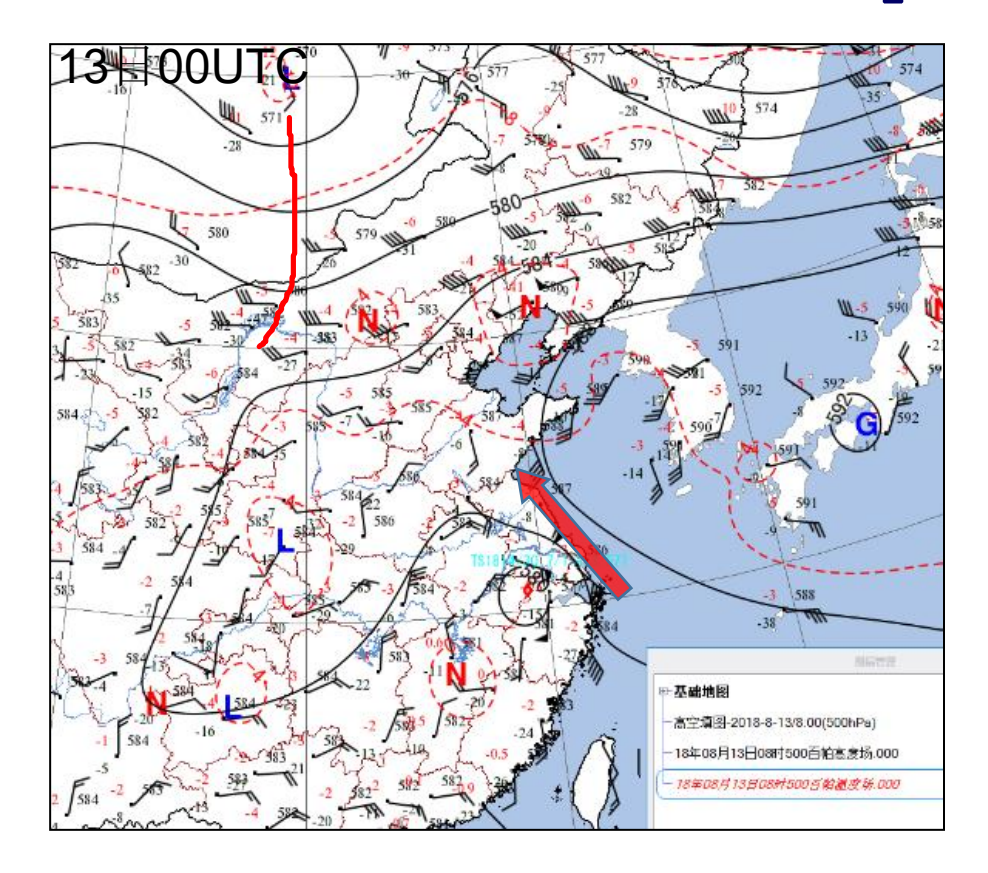


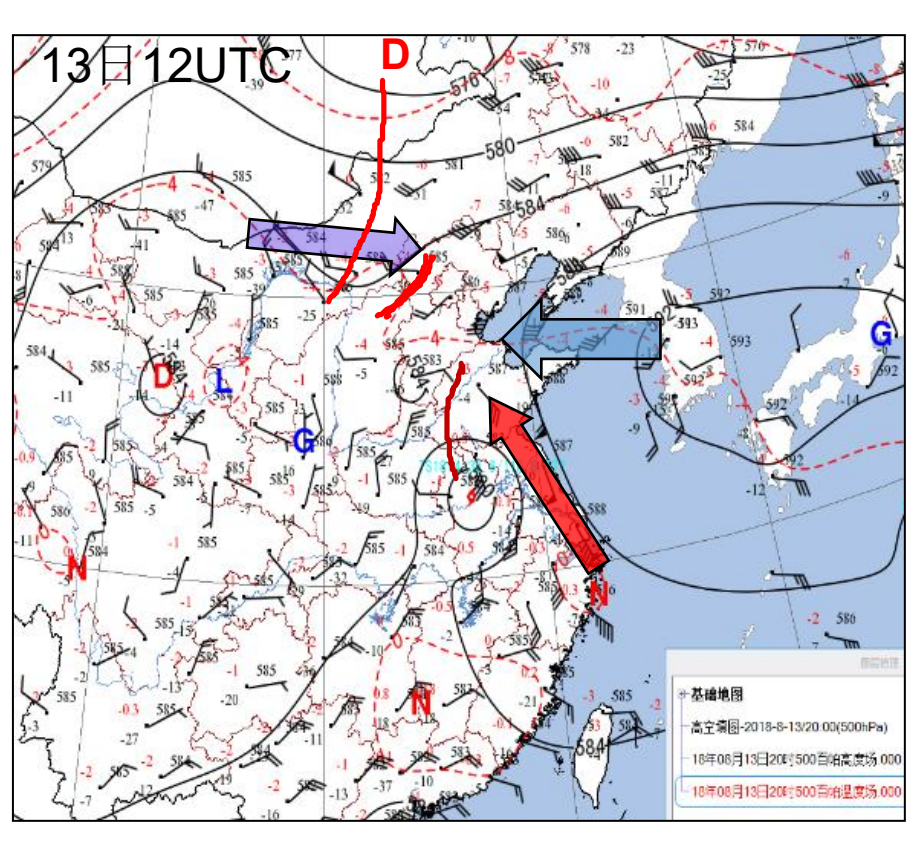




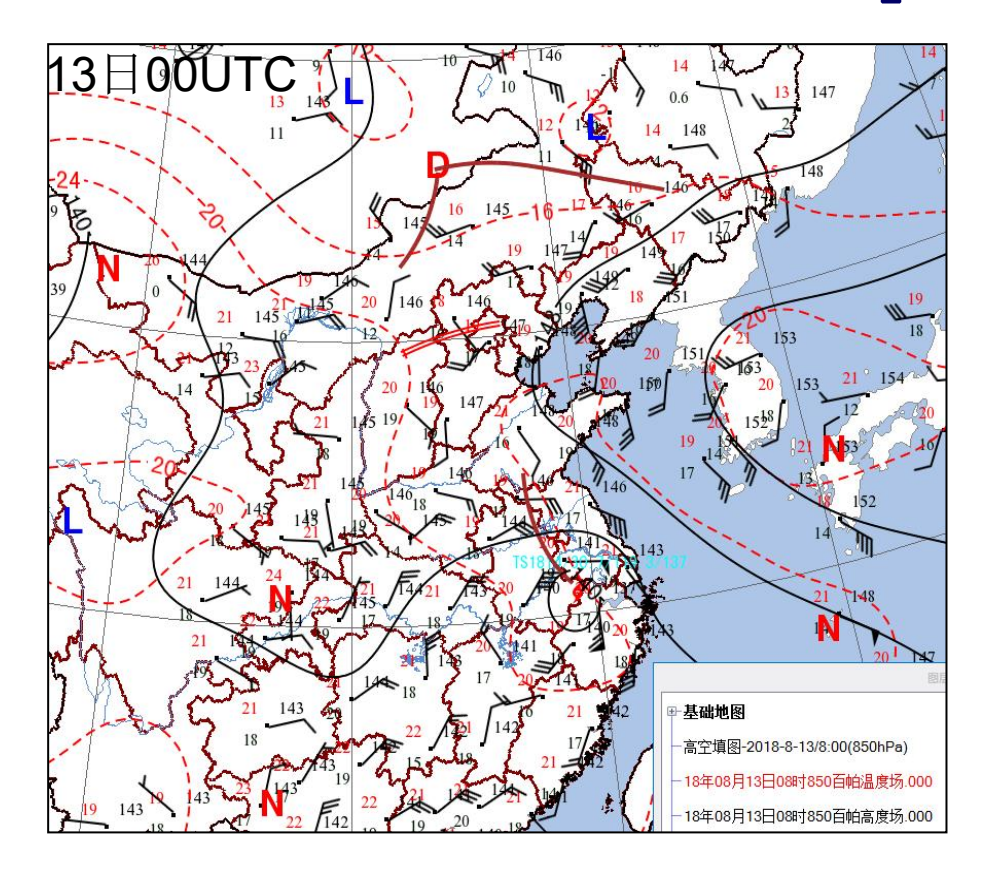


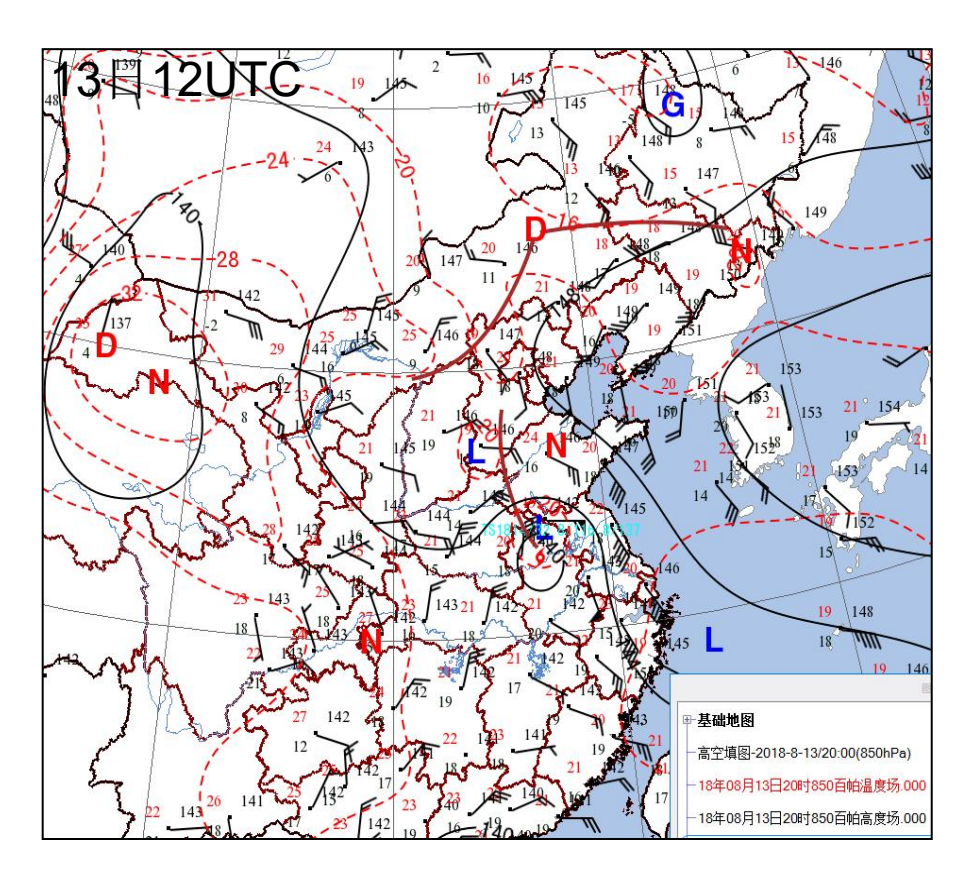
500hPa weather map



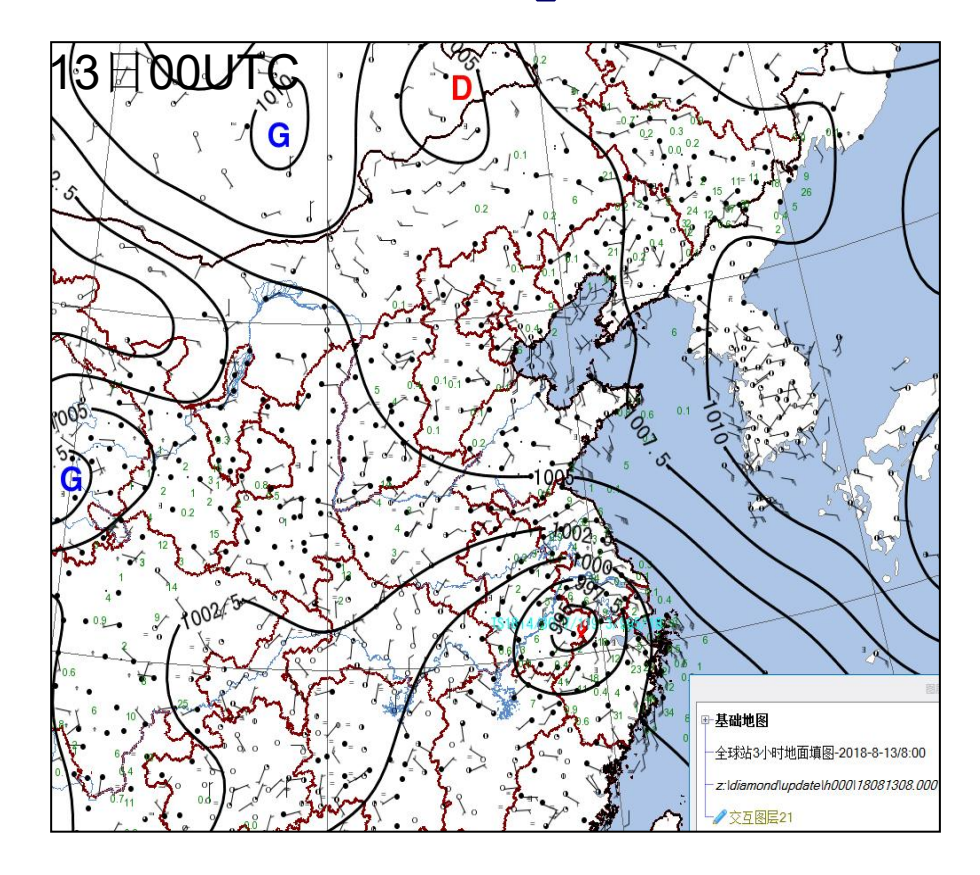


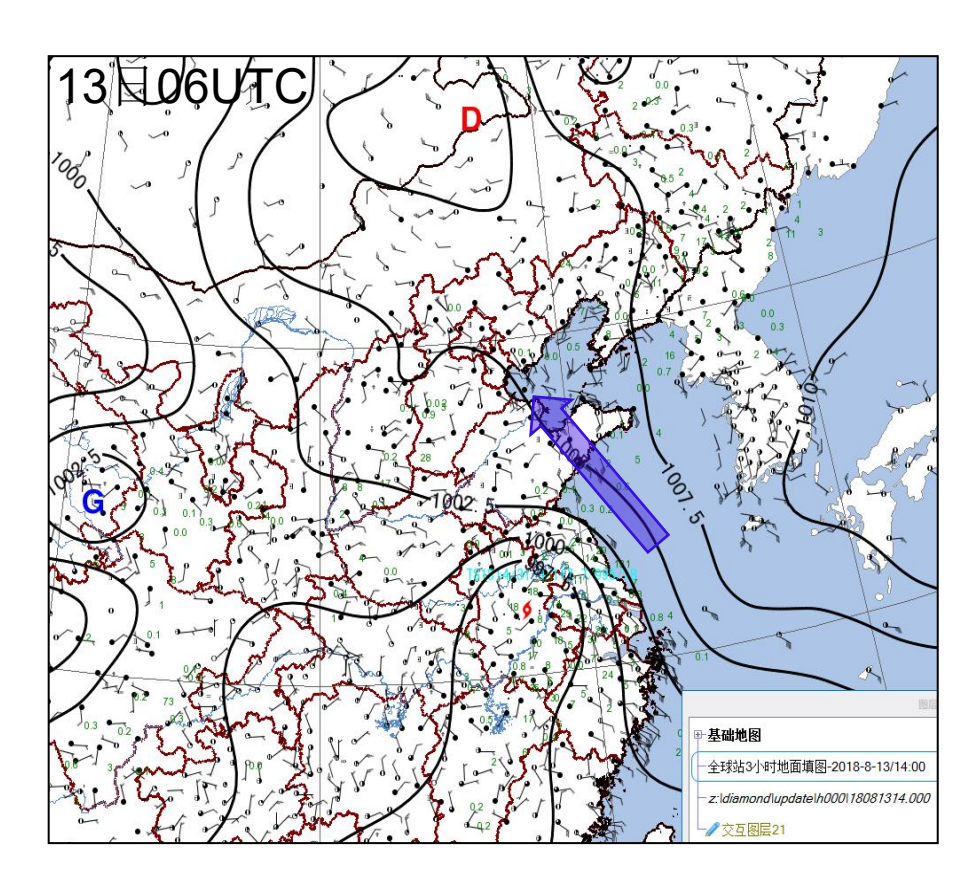
850hPa weather map

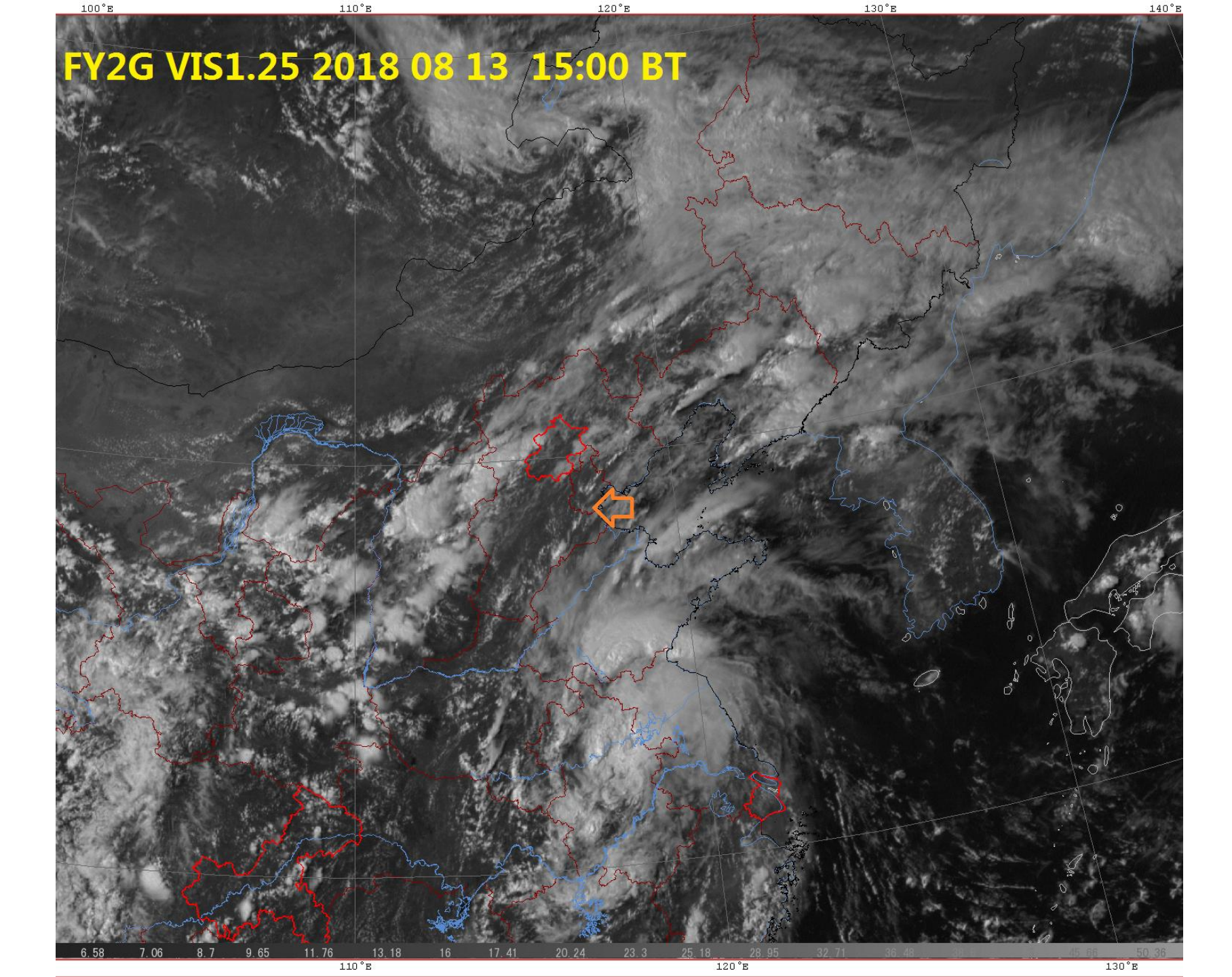




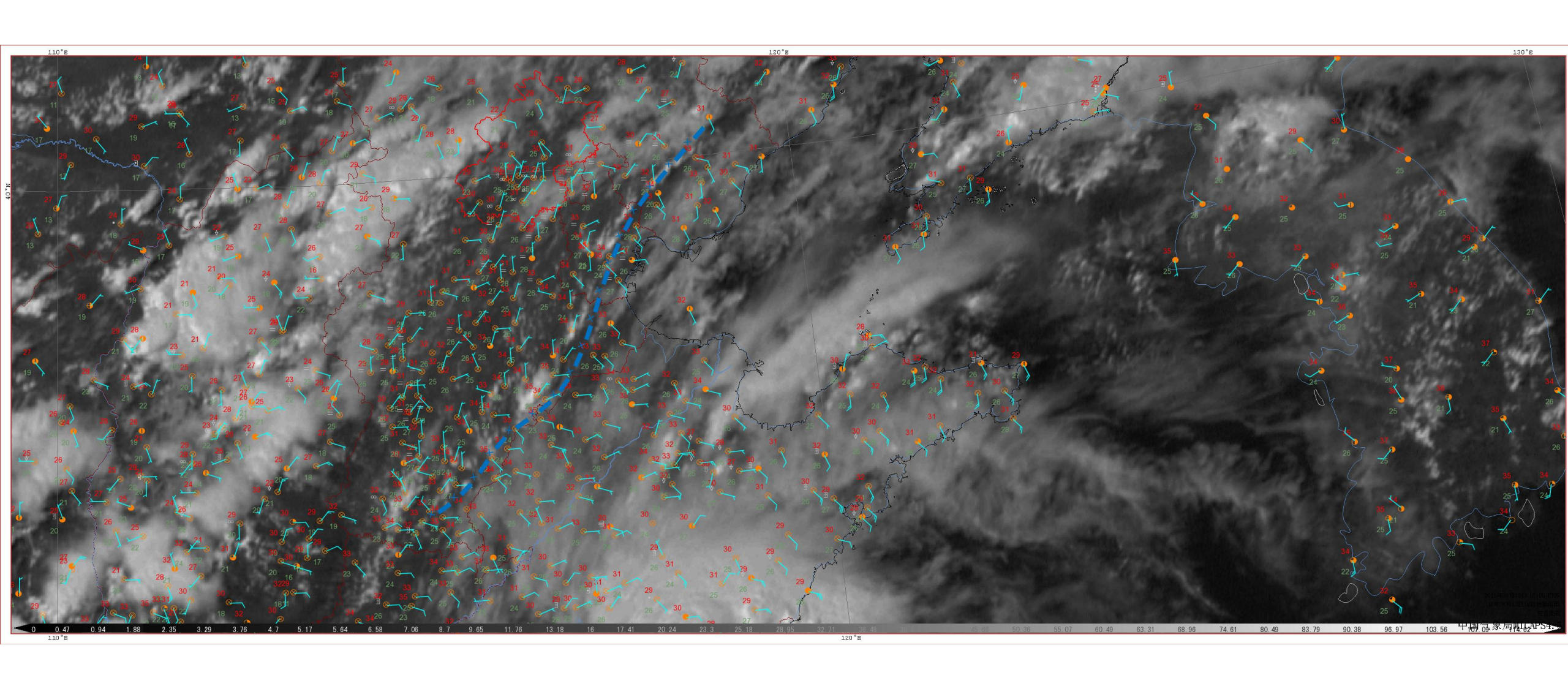
Surface map:

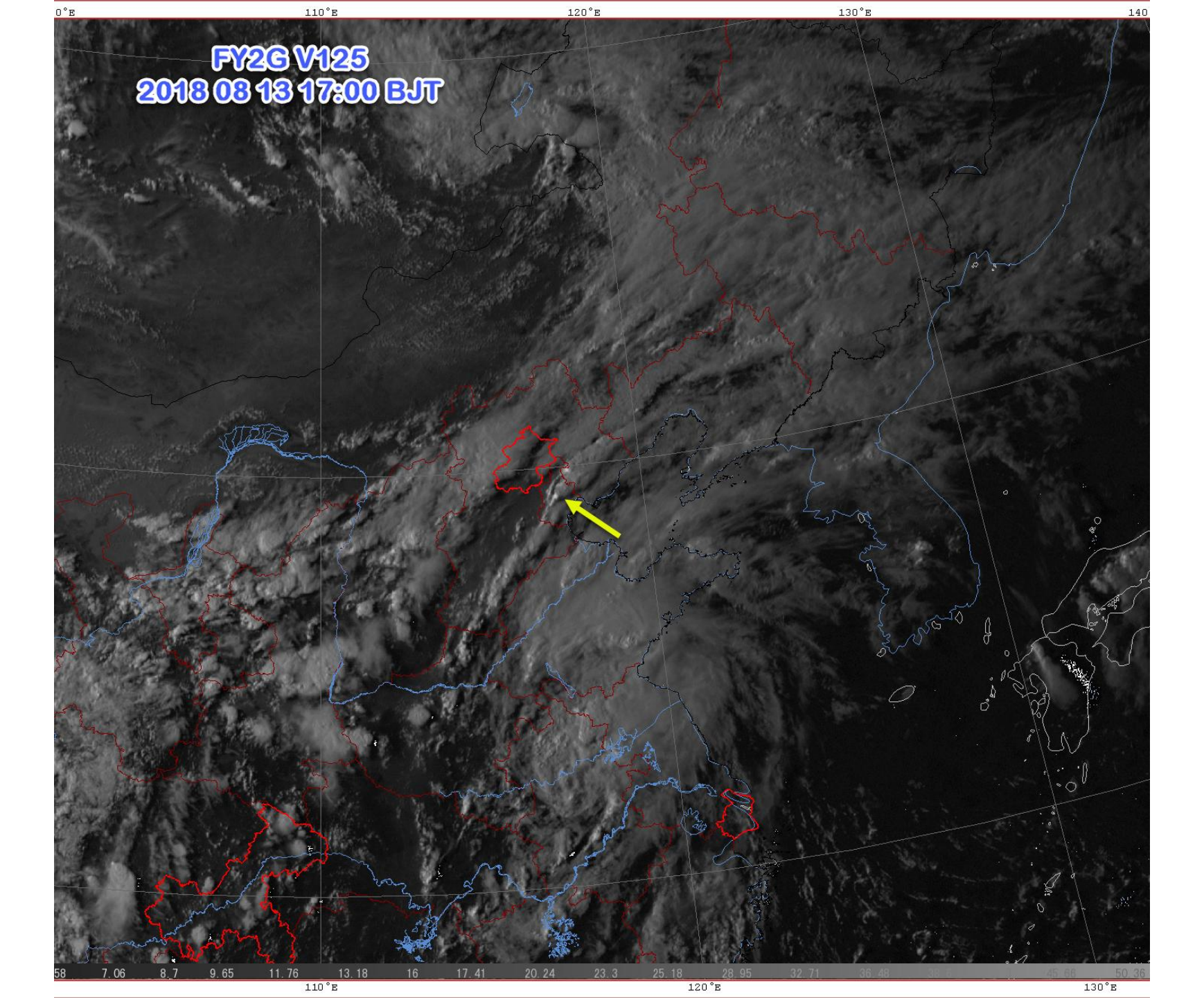




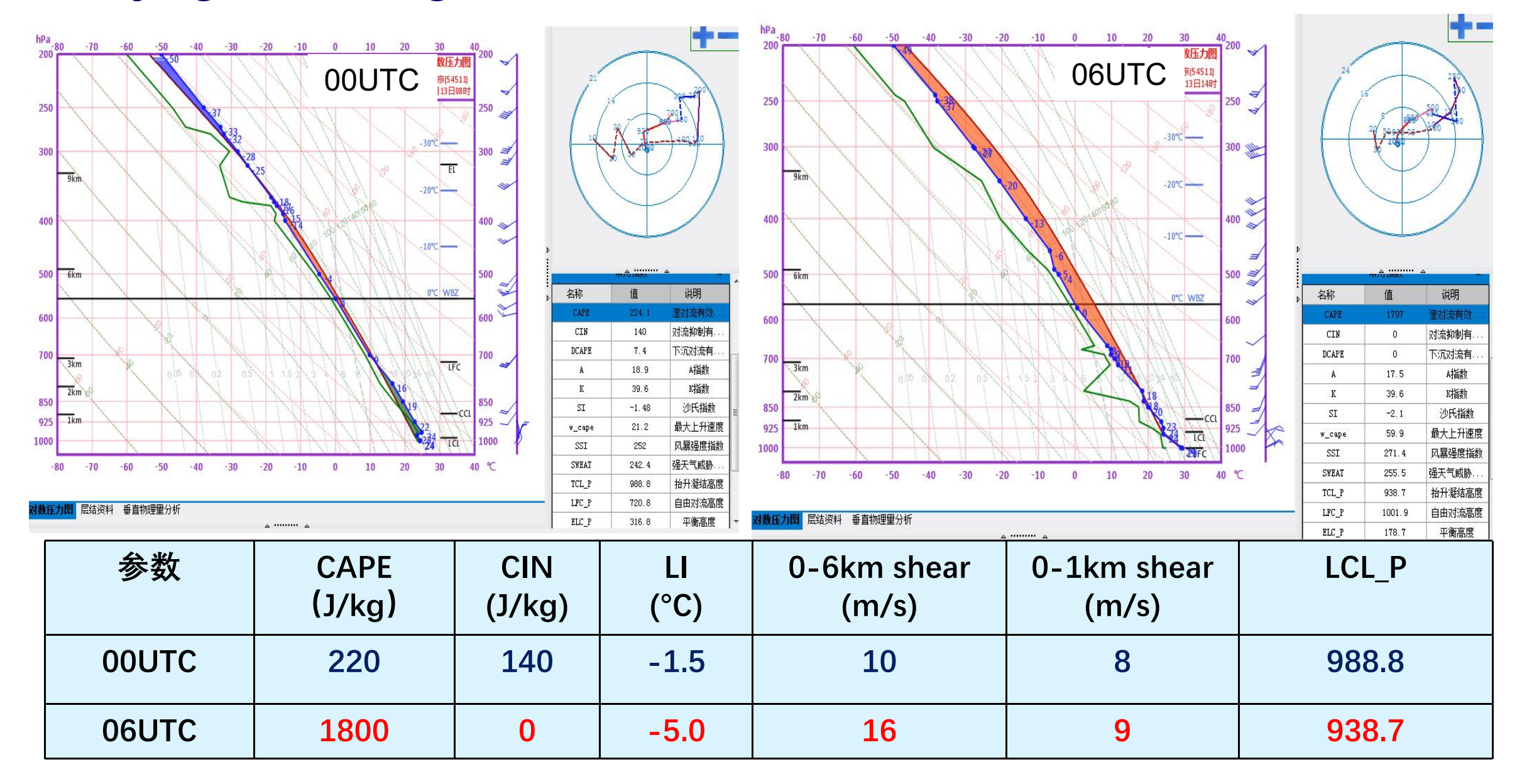


2018 08 13 14:00 BJT surface + 15:00 FY4A VIS

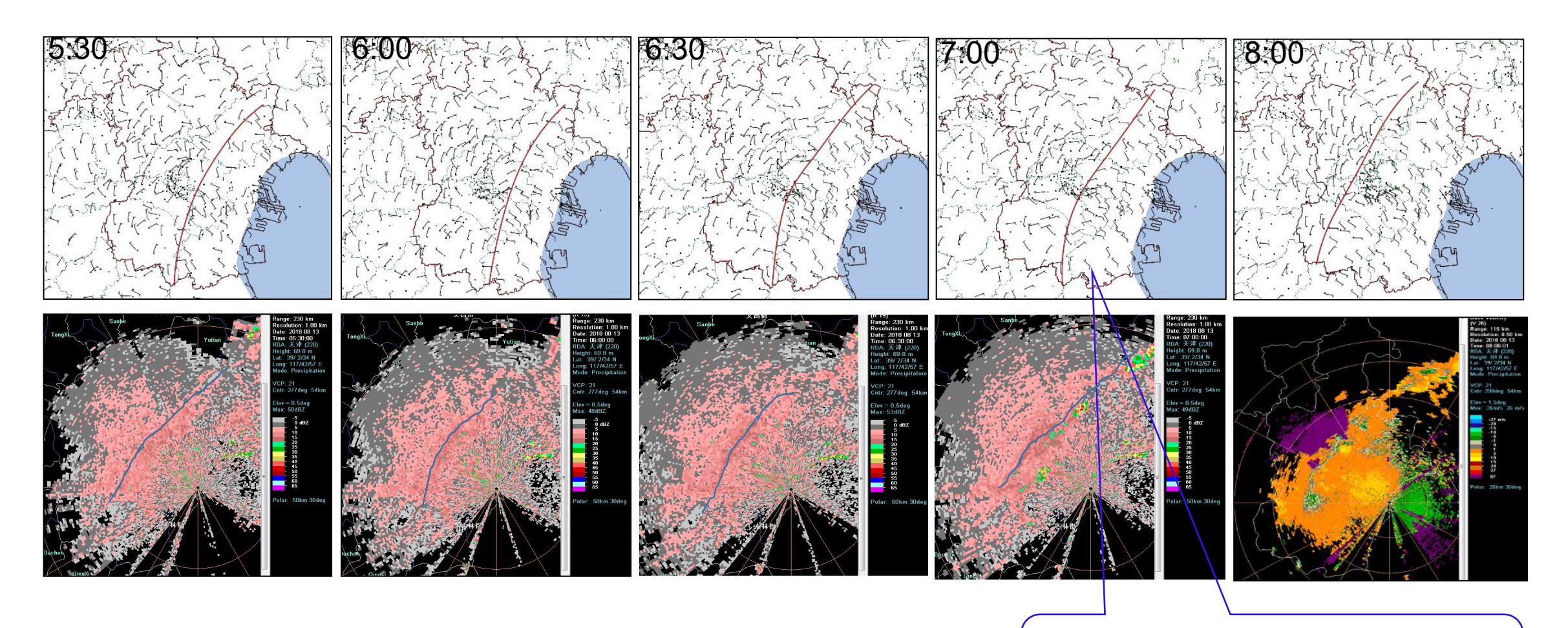




Beijing sounding 2018 08 13

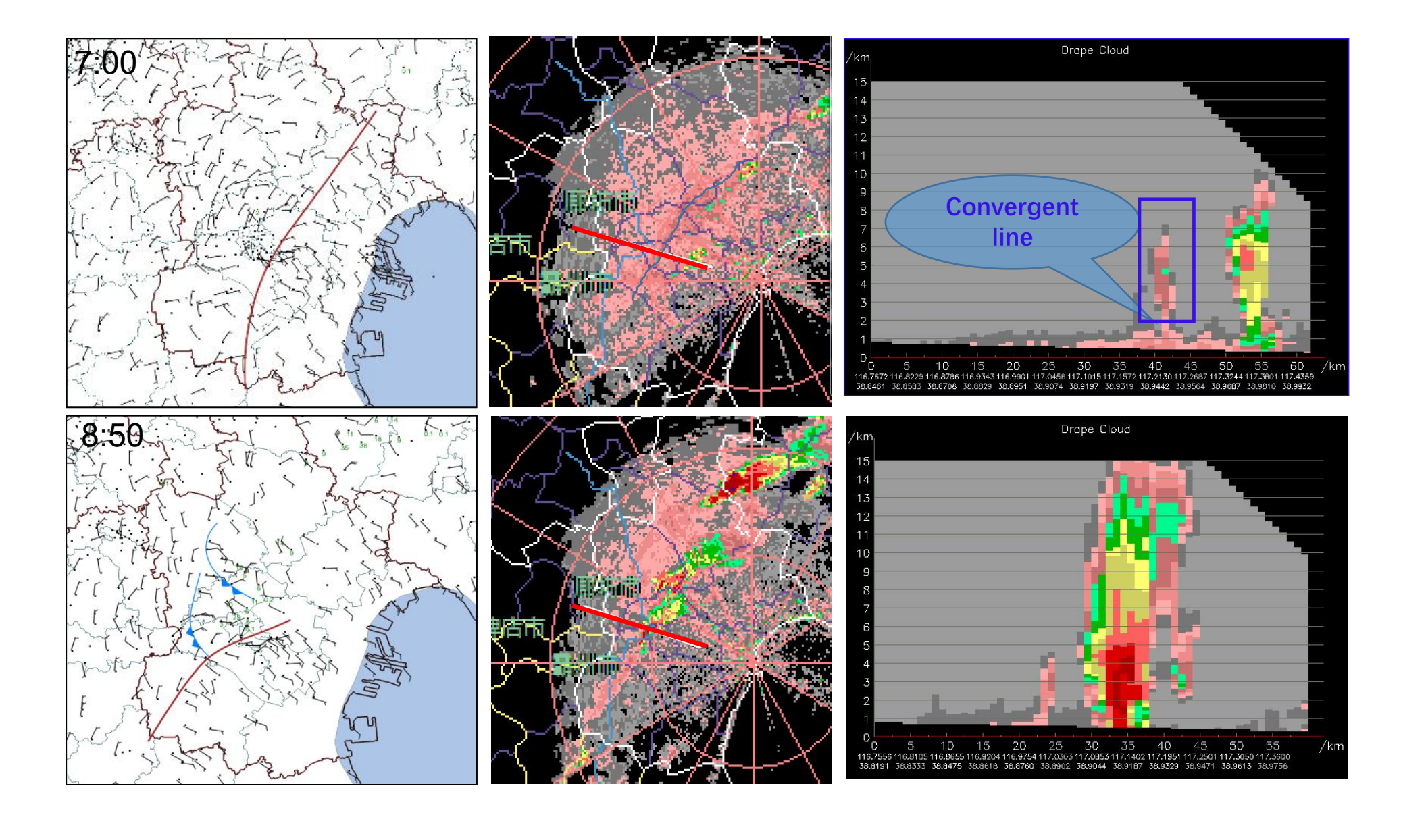


Before the tornado occurrence : convergent line

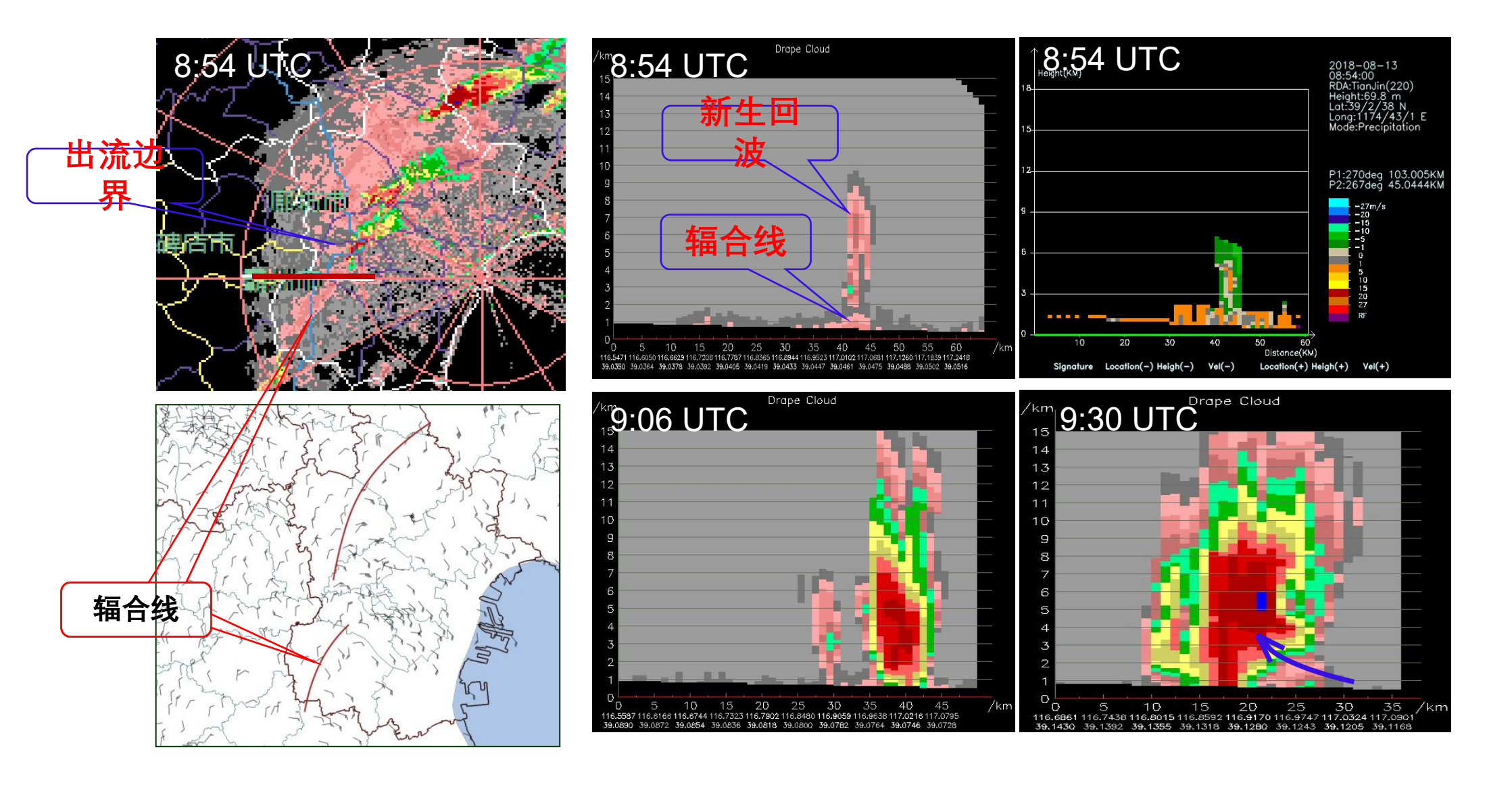


Convection initiation along the convergent line

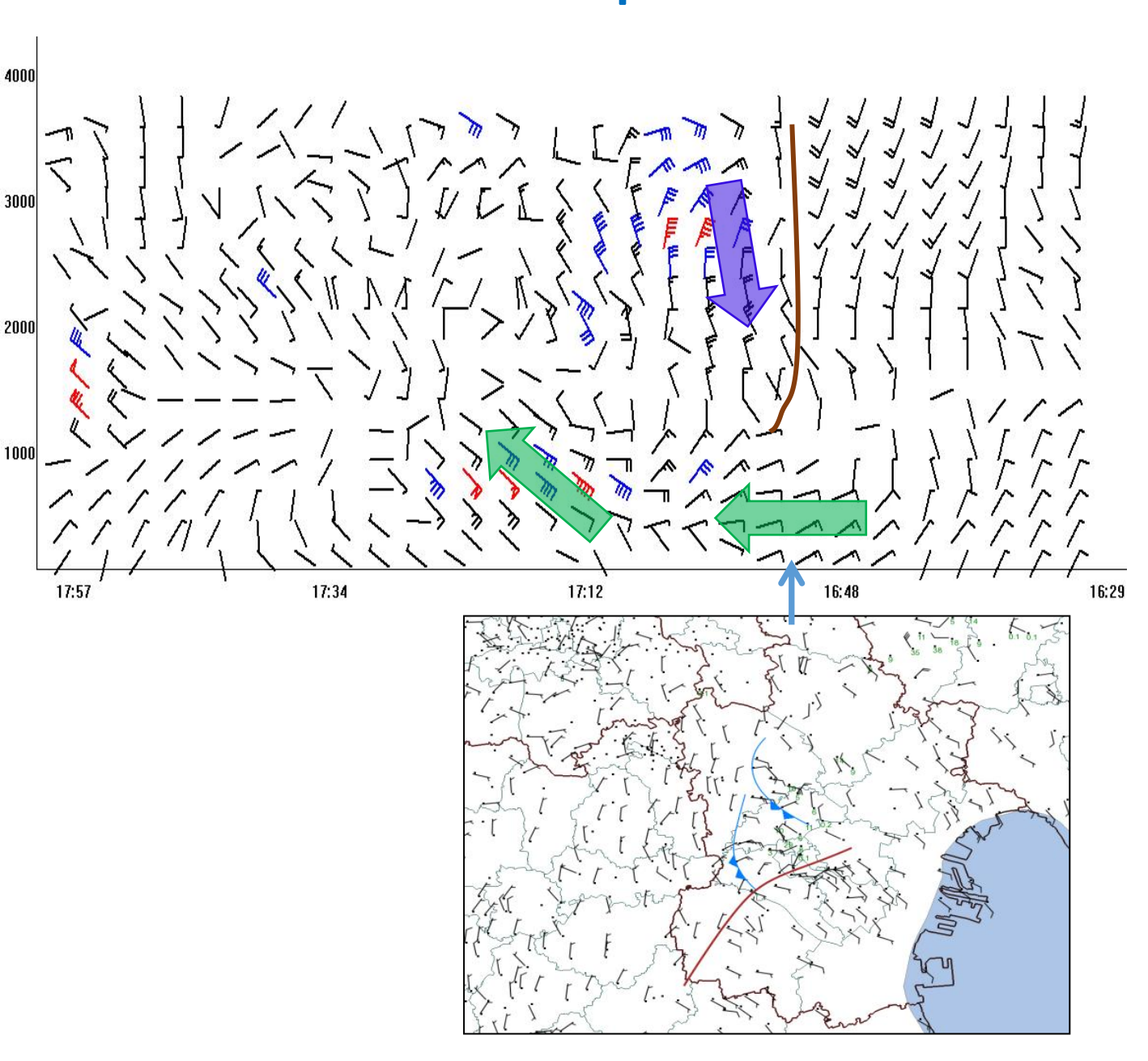
Convection initiation along the convergent line and intensified after



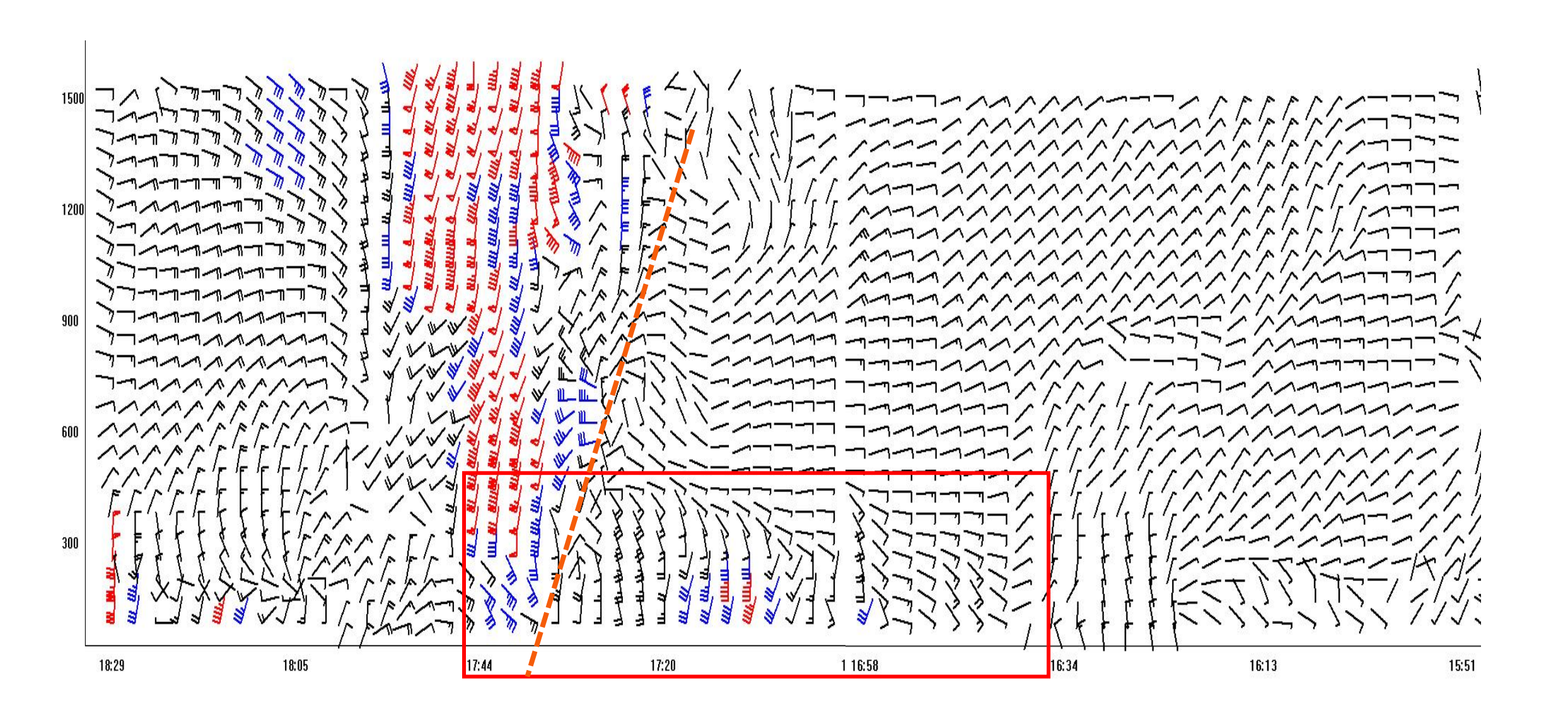
Half an hour after a new echo initiation along the convergent line, the tornado occurred.



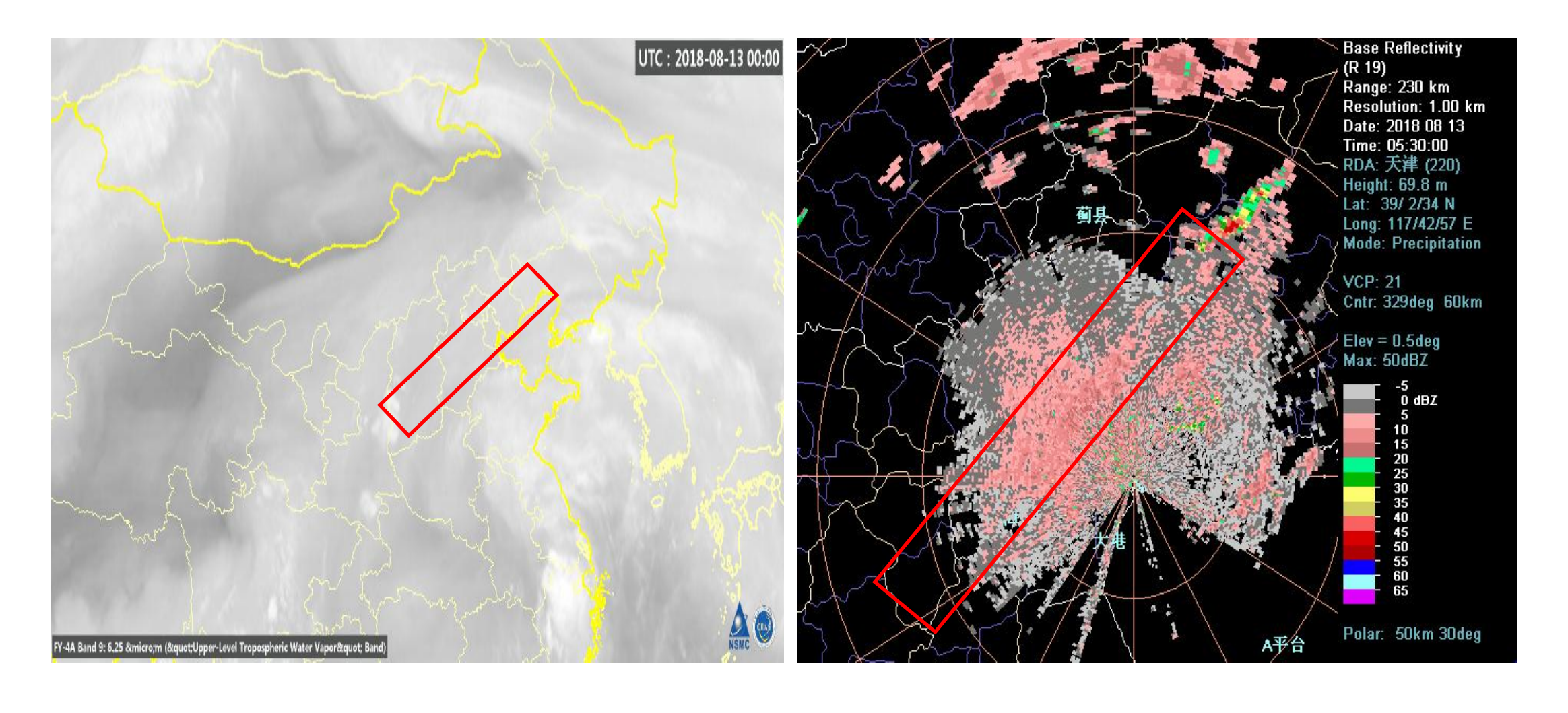
54527 sation wind profiler observation



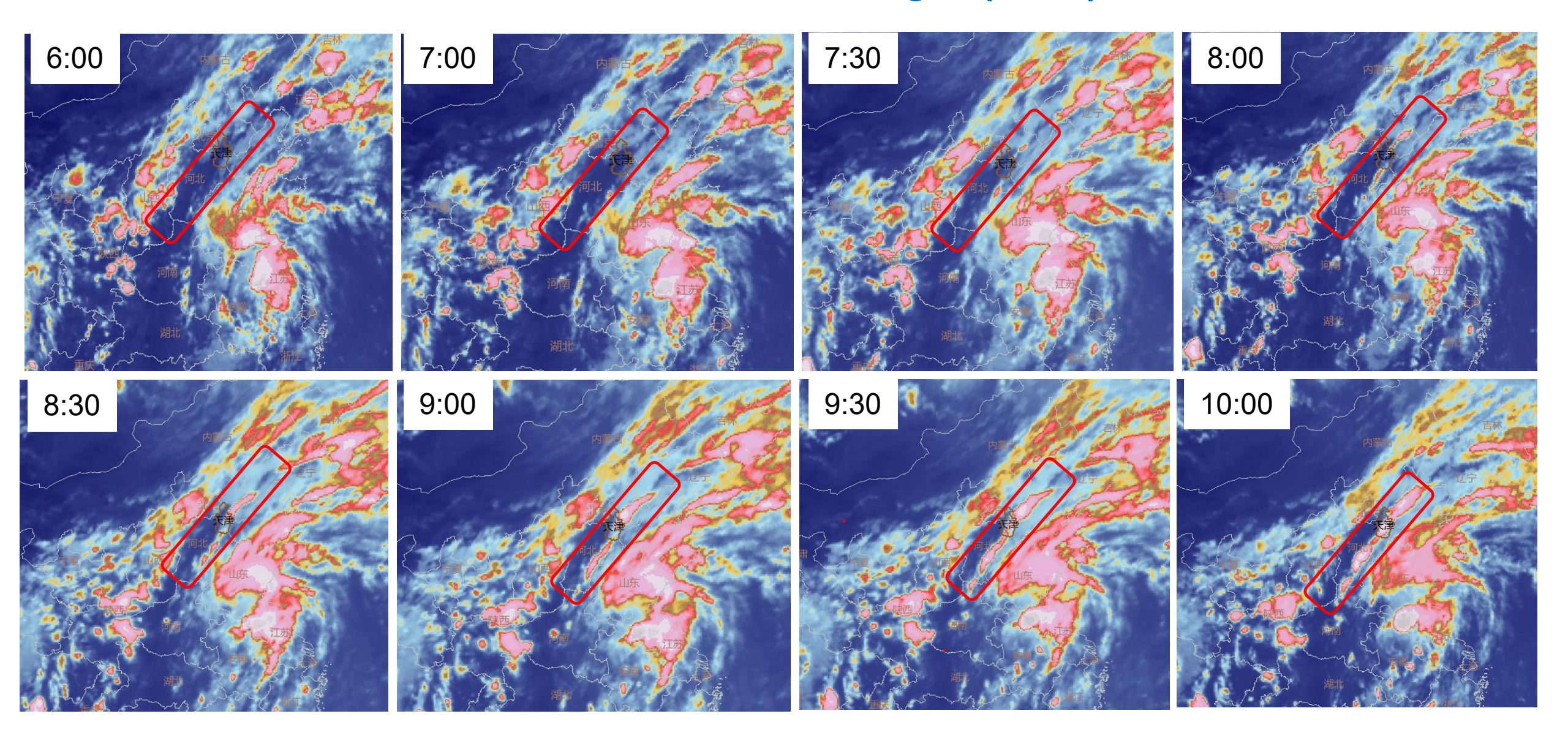
Jinghai (54619) station wind profiler (300-1500m)



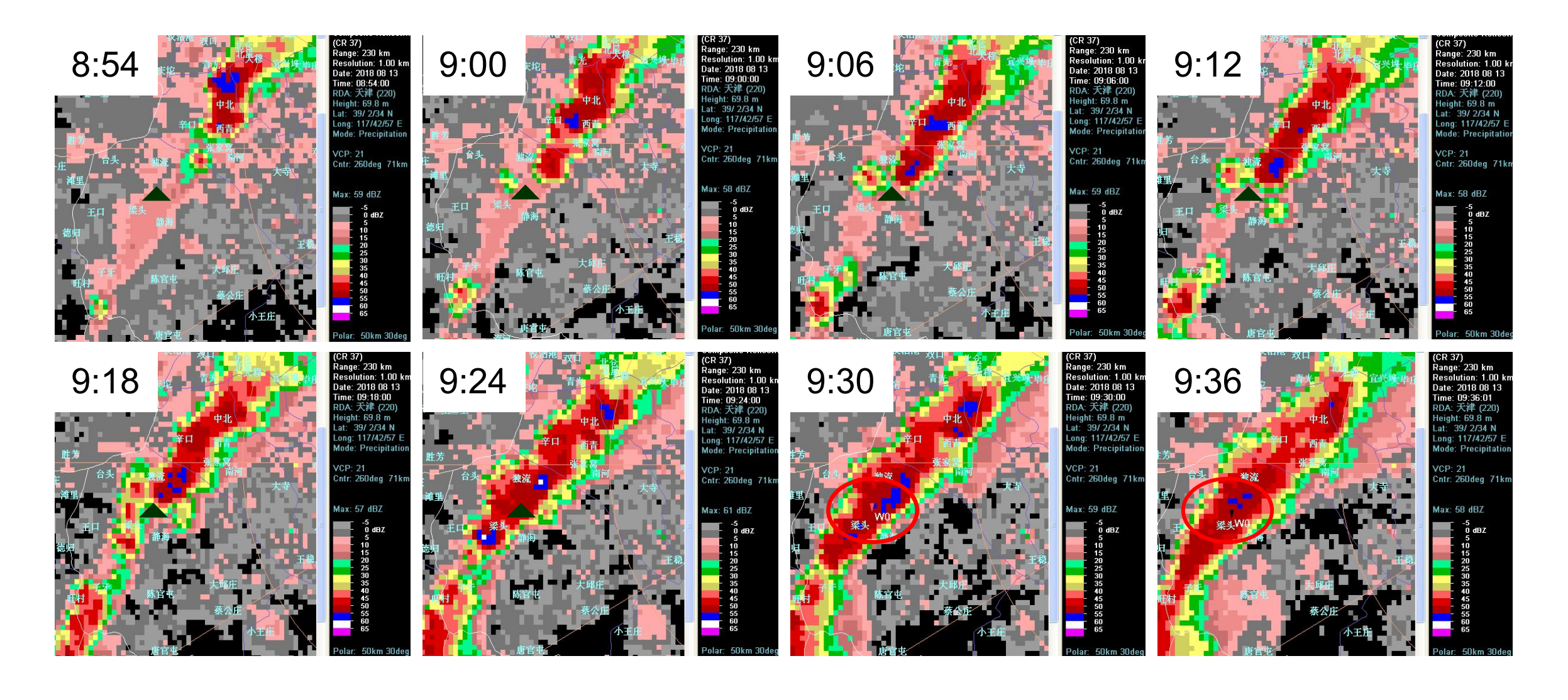
2018 08 13 Satellite and radar images movie :



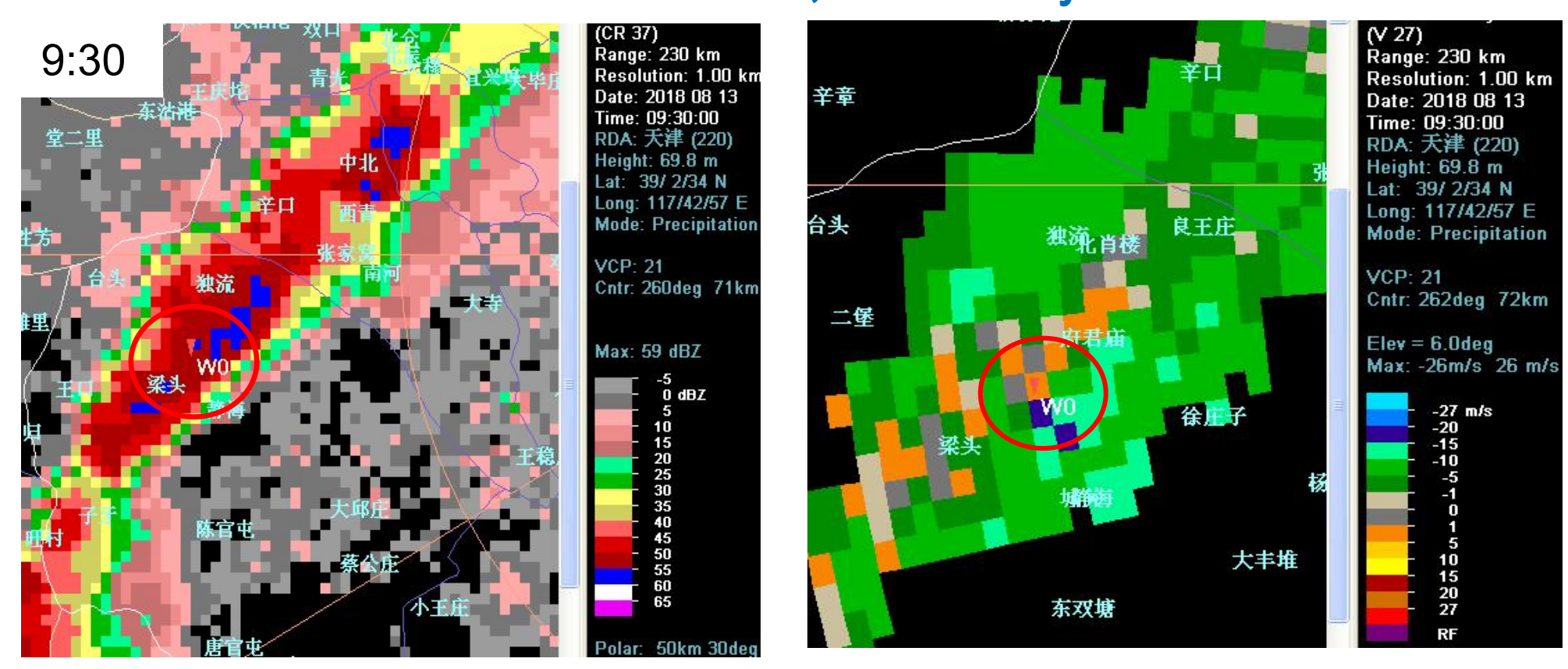
2018 08 13 satellite IR images(UTC)



Before and after the tornado occurrence: radar echoes (UTC)



TVS: 9:30-9:36 UTC detected, no mesocyclone was detected

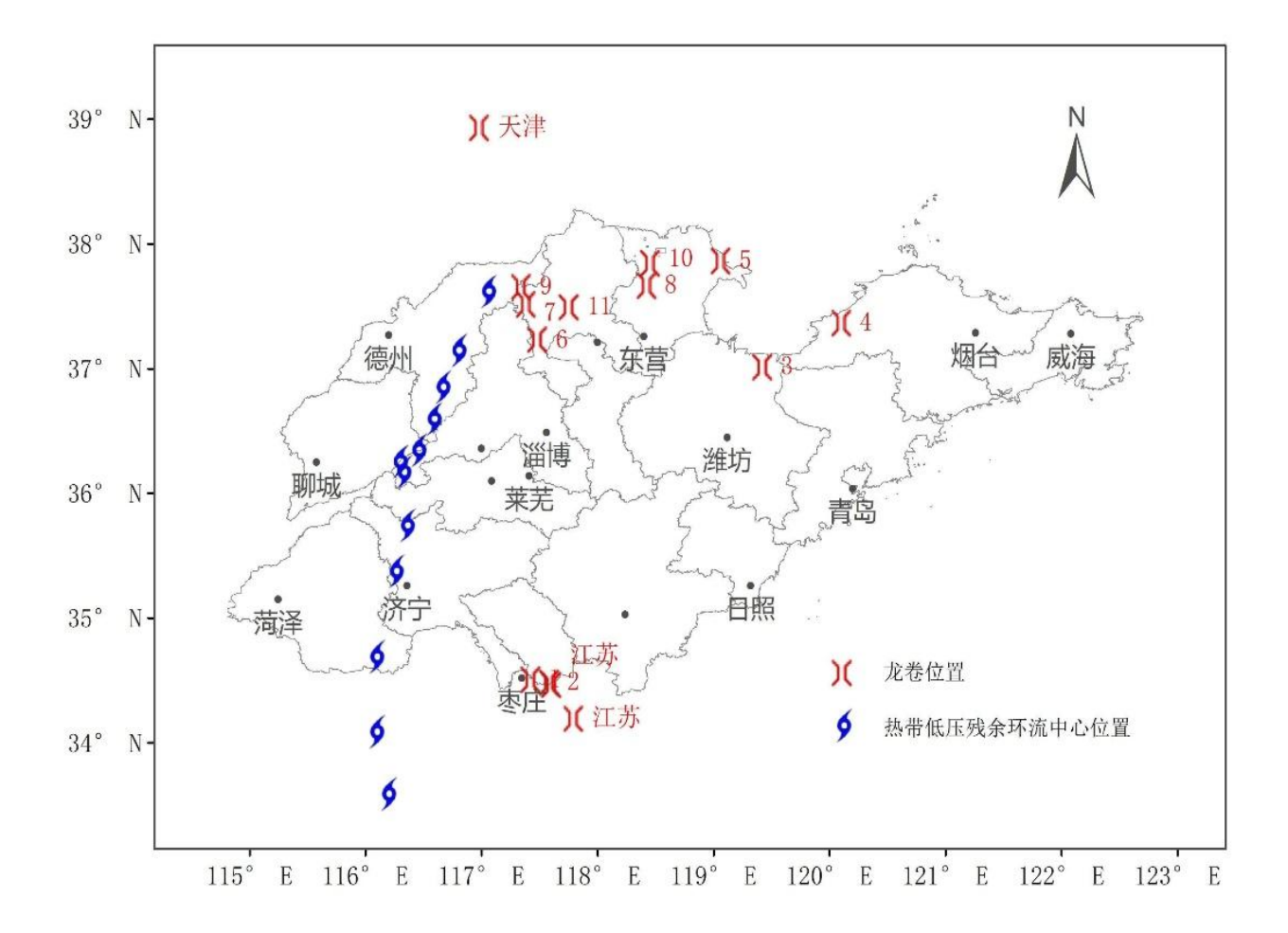


龙卷涡旋 (TVS) 特征参数:

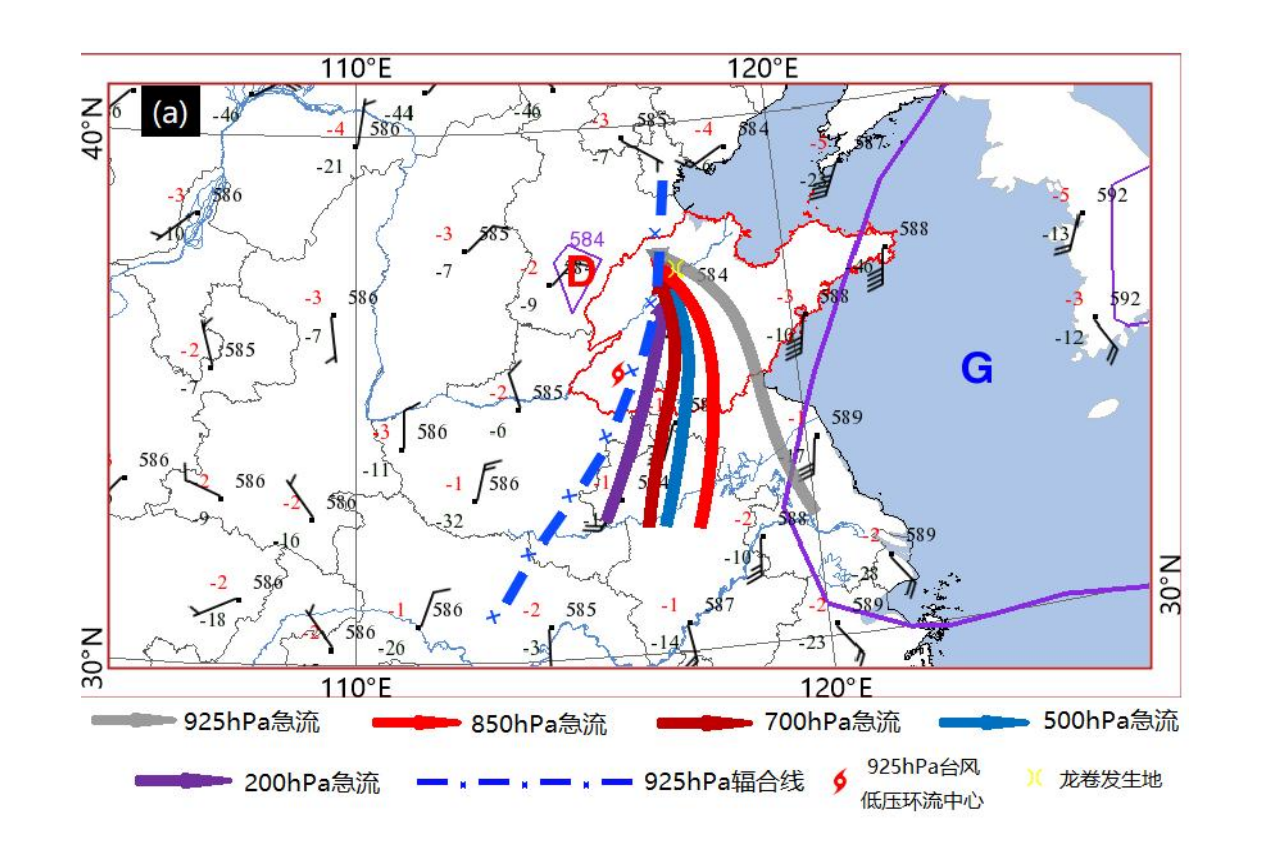
时间/UTC	方位/ °	距离/km	最大速度差	最大速度差高度/km	底高/km	顶高/km	最大切变/10 ⁻³ s ⁻¹
9:30	262	71	22	2. 4	1.1	5.8	37
7:30	201	/3	25	1. 1	1. 1	0. 0	40

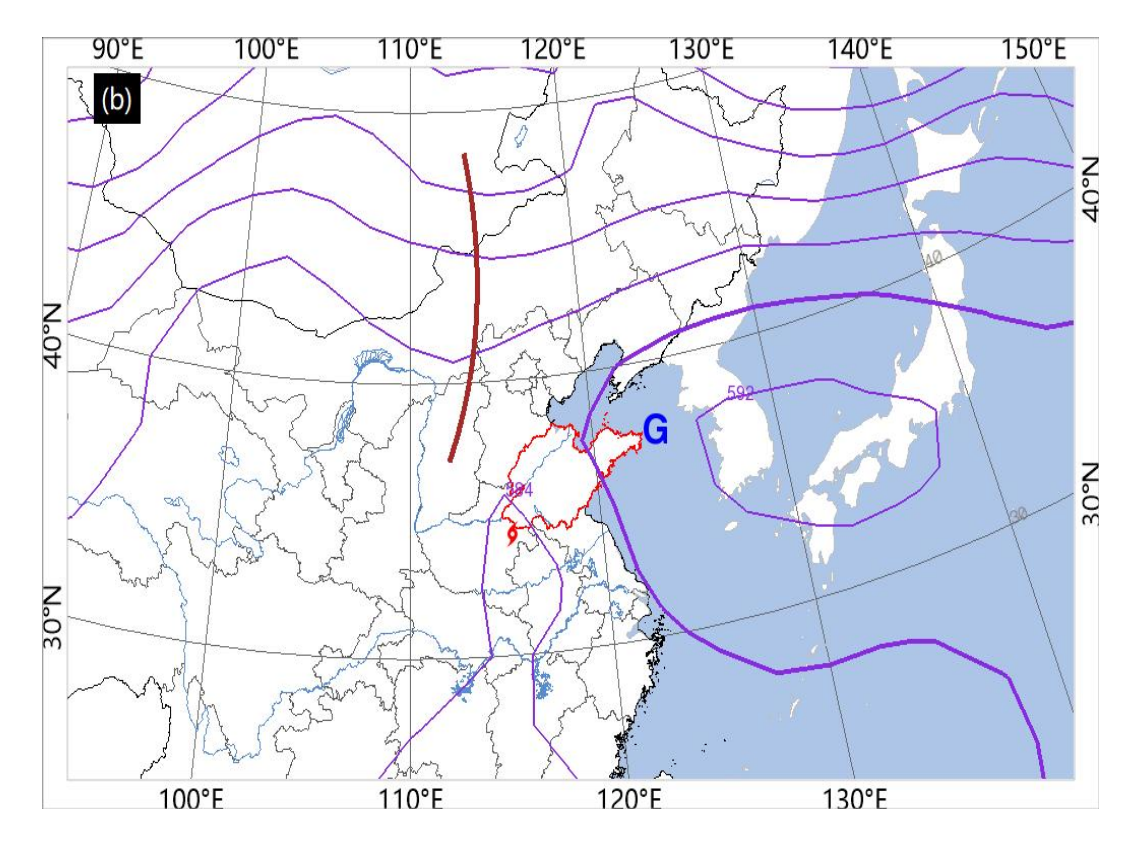
TC Yagi EF2 tornado around 12:15 BJT on 14 August 2018 in Jianglou town, Shandong province

- Ground truth
- Weather pattern
- Radar echoes

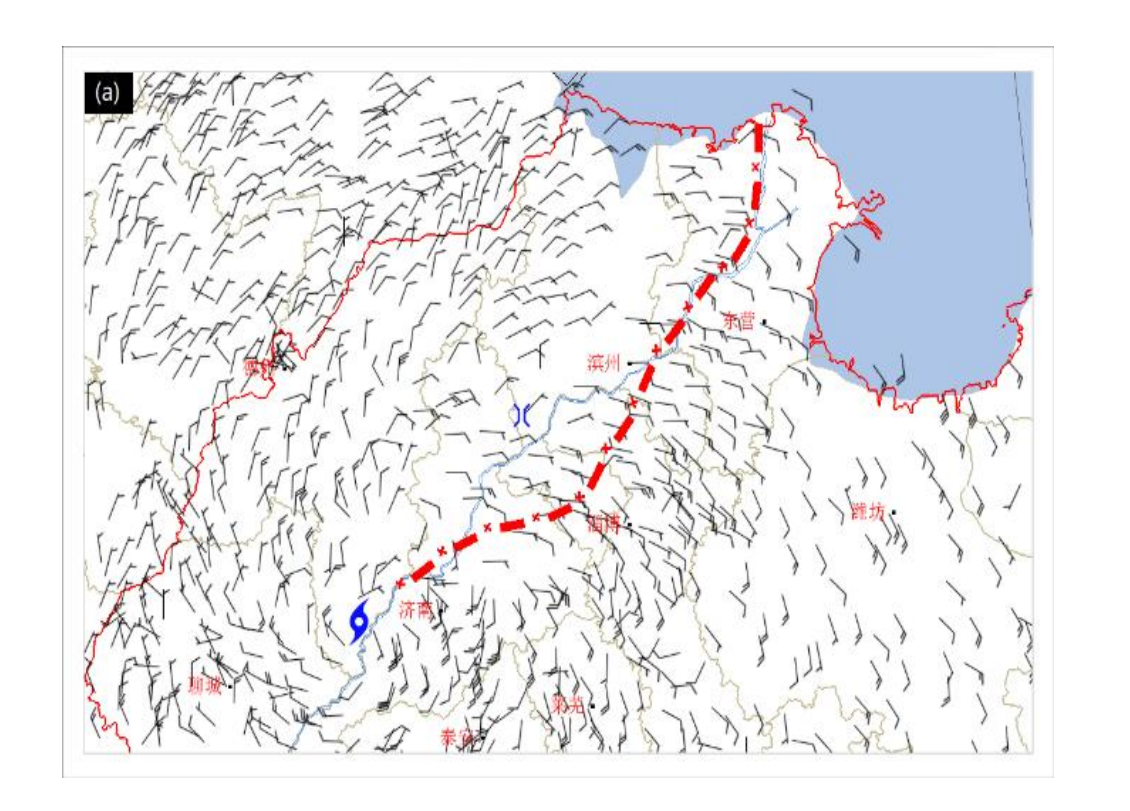


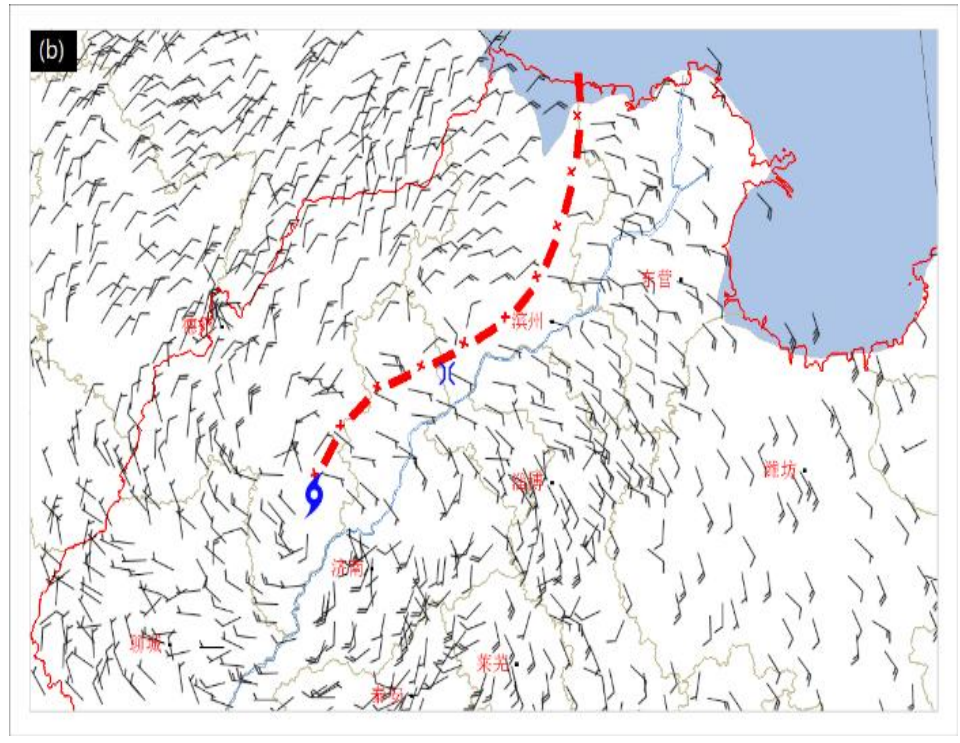
Distribution map of the remnant circulation center of "YAGI" and its tornadoes



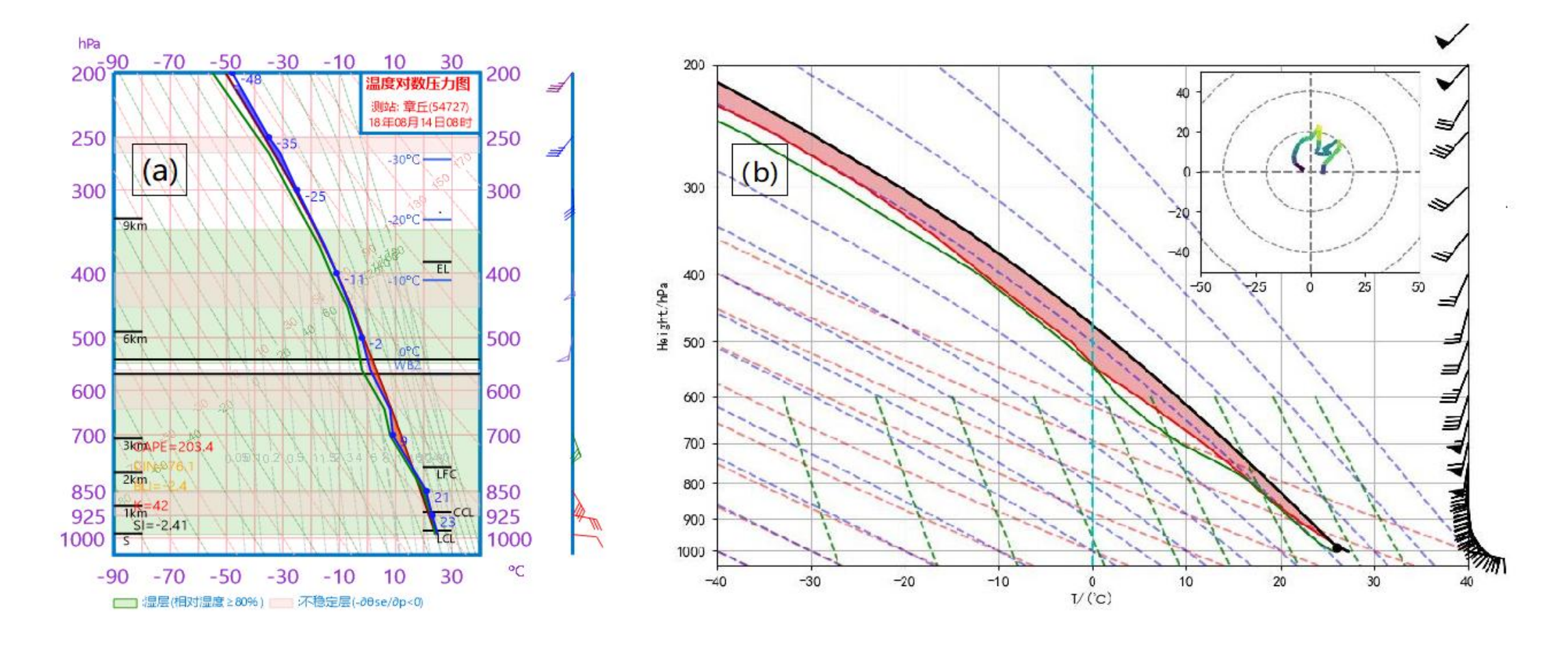


The weather pattern maps of the outer tornado circulation of "YAGI" on August 14 (a. The composite map of the high-altitude situation at 08:00 BST on August 14, b. The high-altitude situation map of 20:00 BST on August 13 at 500hPa)

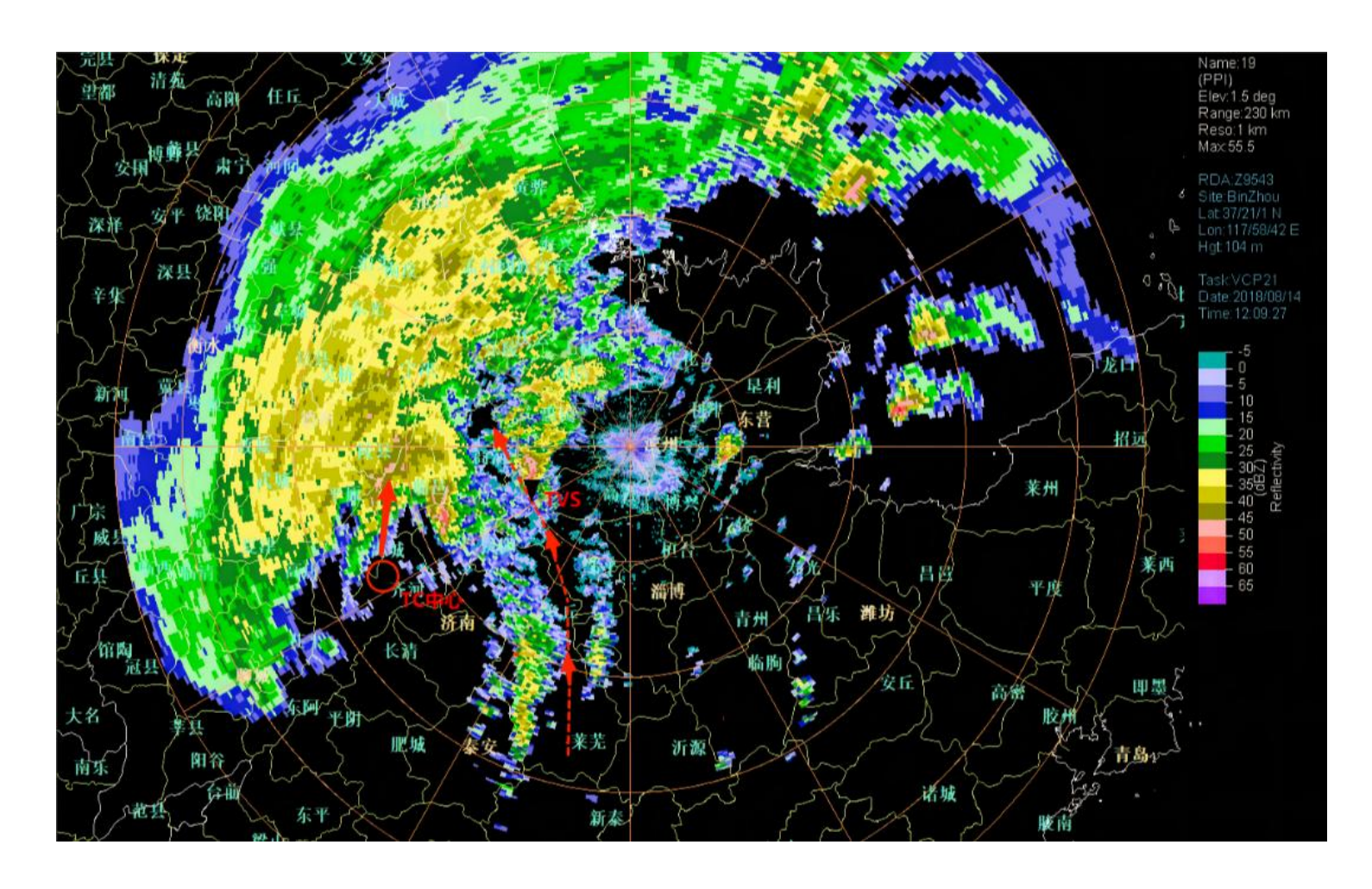




Mesoscale convergence line on the ground in northern Shandong region on August 14 (a. 12:00 BST mesoscale convergence line b. 13:00 BST mesoscale convergence line; position of the EF2 tornado was indicated)



(a)The T-InP diagram of Zhangqiu radiosonde Station (54727) at 08:00 BST on August 14 2018; (b) ERA5 reanalysis data of Huimin Station(54725) at 11:00 BST on August 14 2018



2018 08 14 12:09 BJT Binzhou SA radar 1.5° elevation reflectivity and the track of the tornado parent storm

13:39 BJT

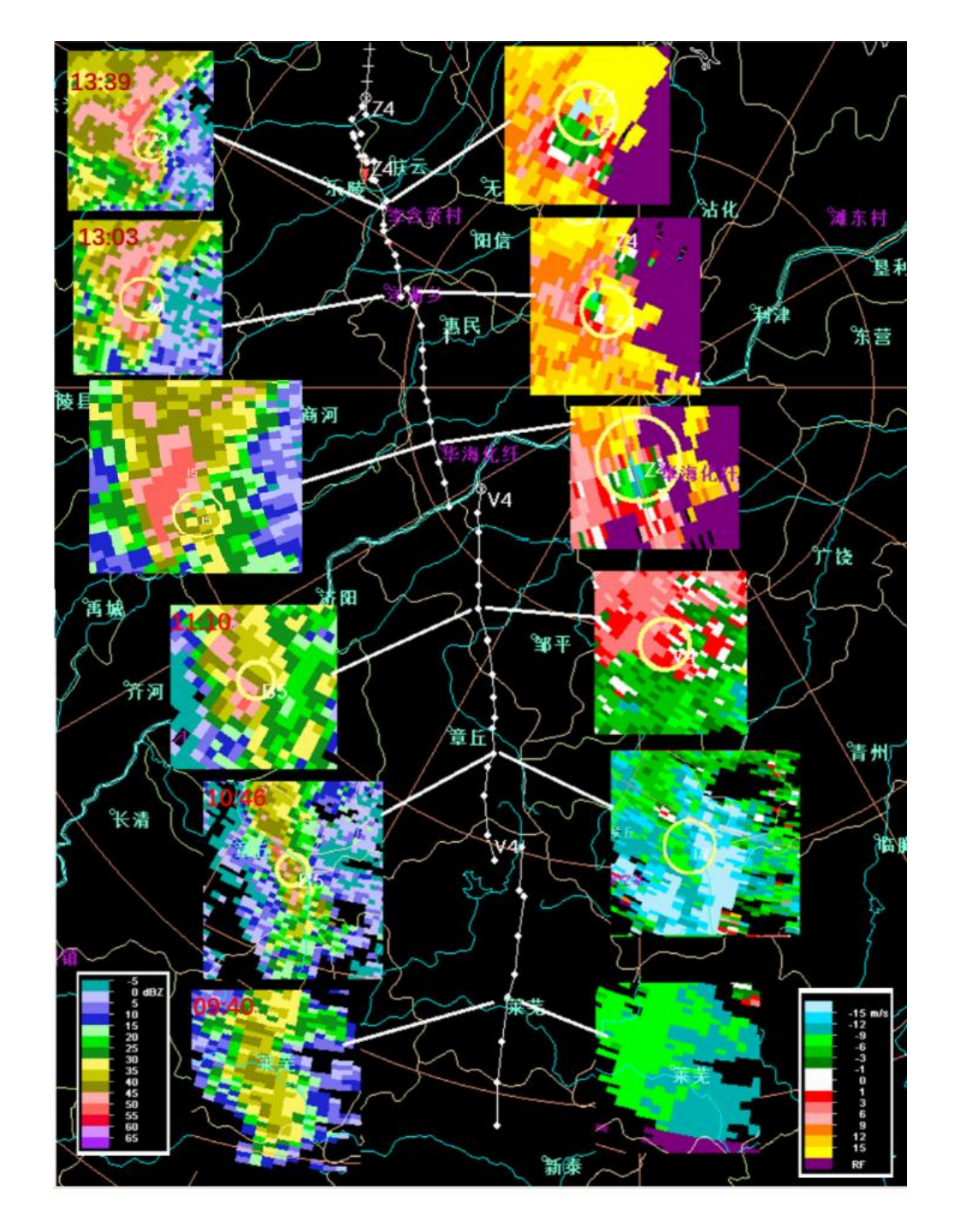
13:03 BJT

12:15 BJT

11:10 BJT

10:46 BJT

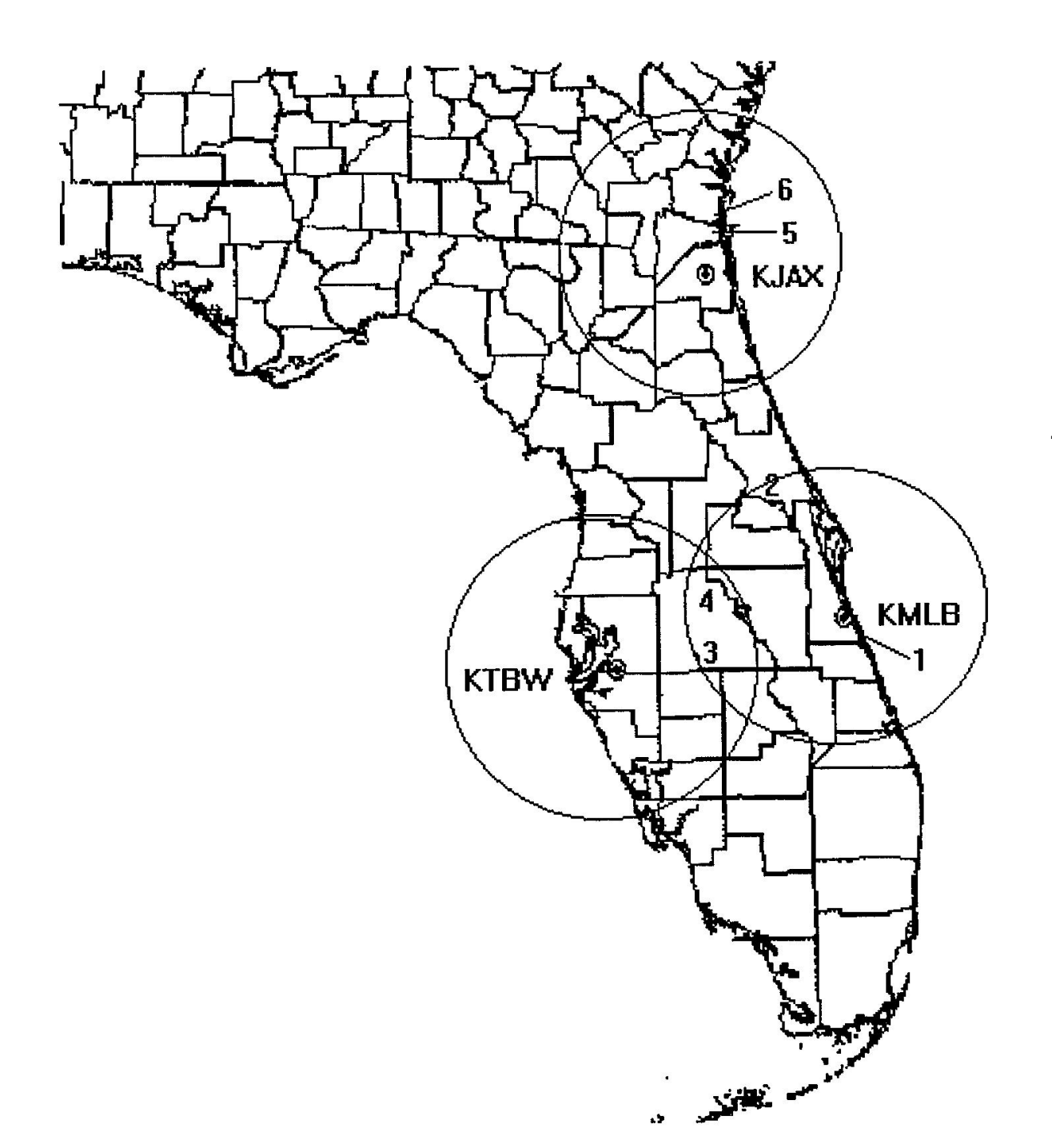
09:40 BJT



The moving characteristic map of the tornado parent storm (STI tracking information of the parent storm (white dotted line), reflectivity (left) and radial velocity (right) at each time)

Tropical Cyclone Outer Rainband Tornadoes in Florida, United States

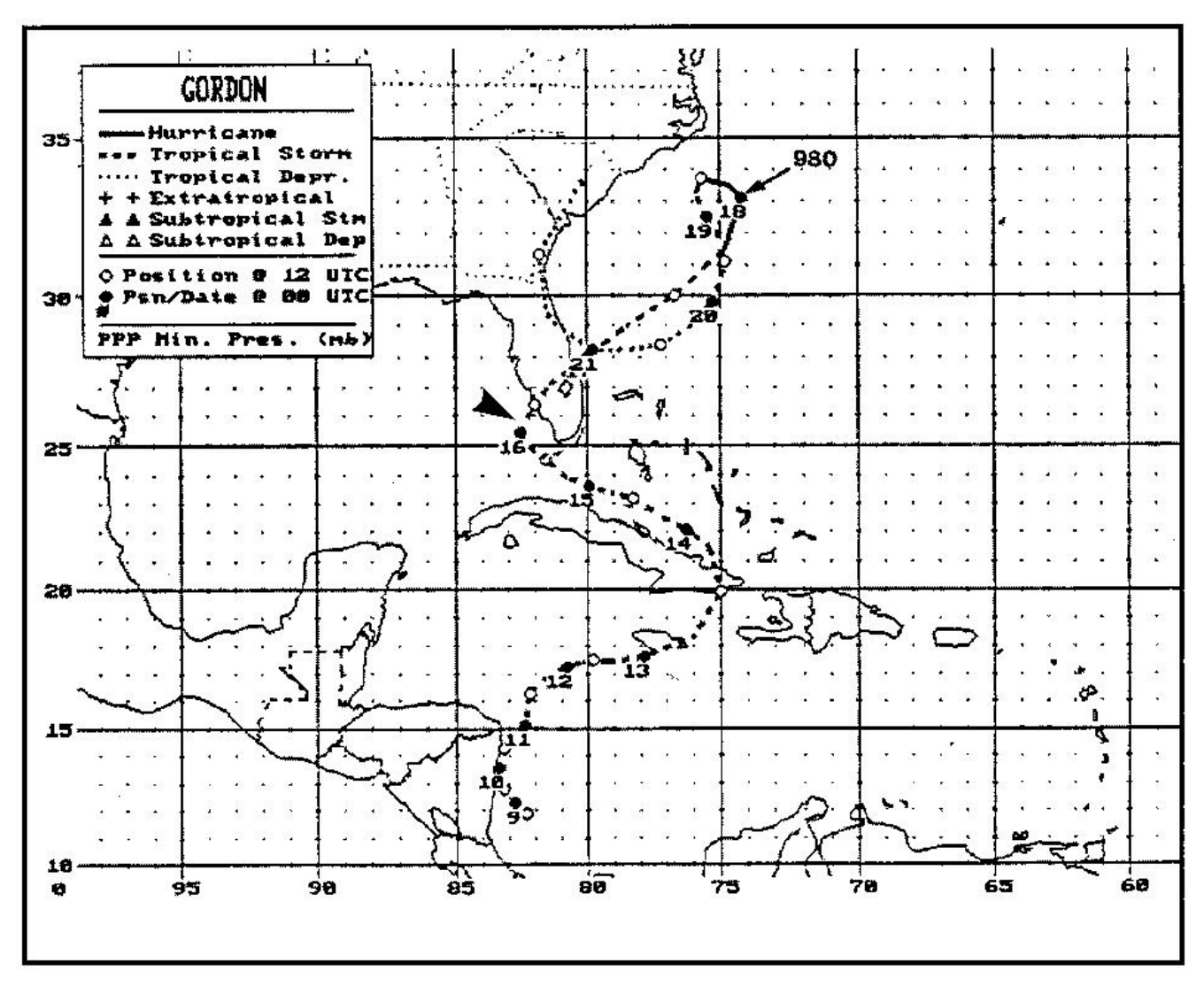
- This study provides a radar-based analysis of known tornadic mesocyclones associated with two mature tropical cyclones that were *not* landfalling in the vicinity of the tornado occurrence, namely, Tropical Storm Gordon (1994) and Hurricane Allison (1995).
- In the United States, tornadoes account for as much as 10% of the total deaths associated with tropical cyclones (Novlan and Gray 1974).
- This study will strictly focus upon outer rainband mesocyclones and associated tornadoes, as observed during TC's Gordon and Allison.



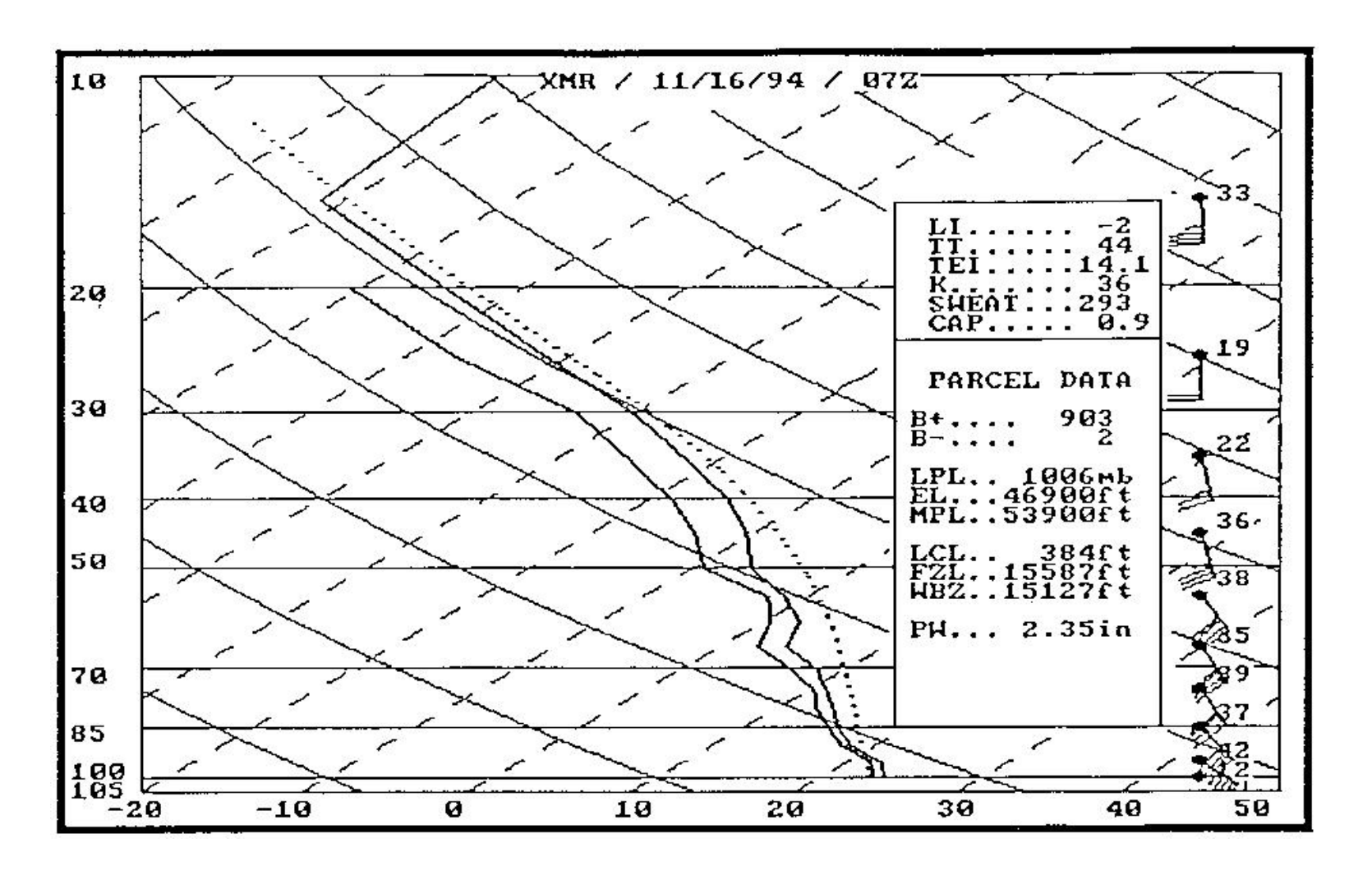
Map of the Florida peninsula and southern Georgia with locations of the Jacksonville (KJAX), Tampa Bay (KTBW), and Melbourne (KMLB) WSR-88D sites. Range rings are indicated around each radar site at radius of 111 km (60 n mi). Tornadoes discussed within the text are labeled chronologically: Barefoot Bay (1), Iron Bend (2), Polk County at Lake Wales (3), Polk County at Haines City(4), Florida–Georgia state line (5), and St. Marys (6).

Tropical Cyclone Gordon outer band tornadoes

- Weather pattern
- Radar Echoes

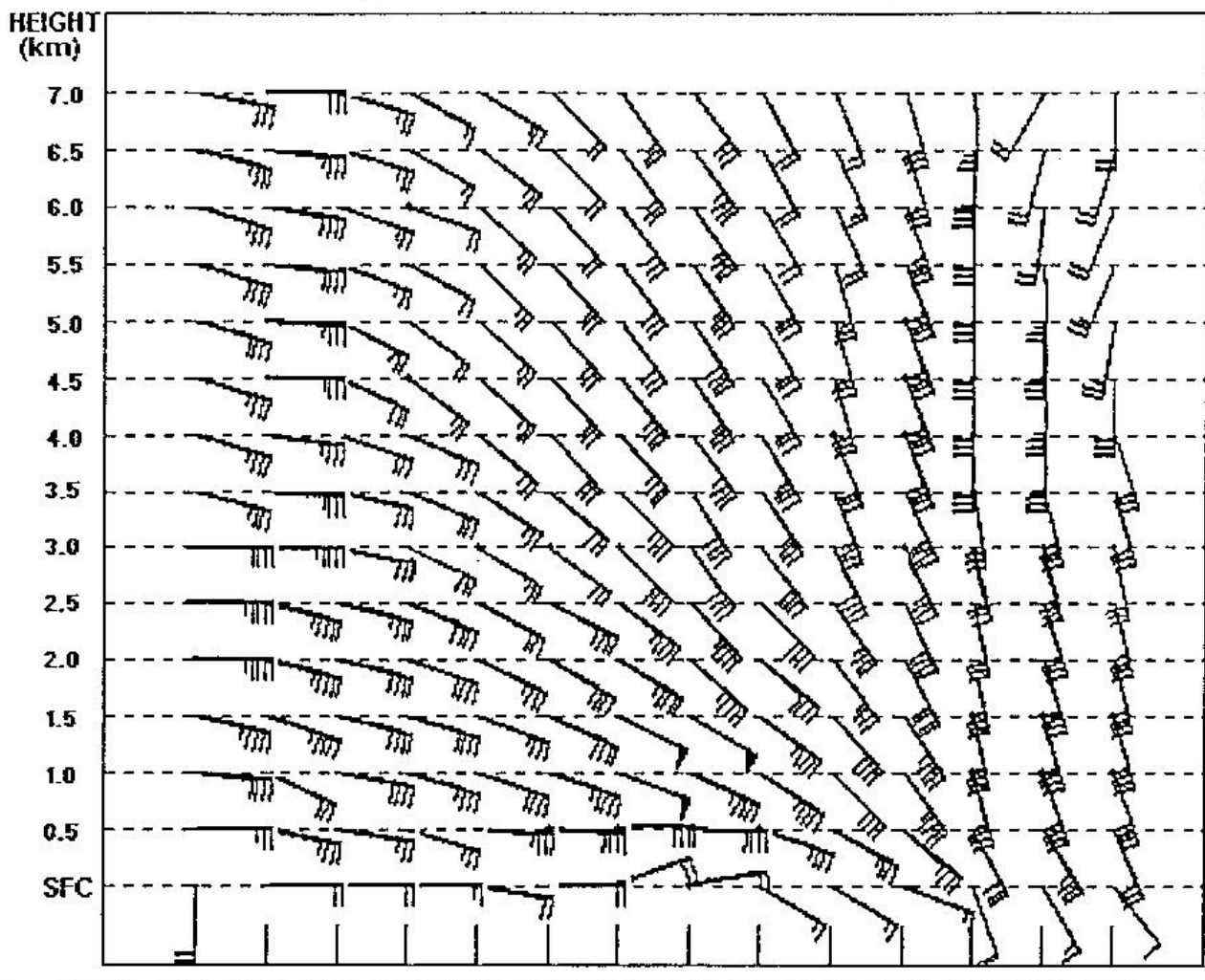


Best track positions of Tropical Cyclone Gordon. The arrow indicates the approximate position of Gordon during the time of the tornadoes across east-central Florida.



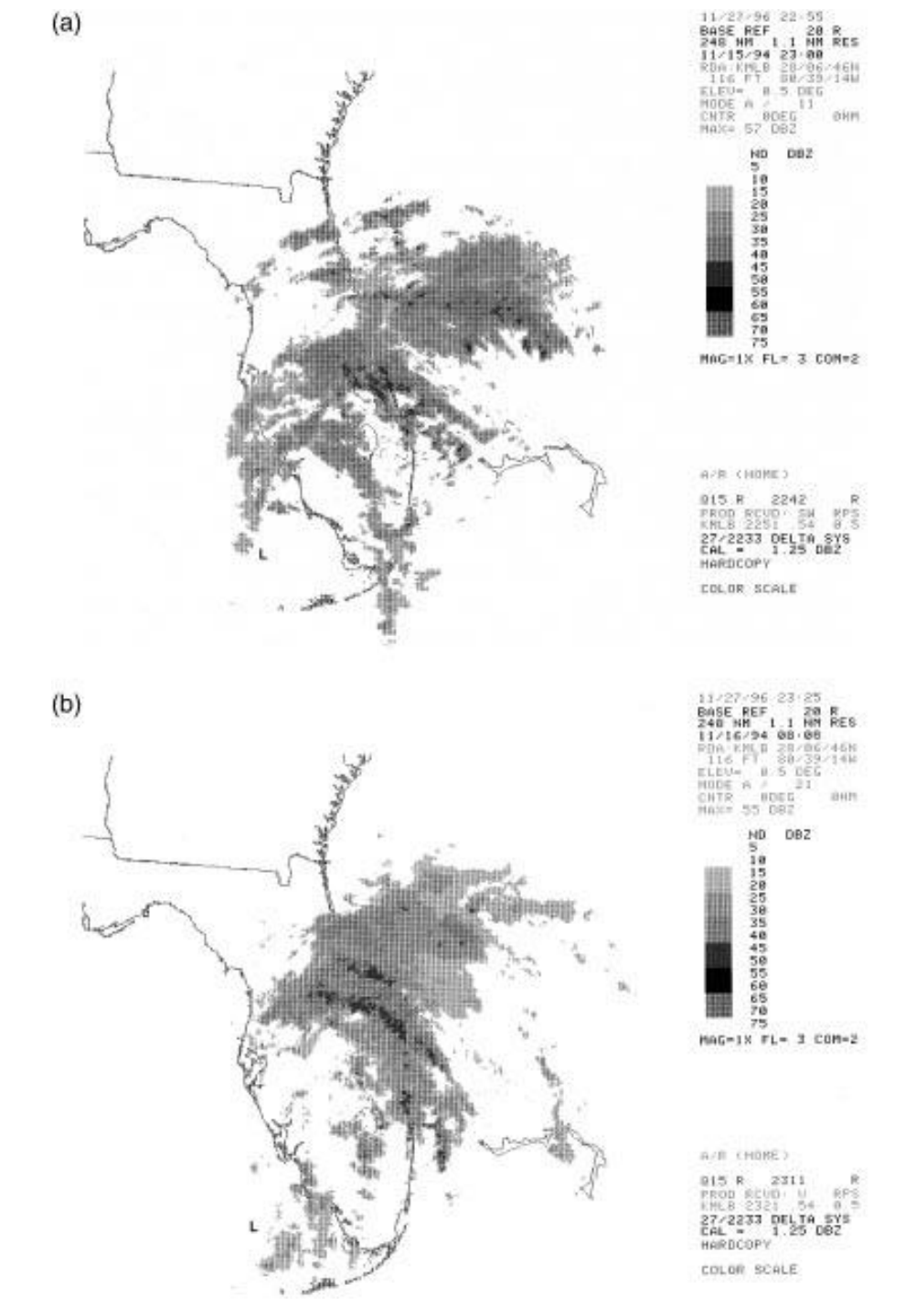
Thermodynamic sounding from Cape Canaveral AFB, FL, at 0700 UTC 16 November 1994 indicative of the deep tropical moisture. The solid lines represent temperature and dewpoint profiles (8C), and the dotted line indicates an adiabatic displacement of a parcel lifted from the surface. Wind direction and speed (kt) are plotted at selected levels.

MELBOURNE, FL VERTICAL WIND PROFILE FOR 15-16 NOV 1994

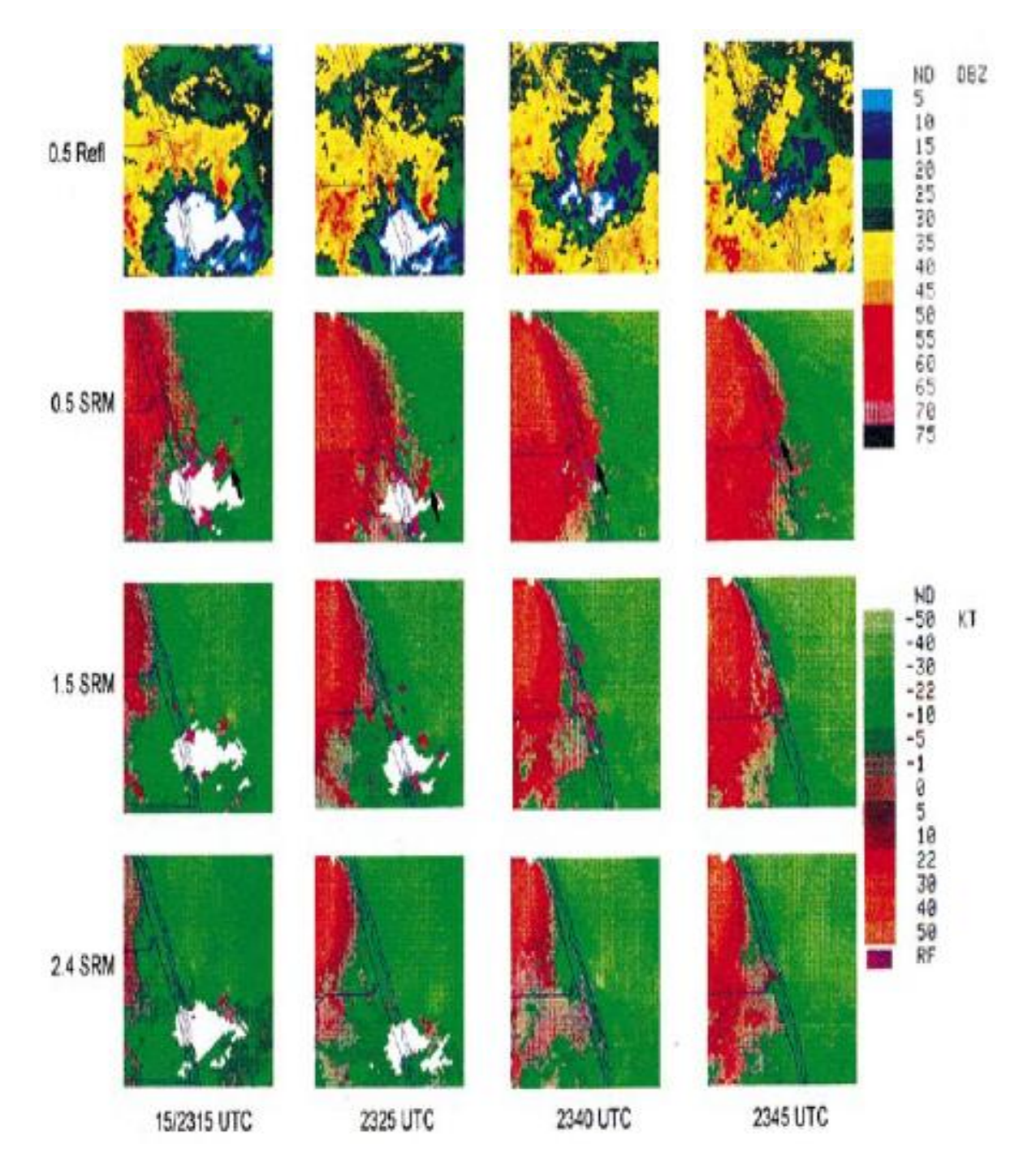


time (UTC) 1201 1357 1600 1803 2000 2200 0002 0056 0306 0356 0559 0801 1004 1203 helicity ($m^2 \, s^{-2}$) 25 -29 21 67 92 151 295 343 136 74 113 13 23 -48

Vertical wind profile (time vs height cross section) between 1200 UTC 15 November 1994 and 1200 UTC 16 November 1994 constructed using winds aloft from the Melbourne WSR-88D VAD Wind Profile and surface winds from Melbourne International Airport. Winds are plotted using the standard model, with one short barb equal to 2.5 m s⁻¹ (5 kt) and a long barb equal to 5 m s⁻¹ (10 kt). Storm-relative helicity (SRH) values based upon the individual profiles are shown below each plot. Storm motion vectors were determined by radar for the rainband cell with the highest reflectivity within 140 km of KMLB.



Large-scale view of TC Gordon's rainbands from the Melbourne WSR-88D 0.5° base reflectivity products at (a) 2300 UTC 15 November 1994 and (b) 0808 UTC 16 November 1994. The letter "L" signifies the location of Gordon's center near the time of the radar product.



Selected low-level base reflectivity (Refl) and storm-relative velocity (SRM) products illustrate the evolution of the tornadic Barefoot Bay cell. The images are sized 56 km × 56 km and centered on the cell of interest. The Melbourne radar site is located north-northwest of the cell. The reflectivity (dBZ) and velocity (kt) scales are shown near the right margin, and arrows mark the cell of interest.

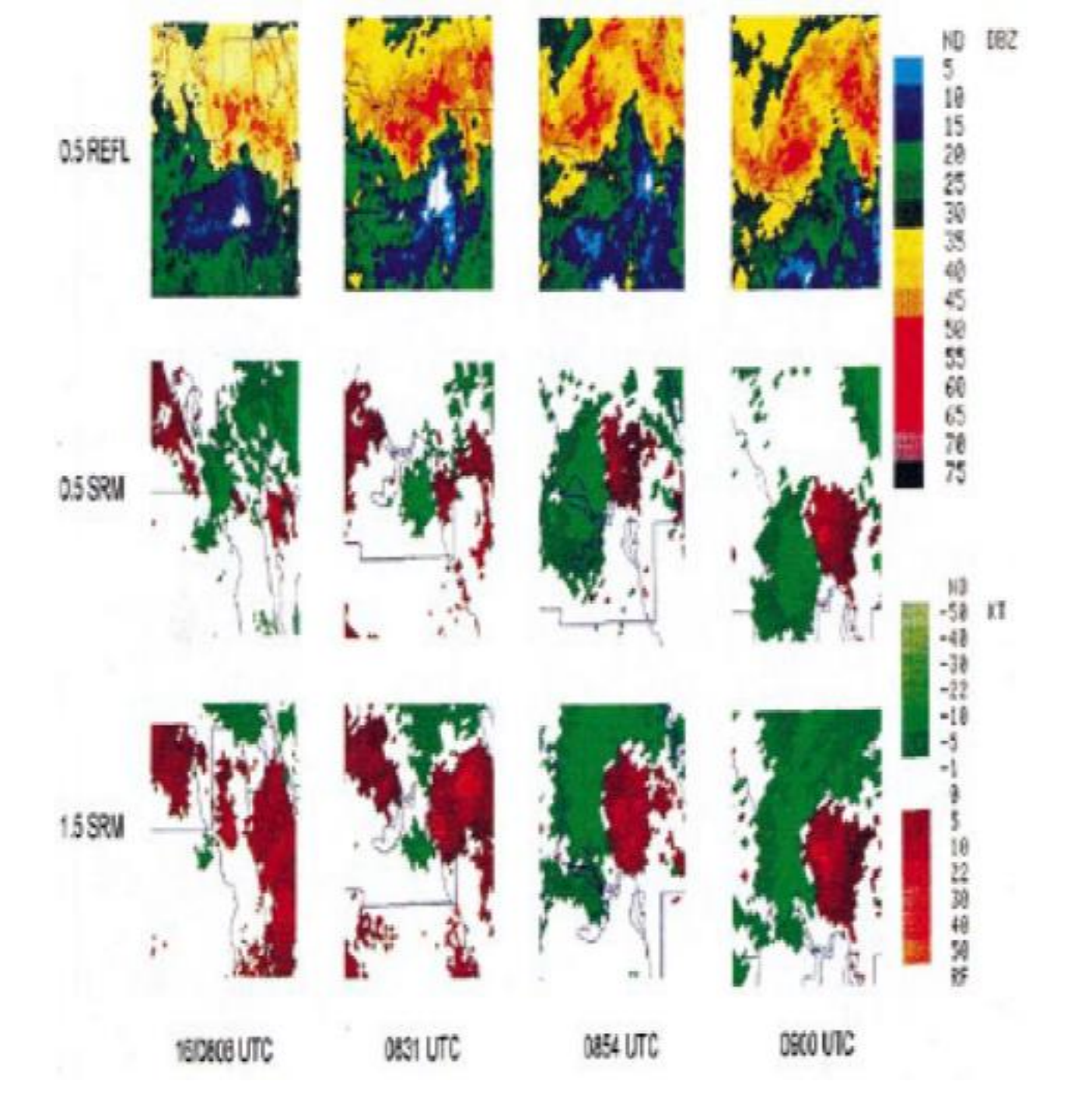


Fig.9. Same as Fig. 8 except for the Iron Bend cell. The Melbourne radar site is located southeast of the cell.

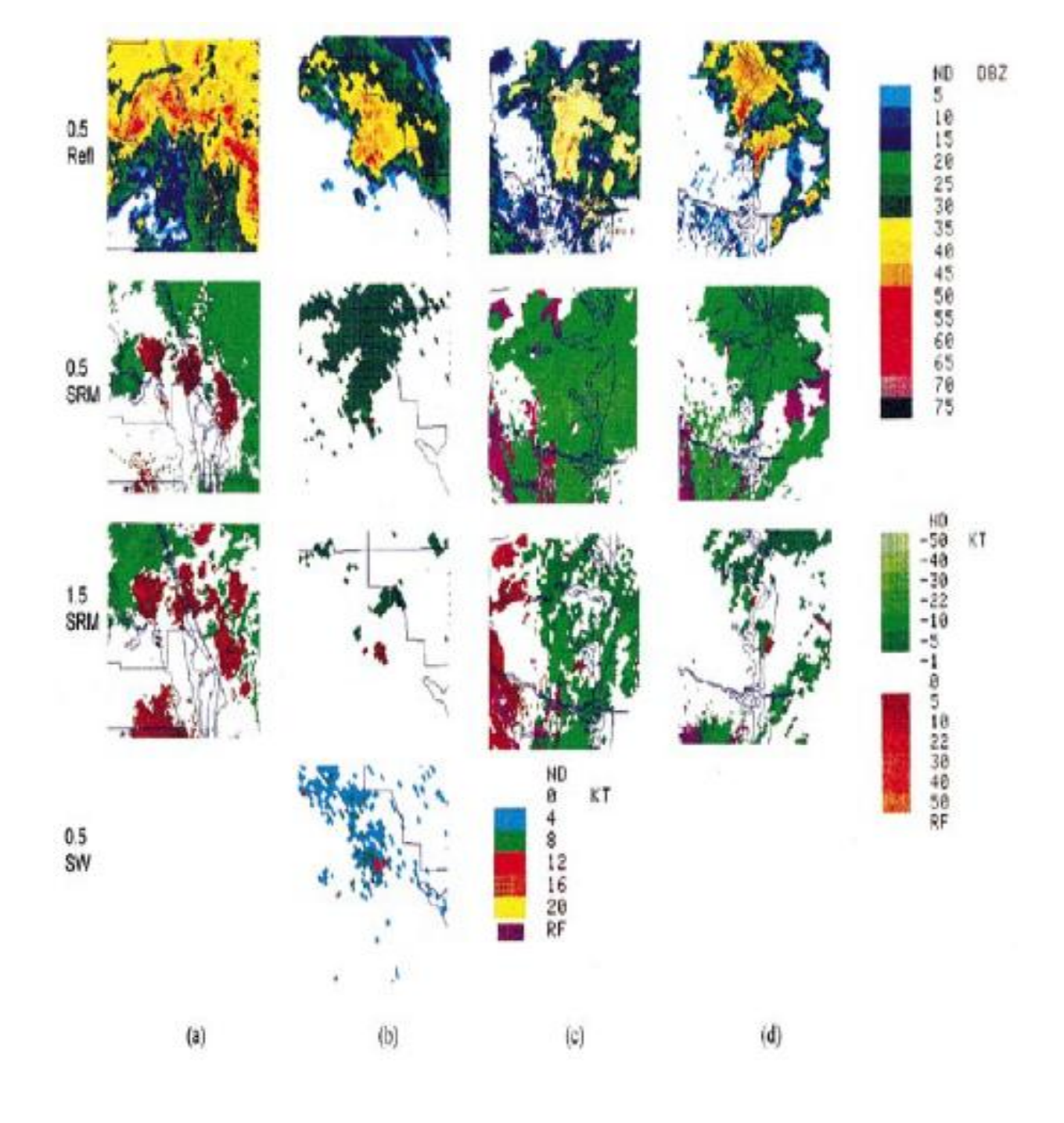
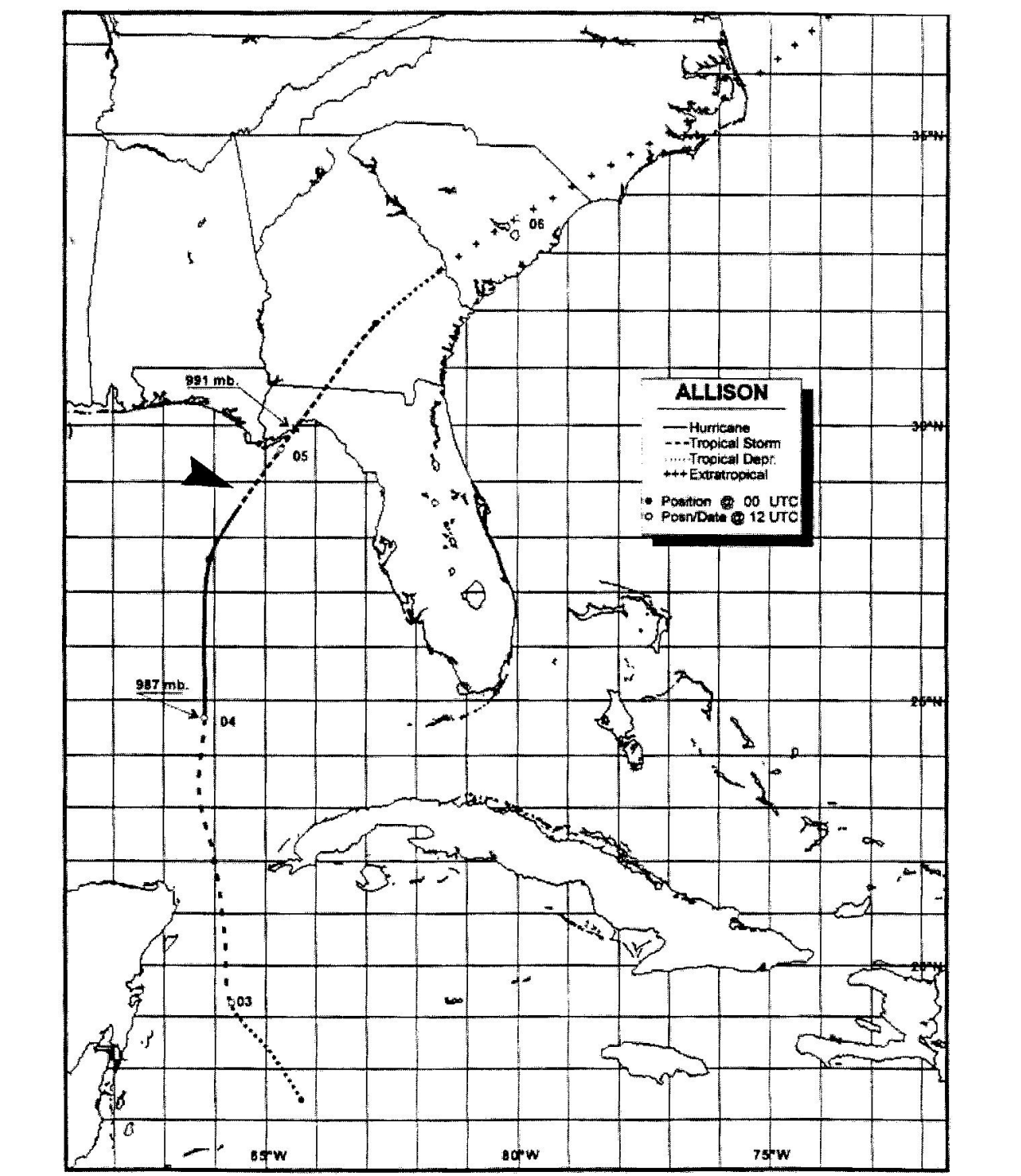


FIG. 10. Selected Refl, SRM, and spectrum width (SW) products illustrate (a) a family of mesocyclones associated with the Iron Bend tropical LEWP at 0900 UTC 16 November 1994, (b) the Polk County mesocyclone at 0305 UTC 5 June 1995, (c) the St. Marys mesocyclone at 0818 UTC 5 June 1995, and (d) a series of mesocyclones downwind from the St. Marys cell at 0957 UTC 5 June 1995. Images in (a) are sized 111 km × 111 km , and the remainder are 56 km \times 56 km. The WSR-88D sites are located southsoutheast of (a) (Melbourne), west of (b) (Tampa Bay), and south of (c) and (d) (Jacksonville).

Tropical Cyclone Allison outer band tornadoes

- Weather pattern
- Radar Echoes

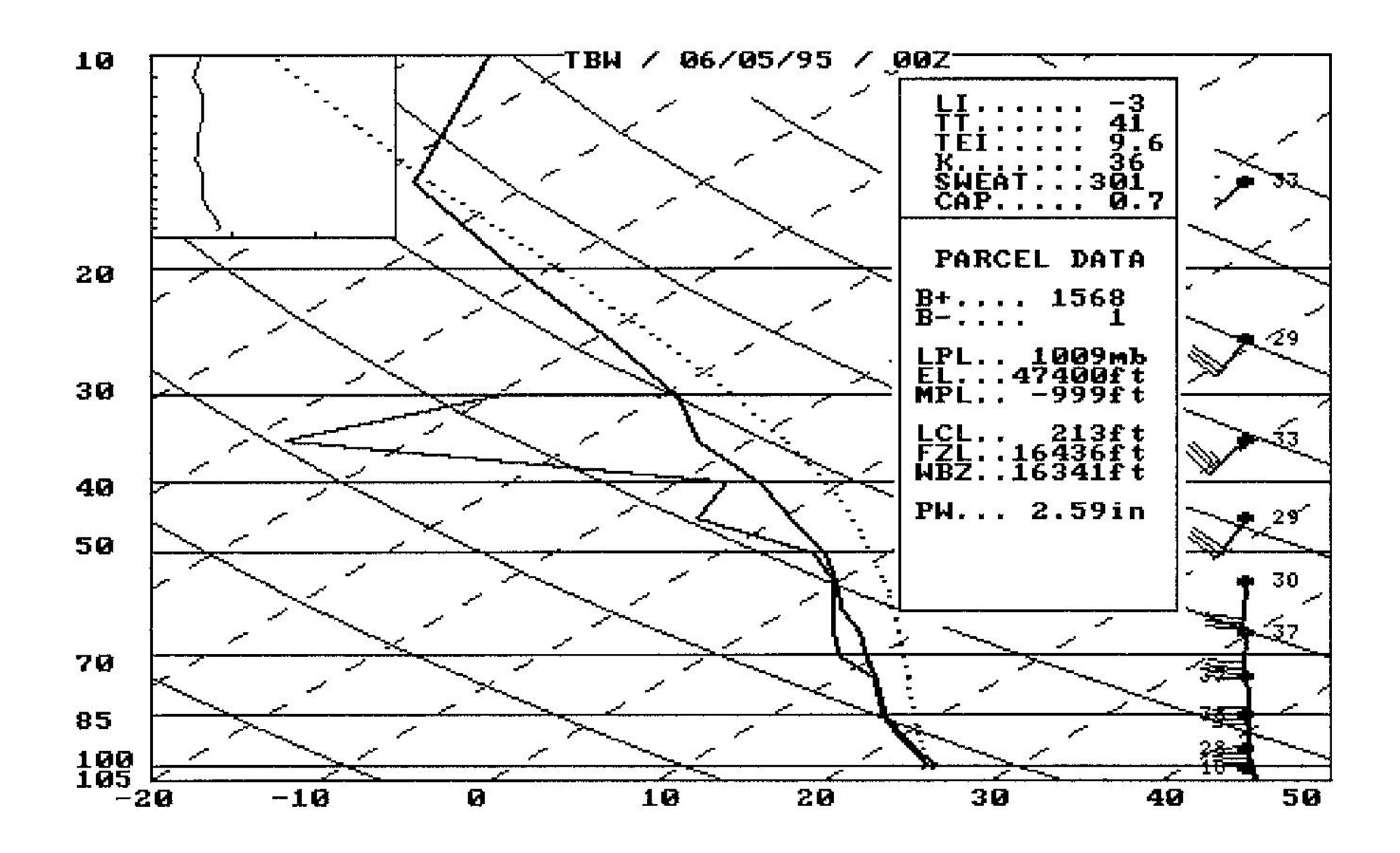


Best track positions of Hurricane Allison, 3–6 June 1995

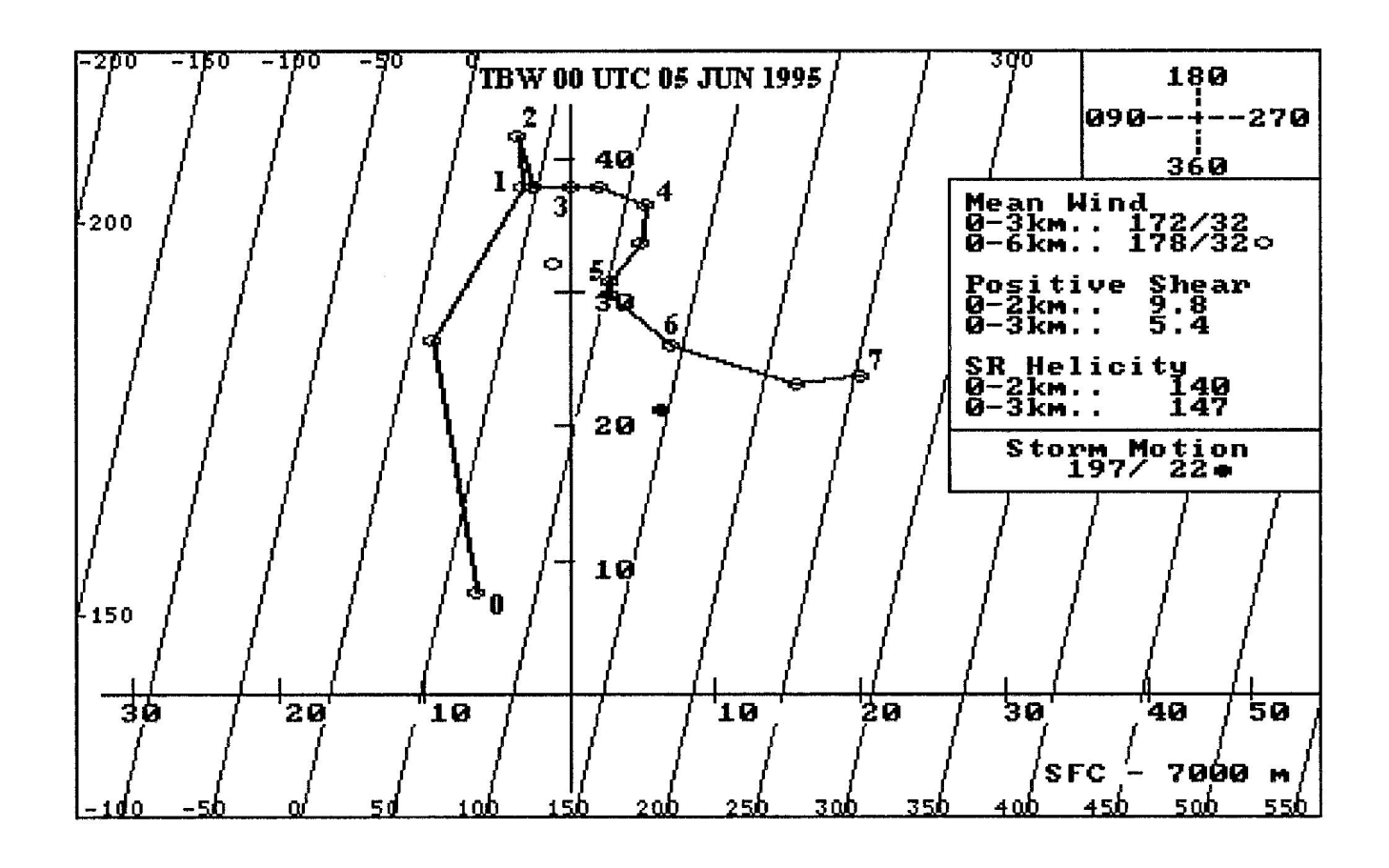
Tropical cyclone summary:

At 0000 UTC 3 June 1995, a tropical disturbance in the northwest Caribbean Sea was upgraded to the first tropical depression of the season. As the system moved north into the eastern Gulf of Mexico, it gradually strengthened and was named Tropical Storm Allison at 1500 UTC 3 June, then reached hurricane status 24 h later. Hurricane Allison made landfall in the "Big Bend" area of Florida the morning of 5 June, then continued north-northeast into Georgia and the Carolinas, where it became extratropical.

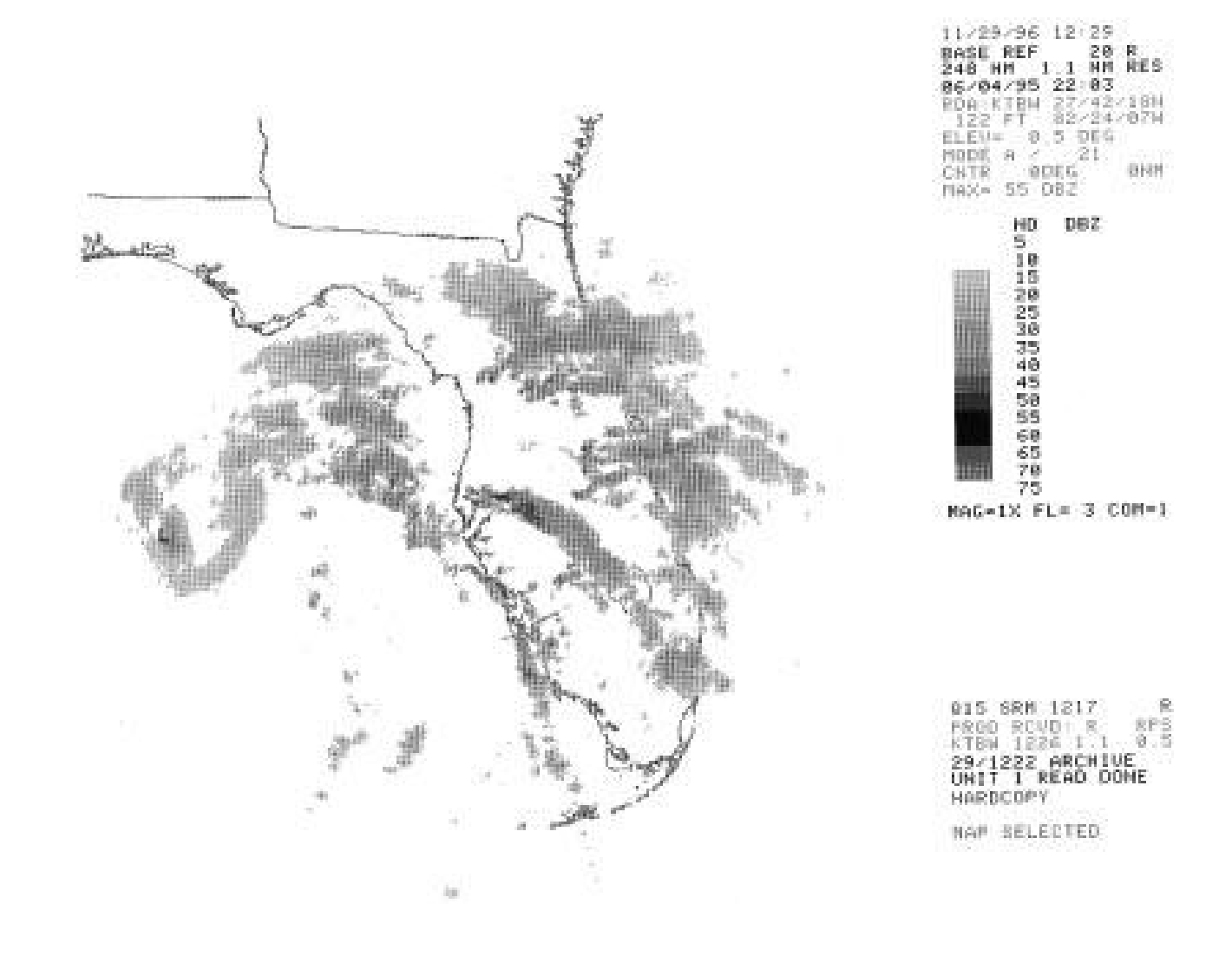
During the evening of 4 June, the center of Allison reached a position favorable for tornado development across west-central portions of the peninsula. Although most of the tropical storm force winds remained offshore, an outer convective band did sweep inland from the gulf during this period. Two weak tornadoes formed within the band in association with the same parent cell. Early on the following day as Allison approached landfall, the favorable tornadic environment shifted northward. Subsequently, eight tornadoes occurred across northeast Florida and southeast Georgia between 0700 and 1300 UTC, several of which were spawned from a single mesocyclone.



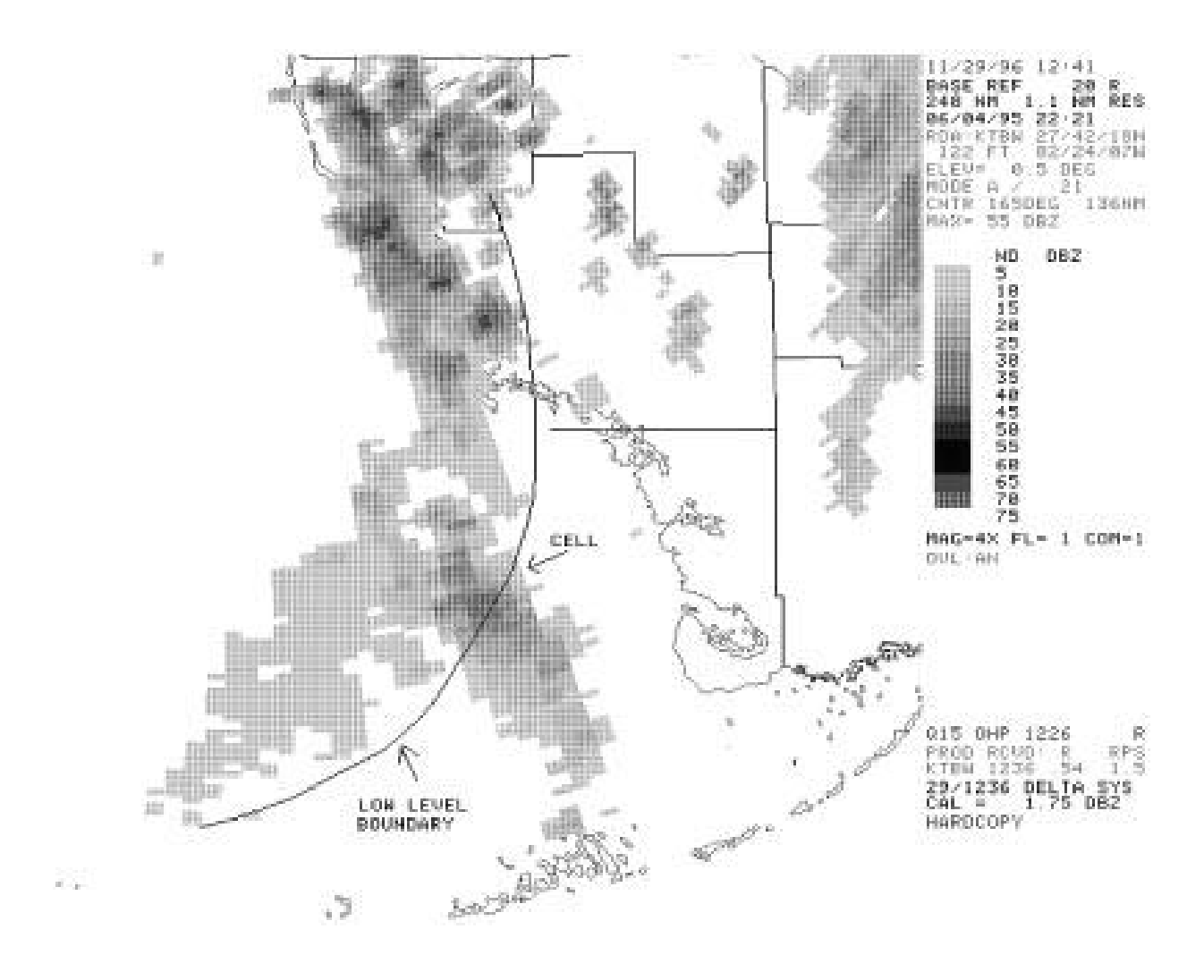
Same as Fig. 4 except for Tampa Bay, FL, at 0000 UTC 5 June 1995.



Hodograph produced using winds aloft from the Melbourne WSR-88D VAD Wind Profile and the surface wind from Melbourne International Airport at 0000 UTC 5 June 1995. Winds are plotted every 0.5 km above ground level (AGL) from the surface to 7 km and labeled every 1 km. The skewed lines represent contours of constant helicity. The table inset lists average wind (kt), shear (1023), and helicity (m2 s22) parameters. Storm motion was determined manually from radar for the highest reflectivity rainband cell within 140 km of KMLB.



The 0.5° base reflectivity product from KTBW illustrating the rainband structure at 2203 UTC 4 June 1995. The letter "L" indicates the center of Allison near the time of the radar image.



The 0.5° base reflectivity product for 2221 UTC 4 June 1995. Note the boundary extending offshore from the southwest Florida coast.

Questions?